The oxidation of **68** proceeded in practically identical yield and regioselectivity, regardless of the oxidant employed. The regioselectivity of 96:4, for 5-methylpyrrole-1-oxides **61** and **62**, can be rationalized along the same lines as before in E 60 (Table 10), and will not be discussed here further. The analytically pure nitrones **61** and **62** could be told apart by ^{13}C NMR by employing the principles already applied for the analysis of rigid diastereoisomeric pairs (i.e. "*β-effects*"; cf. Sections 3.2.3.1).[219-221] For instance, the absorptions for C-2/C-3 in the *trans*-nitrone **61** and the *cis*-nitrone **62** are 74.5/78.1 ppm and 70.3/74.3 ppm, respectively. The relative downfield shifts in *trans*-**61** are proof that a "*β-effect*" is operative, which justifies the structural and regioisomeric assignment in Table 11.

4.3.5 Role of conjugation in the oxidation of 5-anisyl-substituted *N*-hydroxypyrrolidines 41 and 71

From Table 12, a clear preference for the formation of the non-conjugated regioisomers **63** and **64** (r. r. = 96:4 or better, E 63-66) was observed. Since the bromomethyl substituent in the α-L-*lyxo*-configured compound **41** is *syn-clinal* to 2-H, this had a negligible influence on the regioselectivity, as already mentioned above. Instead, the electronic effects dictates the abstraction of the *anti*-standing 2-H with respect to the alkoxy functionality at C-3. This is able to "override" the conjugative effect, as was reported by Goti, Merino and Co-workers,[251,303] for the oxidation of similar substrates. The bromomethylnitrone **63** was obtained in crystalline form (X-ray, below).

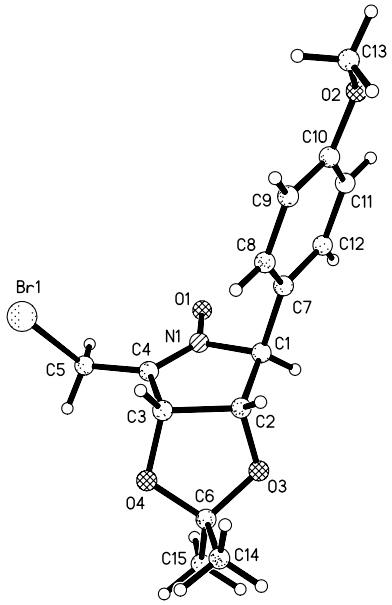

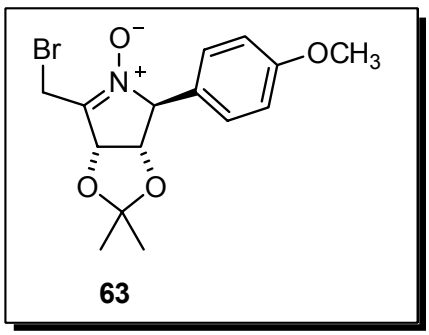

63

Diagram **41**: Solid state representation of bromomethyl-nitrone **63**

Table 12: Regioselective oxidation of 5-anisyl-2-bromomethyl- and 2-anisyl-5-methyl-*N*-hydroxypyrrolidines **41** and **71**. Reagent conditions: mercury(II) oxide (HgO, yellow, Fluka, 99 %; 3 Eq., CH_2Cl_2, 7-8 h, r. t.); manganese(IV) oxide (MnO_2, Fluka, techn. 90 %; 'oxidation active', 1.3 Eq., CH_2Cl_2, 30 min to 1 h, 0 °C to r. t.).

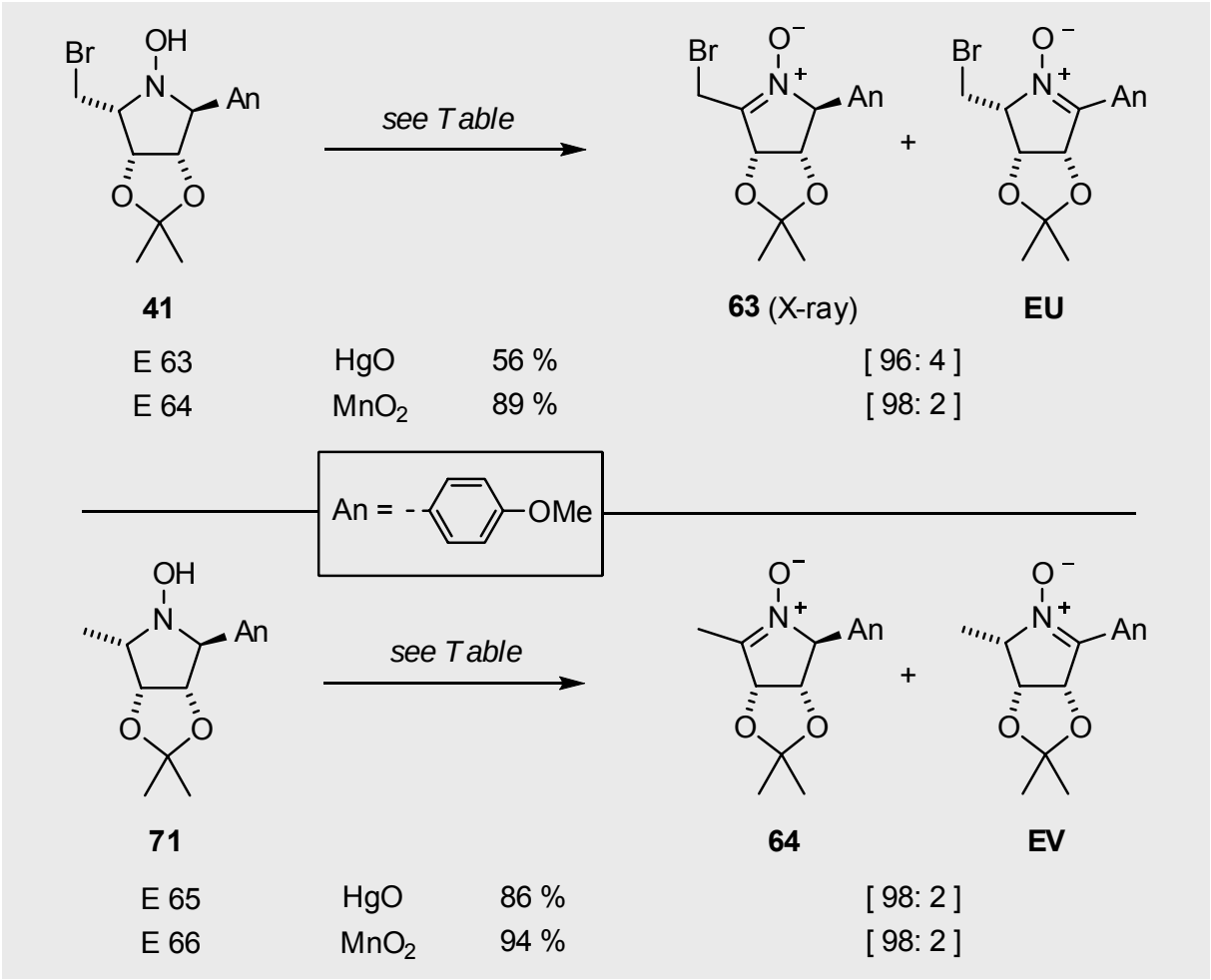

Exp.	Educt	Oxidant	Time [h]		Product r. r. HPLC[a]	^{13}C NMR[b]	$\Delta\Delta G^{\ddagger}_{298}$[c]	Yield [%][d]
E 63	**41**	HgO	7	**63** : **EU**	n/a	[96 : 4]	1.89	56 (**63**)
E 64	**41**	MnO_2	0.5		n/a	[98 : 2]	2.30	89 (**63**)
E 65	**71**	HgO	8	**64** : **EV**	[94 : 6]	[98 : 2]	n/a	86 (**64**)
E 66	**71**	MnO_2	1		[96 : 4]	[98 : 2]	2.30	94 (**64**)

[a] Peak integration at λ_{max} = 265 nm (in CH_2Cl_2/MeOH = 92:2); E 65 contained impurities, occludeding with the minor product peak – ratio may be slightly inaccurate; [b] Integration of isopropylidene methyl signal pairs; [c] kcal/mol; [d] After celite filtration; MPLC purification.

4.4 Reactions of Bromomethyl-Ketonitrones

4.4.1 1,3-Dipolar cycloaddition of 2-anisyl-substituted-bromomethyl nitrone 63

If the work of Bierer[2] and Section 3.1.1 is anything to go by, the 1,3-dipolar cycloaddition of a nitrone and an alkyne should be a facile reaction. Indeed, the reaction of bromomethyl nitrone **63** in the presence of dimethylacetylenedicarboxylate (DMAD) at 75 °C yielded a separable mixture of "4-isoxazolines" in 81 % yield. Elevated temperature was necessary to drive the reaction to completetion, being sluggish otherwise. The minor cycloadduct **EW** was found to decompose rapidly at room temperature evidenced by a change from a solid to a liquid form and the resulting undecipherable ^{1}H and ^{13}C NMR data. The 4-isoxazolines are known to be reactive species, capable of undergoing ring-opening and subsequent rearrangements.[324,325,326] This aspect was not examined further in this work, however.

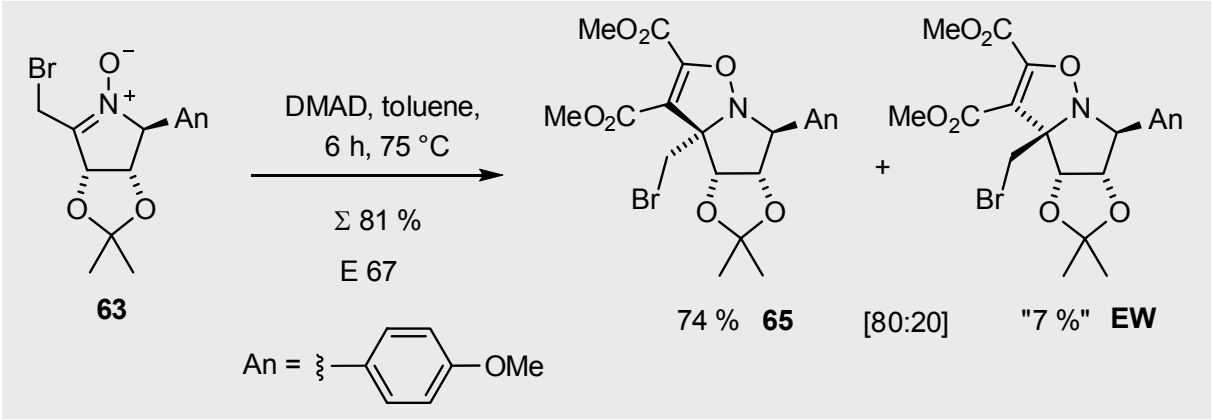

Scheme 39: [1 + 3] dipolar cycloaddition of bromomethyl nitrone **63**

4.4.2 Generation and reactions of cyclic vinylnitrosonium cations from bromomethylnitrones

4.4.2.1 Background of α-chloronitrones from Eschenmoser, Kempe *et al*.

In 1972, Eschenmoser and co-workers at the ETH laboratories introduced *N*-vinyl-*N*-alkyl-nitrosonium cations (in particular, N = cyclohexyl, **FB**) as versatile synthetic equivalents.[100] Interestingly, the inspiration for this work can be traced further north to *swabian* Stuttgart, where Schmidt and co-workers[327] were working on the synthesis of 1,3-oxazines. Their

approach relied on treating, for example, *N*-chloromethylbenzamide **EX** with tin(IV) tetrachloride in the presence of an olefin. This process eliminated chloride to form the hexachlorostannate salt **EY**, a cationic heterodiene, which entered into a [4 + 2] Diels-Alder cycloaddition. Working up the reaction with sodium hydroxide liberated the bicyclic 1,3-oxazine **EZ**. The addition is *cis*-stereo "specific" and normally region "specific" (i.e. additions follow Markovnikov's rule).[328] Following on from Schmidt's lead, Eschenmoser investigated chloride elimination from α-chloro-aldonitrone **FA** with silver tetrafluoroborate to generate to the vinylnitrosonium ion **FB**. This very sensitive and unstable species underwent *in situ* [4 + 2] cycloadditions with unactivated alkenes, generating the 1,2-oxazinium ion framework **FC** in the process. The yields varied between 30-85 % (Scheme 40).[100]

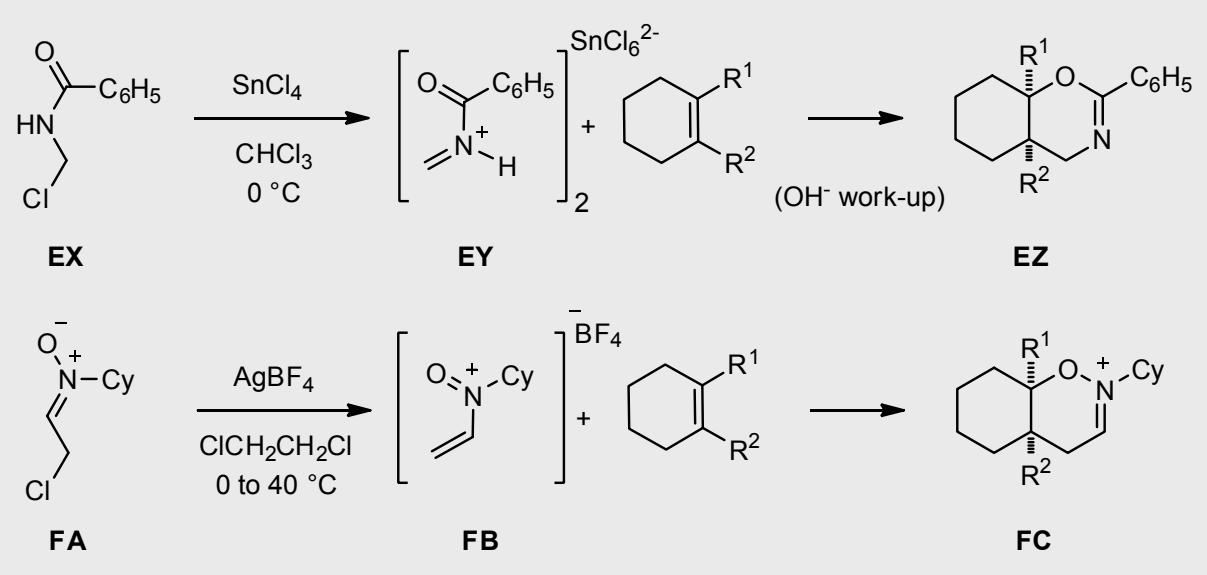

Scheme 40: Relationship between the formation of amidomethylium ions and vinylnitrosonium ions by chloride elimination from Schmidt and Eschenmoser, respectively

The salts of type **FC** may be used directly or undergo cycloreversion when inititated by base promoted proton extraction at C—4 (see Schatzmiller et al.[329]). However, the usual work-up is with aqueous potassium cyanide to give a mixture of epimeric cyanotetrahydro-2*H*-1,2-oxazines, as the transformation of **FD** to **FE** documents (Scheme 41).[330] The nitrile **FE** undergoes cyanide explusion and ring contraction with *tert*-butoxide to provide the imino γ-lactone **FF** and **FG**, following hydrolysis on moist silica gel. Similarily, α-methylidene-γ-lactone **FI** can be constructed if the parent chloronitrone **FA** is exchanged for cyclohexyl-α,β-dichloro-propionaldonitrone **FH**.[331] (Scheme 42). Noteworthy is the selective dissociation of the α-chlorine by the silver ions; though, a mixture of several diastereoisomers is obtained after the KCN work-up step. This was put down to the conformational mobility of the system

(i.e. "*cis*-decalin" like; see Riddell, lit.[275]), meaning that two conformations were available for attack by the incoming cyanide anion. The *axial* addition to the iminium ion (such as in **FD**) is the preferred direction of attack, explained by a stereoelectronic "kinetic anomeric-effect" (i.e. CN takes up an anti-periplanar conformation with respect to the ring nitrogen lone pair).[331] Riediker and co-workers[332] further investigated this, particularly the aspect of conformational mobility,[333] in the related hydroxymethyl cycloadduct **FK**, easily accessible from the epoxynitone **FJ**, which after conversion to the "1,5"-dipole underwent annelation with cyclohexene and analogous transformations to α-methylidene-γ-lactone **FI**.

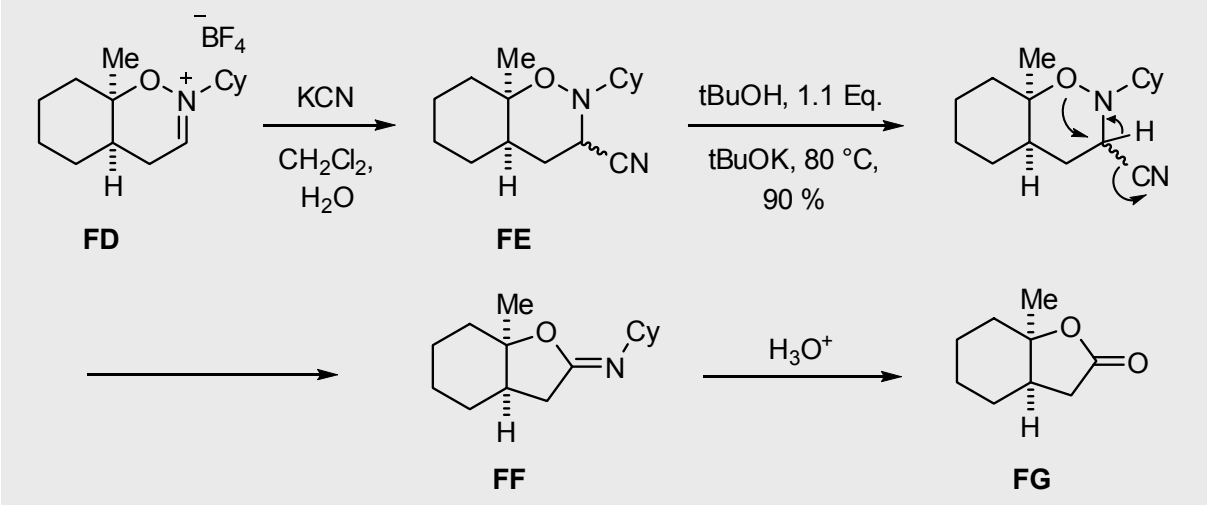

Scheme 41: Addition of cyanide to the 1,2-oxazilium spieces and subsequent transformations leading to bicyclic γ-lactone **FG**.

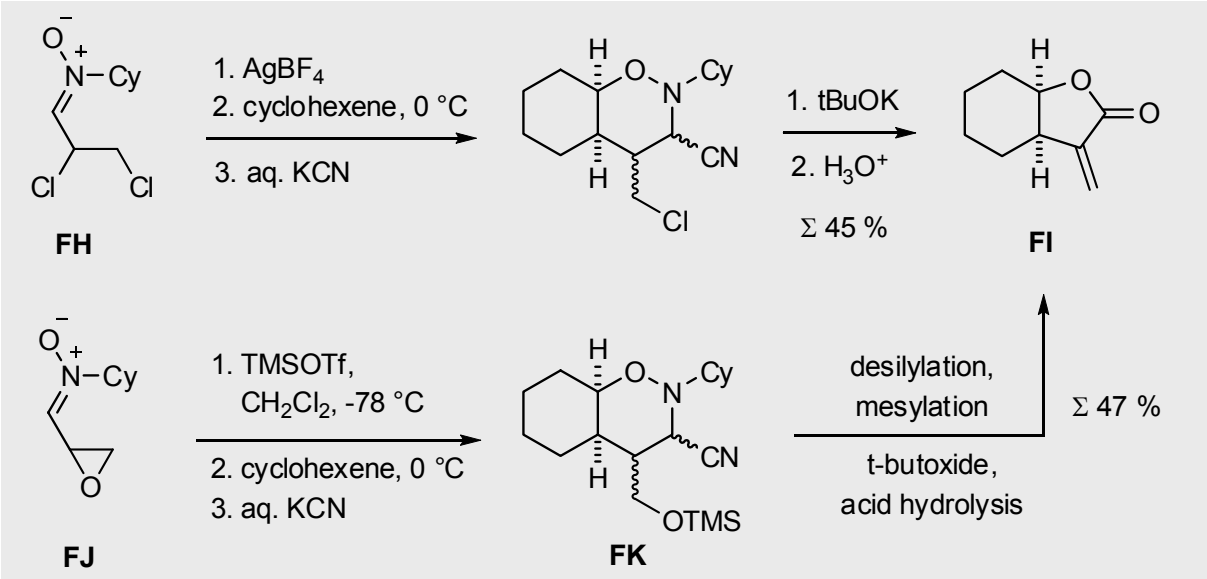

Scheme 42: Convergent route to α-methylidene-γ-lactones using dichloro- or epoxynitrones as precursors for vinyl-nitrosonium species

In generating the β-hydroxylmethyl spiecies from the epoxynitrone **FJ** with trimethylsilyl triflurormethylsulfonate (TMSOTf), it is evident that oxygen functionalities with nucleofuge capacity can be good alternatives to α-chloromethyl, and thus to silver tetrafluoroborate (difficult to handle, light sensitive, etc.) as precursors for the "1,5"-dipoles. Here, interestingly, it seems that Riediker has cobbled together elements of the related "Wharton Rearrangement"[334] and "Epoxyketon–Alkynone Fragmentation" in forming the basis for the epoxynitrone reaction – a relationship he himself openly acknowledges.[332a] The epoxynitrones after treatment with TMSOTf were carefully investigated in solution by ^{13}C NMR and found to dissociate into more stable components through proton elimination to α,β-unsaturated nitrones, inferred to have formed after treatment with aqueous KCN solution and the subsequent isolation of 3-hydroxy-isoxazolidines derivatives.[332a]

One final point, *N*-vinyl-*N*-alkyl-nitrosonium species are strongly electrophilic, meaning that the reaction with olefins is subject to electrophilic substitution in competition with cycloaddition, as also described by Eschenmoser.[335] Conducting the reaction in a highly polar solvent, usually sulfur dioxide at -20 °C, favours the substitution. The geometry of trisubstituted alkenes is retained. Similarly, Eschenmoser[335] and others[336,337] have shown that electron-rich aromatic compounds are alkylated and hydrolytic work up affords α-arylaldehydes. A representative example is shown in Scheme 43, where the 1,4-dipole generated from α-chloro propionaldonitrone **FL** gave the substitution product **FM** and, following hydrolysis, the aldehyde **FN**. Here, the *N*-vinyl-*N*-cyclohexyl nitrosonium ion is a α-acyl carbocation equivalent or **a²** acetaldehyde "*umpolung*" synthon in these reactions.

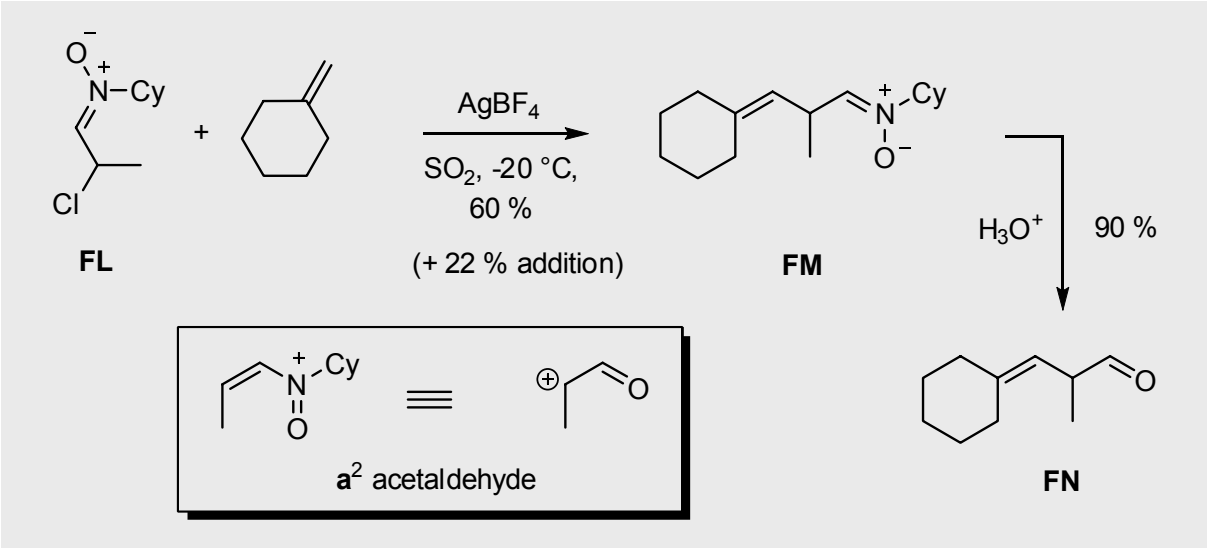

Scheme 43: Preferred electrophilic substitution of chloronitrone **FL** with olefins when conducted in liquid sulfur dioxide[335]

4.4.2.2 Own results: Treatment of bromomethyl-ketonitrone 57 with $AgBF_4$

Using lit.[100] as a guideline, bromo-ketonitrone **57** in 1,2-dichloroethane was added to a solution of silver tetrafluoroborate and cyclohexene in 1,2-dichloroethane, taking care to avoid the influx of moisture and light (Scheme 44). The addition of a few drops of the nitrone led to the immediate precipitation of silver bromide, which as it turned out, can lead to stirring problems later on when not careful. Regular TLC control indicated the formation of two equally intense UV-active spots at R_f = 0.15 (EE 100 %) and rapid disappearance of the starting material. Work-up with KCN solution, followed by filtration through a short column, afforded the diastereoisomeric pair **66**/**67** in a combined, albeit low, yield of 20 % (^{1}H & ^{13}C NMR d. r. = 50:50). Separation led to the isolation of **66** (8.3 %) as a colourless oil that solidified on standing (m. p. 88-91 °C) and **67** (10 %; Σ 18 %) as a crystalline colourless solid (m. p. 119-121 °C), whose X-ray structure could be determined (see below).

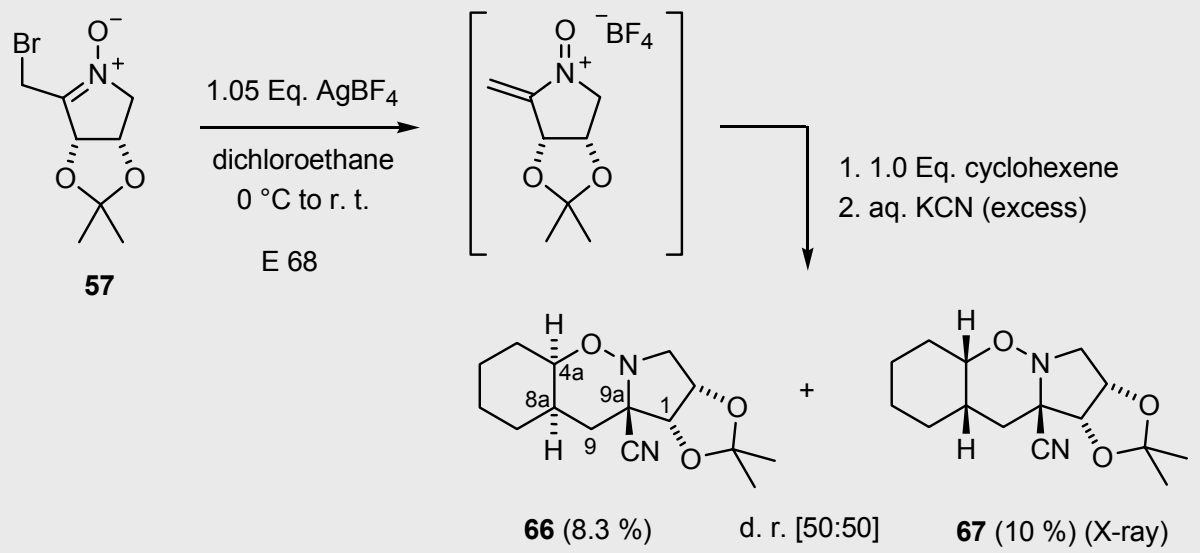

Scheme 44: Reaction cascade of the purported vinyl nitrosonium cation generated from the reaction of bromo-ketonitrone **57** with silver tetrafluoroborate

The low yield of this transformation, unprecedented as it is, throws up a few questions: namely, does the lifetime of the vinyl nitrosonium spieces allow for sufficient time for cycloaddition to occur? Eschenmoser generated the vinyl nitrosonium cations through the slow addition of the nitrone, usually over 2 hours, at around -20 °C. Due to lack of time, the experiments in this Thesis largely ignored Eschenmoser's time and temperature guidelines; the bromo ketonitrone **57** was added to $AgBF_4$/cyclohexene over the course of 10-15 minutes at 0 °C instead. The silver tetrafluoroborate taken in this reaction was not of the "freshest" quality either. Obviously, the individual parameters of the experimental procedure require a

more thorough investigation. Regarding analysis, annelation with cyclohexene gave a 50:50 mixture of cycloadducts with a *cis*-linkage at the C—4a/C—8a juncture; the ^{1}H NMR $J_{4a,8a}$ coupling constants were 7.3 and 4.3 Hz for **66** and **67**, respectively, support this. Conversely, the addition of cyanide proceeded stereo "specifically" with the attack taking place at the least hindered face of the intermediary 1,2-oxazinium salt, probably due to the steric nature of the "acetonide clamp" (cf. nucleophilic additions to L-*lyxo* nitrone **5**, Section 3.2.2.). In the ^{13}C NMR spectra, the quaternary carbons attached to cyanide (i.e. C—9a) resonated at 64.0 and 69.1 ppm for **66** and **67**, respectively, while the nitrile carbon was found at 119.7 ppm. Since a shielding effect invoked by a substituent is attenuated by distance, some deviation in the chemical shift of C—9 should also be observed. We can predict that there is perturbation closer to C—9 when the cyclohexane ring is pointing downwards in **67**, to shield this carbon, than in the diastereoisomer **66**. This is verified by experimental data, where the chemical shift of C—9 in **67** is upfield of C—9 in **66** (i.e. 27.8 *versus* 31.8 ppm).

In the solid state, the bicyclic 1,2-tetrahydro-oxazine system resides in a double-chair conformation (Diagram 42). The conformation of this "*cis*-decalin" system is locked in by the pyrrolidine component and is therefore not conformationally mobile in solution, as judged by ^{1}H NMR. Ample literature is known for the inversion of *cis*-decalin (rapid at room temperature, activation energy of 12 kcal/mol, cf. lit.[277]) and also for bicyclic tetrahydro-1,2-oxazine systems, for example, as reported by Denmark and co-workers.[338]

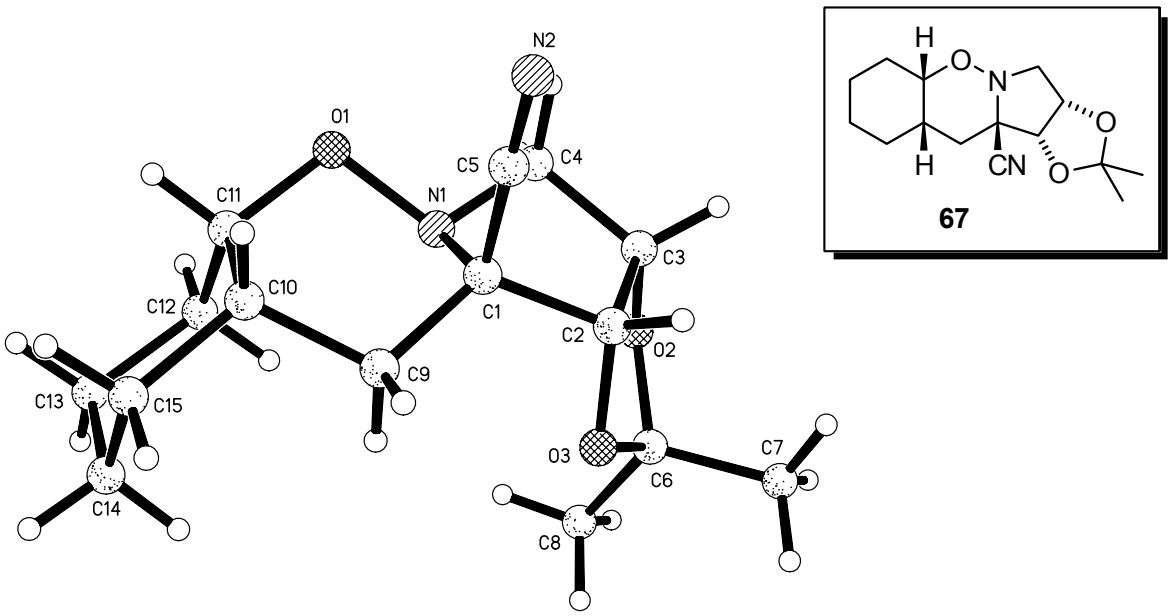

Diagram 42: X-ray of tetra-cyclic nitrile **67**

5 Synthesis of α-L-Fucosidase Inhibitors

5.1 Own Results

5.1.1 Lithium aluminium hydride reduction of the bromomethyl group

The conversion of the tetra-substituted pyrrolidines into inhibition candidates is pretty much self-explanatory and commences with the reduction of the bromomethyl moiety with $LiAlH_4$, using a procedure from Bierer.[2,3] A moderate excess of $LiAlH_4$ in THF at room temperature provided the *N*-hydroxypyrrolidines **68**-**80** in very good yields (Scheme 45). Note: a crystal structure determination of the isopropyl-substituted compound **69** could be obtained. To save space, no X-ray diagram is displayed here (refer to Section 9.10 for full data).

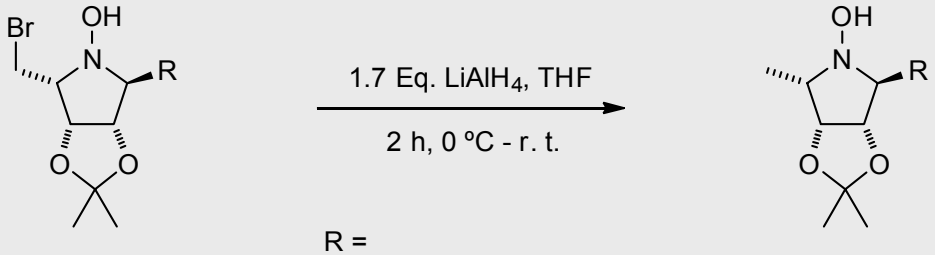

		R =		
35	E 69	methyl	84 %	**68**
36	E 70	isopropyl	66 %	**69** (X-ray)
38	E 71	allyl	81 %	**70**
41	E 72	*p*-methoxyphenyl	97 %	**71**
42	E 73	[(1,1'-biphenyl)-4-yl]	91 %	**72**
43	E 74	*p*-fluorophenyl	89 %	**73**
44	E 75	*p*-chlorophenyl	72 %	**74**
45	E 76	*p*-bromophenyl	92 %	**75**
46	E 77	*p*-methylthiophenyl	89 %	**76**
47	E 78	*p*-methoxybenzyl	91 %	**77**
48	E 79	*p*-phenoxyphenyl	89 %	**78**
49	E 80	(2)-furyl	92 %	**79**
50	E 81	*p*-*N*,*N*-dimethylanilino	88 %	**80**

Scheme 45: Reductve removal of bromine using lithium aluminium hydride

Likewise, reduction of the *p*-*N*,*N*-dimethylanilino substrate **51** in the series to the *N*-hydroxyamine **81** proceeded in high yield (Scheme 46).

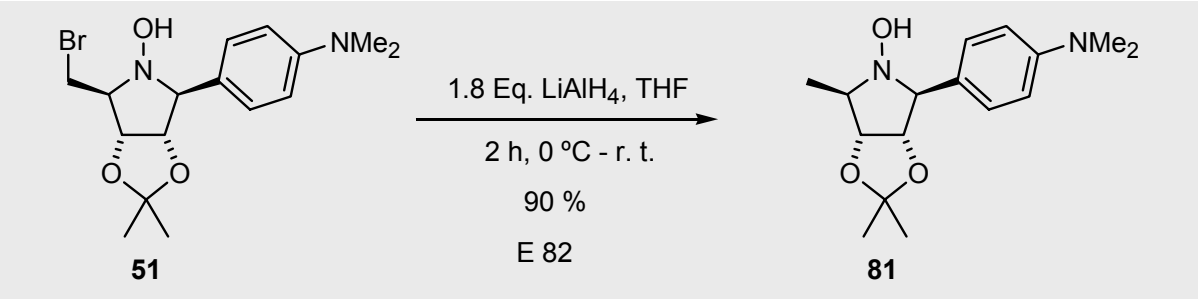

Scheme 46: Analogous reduction of the bromomethyl group with $LiAlH_4$ in the β-D-*ribo* series

5.1.2 Concomitant reduction of C—Br and N—O bonds

Various reagents were tested in the pursuit of a "one pot" concomitant C—Br and N—O bond reduction for the direct entry into the corresponding cyclic amine. The $LiAlH_4$ reduction using excess of reagent under pronounced reflux had no effect.[339] Employing $LiAlH_4$ in tandem with anhydrous nickel chloride[340] to produce a "low-valence" metal couple led only to products of C—Br bond cleavage and no detection of cyclic amines.[341] The use of acid-activated zinc, as carried out by Sayago[190a] led to N—O bond cleavage only, as expected (see below), but left the bromomethyl moiety intact, affording the cyclic amine **FO** in good yield. Noteworthy is that no discernable Boord-like elimination was observed (cf. Section 2.2.1.1, pp. 30-31). Using catalytic hydrogenation to induce N—O bond cleavage was hampered by a competing C—N benzylic reduction, which resulted in product mixtures comprising variable amounts of the cyclic amine hydrogenbromide and ring-opened product, i.e. **FP** and **FQ**, when starting out from substrate **41** (cf. Bierer, Thesis, lit.[2]) (Scheme 47).

In contrast, Yu and Huang, working on the tetra-substituted pyrrolidine framework (alkaloids related to radicamines A and B), reported high yields for the catalytic hydrogenation under similar conditions (i.e. Pd-C, 10 %, H_2, MeOH); no competing benzylic C—N cleavage with was mentioned.[145] Hydrogenation was carried out on the substrate **41** using other supported metal catalysts. This either gave decomposition (i.e. 5 % palladium on $CaCO_3$), or product mixtures arising from the incomplete hydrogenation of the aromatic substituent (with rhodium, 5 % on alumina). On the basis that the liberated acid might promote reduction at the benzylic position, catalytic hydrogentation on the phenyl-substituted pyrrolidine **40** with

Pd-C and hydrogen was buffered with triethylamine.[342] However, these conditions led surprisingly to reduction *and* dehydration to afford the cyclic nitrone **82** in moderate yield (Scheme 47)! X-ray analysis confirmed the structure of the pyrrole-1-oxide **82** (Diagram 43). As discussed already in Section 4, the non-conjugated product should be the one that formed preferentially.

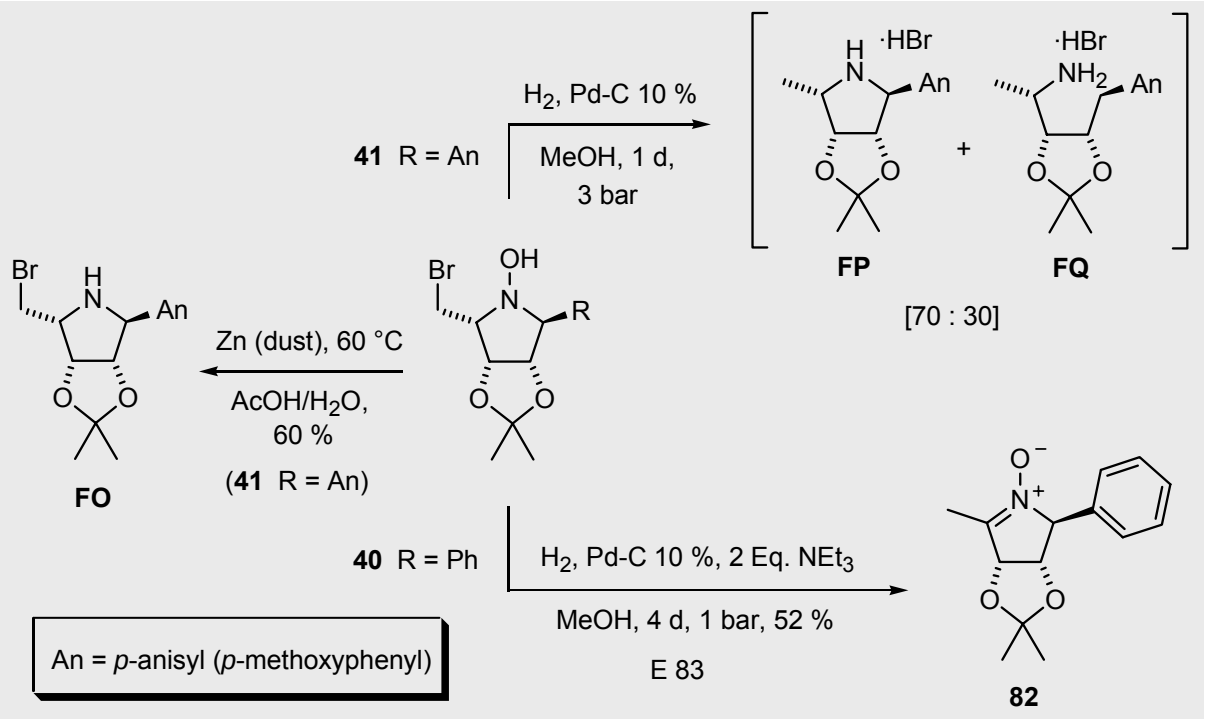

Scheme 47: Interplay between C—N/N—O reduction, depending upon the reagent employed. Catalytic hydrogenation under basic conditions led to nitrone formation **82**.

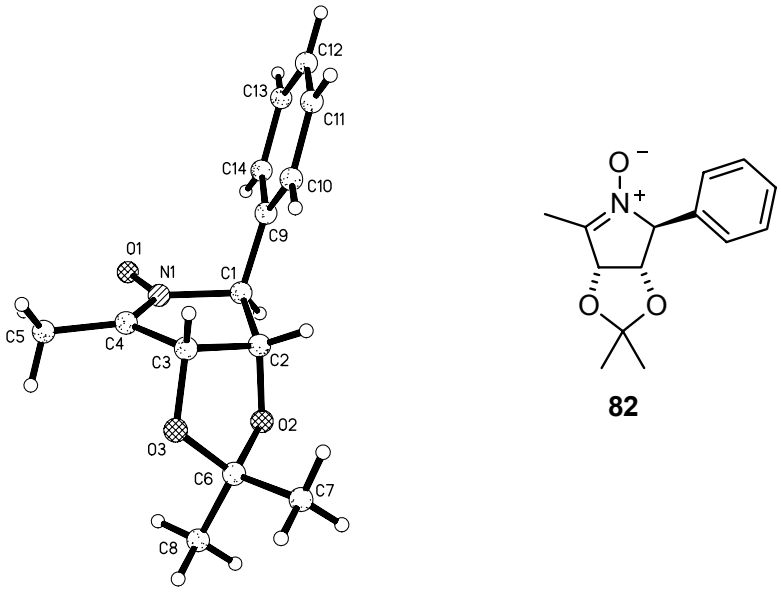

Diagram 43: X-ray structure of 5-phenyl-2*H*-pyrrole-1-oxide **82**

Palladium is a somewhat overlooked reagent in this respect. As shown by Murahashi et al.[130,296] palladium black was an efficient oxidant (80-110 °C, 10 mol %) for *N*,*N*-disubstituted hydroxylamines, providing nitrones with the liberation of hydrogen. Water was among the best reaction solvents examined. Further palladium reagents, i.e. $PdCl_2$, $Pd(OAc)_2$, $PdCl_2(MeCN)_2$, were tested though slightly less efficient. Ruthenium complexes such as Ru black, $RuCl_3$, $Ru(OAc)_3$ gave the corresponding amines, with only traces of the nitrones. The authors rationalized the transformation by initial oxidative insertion of palladium into the O—H bond in **FR** followed by elimination of a [Pd—H] species and reductive coupling to provide the nitrone **FS** and hydrogen (Scheme 48).

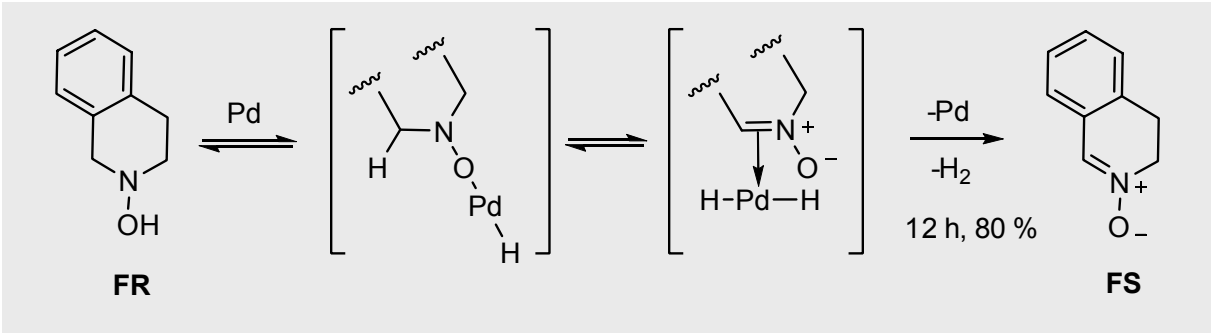

Scheme 48: Palladium dehydrogenation of hydroxylamine **FR** to yield cyclic nitrone **FS**.[296]

In some cases, Murahashi noted the necessity for the addition of 0.1 equivalents of triethylamine, which helped to retard amine formation.[130] In our case (Scheme 47, experiment E 83), the presence of base might also have been beneficial, however, no control experiment was carried out.

Elsewhere, the reduction of C=N bonds and reductive cleavage of N—O bonds (i.e. oximes) to secondary amines,[343] and the dehalogenation of α-bromo ketones in DMF (caution! cf. lit.[344]) was possible using nickel boride (for an overview, cf. lit.[345]). “Nickel boride”, or “Ni_2B”, represents a nominal stoichiometry for the reagent prepared by the action of $NaBH_4$ on a Ni(II) salt (i.e. usually a 1:3 mixture of nickel chloride[340] and sodium borohydride); several other Ni_xB_y spieces have been reported.[345] As far as the author of this Thesis is aware of, no precedent exists for the concomitant N—O and C—Br cleavage using Ni_2B. Pleasingly, both bond clevages were possible following the reduction of the pyrrolidine **41** with 1 Eq. of $NiCl_2$ and 3 Eq. $NaBH_4$ – though, this led to mixtures of *N*-hydroxpyrrolidine and cyclic amine (Scheme 49). The reduction went to completion when a large excess of nickel boride (i.e. 4 Eq. $NiCl_2$/12 Eq. $NaBH_4$) was employed. This provided the analytically pure cyclic amine **86** (numbering taken from Scheme 51, below) in a moderate yield of 45 %.

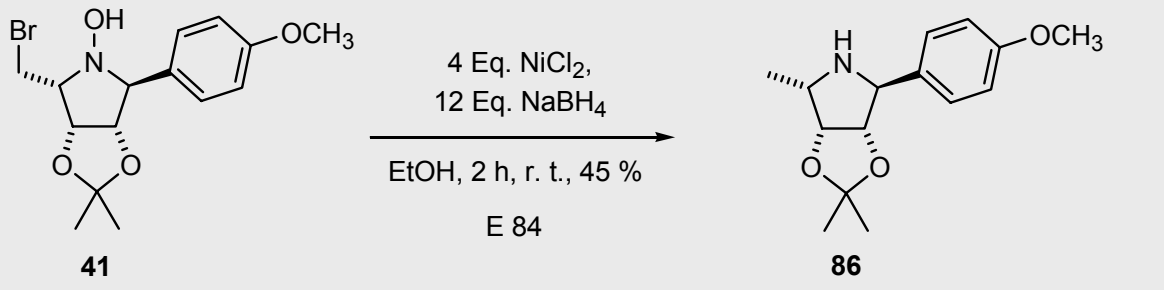

41 **86**

Scheme 49: Concomitant C—Br and N—O reduction of substrate **41** with nickel boride

Note of caution: Employing Ni_2B for the rest of the substrates may perhaps encounter difficulties, since the reagent is particularly deft at dehalogenation of aryl halides (chlorides, bromides, etc.; cf. lit.[346]) and desulfurizations.[345]

5.1.3 Synthesis of *N*-hydroxypyrrolidinetriols

In a straightforward manner, the *N*-hydroxypyrrolidines **71**, **72** and **76** were deprotected in the presence of concentrated hydrochloric acid in methanol to obtain the corresponding crude products as hydrochloride salts. Recrystallisation of the triols **84·HCl** and **85·HCl** (diffusion method; methanol/diethylether, see Experimental Section) led to the isolation of the analytically pure, colourless solids as inhibition candidates in high yields. The *p*-anisyl hydrochloride salt was treated with strongly acidic ionic exchange resin (DOWEX 50WX8, H^+ Form) to afford the free *N*-hydroxypyrrolidine triol **83** in high yield (Scheme 50).

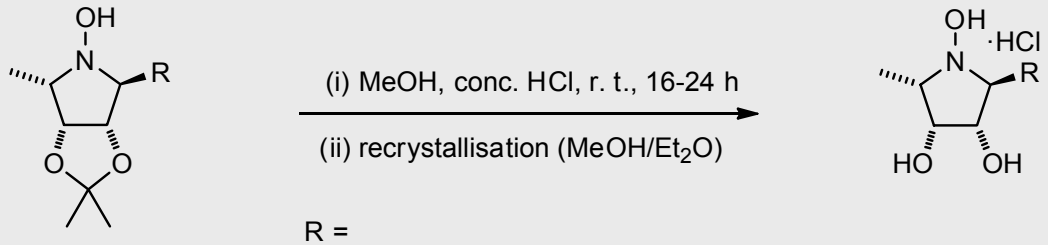

		R =		
71	E 85	*p*-methoxyphenyl	93 % (Σ 27 %)	**83**[iii]
72	E 86	[(1,1'-biphenyl)-4-yl]	91 % (Σ 23 %)	**84·HCl**
76	E 87	*p*-methylthioyphenyl	21 % (Σ 5 %)	**85·HCl**

Scheme 50: Synthesis of pyrrolidinetriols: (iii) then DOWEX 50WX8, H^+ form, elution with 2 N NH_3; combined yield based on D-ribose, 7 steps.

5.1.4 N—O bond cleavage of *N*-hydroxypyrrolidines with zinc/acetic acid or with samarium(II) diiodide

It was convenient to carry out the N—O bond cleavage with zinc in acidic medium, as exemplified in Scheme 51. Reductions were rapid and proceeded in good to high yields.

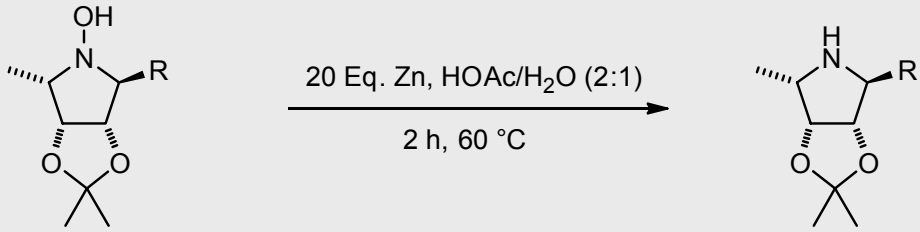

		R =		
71	E 88	*p*-methoxyphenyl	85 %	**86**
72	E 89	[(1,1'-biphenyl)-4-yl]	85 %	**87**
73	E 90	*p*-fluorophenyl	81 %	**88**
74	E 91	*p*-chlorophenyl	73 %	**89**
75	E 92	*p*-bromophenyl	91 %	**90**
76	E 93	*p*-methylthioyphenyl	87 %	**91**
78	E 94	*p*-phenoxyphenyl	96 %	**92**
79	E 95	2-furyl	70 %	**93**

Scheme **51**: Zinc mediated N—O bond cleavage yielded cyclic amines

Sayago expertly tested the reduction method with the *p*-methoxyphenyl substrate **71**.[190a] Following his success, the reduction of the remaining compounds seemed warranted. The procedure is modelled on a report from Varlamov and Co-workers[347] describing the use of an excess of zinc powder heated to 60-70 °C in the presence of a 80 % solution of acetic acid (cf. lit.[348]). The acetonide protecting group under these conditions remained unscathed, as can be inferred from the good to high yields of product obtained.

For the reduction of the *p*-*N*,*N*-dimethylamilino substrates **80** (α-L-*lyxo*) and **81** (β-D-*ribo*), isolation problems were encountered with the use of the zinc reagent, which were attributed to extraction difficulties following neutralisation of the diacetate salt that forms. Thus, a milder reduction under neutral conditions was sought in the form of samarium(II) diiodide (SmI_2).[349] This reagent was chosen on the basis of an encouraging report from Marco-Contelles and co-workers[350] detailing the use of SmI_2 to promote the reductive N—O cleavage of *N*-acetyl-O-benzylhydroxylamines. The reagent was freshly prepared using samarium metal and diiodoethane according to the procedure of Kagan et al.[351] (refer to notes regarding

diiodethane in the Experimental Section). Application of this Prussian-blue solution to α-L-*lyxo* **80** led to a very rapid deoxygenation to provide the analytically pure diamine **94** in a yield of 79 % (Scheme 52). In contrast, the reduction of β-D-*ribo* diastereoisomer **81** to diamine **95** turned out to be a more capricious transformation, requiring an excess of SmI_2 in wet THF and prolonged stirring to drive the reaction to completion. The addition of a proton donor can accelerate N—O cleavage;[350,352] water (20 Eq. with respect to substrate) in this case proved to be essential. Addition of hexamethylphosphoric triamide (HMPA, coordinates to and promotes other SmI_2 transformations, cf. lit.[353]) had no effect.

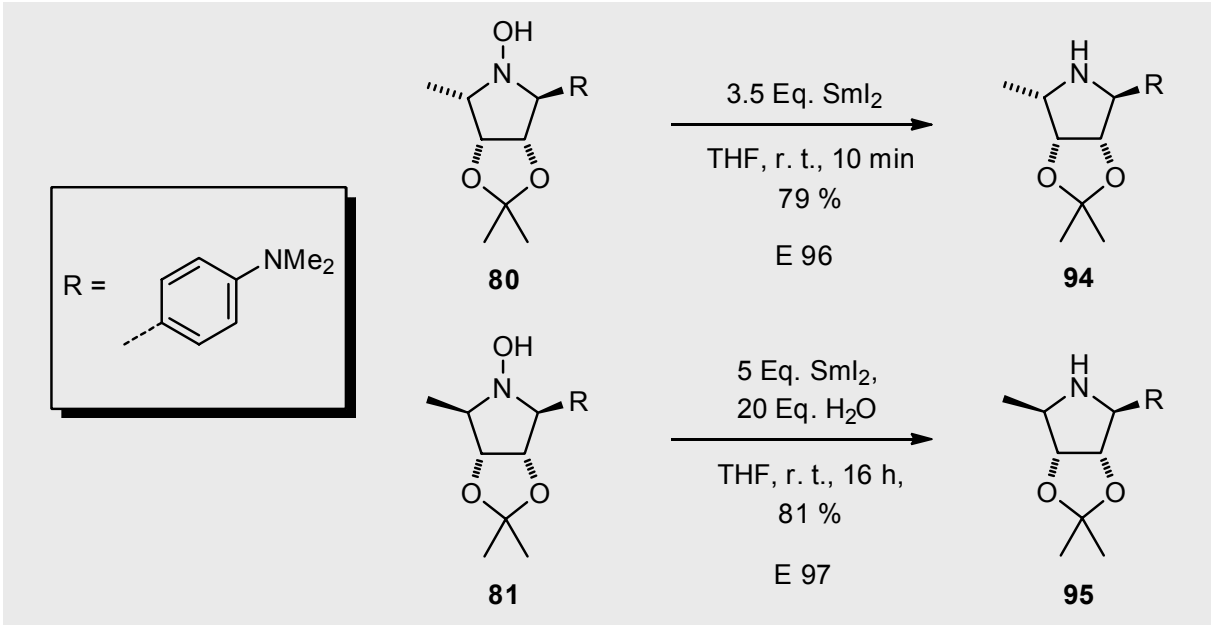

Scheme 52: Samarium diiodide deoxygenation of substrates

5.1.5 Deprotection of cyclic amines and synthesis of pyrrolidinediols with 2-aryl side-chains

The zinc-reduced pyrrolidines were deprotected in the same manner as described already in Section 5.1.3 and by Bierer[2] using methanolic solutions of concentrated hydrochloric acid or hydrobromic acid (Scheme 53). Noteworthy is that, after recrystallisation, the analytically pure hydrochloride or bromide salts were excellent sources of crystals for X-ray structure determination. Indeed, apart from **98·HCl** and **103·HCl**, the solid state structures were elucidated in all cases to provide additional structural proof. The crystal structures of the pyrrolidine diol hydrochlorides **96·HCl** and **97·HCl** are discussed in Section 5.1.7. For all other crystal structure diagrams, the reader is referred to the Section 9 (X-ray data).

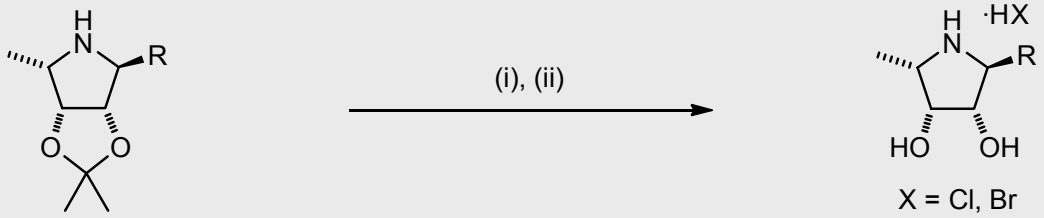

		R =		
86	E 98	*p*-methoxyphenyl	99 % (Σ 23 %)	**96·HCl** (X-ray)
87	E 99	[(1,1'-biphenyl)-4-yl]	95 % (Σ 20 %)	**97·HCl** (X-ray)
88	E 100	*p*-fluorophenyl	95 % (Σ 19 %)	**98·HCl**
89	E 101	*p*-chlorophenyl	90 % (Σ 15 %)	**99·HCl** (X-ray)
90	E 102	*p*-bromophenyl	73 % (Σ 11 %)	**100·HCl** (X-ray)
91	E 103	*p*-methylthiophenyl	63 % (Σ 13 %)	**101·HCl** (X-ray)
92	E 104	*p*-phenoxyphenyl	88 % (Σ 20 %)	**102·HCl** (X-ray)
92	E 105	*p*-phenoxyphenyl	96 % (Σ 21 %)	**102·HBr** (X-ray)
93	E 106	(2)-furyl	82 % (Σ 14 %)	**103·HCl**
94	E 107	*p*-*N*,*N*-dimethylanilino	91 % (Σ 19 %)	**104·2HCl** (X-ray)

Scheme 53: Deprotection of amines **86** to **94**: (i) MeOH, conc. HCl, or conc. 48 % HBr, r. t., 16-24 h. (ii) Recrystallisation (MeOH/Et_2O), 1-4 d; overall yields from D-ribose, 8 steps

Furthermore, several hydrochloride salts were treated further with strongly acidic ionic exchange resin (DOWEX 50WX8, H^+ Form), eluting with 2 N NH_3 to produce the respective free amines **105**, **106** and **107** in yields ranging between 88-95 %. For simplicity in numbering, the sequence starts again at the deprotection step of the respective amine acetonides (Scheme 54). Unfortunately, the free amines **106** and **107** were notoriously difficult to get in aqueous solution which, ultimately, scuppered their chances for an appearance at the ensuing biological tests (solubility in MeOH was better, however).

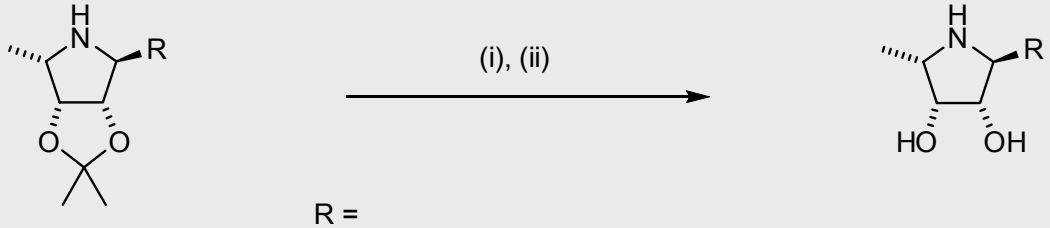

		R =		
86	E 108	*p*-methoxyphenyl	88 % (Σ 21 %)	**105**
89	E 109	*p*-chlorophenyl	95 % (Σ 15 %)	**106**
92	E 110	*p*-phenoxyphenyl	90 % (Σ 20 %)	**107**

Scheme 54: Deprotection, purification by ionic exchange to provide free pyrrolidine diols: (i) MeOH, conc. HCl, 16-24 h. (ii) DOWEX 50WX8, H^+ form, elution with 2 N NH_3; combined yield based on D-ribose, 8 steps

The elemental analysis of the *p*-methoxyphenyl amine **105** for carbon was off by +1.44 %. This prompted a treatment with Boc_2O to afford the analytically pure *N*-butoxycarbonyl carbamate **108** in decent yield (Scheme 55). The ^1H NMR spectrum of the carbamate **108** indicated the appearance of two rotamers in a ca. 2:1 ratio. This is a result of the hindered rotation about the C—N bond of the approximately planar N—C=O framework of the carbamate. The s-*cis* and s-*trans* isomers, with regard to the orientation of the *tert*.-butoxycarbonyl group, are usually similar in energy (barrier to rotation is usually lower than in amides, cf. lit.[354]). The 2:1 ratio is perhaps a reflection of one rotamer's *tert*.-butyl group being in interaction with (or in influence by) the anisotropy of the C_6H_4 moiety (cf. lit.[355]).

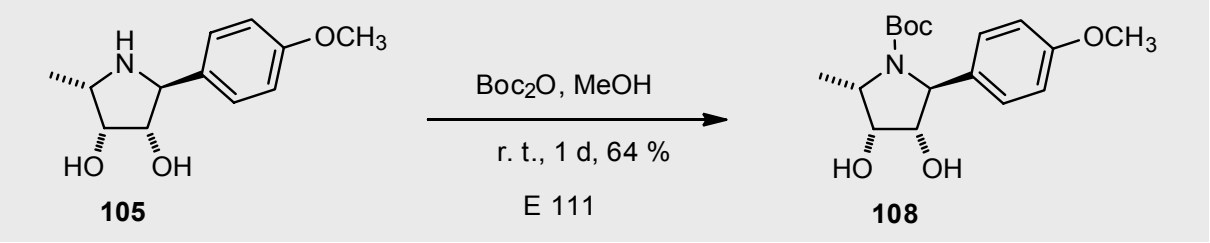

Scheme 55: *N*-Protection of free amine **105** to obtain Boc carbamate **108**

5.1.6 Catalytic hydrogentation followed by deprotection to yield pyrrolidinediol hydrobromides

The absence of a sensitive C—N benzylic position meant that the 5-methyl and 5-methoxybenzyl pyrrolidines **37** and **46** could be subjected to catalytic hydrogenation to yield the intermediary amine hydrobromide salts **109·HBr** and **111·HBr**, respectively. Removal of the acetonide protecting group as described in previous sections led to the isolation of the pyrrolidinediol hydrobromides **110·HBr** and **112·HBr** (Scheme 56).

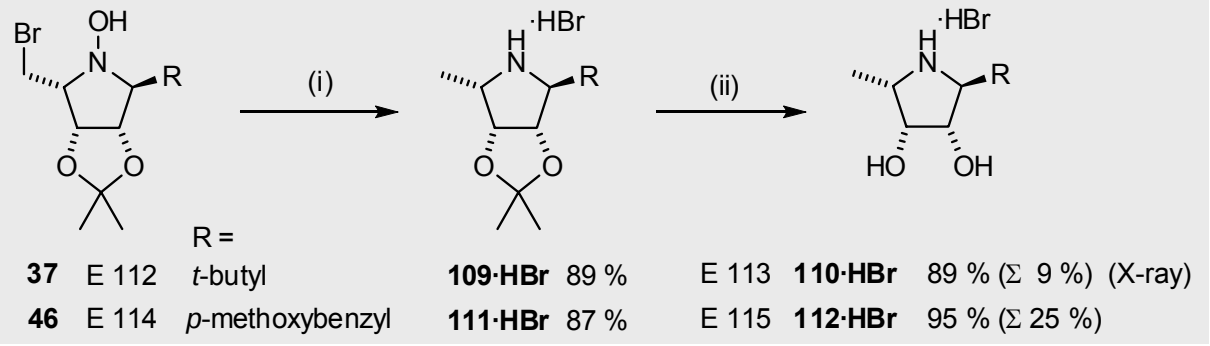

Scheme 56: (i) H_2, Pd/C, MeOH, 3 d, 3 bar; (ii) conc. HBr, MeOH/H_2O, 1 d, recrystallisation (MeOH/Et_2O); combined yield is calculated from D-ribose, 8 steps.

5.1.7 X-Ray crystal structures of selected pyrrolidinediols

5.1.7.1 General remarks

From the nineteen polyhydroxylated pyrrolidines synthesised, the structures of hydrochlorides **96**, **97**, **99**—**102** and **104**, and hydrobromides **102** and **110** could be elucidated by X-ray crystal analysis. However, in order to save space, the asymmetric unit and corresponding stereo images are not shown here. The reader is referred to Section 9 for full structural data. The majority of the crystal structures were found to be in either the space group $P2_1$ (i.e. compounds **97**, **101**, **102·HCl** and **·HBr**) or $P2_12_12_1$ (**96**, **99**, **100** and **104**). According to Glusker's book, these two space groups are, indeed, common systems for chiral, non-racemic, small molecules.[286] The space group $P2_1$ describes a primitive (*P*) monoclinic unit cell where a ≠ b ≠ c, $\alpha = \gamma = 90°$ and $\beta > 90°$; a two-fold screw-axis along the b axis is present. The space group $P2_12_12_1$ denotes a primitive orthorhombic unit cell where a ≠ b ≠ c and all angles, $\alpha = \beta = \gamma$, are equal to 90°; three mutually perpendicular non-intersecting screw axes are in the unit cell.[286-288] The one exception is for the t-butyl substituted pyrrolidine **110·HBr**, which crystallises in the tetragonal space group $P4_12_12_1$. The tetragonal *P*-lattice symmetry is higher than those above, since it contains a 4-fold screw-axis in the c direction. By definition this makes a and b equivalent and consequently a = b ≠ c and $\alpha = \beta = \gamma$ equal 90°. In the diol **109·HBr** the especially long c-axis of 37.1 Å reflects the presence of a 4-fold screw axis where a translation (i.e. c/4) is accompanied by a left-handed rotation through 90°. This is shown in the stereoview below (Diagram 44).

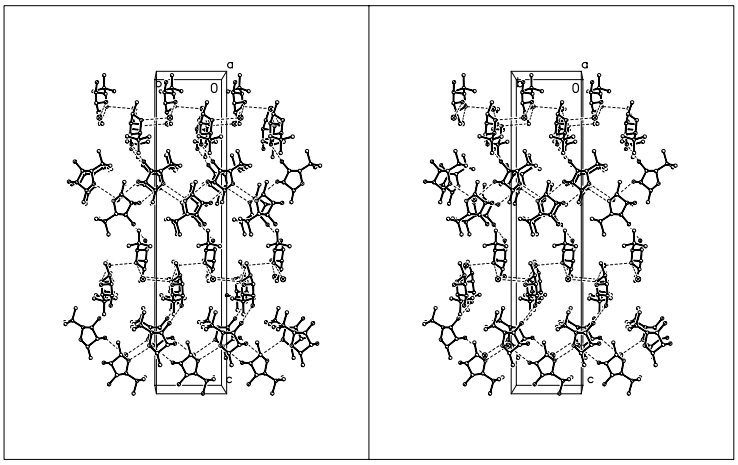

Diagram 44: Stereoview of the 4-fold screw axis along the c direction in pyrrolidine **110·HBr**

5.1.7.2 Discussion of the X-ray crystal structure of the *p*-methyoxyphenyl-substituted pyrrolidinediol 96·HCl

A view of the asymmetric unit of pyrrolidine diol **96·HCl** can be found in Section 9.12. The crystal packing is very similar to that of pyrrolidine hydrochlorides **99·HCl** and **100·HCl**, where co-crystallisation with methanol and a $P2_12_12_1$ space group is found. Taking pyrrolidine **96·HCl** then as an illustrative example, we can see that the crystal packing is defined by the array of hydrogen bonds formed between chlorine with the N^+—H and O—H groups. Chlorine is sandwiched in a "hole" between two independent molecules A and B and constructs an array of hydrogen bonds with O2AH····Cl (2.28 Å) and to the nitrogen's *trans*-H atom, relative to p-methoxyphenyl substitutent at C—2, N1BH····Cl (2.24 Å). The angles deviate from linearity being 165° and 168°, respectively. A further hydrogen bond to a third molecule, C, and to chlorine (O1CH····Cl = 2.38 Å; 170°) completes the "head-to-head" bi-layer arrangement, in which molecule C is aligned between the molecules A and B at 180°. This arrangement keeps hydrophilic and hydrophobic regions well away from each other (Diagram 45). Methanol sits opposite molecule C and is encapsulated in a hydrophobic channel between molecules A and B (cf. stereoview along the a-axis, Section 9.12).

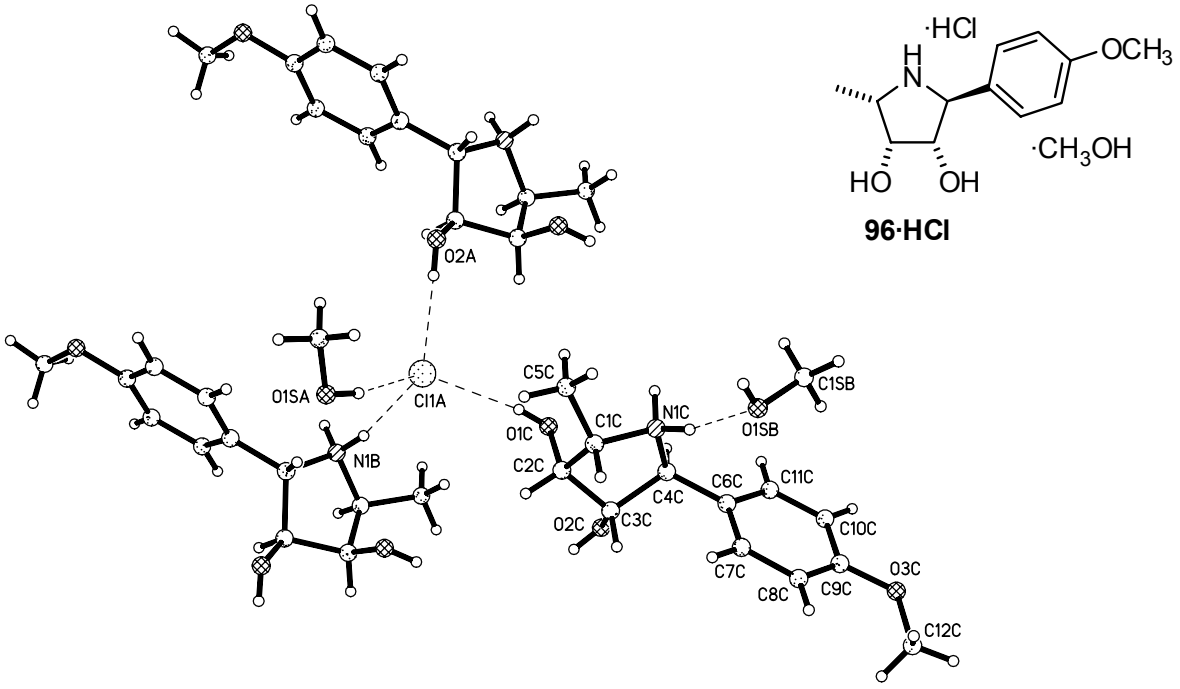

96·HCl

Diagram 45: The "head to head" bi-layer structure of the co-crystal of pyrrolidine diol **96·HCl** with methanol, showing the tetrahedrally coordinated chlorine.

The co-crystallisation of methanol was not forseen. It is therefore of interest to speculate on its role with regard to the packing arrangement. The crystals contain one molecule of methanol per polyhydroxylated pyrrolidine. An interesting observation is that upon standing in air, the crystals tend to disintegrate slowly or sometimes even, as with the thioanisyl derivative **101·HCl**, within a matter of hours. This is probably due to the dissociative loss of solvent of crystallisation, which could be monitored by ^{1}H NMR. For this reason, methanol may be thought as being the "glue" of the crystal: It has a bifunctional role as a hydrogen bond acceptor to chlorine (i.e. O1SAH····Cl = 2.32 Å; 160°) and a donor to the *cis*-H atom on the pyrrolidine's nitrogen, i.e. relative to *p*-methoxyphenyl substituent (N1CH····Cl = 1.82 Å; 163°). This forms the basis for cross-linking between the layers (Diagram 46).

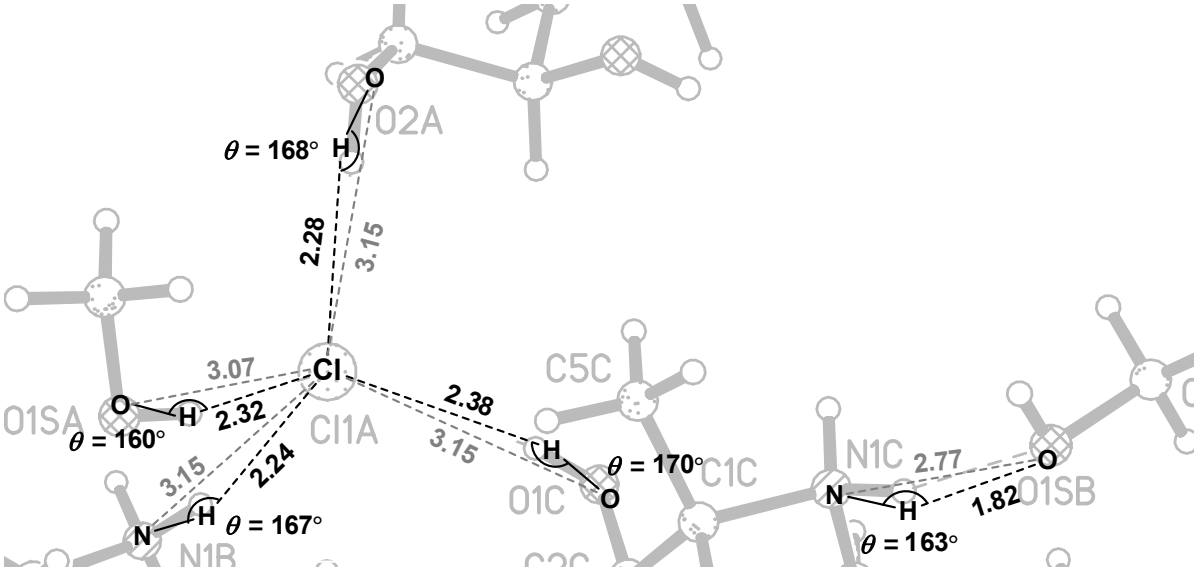

Diagram 46: Detailed view of the donor-acceptor hydrogen bonding region of **96·HCl** with chlorine and solvent of crystallisation, methanol. The hydrogen bond network is represented by the darker dashed lines, interatomic distances by the lighter dashed lines (lengths in Angstroms, 1 Å = 1 x10^{-10} m).

5.1.7.3 Discussion of 2-([1,1'-biphenyl]-4-yl)-substituted pyrrolidinediol 97·HCl

The pyrrolidine diol **97·HCl** features a hydrogen bonding network very similar to that of **96·HCl** but crystallises in the space group $P2_1$. Again, chlorine has a coordination number of 4 (tetrahedral arrangement) and takes up a position as hydrogen bond donor to construct the monolayer with O2AH····Cl (2.46 Å, 169°) and with the pyrrolidine's *trans*-H atom, relative to

the biphenyl group (N1BH····Cl = 2.29 Å; 169°) between molecules A and B. Bonding to methanol (O1SCH····Cl = 1.97 Å; 163°) and to OH on C—4 in molecule D (O1DH····Cl = 2.58 Å, 163°) completes the "head-to-head" bi-layer arrangement (Diagrams 47).

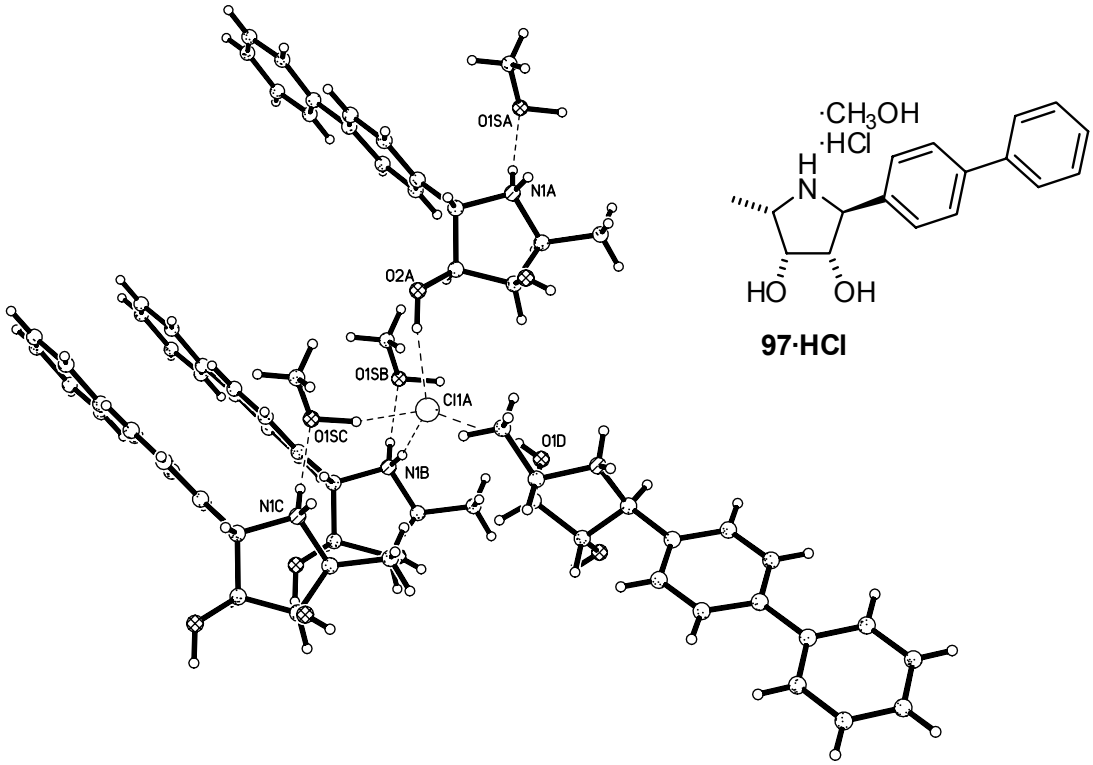

Diagram 47: Hydrogen bonding in the pyrrolidinediol **97·HCl**. Noteworthy is the role of methanol: it is able to interlink the layers through a by acting as a hydrogen bond donor (to chlorine) and as a hydrogen bond acceptor (to N^+—H).

Expanded for clarity in Diagram 48, methanol contacts with the molecules A and B by hydrogen bonding to chlorine (donor) and to N^+—H (acceptor), thereby interlinking the layers to provide structural rigity. A view along the a-axis is depicted in Diagram 49 and shows that the flat biphenyl substituents are stacking along this axis in a "face-to-face" orientation. Further stereoimages are given in Section 9.13. The biphenyl units stack is inclined to ca. 45°. The inclination, according to Glusker, is a result of adjacent aromatic "slabs" being slightly off-set to each other.[288] In doing so, interactions between the the slightly positive charges of the hydrogen atoms of one molecule's π-system are then best aligned for contact with the ring carbon atoms of the neighbours' π-system, and presumably results in van der Waals interactions.

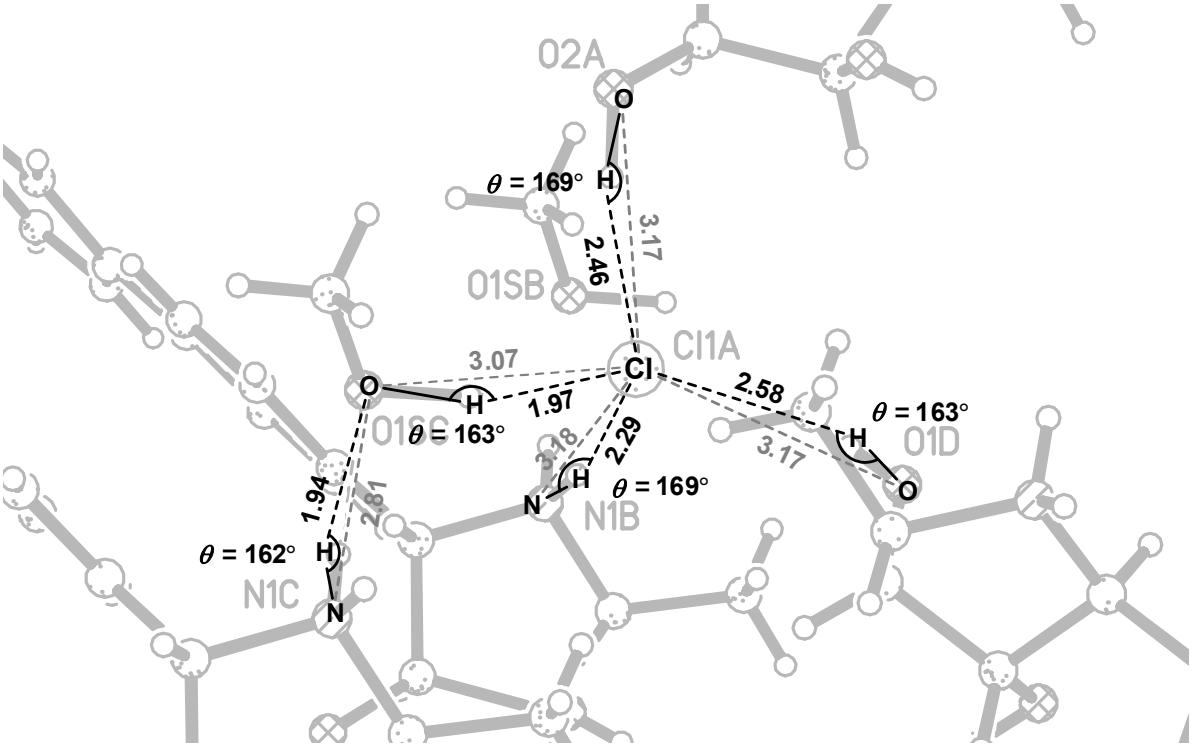

Diagram 48: Scaled-up view of donor/acceptor bonds lenghts and angles in 2-biphenyl-pyrrolidine **97·HCl** and methanol coordinating to chlorine (lengths in Angstroms, Å)

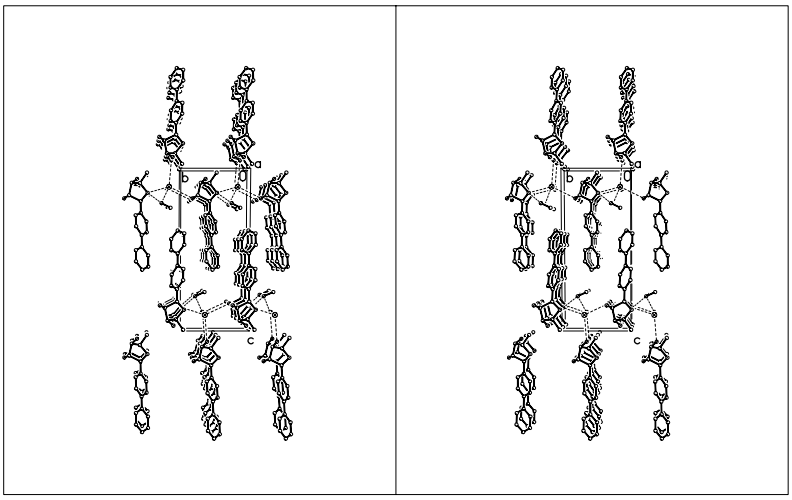

Diagram 49: Stereoplot of the stacking found in pyrrolidine **97·HCl** viewed along the a-axis depicting the biphenyl unit having a face-to-face orientation. Note the degree of inclination of adjacent stacking π-systems

5.1.8 Synthesis of deoxyfuconojirimycin derivatives

The deprotection of the bromomethylpiperidine **52** followed the same sequence as that applied to the bromomethylpyrrolidines (cf. Section 5.1.1). Thus, the key intermediate **52** (Section 3.2.3, p 77) was reduced with $LiAlH_4$ in good yield to the diol **113**. Noteworthy is the concomitant removal of the silyl (TIPS) protecting group; occasionally, this reductive removal of a silyl ether with $LiAlH_4$ can be facilitated when a vicinal alcohol/ether moiety is present.[356] Cleavage of the N—O bond with zinc provided the amine **114** which, following deprotection under acidic conditions, was transformed into the target *C*-linked iminocyclitol hydrochloride **115·HCl** in 12 steps and 4.4 % overall yield starting from D-lyxose (Scheme 57). The question of ring conformation could be remedied by consideration of the ring coupling constants from the ^1H NMR spectrum, displayed graphically below. From the two low energy chair conformations, $^1C_4$ and $^4C_1$, the $^4C_1$ conformation is preferred in solution, dominated by the equatorial preference of the aryl group.

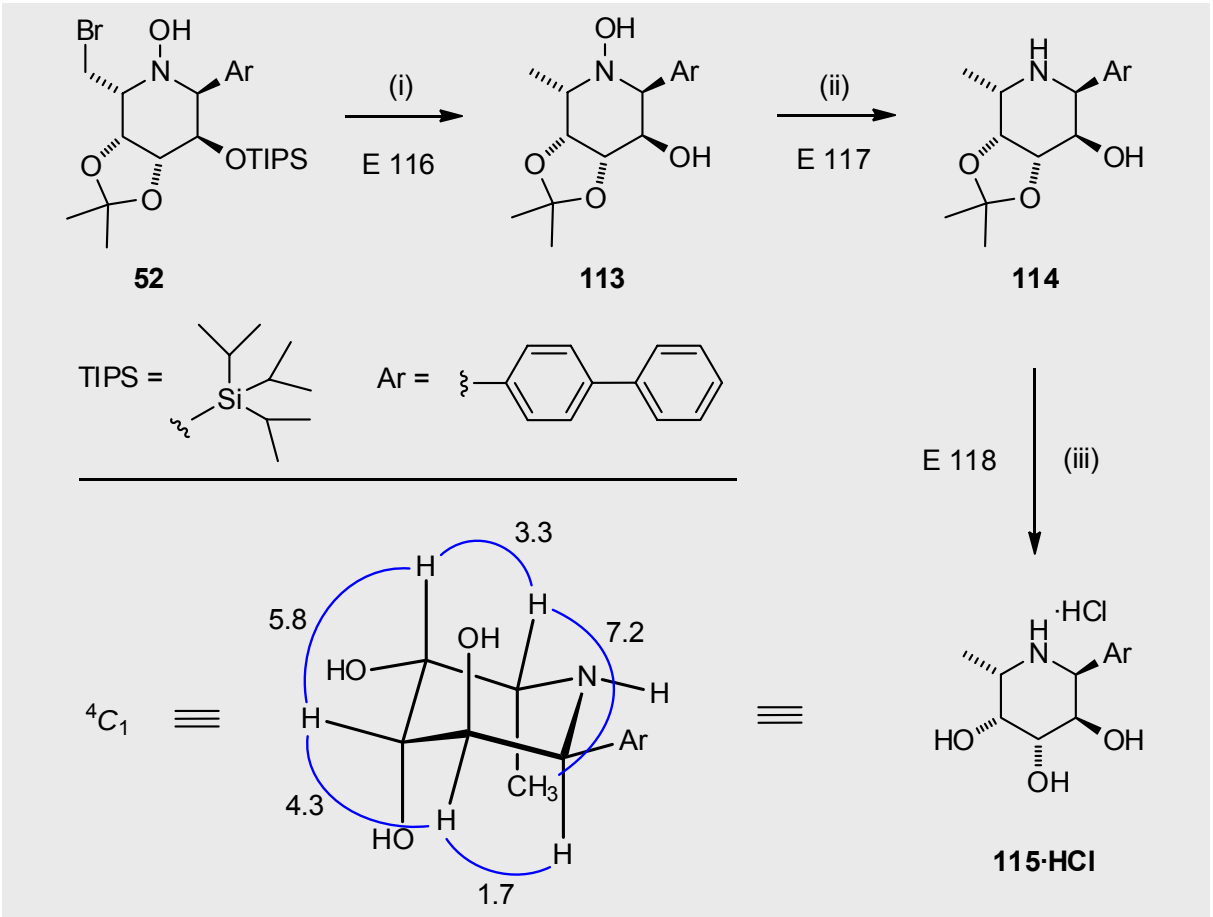

Scheme 57: (i) 2.1 Eq. $LiAlH_4$, THF, 0 °C to r. t., 1 h, 57 %. (ii) Zn (dust), $AcOH/H_2O$, 55 °C, 2 h, 85 %. (iii) conc. HCl, MeOH, 1 d, recrystallisation ($MeOH/Et_2O$), 90 % (12 steps from D-lyxose, Σ 4.4 % !).

Diagram 50: ^{1}H NMR of the “biphenyl”-substituted deoxyfuconojirimycin hydrochloride **115·HCl** (δ [ppm], 300.1 MHz, MeOH-d_4)

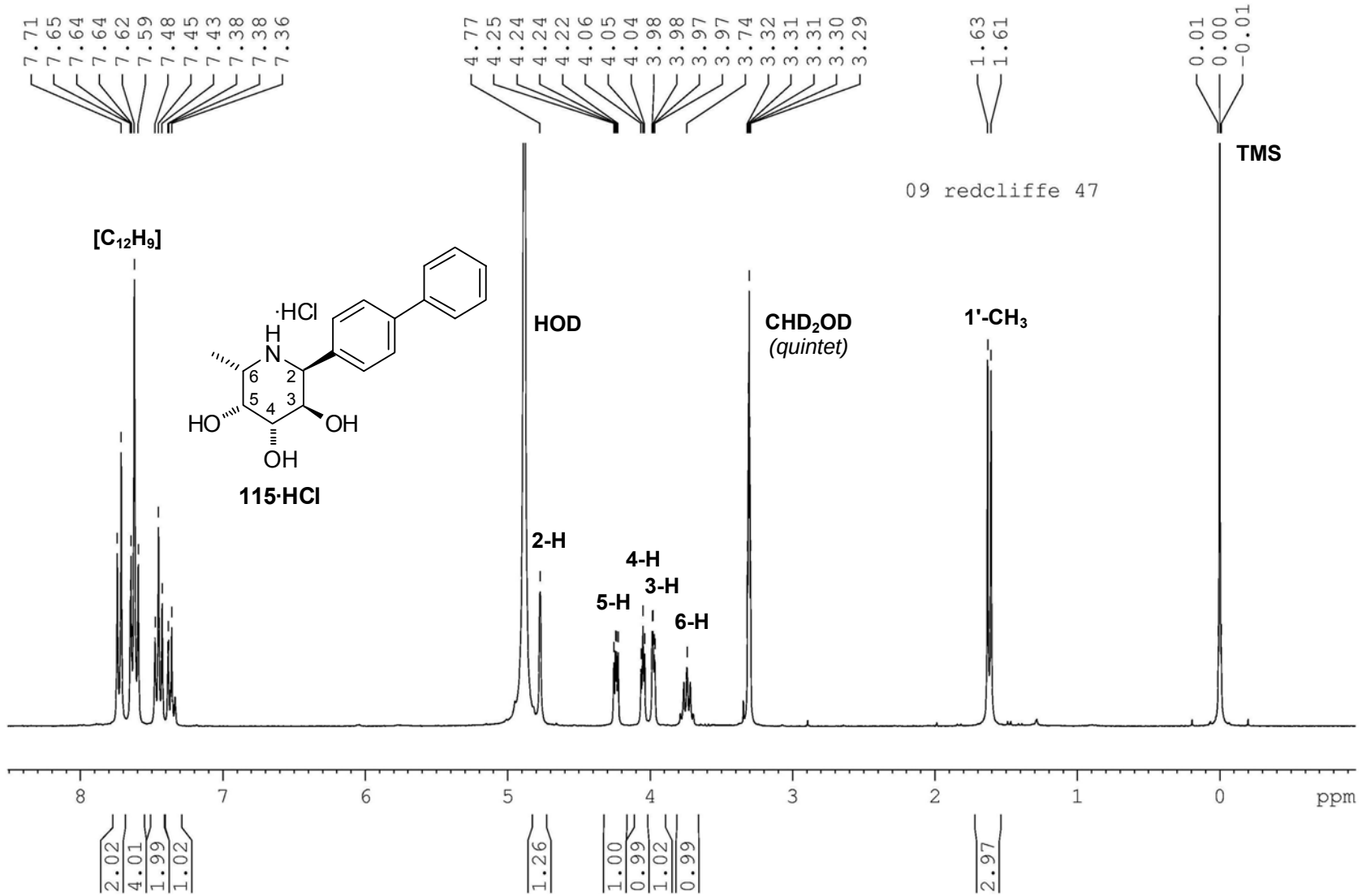

The $^4C_1$ conformation of L-*fuco*-configured C-glycoside **115·HCl** is interesting since the L-fucopyranosyl ring typically adopts the alternative $^1C_4$ conformation, where the C—6 methyl and C—2/C—3 hydroxyl groups are equatorially positioned. These *equatorial* positions obviously change to *axial* ones in **115·HCl** upon ring-flipping. The pertinent ^{1}H NMR coupling constants, $J_{2,3}$ (1.7 Hz), $J_{3,4}$ (5.8 Hz) and $J_{4,5}$ (3.3 Hz), clearly indicate the *gauche*-like orientation, supporting a $^4C_1$ conformation. No large axial-axial coupling constants, typical for DFJ **AI** (cf. Diagram 9 and accompanying literature), were evident. The $^4C_1$ conformation can be easily reconciled if one considers the rotational dynamics of the phenyl-esque substituent *were* it to be axial (i.e. $^1C_4$) and not equatorial. For the former, one of the ortho ring hydrogens would clash unfavourably with the axial hydrogen 6—H of the piperidine ring in much the same way as, for example, the hydrogens at the same ring position of the phenyl group in the axial conformation of 1-phenylcyclohexane or 1-methyl-1-phenylcyclohexane do – as described by Eliel and co-workers.[274,357] However, some L-fucopyranosyl C-glycosides are known to be conformationally labile, in special cases where the "bulky, flat" anomeric substitutent has been separated from the ring by a methylene spacer. This apparently lowers the energy barrier to ring inversion, and gives rise to interesting conformational lability. The reader is encouraged to consult Carpintero and co-workers on this matter.[86] Returning to **115·HCl**, the ^{13}C NMR data indicated that the C—6 methyl group was axial for a $^4C_1$ conformation. Found at 11.9 ppm, the signal for the C—6 methyl in **115·HCl** resonated ca. 5.0 ppm at a higher field than the C—6 methyl in the parent compound, DFJ **AI**, which is known to be equatorial. This is consistent with the shielding value for an axial-methyl substituent, for example, as was found to be the case for methylcyclohexane (cf. Breitmaier et al, lit.[358]).

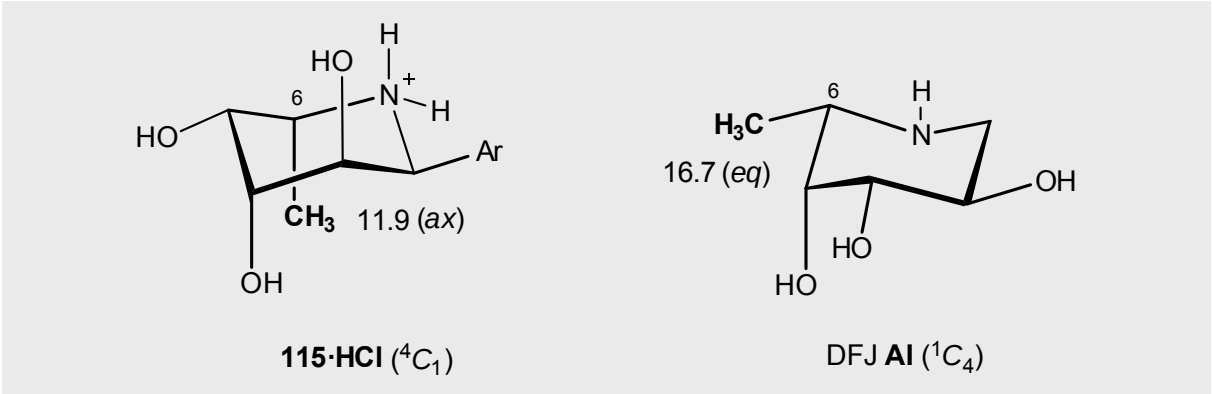

Diagram 51: The ^{13}C NMR chemical shift of the *axial* compared to the *equatorial* C—6 methyl as an indication of ring $^4C_1$ conformation

6 Glycosidase Mechanism and *In Vitro* Tests

6.1 General Remarks

Glycosidases (EC 3.2.1) have been studied extensively due to their importance to biochemistry and therapeutic applications (cf. Section 1). In theory, the non-enzymatic hydrolysis of glycosides is possible, although this would be at a rate which is inherently unsuable for cellular processes. Glycosidases accelerate the cleavage of the bond between the anomeric carbon atom and the glycosidic oxygen atom; two situations arise:

> Should this lead to hydrolysis (i.e. through action of water), then conformationally-liable half-acetals are obtained and the compositions of these products will become entwined in the constants of mutarotational equilibrium.
>
> Certain glycosidases have some transferase activity (e.g. with alcohol) and, in comparison, stereochemically stable products can be obtained which can be examined at leisure (consult review by Sinnott, lit.[6a]).

Wolfenden[359] noted that a k_{cat} of 10 to 1000 s^{-1} is common for most glycosidases. According to Gloster and co-workers,[360] rate enhancement factors of up to 10^{17} are feasible relative to the ratio of k_{cat}/k_{non} – albeit on the basis of the few examples where the measurement of k_{non} (i.e. uncatalysed hydrolysis) was actually possible. This increase in reaction rate would require that the free energy of activation be lowererd by ca. 97 kJ/mol, or ca. 24 kcal/mol. This implies a binding constant for the transition state of the natural substrate falling in to the range of 10^{-22} M. In turn, this makes glycosidases exciting targets for potential inhibitors. In order to "understand" how this may be achievable, exact enzyme-substrate interactions must be known, ideally supported by X-ray analysis. The main contributors to lowering the energy of activation are: a precise orientation of catalytic groups with respect to the bonds to be broken; synergistic effects of one (or more) such groups; formation of reactive intermediates, or as Legler[6c] puts it, favourable changes to the local dielectric constant by the exclusion of solvent water. The later can be important for the lowering of the activation energy, since it will have the effect of making the entropy of activation positive (in the scheme of enthalpy-entropy compensation), and hence the free energy of activation negative

.

6.2 Mechanism of Glycosidase Hydrolysis

The general features of the catalytic mechanism of hydrolysis were set out by Koshland in 1953.[361,362] Still an insightful read, the late Koshland noted that the products generated from glycosidases had either retained or inverted stereochemistry at the anomeric centre in relation to that of the substrate glycoside.[363]

For hydrolysis under inversion of configuration, Koshland suggested a concomitant acid/base catalyst that gives protonic assistance (depicted as **FT**) to the departing aglycon group (and subsequent Brønsted base assistance to nucleophilic attack by water). Very commonly, this cascade of events is refered to in the literature as "*Koshland's single displacement mechanism*", leading to the inverted hydrolysis product **FU** (Scheme 58).

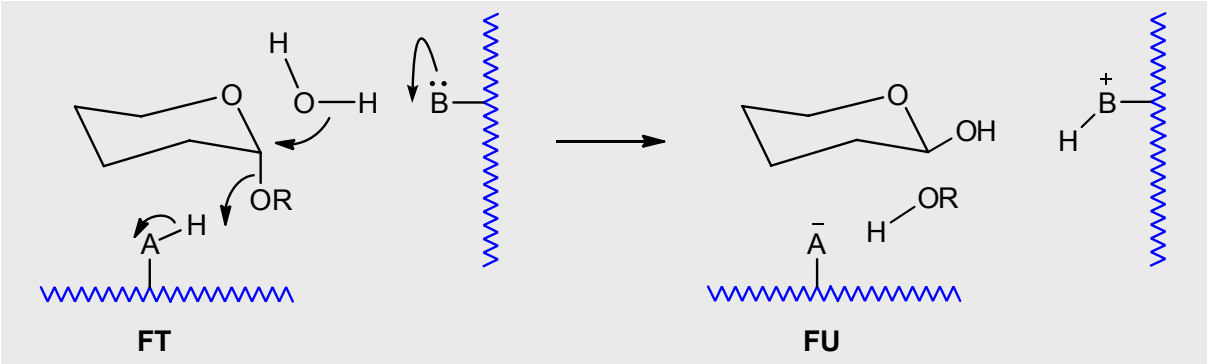

Scheme 58: Glycosidase action leading to inversion of anomeric configuration

For glycosidases that act with retension of configuration, Koshland[361] postulated a "double-displacement mechanism" with a covalent enzyme carboxylate intermediate (Scheme 59). Paraphrasing Vocadlo and Davies,[364] "…*this involves a general acid/base catalyst that in the first step would facilitate departure of the leaving group* (**FV** to **FW**) *while a second residue would stabilize an enzyme sequestered intermediate, either an ion pair* (**FX**) *or by forming a formal covalent glycosyl enzyme intermediate* (**FY** to **FZ**). *The second step (deglycosylation) would be the near microscopic reverse of the first step with the general acid/base catalyst facilitating attack of a molecule of water on the anomeric center to break down this intermediate* (**FZ** to **GB**)*, forming the hemicacetal (lactol) product* (**GC**) *with retained stereochemistry at the anomeric center…"*

The enzymatic deglycosylation that leads to hydrolysis with retention is obviously the more complex of the two possible mechanisms. Such is the complexity, current research in this

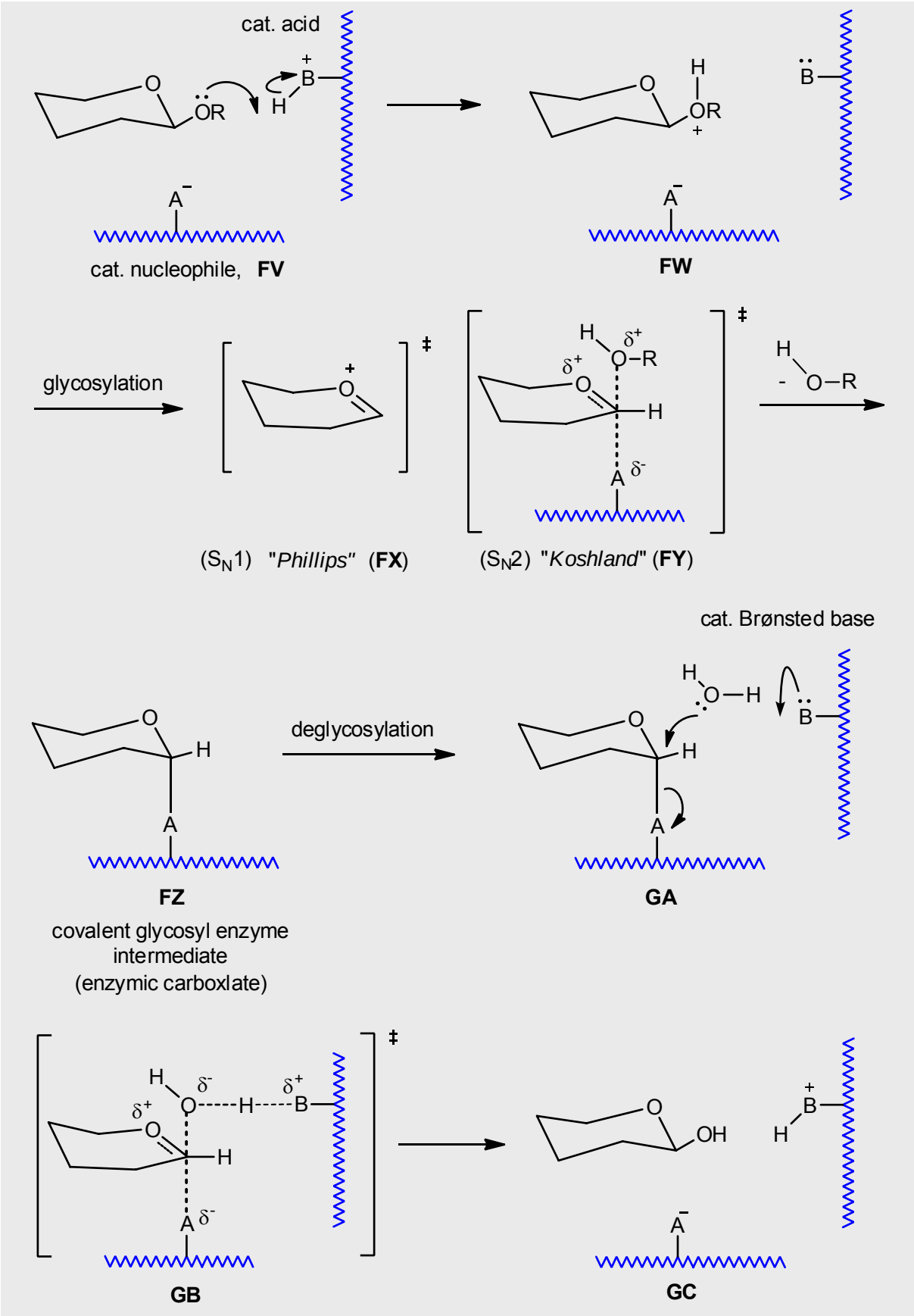

Scheme 59: Mechanism of glycosidase leading to hydrolysis under retention of the anomeric configuration with equatorial leaving groups (i.e. an *e*→*e* hydrolysis; Sinnott, lit.[6a])

field remains very active in discerning the finer points of catalytic process. Further points to the inverting [only point (a)] and retaining mechanism [(a) to (e)] can be made as follows:

(a) The mechanism of glycosidase action is linked to the geometry of the catalytic carboxylic acid groups. That is to say, the structure of the "protonation machinery" indicates if hydrolysis occurs *via* the retaining or inverting mechanism. The barometer taken for this is the distance between the carboxylic acid residues. A fairly consistant distance of 9.0–9.5 Å is found for inverting glycosidases.[365] For retaining glycosidases, the distance between the carboxylic acid groups may vary considerably, though on average the groups are closer in space, around 5 Å apart.[365]

(b) The catalytic acid/base and enzymic nucleophile have been identified as the side chain carboxylic acid groups of aspartate or glutamate residues. They are essential for catalytic activity. This has been verified through specific point-group mutations (substituting aspartate or glutamate residues for alanine, asparagin, or glutamine, etc.). The "mutated" glycosidase will shown associated changes in the enzyme kinetics, for example, in the affinity of the enzyme-substrate, the K_m value, or to k_{cat}/K_m, as a result of the reduced rate of hydrolysis, and the accumulation of glycosyl-enzyme intermediates.

(c) The exact nature of bond-breaking and bond-making at the anomeric centre in the formation of the Michaelis complex is of great debate. This surrounds the degree of S_N1 *versus* S_N2 character at the transition state – although both "extreme" cases are considered to be highly unlikely. The "Phillips mechanism" for β-glucosidase, based on the catalysis of hen egg-white lysosyme (HEWL),[366,367] describes a step-wise S_N1 mechanism where water leaves through a proton-assisted ionization from the catalytic acid to yield the glycosyl oxocarbenium ion (**FW** to **FX**, Scheme 59), which is then attacked by a "waiting" nucleophilic residue. The resulting ion-pair intermediate is a source of contention. Sinnott[6a] remarked that they are at most transitory species and "*in nothing else than aqueous solution so unstable as to be on the borderline of real existence, with lifetimes around* 10^{-10} *s*." The alternative and more plausible mechanism concerns the loss of water to form the covalent intermediate *via* a S_N2 mechanism. Sinnott and Souchard[368] reported grounds for a "S_N2-like" mechanism on the basis of α-detuerium kinetic isotope effects. They found that the breakdown of the intermediate is rate determining, meaning that k_H/k_D was greater than unity (i.e. >1). If this is the case, as measured on the second step, it suggests that the anomeric centre undergoes rehybridisation from sp^3 in the intermediate to sp^2 in the transition state. This is only

consistent with the collapse of a covalent tetrahedral intermediate through an oxocarbenium ion-like transition state. Schematically, this could be either **FZ↔FY** or **GA↔GB** (Scheme 59). The long-lived ion pair of Phillips,[366] i. e. step-wise S_N1-like, cannot be reconciled with these observations.

(d) "Activated" 2-deoxy-2-fluoroglycosides are often the key for the ability to observe covalent intermediates.[6a] An electronegative fluorine substituent at the 2-position will inductively destablise the hydrolysis, whose covalent intermediate then becomes trapped on-enzyme causing it to accumulate. An important covalent intermediate was "captured" by this method in the determination of the catalytic mechanism of HEWL (see above).[369] These trapped species are often conformationally distorted.

(e) Many advances have been made in identifying the conformation/distortions of the Michaelis complexes (i. e. the formation of the Michaelis complex in classical enzyme kinetics: E + S ↔ ES) and those of the glycosyl-enzyme intermediates.[364] By knowing the conformation/distortion of these intermediates (species which flank either side of the transition state along the reaction coordinate), a guess can be made at the conformation of the ensuing oxocarbenium ion-like transition state. During hydrolysis the pyranose ring will become distorted because of the significant charge development on the anomeric center as the transition state is approached. This means that these structures will have a geometry where the C—5, O—5, C—1 and C—2 atoms approach coplanarity. This places a restriction on the number of conformations that the pyranose ring can adopt. The stabilisation of the developing positive charge at the anomeric centre by the p-like lone pair of the endocyclic oxygen assists the oxocarbenium ion-like transition state in adopting certain conformations (Diagram 52a). Sinnott[6a] was first to emphasize the stereochemical implications i. e. the distortion of the glycoside at the transition state will result in either a half-chair ($^4H_3$ and $^3H_4$ or equivalent ^4E and ^3E envelopes) or boat ($^{2,5}B$ or $B_{2,5}$) conformation (Diagram 52b). From crystallographic data, many distorted complexes and covalent intermediates have been identified: For example, in β-D-glucosidase hydrolase (GH 26), a $^1S_3$ Michaelis complex and $^4C_1$ glycosyl-enzyme intermediate was observed. Consequently, a $^4H_3$ transition state conformation was postulated.[370] The grounds for this postulation can be understood by considering the itinerary for pyranoside ring inter-conversion. This states that a pyranoside ring undergoing a $^1S_3$ to $^4C_1$ transformation must go through an intermediary $^4H_3$ conformation. It is precisely this "flattened" conformation that resembles the transition state conformation referred to by Sinnott (Diagram 51c).[371] The anomeric carbon has the largest vector during this transformation. Davies and other authors

advocate the term “electrophilic migration” to describe this movement, “above to below plane”, by which the gap from the Michaelis complex to the covalent intermediate is bridged (Diagram 51d). Interestingly, within the same GH family, several conformational itineraries are known: For β-D-mannosidase (GH 26), “snapshots” of the Michaelis complex and glycosyl-enzyme intermediate revealed $^{O}S_2$ and $^{1}S_5$ skew boat conformations, suggesting therefore a $B_{2,5}$ transition state. The different transition state conformation in β-D-mannosidase to β-glucosidase is not entirely due, as one would might think, to the *gluco* versus *manno* configuration at C—2.[372] Other “snapshots” have led to the determination of a $^{2,5}B$ transition state in, for example, GH 11 xylanases.[373] For the GH 29, *T. maritima* α-L-fucosidase, snapshots of the complexes led to the postulation of a $^{3}H_4$ transition state. The reaction pathway is therefore $^{1}C_4 \leftrightarrow {}^{3}H_4 \leftrightarrow {}^{3}S_1$.[374,375] Although any distortion of the ring will result in an energetic penalty, there are geometrically sound reasons in doing so. Mainly, in the distorted complexes, the leaving group can be placed in an axial orientation to facilitate an in-line attack to the σ* anti-bonding orbital at the anomeric carbon (Deslongchamps anti-periplanar lone-pair hypothesis, see lit.[376]). Distortion may minmise steric hindrance to nucleophilic attack and also alleviate *cis*-1,2 and 1,3-diaxial clashes.

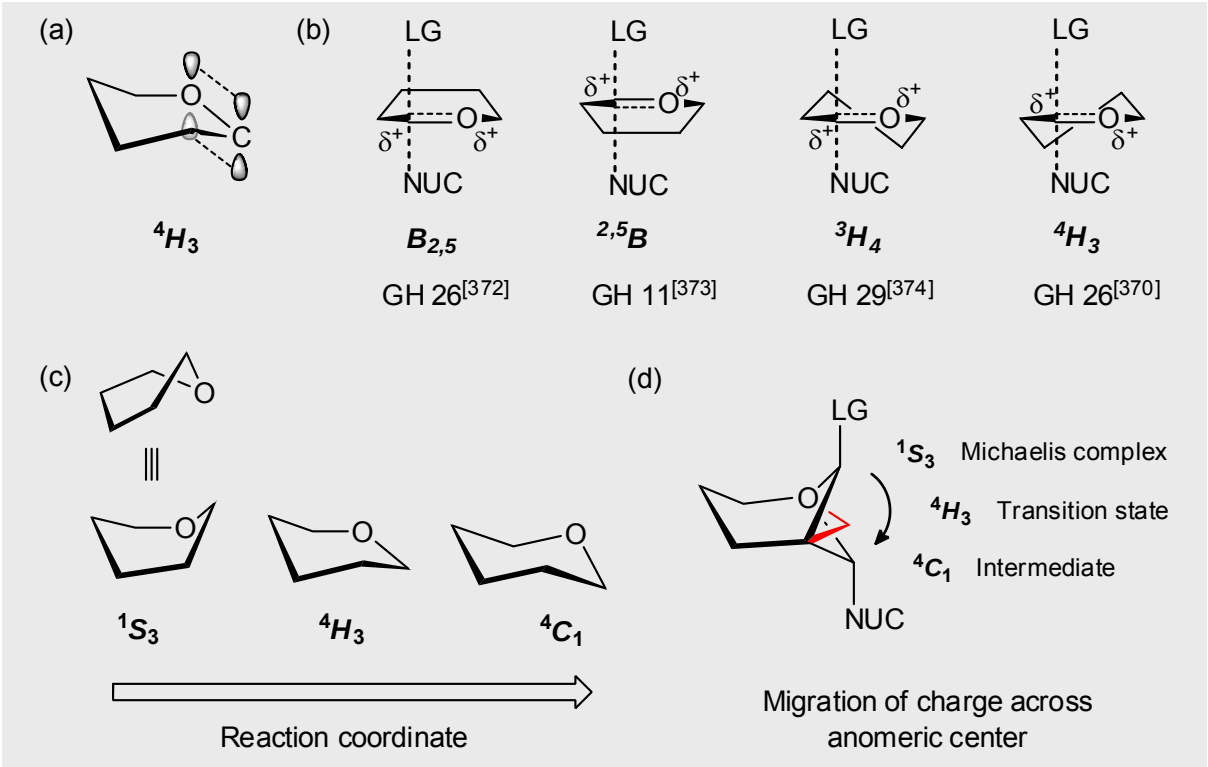

Diagram 52: The reaction coordinates of different glycosidase hydroylases follow different conformational itineraries that proceed through specific transition states.[6a,364,375]

6.3 Enzymatic Inhibition from Iminopolyols

Bartlett[377] has pointed out that "*it is usually on a conceptual basis that an inhibitor is classified as a transition state analogue, for example as a reflection of the design process or rationalisation of its high affinity rather than through a verification of its actual mode of binding*". In other words, a good transition-state analogue can be a strong inhibitor, but a strong inhibitor does not necessarily have to be a transition-state analogue. In fact, it is worth mentioning that a strong inhibitor may not even bind to the active site.[6e] For iminopolyols, the main criteria for potent enzyme inhibition is, to quote Wong,[378] "*[the ability] as protonated iminocyclitols to mimic the oxonium ion transition state of sugar transfer reactions.*" While this is superficially a persuasive and intuitive proposal there is usually little or no evidence to suggest that this is the *defining* reason for an inhibitor's potency. This explains only part of a situation which is in reality much more complex. According to Wolfenden,[379] "true" transition state mimics should bind with a large negative enthalpy, ΔH_a, as is true of the real transition state. However, there are often cases where the enthalpy term is, for example, off-set by an unusually large entropy contribution, $T\Delta S_a$.[360,380] This scenario is termed as enthalpy-entropy compensation, a phenomenon that likely arises from the desolvation of the iminopolyol inhibitor on binding to the enzyme. Inhibitor binding, rather like protein folding, results in a small favourable energy derived from the sum of exceedingly large and conflicting terms and reflects a rather complex footprint of thermodynamical signatures, which are often unaccounted for in studies (cf. *Own Results*, Section 6.5).

Nonetheless, at a superficial level, it is still possible for us to demystify the efficacy of iminopolyols by dissecting the structural and thermodynamical aspects of their binding. The design of iminopolyols inhibitors can be put roughly into two categories to emphasise either the *charge* or *geometry/shape* of the structural motif. *Charge* can be taken to mean: The basic atom or group of the iminopolyol, protonated at physiological pH, through which the conjugate acid mirrors the development of charge at the endocyclic oxygen or the anomeric carbon in order to engage in electrostatic interactions with the catalytic residues. Whilst *geometry* can be thought as referring to: Either inhibitors that reside in the native low engery *chair* conformation (such as the $^4C_1$ of deoxynojirimycin, DNJ **L**), or contain sp^2 hybridization (such as *gluco*-hydroximolactam **GD**) at the anomeric region and, theoretically, are better adapted at mimicking the *half-chair*, for example the $^4H_3$ of β-glucosidases,[370] at the transition state. Polyhydroxylated pyrrolidines also fall into this category; the native *E* (envelope) conformation, for example, of the protonated pyrrolidine **GE** is purported to be a good mimic of a "flattened" or *half chair* conformation (Diagram 53).[381,382]

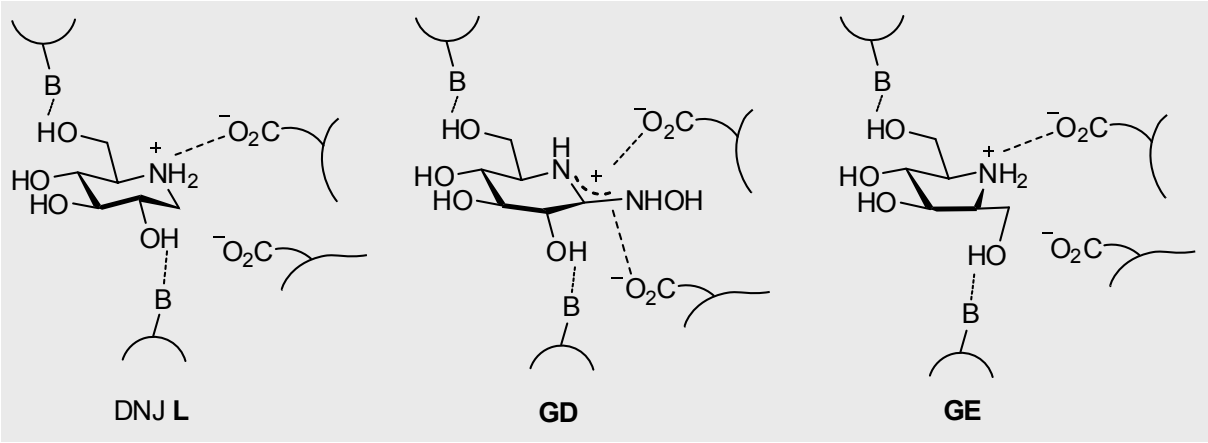

Diagram 53: Binding and imitation of the chair (DNJ **L**) or *half-chair* transition states (**GD** and **GE**) of the enzymatic glycoside cleavage

The enzymatic stereochemical discrimination for *half-chair*-like is not as pronounced as for a *chair*-like inhibitor, evidenced by their respective inhibition profiles: The glucosidase inhibitor DNJ **L** does not inhibit β-galactosidase or α-mannosidase, and its *manno*-configured analogue, DMJ **E** (cf. Diagram 5), is a poor inhibitor of glucosidase.[383] The *gluco*-configured pyrrolidine **GE**, on the other hand, is known to exhibit broad spectrum inhibition against both α- and β-glucosidases and others.[384] The inhibition selectivity of the deoxynorjirimycins is due to the tight fit of the chair in the "hydrophilic portion" of the enzyme pocket. A axial ↔ equatorial epimerisation of one ring hydroxyl can lead to inactivity, since this may erase specific hydrogen bonding networks at a substantial cost to enthalpy. For example, the substrate 2-OH contributes at least 4.5 kcal/mol to the transition state stabilisation by GH 1 family β-glucosidases.[385] Furthermore, an epimerisation may lead to a perturbation of the subtle "dispersion forces" (CH→π interactions), as *ab initio* calculations have shown,[386] between the "hydrophobic faces" above and below the pyranosyl ring. For polyhydroxylated pyrrolidines, glycosidases are less sensitive to changes in the hydroxyl group topography. This has been ascribed to the overriding significance of the electrostratic interaction and the "loose-fit" of the flattened shape of the inhibitor.[382]

Apart from ring conformation and hydroxyl group topography, other parameters are available to study the inhibition of glycosidases by iminopolyols. It is often interesting to establish whether a particular inhibitor class is functioning as a transition state inhibitor or not. For this purpose, aside from superficial yard stick of inhibiton potency, other criteria can be measured. For example, one option is to measure linear free energy relationships, where the ln K_i values of an inhibitor toward a series of enzymes or enzyme mutants are compared with the ln(k_{cat}/K_M) values of a substrate toward those enzymes. Alternatively the same

comparison is done with one enzyme but with a series of similar structural analogues of an inhibitor and the substrates. In both cases, a linear relationship should be obtained if the inhibitor or inhibitor-type is a transition state analogue of the enzymatic reaction of that substrate provided that $k_{cat}/K_M \approx k_{cat}/K_S$, which is a good assumption. It should be noted that a linear relationship will only reveal similarity between the transition state and the inhibitor with regard to what has been varied.[6e]

In addition, it is known that the binding of the iminopolyol is influenced by factors (pH, temperature, etc.) in the same way that k_{cat}/K_m is influenced by these factors. That is to say, when we measure the pH dependence on $1/K_i$ and the influence of pH on k_{cat}/K_m both should give characteristic "bell shaped" curves. If the two curves cover each other up, then the affinity of an iminopolyol inhibitor for a particular glycosidase does not change with changing pH in a way that completely resembles the influence of pH on k_{cat}/K_m for normal substrates. This is another Wolfenden[387] criteria – aside to a negative large enthalpy – for defining an inhibitor as an ideal transition state analogue. For three classes of iminopolyol inhibitors, a stylised picture of pH against $1/K_i$ and pH against k_{cat}/K_m is presented in Diagram 54 (actual data in lit.[360]). The enzyme in question is *Thermotoga maritima* β-glucosidase (GH 1) with a pH optimum for catalysis at 6.1 (i.e. the constant grey curve); the acid and basic limbs for catalysis have pK_a values of approx. 5.3 and 7.0, respectively.

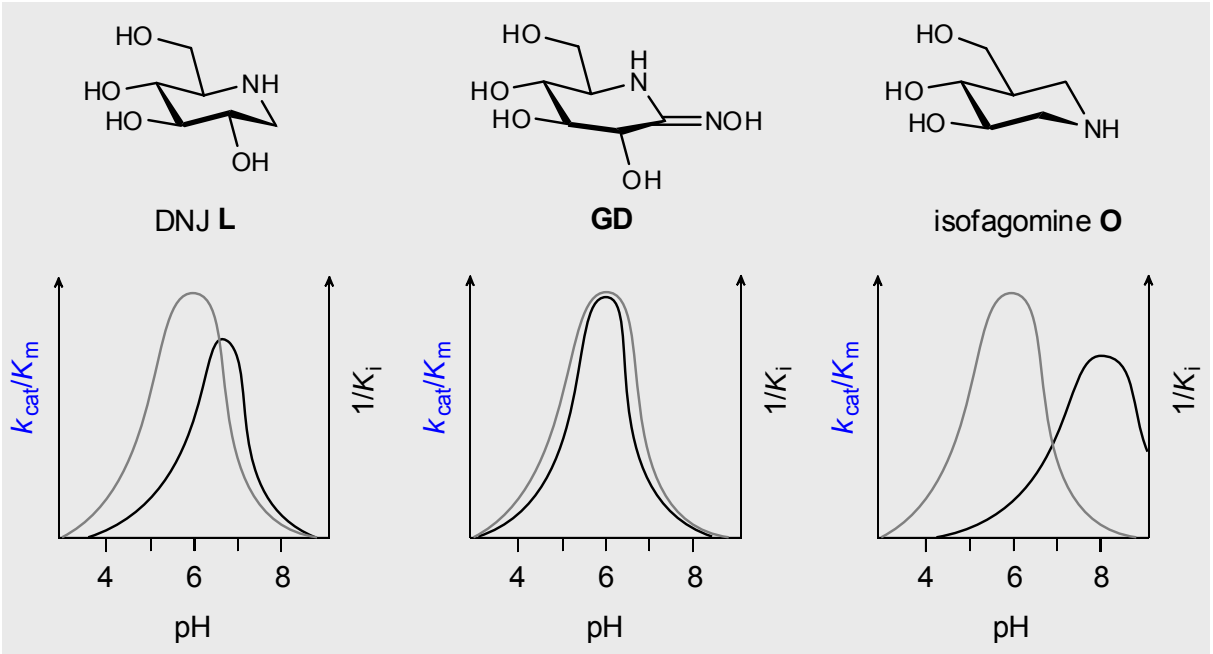

Diagram 54: Relative pH profiles for inhibition of three different classes of iminopolyols (black curves); maximum K_i (pH) for inhibition: DNJ **L** = 3.8 μM (6.85), hydroximo lactam **GD** = 0.28 μM (6.0), isofagomine **O** = 0.0034 μM (7.8)

The pH profile for 1-deoxynojirimycin (DNJ **L**) indicates that the the acid leg is shifted to the alkaline region, whereas the alkaline leg drops off with that of k_{cat}/K_m. The maximum K_i value of 3.8 μM was found at pH 6.85 – away from the optimum pH of 6.1 for catalysis (i.e. where the curves intersect). Since the pK_a of the nitrogen group for DNJ **L** is 7.3, and optimum inhibition is at a pH of 6.85, there is obviously some ambiguity as to whether the inhibitor binds in a (completely) protonated form. Nethertheless, the shift of the acid leg to the right (alkaline region) simply reflects that a protonated inhibitor cannot bind tightly due to protonation of the acid/base. Consequently, this indicates that the ionisation of the piperidine nitrogen group interacts best with the ionized enzyme (Diagrams 55). The pH profile of hydroximo lactam **GD** correlates perfectly with k_{cat}/K_m. A simplistic view is that lactam **GD**, on account of its sp^2 hybridization and charge, is able to better track the $^4H_3/^4E$ conformation of the substrate along the catalysis coordinate for this Family GH 1 enzyme. For isofagomine **O**, the optimum K_i = 3.4 nM (pH 7.6) – where the enzyme becomes ionized and also at a point, as can be seen from the k_{cat}/K_m curve, where its activity is greatly reduced. The shift of the acid leg to the alkaline region can be explained in similar terms to the case of DNJ **L**, above. The large alkaline shift was interpreted as a special "clamping mode" where very strong interaction with the nucleopile and acid/base catalytic residues results, i.e. due to favourable geometry. A similar "clamping mode" was observed in *sweet almond* β-glucosidase: in both cases, the catalytic carboxylate is located directly below the ring therefore interacting strongly with the protonated isofagomine **O**, whereas no favourable interaction can be made directly with the protonated 1-deoxynojirimycin, DNJ **L**.[6d]

The difference in the thermodynamic data of the binding of DNJ **L** and isofagomine **O** was negligible for the (negative) enthalpy parameter (i.e. $T\Delta\Delta H_a$) though differed substiantially in entropy ($T\Delta\Delta S_a$) by -4.0 kcal mol^{-1} (compare Bols' data, lit.[388]).[380] This is reminiscent of the unfavourable contributions of ordered water molecules at the molecular interface. Each water molecule has been estimated to contribute -0.5 to 3.0 kcal mol^{-1} to ΔH,[389,390] but also with a corresponding negative effect on $T\Delta S$.[390,391] For the binding of DNJ **L** this would mean an additional 1-3 ordered water molecules in line with these thermodynamic differences. Indeed, a single ordered water molecule (shown as the grey sphere in Diagram 55) was observed to hydrogen bond to the nitrogen of DNJ **L** in the active site; no ordered water molecules were found in the active site of isofagomine **O** binding to the enzyme (X-ray, lit.[380]). In a related structural report, for the inhibiton of *Streptomyces lividans* xylanse Xyn10A by xylobiose-derived DNJ **L** and isofagomine **O**, *two* water molecules have occupied the active site for the DNJ-glyco-conjugate, while none were present in the isofagomine-enzyme complex. Similar entropy trends and K_i differences were observed.[392]

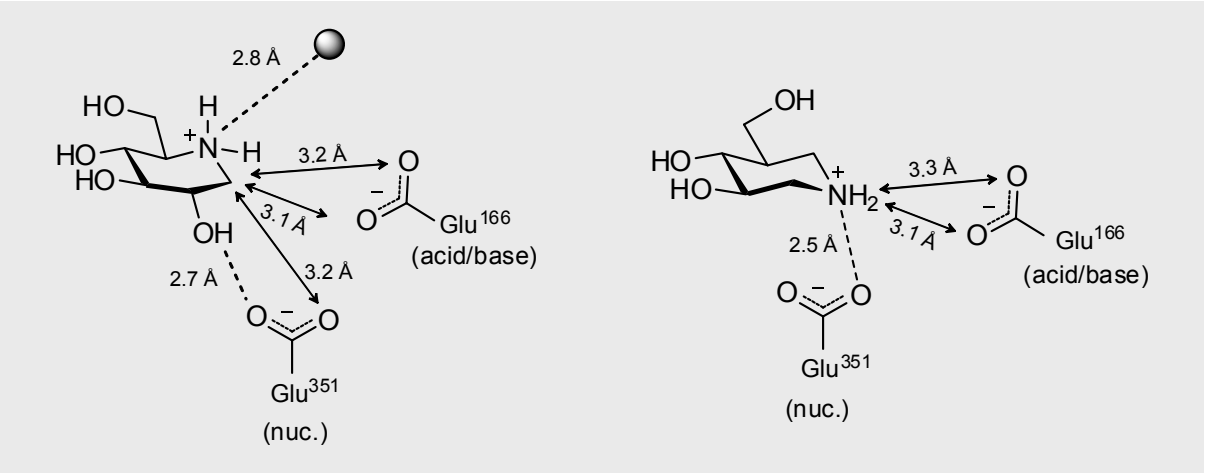

Diagram 55: An aspect of DNJ **L** (*left*) and isofagomine **O** (*right*) binding to *T. maritima.* β-glucosidase, based upon pH profiles (see above) and atomic resolution data (see lit.[380]). The stronger inhibition of isofagomine **O** is put down to the release of water (entropic gains) and the stronger electrostatic interactions in the "double-clamp" mode of binding.

The question if DNJ **L**, lactam **GD** and isofagomine **O** are good transition state mimics or fortuitous binders is difficult to answer. Although DNJ **L** and isofagomine **O** bind with a large negative enthalpy, there is no correlation between pH and K_i and k_{cat}/K_m. This is presumerably because the structures of DNJ **L** and isofagomine **O** are absent of constraints that force the ring to the adopt the $^4H_3$ conformation of the transition state, as is quite the opposite for the hydroximo lactam **GD**. This non-correlation occurs typically when the inhibitor changes charge and thus shape under the observed pH range, and though this may be regarded as an imperfection, the inhibitors DNJ **L** and isofagomine **O** could still be transition-state analogues at one pH and not another.[6e] Even so, isofagomine **O** inhibits most effectively when the enzyme is largely inactive, suggesting it cannot be a true transition state mimic as, by definition, a catalytically inactive enzyme cannot bind the transition state.

The favourable $T\Delta S$ term for the binding of isofagomine **O** is intruiging since it demonstrates the importance of ligand solvation/desolvation events, primarily in relation to structured water networks. Such "enthalpy-entropy compenstations" have been exploited to arrive at extremely potent glycosidase inhibitors: A case-in-point concerns the glucoimidazole **GF** and the phenylethyl-substituted derivative **GG** for the inhibition of *T. maritima* β-glucosidase (Diagram 56).[360,393] Both imidazoles **GF** and **GG** were found to bind with large negative enthalpy and contain structural motifs that force the piperidine ring to adopt the postulated $^4H_3$ transition state. However, the phenylethyl-derivative **GG** is a 25-fold stronger inhibitor of this GH 1 β-glucosidase. The aryl appendage improved the potency by presumerably

harnessing binding interactions in the aglycon (-1) subsite; interestingly, the aryl group, according to structural data from Gloster and co-workers,[393] did not appear to bind in an ordered manner.

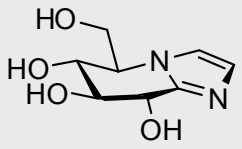

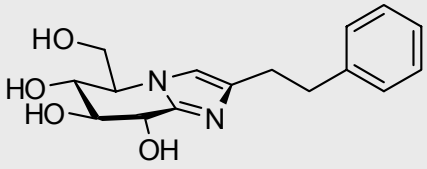

	GF	**GG**
K_i (pH 5.8)	138 nM	7.5 nM
K_i (inhib. opt.)	74 nM (pH 6.6)	2.8 nM (pH 6.8)
ΔH^o_a	-8.96	-4.64
$T\Delta S^o_a$	+0.94	+6.29
ΔG^o_a	-9.90	-10.93

T = 298 K; kcal/mol

Diagram 56: A “cherry picked” example of a enthalpy-entropy compensation. Both inhibitors bind with a negative enthalpy. Nonetheless, the thermodynamic signature is dominated by large positive entropy term, elicited by inclusion of the liphophilic phenylethyl side chain.[360]

The increased potency appeared to stem from the more favourable entropy, i.e. the dominant $T\Delta S$ term, measured by isothermal titration calorimetry, a phenomenon that likely arises from desolvation of the inhibitor on binding as a result of the loss of bound water molecules: These contribute favourably to the disorder of the system, and consequently to entropy, but unfavourably to enthalpy because hydrogen bond interactions are lost, as indeed the data seems to suggest (Diagram 56). However, as stressed at the start of this section, the binding of an inhibitor reflects a rather complex thermodynamical footprint. It should be emphasized, as a comprehensive investigation of 18 potent inhibitors with β-glucosidases has shown,[360] that the thermodynamic parameters of binding of these inhibitors may vary in a somewhat unpredictable manner. This means that there is, generally, no apparent correlation between inhibitor potency, chemistry and the degree of enthalpy-entropy compensation. A way of enhancing inhibitor binding could be to augment the number of enzyme inhibitor interactions. One concept that aimed to do this was considered by Jäger and Palmer,[3,4] who prepared a series of D-*ribo*-configrued *N*-oxide-*N*-butyl pyrrolidine diols, including the candidate **GH** (Diagram 57). The question of ring protonation would in this case, obviously, not be an issue for these quaternary ammonium species. Unfortunately, this class of iminopolyols were

devoid of any useful glycosidase inhibition. This result did not stand in isolation, however, as the weak inhibition from the next biggest homologues, piperidine *N*-oxides, was already known. For example, the *N*-oxide-*N*-methyl *gluco*-deoxynojirimycin derivative **GI** inhibited *almond* β-glucosidase 30-fold weaker than the parent DNJ **L**.[383]

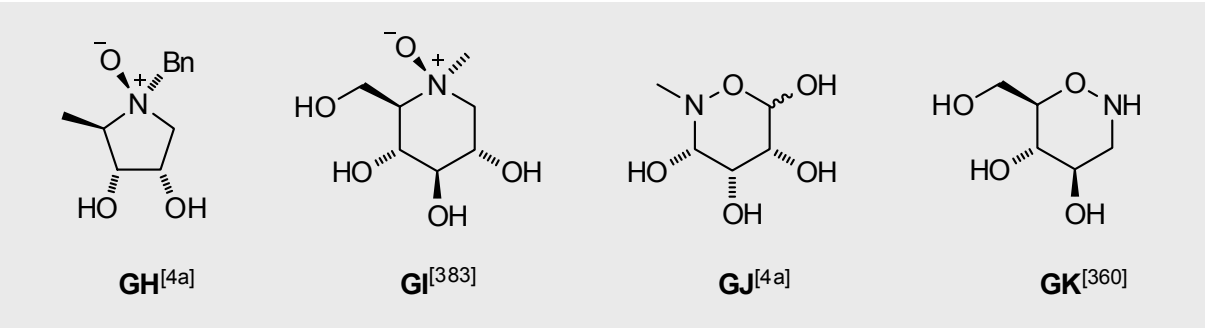

GH[4a] **GI**[383] **GJ**[4a] **GK**[360]

Diagram 57: Poor "quaternary ammonium" and "weakly-basic" glycosidase inhibitors

Likewise, the 1,2-oxazines of type **GJ** from Palmer[4a] were inactive. This can be reconciled well with the poor activity of the related tetrahydrooxazine **GK**.[360] This oxazine was not protonated under the assay conditions in the inhibition studies with *T. maritima* β-glucosidase and, essentially, this "oxy-isofagomine" derivative was a 20-fold weaker inhibitor in comparison to isofagomine **O**.[360] Since **GK** and **O** are similar in many ways, the reason for the considerable loss in activity of **GK**, and consequently **GJ**, could be related to lower base strength of the oxazine (pK_a = 3.6). In Palmer's choosen strategy, we assume that an attempt was made to mimic the build of a charge at several places to model the transition state better, notwithstanding the obvious (problematic?) lability of the halb-acetal species.

6.4 Fucosidase Inhibition

α-L-Fucosidases are lysosomal enzymes involved in the degradative pathway of L-fucose containg glycoproteins and glycolipids (cf. Section 1.4 and Diagram 9, p 15). The enzyme is strongly inhibited by the basic iminocyclitol analogues of the natural substrate, L-fucose, with binding energies, for example for the paradigm inhibitor DFJ **AI**, in the low nanomolar range.[87-91] The potent binding of α-L-fucosidase to this class of iminocyclitols is due to the very tight interactions of the enzyme with the inhibitor, which according to Sulzenbacher and co-workers,[374] "*leaves barely any space for potential modifications of, or substituents upon, the sugar hydroxyl groups*". Interestingly, the tight hydrophilic region opens up into a vast groove at the aglycon site, as has been discerned from structural studies of *Thermotoga maritima* α-L-fucosidase.[374] This is consistent with biological role of α-L-fucosidases and

their structural diversity because their substrates are mostly branched and have a highly varied linkage compostion (i.e. α-1,2, α-1,3, α-1,4 or α-1,6) – though significant linkage specifcity for hydrolysis has been documented.[394,395] The discovery of a "groove" also explains the receptivness of α-L-fucosidase to iminocyclitol *C*-glycosides, where apparent K_i values as low as 0.47 pM have been reported – an alleged record-low for glycosidase inhibition.[97] However, two recent X-ray structures have shed light on the nature of aglycon binding of several α-L-fucosidases with 6-membered iminocyclitols C-glycosides to reveal that the aglycon region is not conserved. Accordingly, striking differences in binding between *bovine kidney*, *T. maritima* and *Homo sapiens* α-L-fucosidase have been found.[396,397] This binding, along with mechanistic aspects, will be discussed in more detail below.

6.4.1 Structure activity relationships

6.4.1.1 General notes

For glycon analogues, replacing the ring oxygen atom by the NH-group has an profound effect on enzymatic inhibition. One explanation for the potent inhibition is the strong electrostatic interaction of the protonated imino group with the carboxylate of the active site. As inhibition is pH dependence, this should therefore depend on the ionization state of both the inhibitor and the carboxylate. Fucose itself is a moderate inhibitor of α-L-fucosidase and here a pH dependence on inhibition can be observed: At pH 5.0, its K_i value (205 μM) drops to 30 μM and 25 μM at pH 6.0 and 7.0, respectively.[89] This pH dependence is tentatively explained by a hydrogen bond of a anomeric hydroxyl group as donor with an active site carboxylate with pK_a 6.1 as acceptor. Where no H-bonding is possible, for example for methyl α-L-fucopyranoside, the binding was in comparison 100-fold weaker over the same pH range (K_i = 3600-4500 μM) (Diagram 58). For L-fucosylamine **GL**, although prone to quick hydrolysis under the assay conditions at pH 5.0 and 7.0, and to a lesser extend at pH 6.0, the K_i value at pH 7.0 differs from the other ainhibitors listed in being consistently higher than at pH 6.0. This underlines that α-L-fucosidase is stronger inhibited by the cationic form of basic glycon derivatives, whereas L-fucosylamine **GL** (p$K_a \leq 7.0$) would be less than 50 % protonated at pH 7.0. The glycon also provides a close fit to the methyl group of L-fucose. The replacement of methyl by hydrogen in the *nor*-DFJ-derivative **GM** caused the K_i to increase 1600-fold over the K_i of DFJ **AI** at pH 7.0. The drop in potency translates into a $\Delta\Delta G$ = 4.3 kcal/mol. This is around five-fold larger than expected for the hydrophobic "effect" of a methyl group alone.[89]

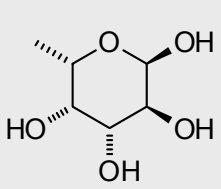
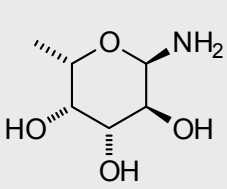
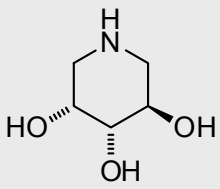
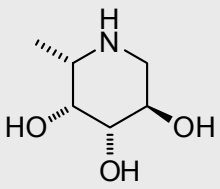

pH	α-L-fucose	**GL**	**GM**	**AI**
5.0	205	4.9	24.0	0.017
6.0	30	0.75	4.3	0.0027
7.0	25	1.2	2.2	0.0013

K_i in μM; *bovine kidney*, lit.[89]

Diagram 58: The pH dependence on the inhibition constant, K_i, for fucose and nitrogen containing analogues. Data taken from lit.[89]

Changes to the ring hydroxyl topography or the "doubling up" of substituents at any hydroxyl group position will result in large reduction in inhibition potency, as was demonstrated by the 4-methyl appendage in Fleet's DFJ derivative **AL** (cf. Diagram 9, p. 15). That said, the indifference of α-L-fucosidase to substituents at the anomeric position of either configuration is worth reiterating: The homomethyl-deoxyfuconojirimycin (α/β-HFJ, **AJ** & **AK**, respectively; K_i = 0.0053-0.0058 μM, Diagram 9) is a prime example. Quaternary centres and sp-hybridization is tolerated with no drastic loss in potency, as featured in nitrile **GN**.[398] The C=N unsaturation as found in cyclic imines **GO**[399] and **GP**[400] brought about no considerable inhibition loss in comparison to the K_i values for the fully saturated derivatives of their respective substance classes (Diagram 59).

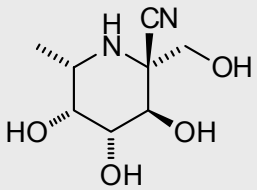
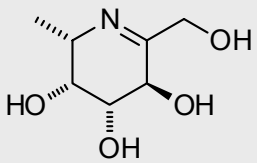
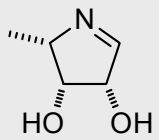
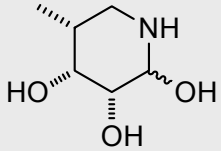

GN	**GO**	**GP**	**GQ**
IC_{50} = 0.075[398] b.k.	K_i = 0.0069[399] b.e.	K_i = 0.010[98b,400] b.k.	K_i = 0.0044[401] b.k.

α-L-fucosidase: b.k. *bovine kidney*, b.e. *bovine epididymis.* Concentrations and constants in μM

Diagram 59: Variations of structural motifs around the anomeric position

The sp^2-hybridization structural motif might force the ring to adopt a transition state-like conformation. Relevant to the glycosidase mechanism of α-L-fucosidase, discussed in the

next chapters, this may be a $^3H_4$ conformation for tetrahydropyridine **GO**; conceivably, this could be modelled equivocally by the co-plainarity of C—2/N—1/C—5/C—4 and envelope "flap" at C—3 in the L-*lyxo*-pyrrroline **GP**. The isofagomine-like **GQ** was demonstrated to be a nanomolar inhibitor of α-L-fucosidase. Interestingly, this hemiaminal, discovered independently by Bols[401] and Nishimura,[402] and other "noeuromycin" derivatives like it, are known to form hydrated ketones at neutral pH through the Amadori rearrangement.

6.4.1.2 Aminocyclopentanetriols and derivatives thereof

This brings us to the aminocyclopentanetriols, **GR**-**GU**, from Raymond (Diagram 60).[403,404,405,406] The exact nature of transition-state mimicry ascribable to this class of compounds is debatable. This uncertainty surrounding the biological efficacy can be extended to the likewise synthetic amino(hydroxymethyl) cyclopentanetriols and the related, though naturally-occurring, mannostatins.[407] It was proposed that mannostatin A, a potent Golgi α-mannosidase II inhibitor (K_i = 34 nM; lit.[408]), is a good mimic for the mannosyl cation.[407] This has been supported by comparing the inhibitor with a molecular orbital-optimsed half-chair of the mannosyl cation. By superimposing the assumed transition state on mannostatin A, very good overlap of the 2- and 3-OH of the mannosyl oxocarbenium ion and two of the hydroxyl groups at mannostatin A was seen, and that the nitrogen of mannostatin A is placed near the oxocarbenium ion.[409] However, as pointed out by Bols,[6e] whether the amino group of mannostatin A mimics charge at ring oxygen or anomeric carbon in the mannosyl oxocarbenium ion or if it corresponds to the protonated exocyclic oxygen of the substrate has yet to be determined. Newer research even suggests that the efficacy of mannostatin A may not be due to resemblance to the transition state at all (more below).[408]

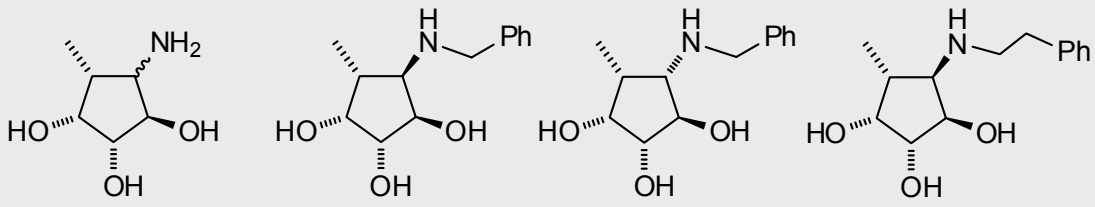

source	α/β–**GR**	α-**GS**	β–**GT**	α-**GU**
b.k.	15 / 28	0.7	110	0.4
b.e.	12 / 18	0.6	28	0.3
h.p.	n/d	n/d	18	0.09

α-L-fucosidase: b.k. *bovine kidney*, b.e. *bovine epididymis,* h.p. *human placenta; K_i* in μM

Diagram 60: The "L-*fuco*" aminocyclopentitols; K_i-improvement with N-substituent

Nevertheless, despite this ambiguity, Raymond argues along the same lines, as described for mannostatin A, in explaining the biological efficacy of the "L-*fuco*"-amino-5-methylcyclopentane-1,2,3-triol **GR** in terms of a mimic of the "*high-energy endocyclic fucosyl cation*".[403] In later work, Raymond states that the amino group might correspond to "*exocyclic oxygen of the protonated substrate*."[404-406] Both statements are bold, especially in reference to the limited scope of his results and the properties of α-L-fucosidase. For the latter argument to be valid, one criteria is that there should be at least some anomeric inhibition specificity, as was suggested by Bols.[6e] However, for the parent inhibitor, bearly no difference in fucosidase inhibition was observed between α-**GR** and β-**GR** (cf. Greul, lit.[102])

This is not suprising because Family 29 α-L-fucosidase is known to be notoriously indifferent to the configuration of the anomeric subsitutent – demonstrated aptly in the case of homomethyl-deoxyfuconojirimycin (α/β-HFJ, **AJ** & **AK**, Diagram 9) – due to large cavity that exists presumerably at the entrance to the aglycon pocket. Sticking something bulky into this groove will, obviously, elicit a biological response: The addition of the *N*-benzyl substituent to "L-*fuco*" **GR** led to a marginal improvement in inhibition for the "correct" α-anomer **GS** (i. e. K_i = 0.7 μM). This translates energetically as 1.8 kcal/mol contribution to the ΔG by the benzyl moiety and, according to Raymond, qualified it as being a "*aglycon leaving group mimic*"![405] Weaker binding was observed for the β-L-*fuco* **GT** (K_i = 110 μM, *bovine kidney*).[405] This is not unreasonable because if the *N*-substituent is large it may be required that it can fit into the aglycon subsite of the enzyme.

The flexibility of the aglycon can affect the compactness of the enzyme-inhibitor complex. If this relationship is synergistic, dramatic improvements in inhibition potency are possible. Jäger and co-workers could demonstrate a dramatic increase in inhibition of *E. coli* β-galactosidase, for example, when the parent *galacto*-configured amino (hydroxylmethyl) cyclopentanetriol (K_i = 4.5 μM) was converted into its corresponding *N*-benzyl derivative (K_i = 0.002 μM).[165,166] Clearly, with a contribution of 4.6 kcal/mol to the free energy change, the *N*-benzyl unit was an adventitious binding partner for β-galactosidase. Because Jäger and co-workers did not investigate the mode of enzyme contact nor the thermodynamic parameters – save for an X-ray structure of a related *para*-bromobenzyl derivative –[102] any explanation of the tight binding can be based on nothing more than pure conjecture. Interestingly, only two of Jäger's derivatives showed any inhibition of α-galactosidase (i.e. *coffee bean*). This seemed to show that this class of inhibitors *is* anomeric selective; thus, the amino group might correspond to the exocyclic oxygen of the protonated substrate instead of mimicking the galactosyl cation. However, this would have been more convincing if a series of

α-*galacto*-configured inhibitors had been synthesized by Jäger's group and their inhibitory properties had confirmed a similar trend.[165,166]

When Raymond extended the alkyl-spacer by one carbon in *N*-phenylethyl **GU**, only small gains in inhibition for the *bovine kidney* and *bovine epididymis* sources were found. In comparison, for *human placenta* α-L-fucosidase, the K_i dropped to 0.09 μM (Diagram 60). The tighter binding of **GU** to the *human placenta* enzyme is an indication that the enzyme structure at the periphery of the active site is not conserved between Family 29 *mammalian* and *homo sapien* α-L-fucosidases. This gives rise to several different ground state conformations between the enzymes which bind the inhibitor. Some – but not all – fucosidases upon binding are known to undergo a conformational change in order to bind the transition state of the inhibitor better. This time-dependent conformational change is hallmarked by the observation of slow onset of inhibition. The nature of the sequence alignments between fucosidases of *mammalian* and *homo sapien* origin have been underpinned by recent X-ray analyses of enzyme-inhibitor complexes.[396,397] The cause of this structural diversity is ostensibly *Darwinian* in origin. A brief discussion of these structural attributes and the effect on inhibition potency is given in the next section.

Returning to the aminocyclopentanetriols, if one is disinclined to pander to the shortcomings of Jäger's[102,165-166] and Raymond's[403-406] take on "substrate mimicry" – i.e. the putative exocyclic oxygen and/or glycosyl cation – there is an extra piece to the puzzle which goes some way to explain the glycosidase inhibition. Specifically, we are referring here to a recent study of mannonstatin A.[408] This combined structural and molecular modelling study revealed that the potent (K_i = 34 nM) Golgi α-mannosidase II (GMII) inhibitor mimics not the transition state but instead the covalent glycosyl-enzyme intermediate. Molecular dynamics simulations and NMR studies showed that the cyclopentane ring of mannostatin A was rather flexible occupying pseudorotational itineraries between $^2T_3$ and ^5E, and $^2T_3$ and ^4E (cf. note on *pseudorotation* of five-membered rings, Section 3.2.2.1). In comparison, in the bound state, mannostatin A adopted a $^2T_1$ twist envelope conformation, which was not significantly populated in solution. Possible conformations of the mannosyl oxacarbenium ion (cf. lit.[409]) and a glucosyl-enzyme-linked intermediate were compared to the conformation of the bound mannostatin A in the cocrystal structure with *Drosphilia melanogaster* GMII. It was found that mannostatin A best mimics the covalent enzyme-linked mannosyl intermediate, which adopts a $^1S_5$ skew boat conformation (Diagram 61). In this conformation, the leaving group of the natural substrate would be *anti-periplanar* to the lone pair of the ring oxygen – a requirement

for the departure of the leaving group according to Deslongchamp's anti-periplanar lone-pair hypothesis (cf. corresponding book chapter on *Acetals*, ref.[376] and Section 6.2, p. 129).

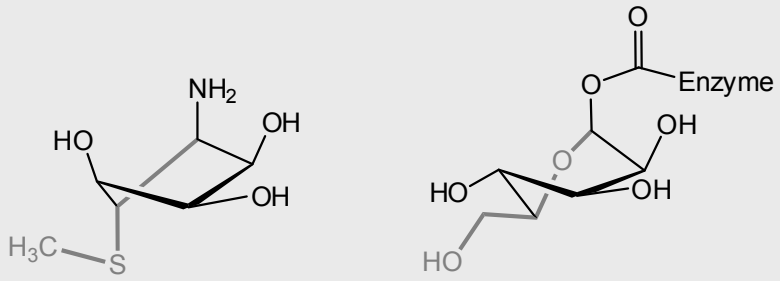

$^2T_1$ $^1S_5$

mannostatin A

Diagram 61: Mannosatin A adopts a $^2T_1$ conformation that resembles the $^1S_5$ conformation of the mannosyl-enzyme intermediate.[408] This finding emphasises that the pursuit of transition state analogy is not the only route to high potency.

The authors of this studies sought not to debunk the commonly accepted belief that potent glycosidase inhibitors mimic only the flattened six-membered ring – or exocyclic oxygen leaving group – of the glycosyl oxacarbenium ion. Instead, the message was that emphasis should be placed on designing inhibitors that can mimic reaction intermediates such as the Michaelis complex or enzyme-linked intermediate. However, conservative chemists could argue that it is unreasonable to compare the mannostatins to the amino(hydroxymethyl) cyclopentanetriols of Jäger and Reymond, for example, as the thiomethyl moiety is able to generate additional ligand-protein interactions which the hydroxymethyl moiety can not.

6.4.1.3 β-Amido L-fucosyl-nojirimycin *C*-glycosides

Fleet and co-workers set the impetus for the development of β-linked C-glycon DFJ-derivatives through the synthesis of α/β-homomethyl-deoxyfuconojirmycin (**AJ**/**AK** –cf. Diagram 9, p. 15) in 1989.[88] The biological tests showed that inhibition potency of either **AJ** or **AK** was not affected by the stereochemistry of the tether extending from C-1, in relation to the activity of the parent DFJ (**AI**).[88,90,94] This trend was confirmed by the β-linked DFJ diamine **GV** (IC_{50} = 0.0025 μM, cf. Diagram 62). Lin, Wong and co-workers thought of using this amine – although of incorrect anomeric configuration – for the identification of new binding components.[96] In their studies they reasoned that the β-linked FNJ amine may be used for the identification of GDP-β-fucose (the glycosyl donor of α-fucosyltransferases)

mimics as fucosyltransferase inhibitors. It is also known that GH 29 α-L-fucosidases process fucosylated-conjugates through the formation and subsequent breakdown of a covalent β-linked fucosyl-enzyme intermediate *via* a double-displacement mechanism (cf. Section 6.4.2). Despite all this, it is worth remembering that Lin and Wong had little choice but to use the β-configured FNJ diamine **GV**, since their chosen synthetic strategy (i.e. Fleet's synthesis of the homomethyl-deoxyfuconojirmycins **AJ**/**AK**, lit.[88]) provides access to the "wrong" pre-requisite (1*S*)-β-primary alcohol only. This is then transformed to an azide at a late stage through a Mitsunobu reaction and reduced by hydrogenation to the (1*R*)-β-diamine.[96] Davies and co-workers commented recently that the success of the "β-linked" inhibitors was enough to off-set the "synthetic problems of accessing α-linked inhibitors" which, they add, "would better mimic the substrate".[410] In this Thesis, however, a viable route to α-linked FNJ derivatives was demonstrated through the diastereoselective addition of nucleophiles to the easily-accessible L-*fuco*-nitrone **28** (cf. Section 3.2.3). The α-congener of the β-amino DFJ **GV** could conceivably be made by our method *via* the nitroaldol reaction of nitromethane, a weak base and L-*fuco*-nitrone **28** (Henry Reaction) to afford the β-nitrohydroxylamine, followed by reduction. Indeed, this is a synthetic protocol that has found diverse application in the group of Prof. Jäger.[5,177,257]

A selected sample of 1-aminomethyl FNJ derivatives (**AM**, **GW**-**GY**) are displayed in Diagram 62. The amides were formed after treating 1-aminomethyl FNJ **GV** with the corresponding acid in the presence of (1*H*-benzotriazole-1-yl)-1,1,3,3-tetramethyluronium hexafluorophosphate (HBTU) and diisopropyl ethylamine. The original method by Wong and Lin[96,97] has been employed in several, in essence, follow-up reports from Lin and co-workers,[411] Lin, Wang and co-workers,[412] as well as a recent collaboration between Lin, Davies and co-workers.[410] The results with the *bovine kidney* α-L-fucosidase are interesting because they illustrate that the enzyme inhibition can be significantly enhanced by introduction of a amide-linked hydrophobic group, even though the existence of an alkyl amide bond had a negative effect [i.e. compare activity of **GW** to the reference diamine **GV** or parent inhibitor DFJ (**AI**)]. The term *significant*, however, should be used with caution, since the extended fluoro-indole moiety, for example, brought only a ca. 10-fold improvement in binding compared to the parent DFJ (**AI**) despite the obvious proliferation in molecular complexity. Indeed, closer inspection of Wong and Lin's[96] results serve as a warning that "packing the aglycon" with a rather flexible aglycon may not necessarily bring the benefits to binding potency as one would desire: for example, the "methylene"-extended indole **GX** elicited only a 20 % inhibition, whereas the "ethylene"-linked candidate **GY** showed no inhibition against *bovine kidney* α-L-fucosidase at 10 nM inhibitor concentration.

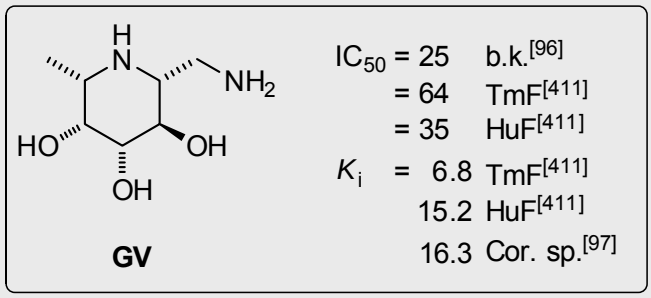

GV

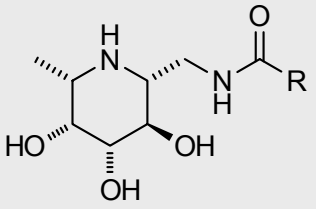

AM, **GW**-**GY**

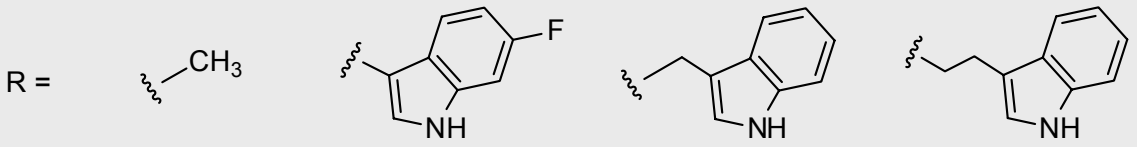

	GW	**AM**	**GX**	**GY**
b.k.[96]	100	0.6	20 %[*]	n.i.
Cor. sp.[97]	—	1.15 *(K_i* = 0.049)*	—	0.32 *(K_i* = 0.00046)*
TmF[411]	4.47[412]	0.259 *(K_i* = 0.063)*	—	0.105 *(K_i* = 0.00041)*
HuF[411]	—	9.7	—	5.6

α-L-fucosidase: b.k *bovine kidney;* Cor. sp. *Corynebacterium sp.* (α1,2-fucosidase)
TmF *Thermotoga maritima;* HuF human

K_i and IC_{50} values in nM; K_i* = time-dependent, slow binding inhibition constant
[*] = % inhibition at 10 nM inhibitor concentration
n.i. = no inhibition at 10 nM inhibitor concentration

Diagram 62: Fucosidase inhibition from selected β-linked fuconojirimycin derivatives. The extended C-1 sidechain can only contribute to binding potency if the enzyme's aglycon allows for specific binding interactions. These interactions may be in the form of extra hydrophobic binding sites.

In the same article,[96] the activity of candidates **AM**, **GW**-**GY** against *Corynebacterium sp.* was also tested. The subsequent full-paper from Lin and co-workers[411] on *Corynebacterium sp.* fucosidase re-affirmed the contrasting aglycon preferences in comparison to the *bovine kidney* enzyme. This should be of no surprise, however, since the former is a bacterial 1,2-α-L-fucosidase exoglycosidase, hydrolysing the specific glycosidic linkage, for example, of Fucα1-2Gal (**AG**) (cf. Section 1.4, Diagram 9, p. 15) *via* an inverting mechanism (GH 95), whereas the latter, as is usual for mammalian sources, has a broad substrate specificity and *retaining* mechanism (GH 29). The structural characteristics of *inverting* α-L-fucosidases will,

by definition, differ substantially to *retaining* α-L-fucosidases (cf. notes in Section 6.2, p. 128-129). Incidentially, a recent crystal structure of 1,2-α-L-fucosidase isolated from *Bifidobacterium bifidum* has been reported,[413] though this will not be discussed further in this Thesis. All candidates tested by Lin and Wong[96] were found to be reversible inhibitors against *bovine kidney*, whereas a time dependent picomolar slow onset of binding was found for *Cor. sp.* with indoles **AM** and **GY** (Diagram 62).[97] Kinetically, this is characterised by a two-step mechanism going from K_i to K_i^*, reflecting the interchange between E + I ⇆ E ▪ I (K_i, ΔG_1) and E ▪ I ⇆ E ▪ I* (K_i^*, ΔG_2). For the fluoroindole **AM** and ethylene-bridged indole **GY**, a 23-fold ($\Delta\Delta G$ = -7.8 kcal/mol) and 696-fold ($\Delta\Delta G$ = -16.2 kcal/mol) tightening, respectively, was observed. The slow binding or slow onset is prevalent amongst potent glycosidase inhibitors, particularly certain iminocyclitols.[6c,414] The phenomenon has been attributed to a slow interchange between protein conformations. Lin and co-workers argued that there was an implicit conformational change in the α-fucosidase in the isomerisation of the E ▪ I to E ▪ I* complex on account of changes to intrinsic protein fluorescence. Whatever the reason, in comparison to the mammalian enzyme, there is obiviously a different set of steric restraints that are exercised upon aglycon binding in this 1,2-α-L-fucosidase. The enhanced inhibitory potency of **AM** and **GY** to the *Corynebacterium sp.* enzyme is probably due to the additional hydrophobic interaction (i.e. entropic gains). The hydrophobic extension may also bring the enzyme and inhibitor closer together – after localized conformational change – so that the enzyme-inhibitor complex supports shorter distances of H-bonds than in the Michaelis complex of the enzyme-substrate (i.e. enthalpic gains).

The first solved crystal structure of α-L-fucosidase was from the marine hyperthermophilic bacterium *Thermotoga maritima* (TmF) by Sulzenbacher and co-workers.[374] With ~ 38 % sequence similarity to human fucosidase (HuF), the TmF X-ray structure provided a basis for the modelling of HuF.[374] Sulzenbacher also noted that the shape of the catalytic potcket is conserved between TmF and HuF, with 11 side chains of 13 in contact with fucose conserved both in sequence and position. A more recent report by Lin, Liu and co-workers[396] has elucidated the essential residues in HuF. They discovered, however, that in this GH family the catalytic acid/base did not align at the amino acid sequence level but appears, at least, to align structurally for all known GH 29 structures. Furthermore, according to Davies and co-workers the region of the loop 2 may play an important role in stabilizing/positioning the catalytic acid/base residue.[410] Between TmF and HuF, drastic differences were found at the periphery of the active site. Specifically, this refers to a 20-residue deletion in HuF within the surface loop 1 (i.e. TmF residues: 44-63) and allows for an enlarged access to the catalytic site.[396] The sequence dissimilarity in the aglycon-binding

site between TmF and HuF reflects the large differences in inhibitor affinity found for indoles **AM** and **GY**, as investigated by Lin, Ho and co-workers.[411] The binding affinity of fluoroindole **AM** for TmF (K_i* = 0.063 nM, slow-onset) was higher than that with HuF (K_i = 9.7 nM), and significantly so for "ethylene"-indole **GY** (TmF: K_i* = 0.00041 nM *versus* HuF: K_i = 5.6 nM), up 13700-fold (Diagram 62). The authors maintained that the two methylene units between amide and indole group in **GY** has more flexibility to allow better adjustments and fit for tighter binding.[411] This statement was strengthened by the findings of the X-ray crystal structure of TmF in complex with **GY** and, as a comparative, with 1-aminomethyl FNJ **GV**:[397] The conformation of loops 1 and 2 of the TmF-**GV** complex remained the same as those of the TmF-**GY** complex; however, the aglycon in TMF-**GY** is able to generate additional hydrophobic interactions, block entrance into the active site groove and "squeeze" out coordinated water. The enzyme conformation of the TmF-**GY** complex leaves little space for water after the binding channel has become closed by the two loops and aglycon: in TmF-**GV** there are two ordered water molecules, while only one in TmF-**GY** (cf. figures in lit.[397]). Furthermore, in the TMF-**GY** complex, shorter H-bonds and, therefore, stronger electrostatic interactions of the endocyclic and exocyclic nitrogens with the catalytic residues are evident. This is consistent with the thermodynamic parameters established by isothermal titration calorimetry (Diagram 63). Especially noteworthy here is the enthalpy contribution in **GY** (cf. thermodynamic signatures between glucoimidazoles **GF** and **GG**, Diagram 56).

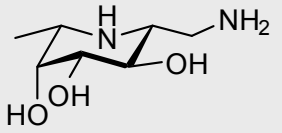

GV

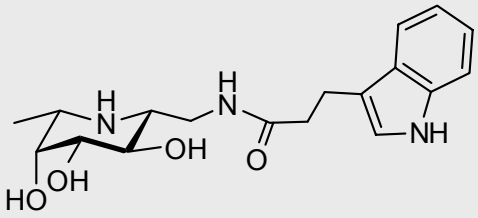

GY

	GV	**GY**
K_i	16.3 nM (HuF: 15.2 nM[411])	0.105 nM (HuF: 5.6 nM[411])
K_i*	n/a	0.00047 nM
ΔH	-2.48	-6.23
$T\Delta S$	+8.22	+10.69
ΔG	-10.70	-16.90

pH 7.5; T = 298 K; kcal/mol

Diagram 63: Binding constants for **GV** and **GY** derived by kinetic and thermodynamic methods.[397] The flexibility of the aglycon **GY** was essential for a "snug" fit with TmF – less so, however, in the binding of **GY** to HuF. Here, a rigid aglycon is better suited.

Although the β-amido-linked fuconojirmycin derivatives achieved impressive binding affinities with TmF, this result may have only minor significance in terms of the role of substances of this "linker category" in the identification of potential fucosidase inhibitors as possible drug candidates. The therapeutically important α-L-fucosidases, such as lysosomal human α-fucosidases FucA1 and FucA2, are *exempt* from the conformational changes that afflict the extended active-centre loop regions, described in TmF. This explains the apparent unreceptivness of HuF to the β-amido-linked inhibitors with "flexible" aglycons, where no significant (or even worse) binding improvements were observed over the parent inhibitor DFJ **AI** (Diagram 62). This has been put down to a truncated surface loop 1 region. Interestingly, amino acid sequencing has shown that loop 1 is completely missing from the therapeutically-relevant FucA1.[410] In HuF, important missing residues in loop 1 are comprised of Trp58, Phe59 and Tyr64, from which TmF forms a hydrophobic domain that lines up to face the active site. This domain could be exploited by the inhibitor's aglycon, in the TmF-**GY** complex, because it was "flexible enough" to manoever itself into position.[397]

As mentioned above, for the HuF enzyme, the curtailment of this surface loop 1 region results in an enlarged entrance to the active site of the enzyme. The structural differences between TmF and HuF will therefore have significant repercussions on the design of the inhibitor's aglycon. For instance, Wu, Lin and Wang[397] hypothesised that FNJ derivatives with more rigid aglycons at C-1 would probably inhibit HuF more effectively. The authors took 1-aminomethyl FNJ **GV** (K_i = 15.2 nM, HuF), coupling it with 9-fluorene-1-carboxylic acid to produce the corresponding "rigid amide" aglycon, and found that a 38-fold improvement in HuF inhibition (K_i = 0.40 nM) was obtained over diamine **GV**. However, in the follow up paper,[410] the inhibition of 1-aminomethyl FNJ **GV** and the same "rigid" fluoren-9-one derivative against α-L-fucosidase from *Bacteroides thetaiotaomicron* (termed "BtGH29") gave contrasting results. The BtGH29 enzyme, according to amino acid sequence alignments, is a good model for conformationally-rigid and therapeutically important FucA1 enzyme as it too is missing the loop 1 region. Interestingly, the contribution of the amide linker and/or the "rigid" fluoren-9-one moiety to the inhibition potency could not be rationalised, since the extended aglycon did not make any additional hydrogen bond contacts with the enzyme than did the parent diamine **GV**. Although binding of the "rigid" fluoren-amide derivative across the pH range of 6.0 to 7.0 was shown to be "entropically driven" – in accordance with the foregoing discussions – the potency remained surprisingly weaker than the diamine **GV**. The authors also mentioned the difficulities involved in the interpreting the mode of inhibition as a function of pH-dependency, as this involves non-uniform composites of pK_a values for the free enzyme, free inhibitor (of which the two differed substantially) and the E ▪ I complex.

6.4.1.4 Derivatives of 3,4-dihydroxy-5-methylpyrrolidines

There is an ever growing number of five-membered iminopolyols that elicit high activity against α-L-fucosidase. Specifically, as this Thesis has endeavoured to set out, we are referring here to a class of polyhydroxylated pyrrolidines ("1,4-dideoxy-1,4-iminoalditols") which have aromatics or heteroaromatic substituents attached at the 2-position. These tend to be more effective than the "usual" hydroxymethyl substitutents, since the lipohilic aromatic component may contribute to the binding constant through unspecific hydrophobic interactions. The "bulky" substituent may also – as has been discussed above in previous chapters – induce ligand desolvation, i.e. bulk water, in the binding pocket and therefore contribute favourably to the entropy component of binding.

The hydrophobic effect is hard to quantify, although it would seem that this effect is borne out by the improved inhibition of the more lipohilic hydroxyethyl-candidate **HA** (K_i = 0.008 μM)[98b] as compared to hydroxymethyl-derivative **GZ** (K_i = 1.4-0.080 μM) – in this anomeric series at least. With hydroxymethyl as the C-2 substituent an interesting annomerly in enzyme potency is presented concerning the inhibition profile of the "correctly"-configured α-L-lyxitol **GZ**[2,382] and "incorrectly"-configured β-L-lyxitol **HB** (Diagram 64).[415,416} The term "correct" in this case is in reference to the "natural" all-*cis* orientation of C-5, C-4, C-3 substitutents and *trans*-C-3/C-2 (α-anomer) configuration as opposed to the "unnatural" C-2 epimer, i.e. β-anomer, where C-3 and C-2 are *cis*-configured. Surprisngly, β-**HB** (K_i = 0.0049 μM) is the more potent fucosidase inhibitior from *bovine kidney*, according to Clapés and co-workers.[415] Although in their hands, however, the activity of the α-L-lyxitol **GZ** was found to be K_i = 0.080 μM; this value deviates significantly from the inhibition constant published by two other groups (i.e. Jäger: 0.40 μM[2]; Wong: 1.40 μM[382], *bovine kidney*). This invites questions regarding their biological testing procedure. Interestingly, Defoin and co-workers[417] recently reported a synthesis of *racemic* β-**HB** hydrochloride and also found this salt to be a potent fucosidase inhibitor (K_i = 0.015 μM, *bovine kidney*).

Clapés and co-workers[415] carried out docking experiments of β-**HB** with 3D-data taken from Sulzenbacher's structural elucidation of *T. maritima* α-L-fucosidase.[374] Their findings emphasised the presence of several hydrogen bonds – especially a strong electrostatic between the ring nitrogen and the catalytic E266 residue. As this was a mere docking "simulation" instead of a protein-inhibitor co-crystal, no ITC data was available, meaning that no thermodynamic parameters could be established. The effect of water/entropy

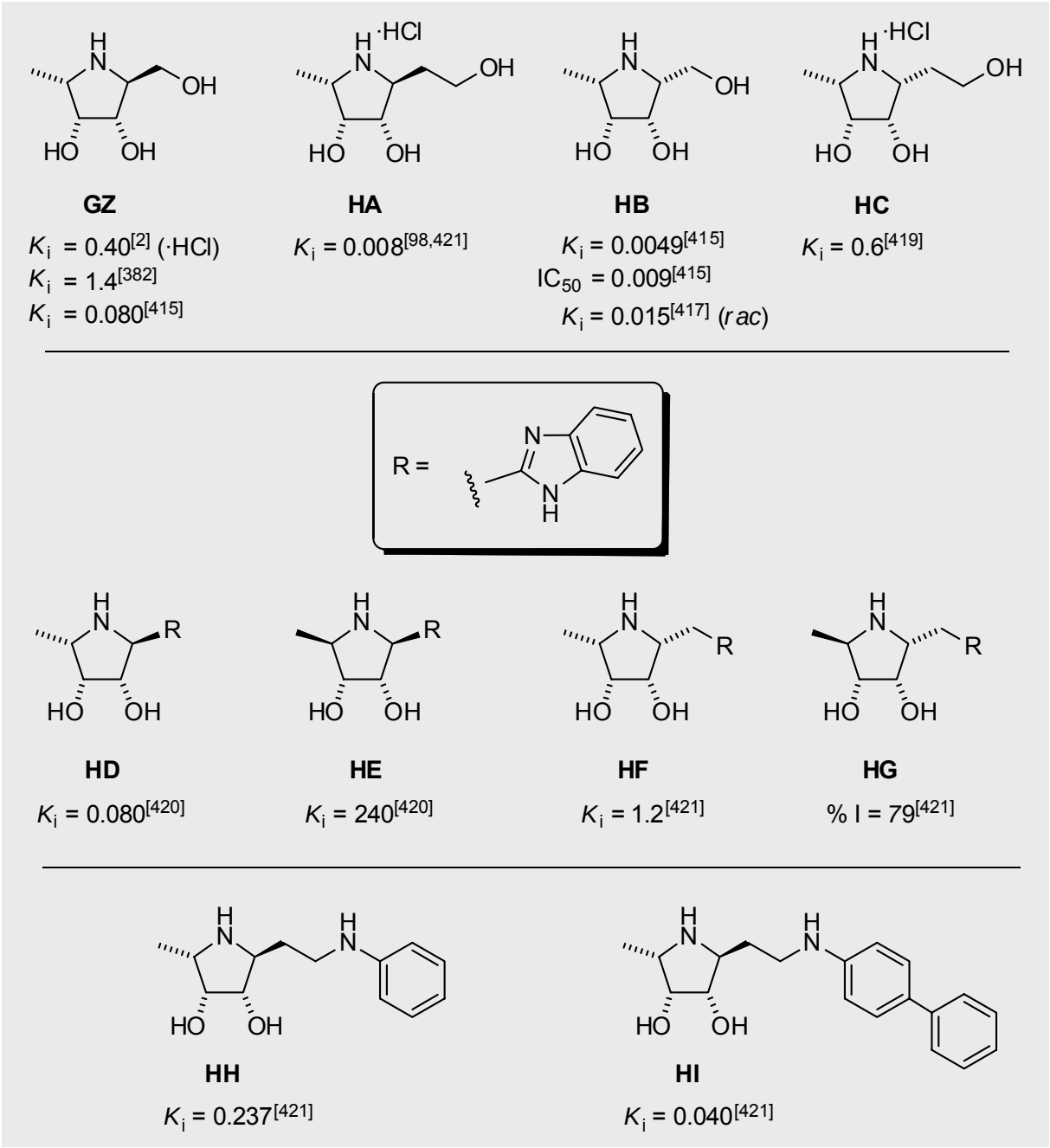

Diagram 64: Effect of the side chain at C-2 on the inhibition potency against *bovine kidney* α-L-fucosidase. *rac* = racemic compound.

was therefore not investigated.[415] Interest in these "all-*cis* β-fucitols" centres on them being "potential non-hydrolysable precursors of GDP-fucose analogues" – according to Defoin.[417] A lengthening of the chain in the β-anomeric series is tolerated less well by *bovine kidney* fucosidase. This is evident for the inhibition value for the hydroxyethyl β-L-lyxitol **HC**, synthesised[418] and tested[419] by Robina and co-workers. In terms of free energy, the presence of one extra carbon "destabilized" the binding energy by approx. 2.9 kcal/mol. Clearly, there is a major augmentation of binding interactions through lengthening the chain.

Diagram 64 presents several pyrrolidines bearing a benzimidazole sidechain, also from Robina and co-workers.[418,420,421] The "natural" diastereoisomer **HD** is the most potent inhibitor. The aromatic moiety enhanced the inhibition by a factor of approx. 9 over "parent" pyrrolidine diol **AN** (cf. Diagram 9, p. 15). As expected, the diastereoisomer **HE** is a much weaker inhibitor – presumerably because the 5-(*R*)-methyl substitutent points away from the hydrophobic patch of the enzyme. The injection of a methylene or deviation of the stereoconfiguration at positions C-2 and C-5 away from **HD** brings with it reductions in inhibition potency with this subsituent, i.e. the all-*cis* **HF** and, even worse, the 5-(*R*)-methyl α-D-ribitol **HG**. This underlines again the importance of a correctly-configured methyl substituent and the negative influence of "flexible" (and bulky) aglycons (cf. Section 6.5). This explains why the enzyme did not tolerate the lengthened benzimidazole side chain in **HG** where only 79 % of fucosidase was inhibited at 1 mM inhibitor concentration. Reverting back to diamines of **HH** and **HI** presents a faimilar picture: In the α-anomeric series, the hydrophobic "pocket" in the aglycon subsite of the enzyme is still accessible by lipohilic aromatic substitutents – even with relatively long ethylamine tethers attached to C-2. However, the change from phenyl to "biphenyl" with the added tether results in a less pronounced improvent in inhibition potency (i.e. **HH**/**HI** = 1.1 kcal/mol) than for the equivalent substituent pair with our inhibitors: i.e. the 2-phenyl (**AP**: K_i = 0.05 μM)[2] and 2-"biphenyl"-substitued pyrrolidine diol **97·HCl** (K_i = 0.0012 μM), where a 2.3 kcal/mol difference is ascribale to the extra phenyl unit.

6.4.2 Fucosidase Mechanism

All known α-L-fucosidases, included *bovine kidney* taken in this work, are classified into the glycoside hydrolase (GH) family 29 (*retaining*). The lesser-known α-L-fucosidases such as the 1,2-α-L-fucosidase isolated from *Bifidobacterium bifidum* (X-ray structure, lit.[413]) are grouped in GH 95 (*retaining*). Previous work on these retaining enzymes, i.e. which act with net retention of anomeric configuration (cf. Section 6.2), postulated a $^3S_1$ covalent intermediate providing the first insight into their conformational itinerary.[374] Recently, Davies, van Bueren and co-workers were able to provide X-ray "snapshots" of the reaction coordinate of α-L-fucosidase sourced from *Bacteroides thetaiotaomicron* (Diagram 65).[422] The advantages in terms of a therapeutic perspective is that this enzyme source shows high homology to human enzymes, as discussed previously in Section 6.4.1.3. The Michaelis

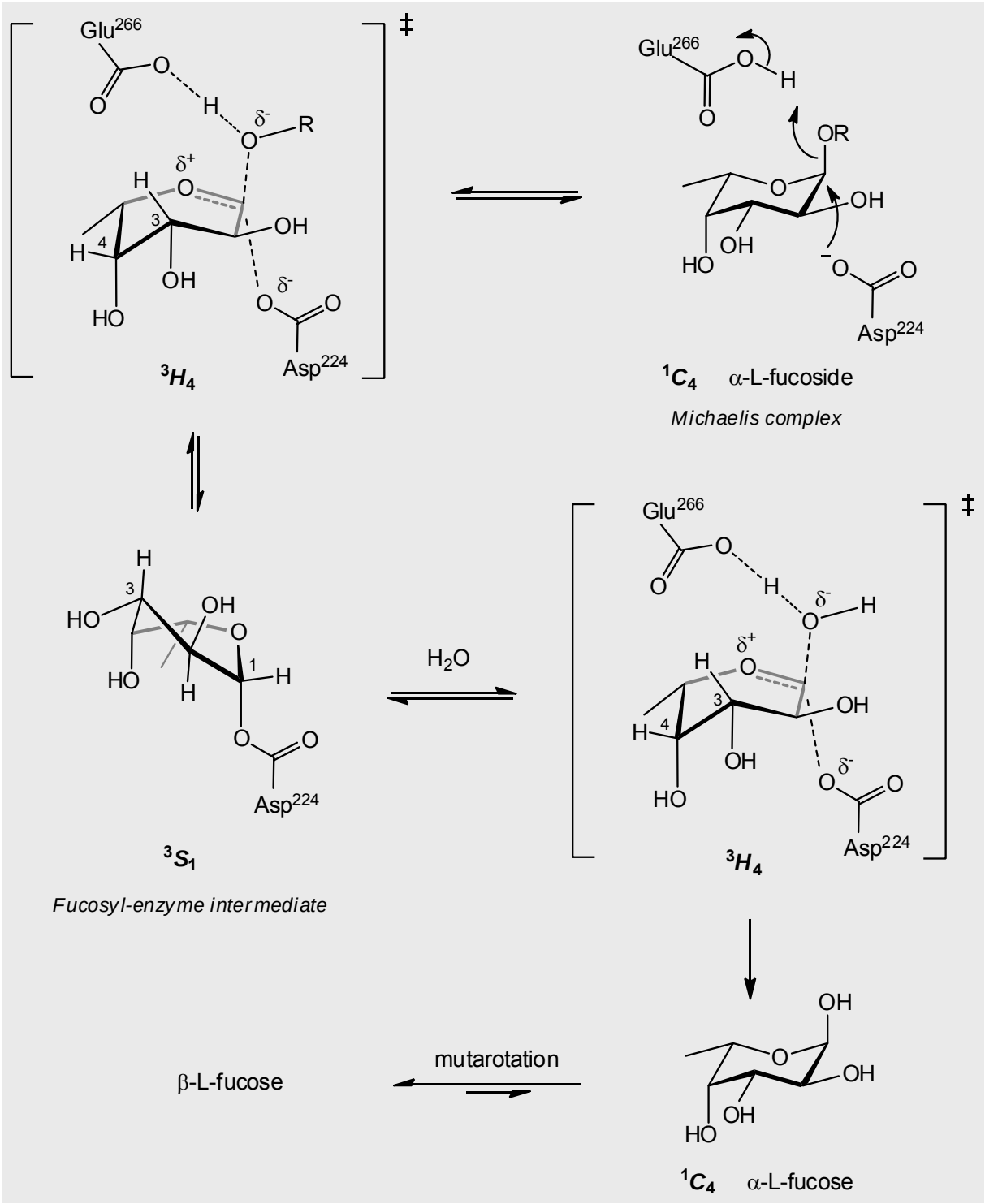

Diagram 65: Likely reaction coordinate for GH 29 α-L-fucosidase catalysed hydrolysis of fucosides.[422] The Michaelis complex binds in the $^1C_4$ conformation affording unhindered in-line nucleophilic attack and "electrophilic migration" of the anomeric carbon to the intermediate in the $^3S_1$ conformation which is subsequently deglycosylated by water. Each intermediate must go through the $^3H_4$ (or close to) transition state conformation. Hence, a $^1C_4 \leftrightarrow {}^3H_4 \leftrightarrow {}^3S_1$ "latitudinal" pathway for the formation of the covalent intermediate is probable. Amino acid labels correspond to the structural data from *T. maritima* α-L-fucosidase.[374]

complex is observed in a $^1C_4$ conformation, a trapped intermediate in the $^3S_1$ skew-boat which together provides structural evidence for the – as Davies and co-workers describe it – "latitudinal" Southern Hemisphere $^1C_4 \leftrightarrow {}^3H_4 \leftrightarrow {}^3S_1$ pathway for terminal α-L-fucosidase hydrolysis. In this itinerary in-line nucleophilic attack on the α-L-fucoside substrate (in $^1C_4$ conformation) with its axial leaving group orientation, results in "electrophilic migration" of the anomeric carbon. The reader may wish to refer to Section 6.2 for more detailed information and lit.[364] The trapping of these "snapshots" was done in the usual way: In order to observe a Michaelis complex or covalent intermediate, the enzyme has to be modified, or even "crippled", so that it is unable to quickly turnover the substrates (for trapping the Michaelis complex the *para*-nitrophenyl-α-L-*fuco*-pyranoside is used; for observing the covalent fucosyl-enyme intermediates, 2-deoxy-2-fluoro-L-fucose is taken – see notes on fluorinated species, Section 6.2) that are taken and soaked into crystals of the enzyme variant, prior to freezing and data collection (i.e. X-ray diffraction). α-L-Fucosides can adopt two low energy chair conformations, $^4C_1$ and $^1C_4$, the $^1C_4$ conformation being predominately preferred in solution. Davies and co-workers[422] used metadynamics simulations to analyse the "conformational free energy landscape": What came out was confirmation that the $^1C_4$ conformation for α-L-fucose is indeed the lowest in free energy and that a second minimum also occurs in the $^3S_1$ twist-boat region. This, of course, is perhaps not suprising since the twist-boat is the next highest intermediate, in terms of energy, found in a local energy minima in the chair-chair interconversion of pyranoses (cf. Eilel's book, ref.[274]).

6.5 Own Results – In Vitro Tests

6.5.1 Test Methodology

Commercially available glycosidases were employed for the test assays (Table 13) and carried out at the University of Stuttgart by Mrs. S. Saring, Mrs. J. Krenz (Dipl.-Chem.) and Miss A. Castiglia (MSc). Full details of the test procedure and enzymatic kinetics can be found in the doctoral work of P. Hilgers,[167] which is why in this Thesis the methodology will not be described in detail. The *in vitro* tests were carried out under standard conditions. As enzyme substrate, only the corresponding *p*-nitrophenyl-glycosides (pnp-glycosides) were employed. The products of the enzymatic cleavage of this substrate are coloured yellow, i.e. *para*-nitrophenolate anion. The concentration and thus colour intensity is inversionally proportional to inhibitor activity (Scheme 60). The inhibition constants of the pyrrolidine and piperidine inhibitors were done in buffered solution at the pH optimum of each enzyme. The

test procedure consists of three parts: Firstly, a determination of the enzyme inhibition (in %) at 1 mM inhibitor concentration. The inhibitor and enyzme are pre-incubated for 5 min. The reaction is then started through the addition of the respective pnp-glycosidase as substrate. After 20 minutes at 37 degrees centigrade, the reaction is stopped by quenching the reaction with 0.25 ml of a 0.2 M borax buffer solution. The resulting concentration of *p*-nitrophenolate is measured at 405 nm as a function of absorbtion.

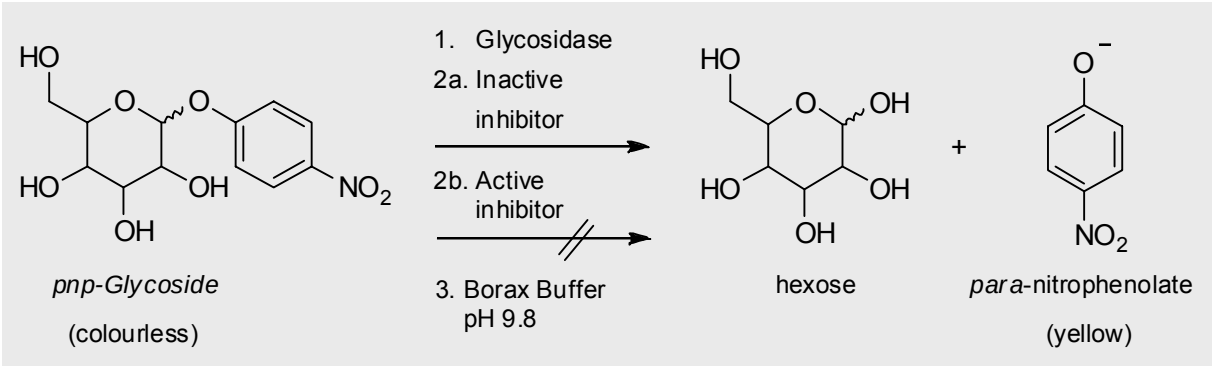

Scheme 60: Enzymatic clevage of *p*-nitrophenyl-glycosides is a colour-indicator method to measure the activity of a inhibitor.

If the inhibition should be higher than 50 %, the inhibition constants IC_{50} and K_i are then determined. The values obtained for IC_{50} represents the concentration of inhibitor required to reduce the maximum velocity of the enzymatic reaction by 50 % (i.e. $v_{max}/2$). The value of K_i represents an inhibition constant obtained from the Michaelis Menten kinetics and represents also the affinity of the inhibitor for the enzyme. The affinity for the enzyme is measured over a range of substrate concentrations, while keeping the concentration of the inhibitor constant. In the case of a purely competitive, reversible inhibition, the IC_{50} and K_i values should be the same (corresponding to the Michaelis-Menten constant, K_m). However this is seldom the case, since fundamentally different test conditions are used. For example, the measurement of the K_i value is done using a Lineweaver-Burk plot, taking the reciprocal of the reaction rate (or an equivalent measure, in this case the recprical of absorption, 1/A, at 405nm of the release of from the pnp-glycosides) against the recpriocal of substrate concentration 1/[S].

6.5.2 Tables of the biological results

In this chapter, the determined inhibition constants for 18 of the synthesised iminipolyols is given. The key to the meaning of the values in Tables 14-18 is displayed below in Table 13. The Enzyme Classification number (EC Nr.) is used to break the glycosidases down into GH

families according to the sequence-based CAZy classification (http://www.cazy.org). For the tert.-butyl-substituted pyrrolidine **110·HBr** and the "biphenyl"-substituted fuconojirimycin derivative **115·HCl**, *in vitro* testing was carried out with *bovine kidney* α-L-fucosidase only.

Table 13: List of the enzymes employed for the inhibition tests

Nr.	EC Nr.	Enzyme	Source	Enzyme Family[2]	pH
28	3.21.51	α-L-fucosidase	bovine kidney	29	6
2	3.2.1.22	α-galactosidase	coffee beans	27	6
3			*Aspergillus niger*	27	4
4			*Escherichia coli*	36	7
5	3.2.1.23	β-galactosidase	*Escherichia coli*	2	7
6			bovine liver		7
7			*Aspergillus niger*	35	4
8			*Aspergillus oryzae*		5
9			jack beans		4
10	3.2.1.20	α-glucosidase (maltase)	yeast	13	7
11			rice		7
29			*Sacc. Cerevisiae*		?
12	3.2.1.10	α-glucosidase (isomaltase)	baker's yeast		7
13	3.2.1.3	amyloglucosidase	*Aspergillus niger*	15	5
14			*Rhizopus* mould		5
15	3.2.1.21	β-glucosidase	sweet almonds		5
24			*Caldocellum saccharolyticum*	1	5
16	3.2.1.24	α-mannosidase	jack beans		5
17			sweet almonds		5
18	3.2.1.25	β-mannosidase	*Helix pomatia*		4
26			small acetone powder		4
19	3.2.1.37	β-xylosidase	*Aspergillus niger*	3	5
20	3.2.1.49	α-*N*-acetylgalactosaminidase	chicken liver	27	4
21	3.2.1.30	β-*N*-acetylglucosaminidasse	jack beans		5
22			bovine epididymis A		4
23			bovine epididymis B		4

Table 14: Biological results of the fucosidase inhibitors synthesised in this work. Inhibition in [%] at 1 mM substrate concentration; IC_{50} and K_i in [μM]

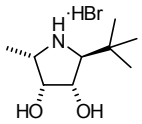

110·HBr

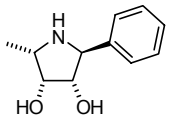

AP[a]

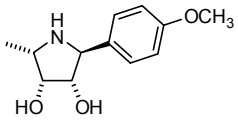

105

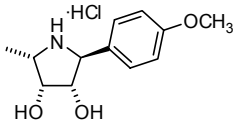

96·HCl

Enzyme family												
Nr.	% I	IC_{50}	K_i	% I	IC_{50}	K_i	% I	IC_{50}	K_i	% I	IC_{50}	K_i
28	45	1238		100	0.35	0.050	100	0.15	0.025	100	0.16	0.013
2				5			17			25		
3				0			0			0		
4												
5				15			0			30		
6				15			5			11		
7				0								
8				5			0			0		
9												
10				5			31			0		
11				5			0			14		
29							75	390	395	90	190	315
12												
13				10			27			35		
14				10			50	984		47		
15				6			0			11		
24				0			3			28		
16				0			0			0		
17				15			1			0		
18							0					
26				0			7			19		
19				7			1			0		
20				0			5			6		
21				0			10			0		
22				23			0			8		
23				0			8			0		

Not tested

[a] For fucosidase sourced from *bovine epididymis*, % I = 100, IC_{50} = 0.40, K_i = 0.040.

Table 15: Biological results of the fucosidase inhibitors synthesised in this work. Inhibition in [%] at 1 mM substrate concentration; IC_{50} and K_i in [μM]

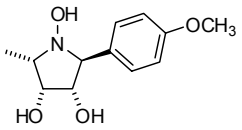

83

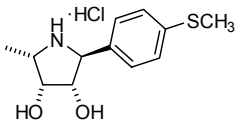

101·HCl

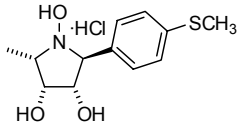

85·HCl

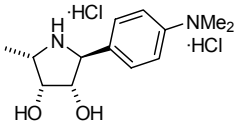

104·2HCl

Enzyme family / Nr.	% I	IC_{50}	K_i	% I	IC_{50}	K_i	% I	IC_{50}	K_i	% I	IC_{50}	K_i
28	100	28	6.3	100	0.14	0.0055	100	0.14	0.016	100	0.14	0.029
2	0			0			0			0		
3	0			3			0			7		
4												
5	82	89	87.1	9			41			26		
6	9			11			40			10		
7												
8	0			4			0			0		
9												
10	95	100	21.4	0			15			0		
11	0			1			11			0		
29	96	28	21.0	49	390	395	100	13	2.69	32		
12												
13	2			31			2			29		
14	41			28	984		45			17		
15	2			2			15			0		
24	6			1			27			2		
16	0			4			0			0		
17	0			4			3			0		
18												
26	6			0			11			11		
19	0			5			0			0		
20	2			0			4			1		
21	5			1			0			9		
22	18			0			5			18		
23	15			5			0			4		

Table 16: Biological results of the fucosidase inhibitors synthesised in this work.
Inhibition in [%] at 1 mM substrate concentration; IC_{50} and K_i in [μM]

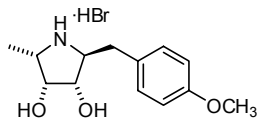

112·HBr

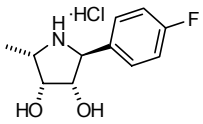

98·HCl

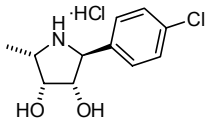

99·HCl

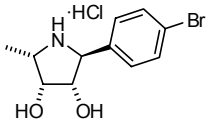

100·HCl

Enzyme family												
Nr.	% I	IC_{50}	K_i	% I	IC_{50}	K_i	% I	IC_{50}	K_i	% I	IC_{50}	K_i
28	99	18	3.4	100	0.18	0.044	100	0.19	0.036	100	0.17	0.031
2	0			5			0			2		
3	0			0			6			0		
4												
5	7			4			7			6		
6	10			0			8			4		
7												
8	0			6			3			4		
9												
10	48			24			2			5		
11	1			3			0			2		
29	48			61	1329		9			15		
12												
13	1			23			14			22		
14	5			33			19			36		
15	1			8			0			0		
24	0			5			0			3		
16	2			1			4			0		
17	0			3			2			1		
18												
26	0			30			3			14		
19	2			0			0			5		
20	1			8			10			15		
21	3			0			0			5		
22	7			0			1			0		
23	6			10			2			0		

Table 17: Biological results of the fucosidase inhibitors synthesised in this work. Inhibition in [%] at 1 mM substrate concentration; IC_{50} and K_i in [μM]

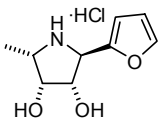

103·HCl

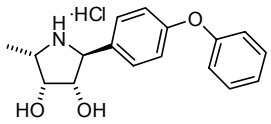

102·HCl

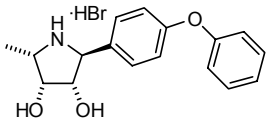

102·HBr

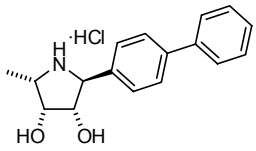

97·HCl

Enzyme family / Nr.	% I	IC_{50}	K_i	% I	IC_{50}	K_i	% I	IC_{50}	K_i	% I	IC_{50}	K_i
28	100	0.36	0.103	100	0.13	0.0092	100	0.014	0.0126	100	0.016	0.0012
2	5			0			0			0		
3	1			0			0			0		
4												
5	3			17			29			43		
6	0			41			27			25		
7												
8	0			0			0			0		
9												
10	3			0			0			22		
11	2			19			18			0		
29	20			0			100	46	25.3	46	1186	
12												
13	9			59	815		54	910		36		
14	18			64	528		74	682		47		
15	1			8			6			0		
24	2			27			27			0		
16	2			0			0			3		
17	1			0			4			0		
18												
26	4			7			20			0		
19	0			0			0			2		
20	0			4			24			14		
21	0			0			0			2		
22	3			0			9			2		
23	2			0			0			2		

Table 18: Biological results of the fucosidase inhibitors synthesised in this work. Inhibition in [%] at 1 mM substrate concentration; IC_{50} and K_i in [μM]

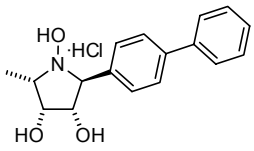

84·HCl

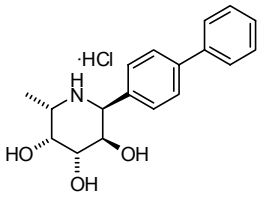

115·HCl

Enzyme family						
Nr.	% I	IC_{50}	K_i	% I	IC_{50}	K_i
28	100	0.14	0.072	98	0.18	1.5
2	0					
3	0					
4						
5	42					
6	41					
7						
8	0					
9						
10	82	777				
11	6					
29	100	0.49	0.65			
12						
13	2					
14	25					
15	11					
24	32					
16	0					
17	0					
18						
26	0					
19	0					
20	0					
21	0					
22	8					
23	0					

Not tested

Diagram 66: Inhibition selectivity of selected polyhydroxylated pyrrolidines towards glycosidases

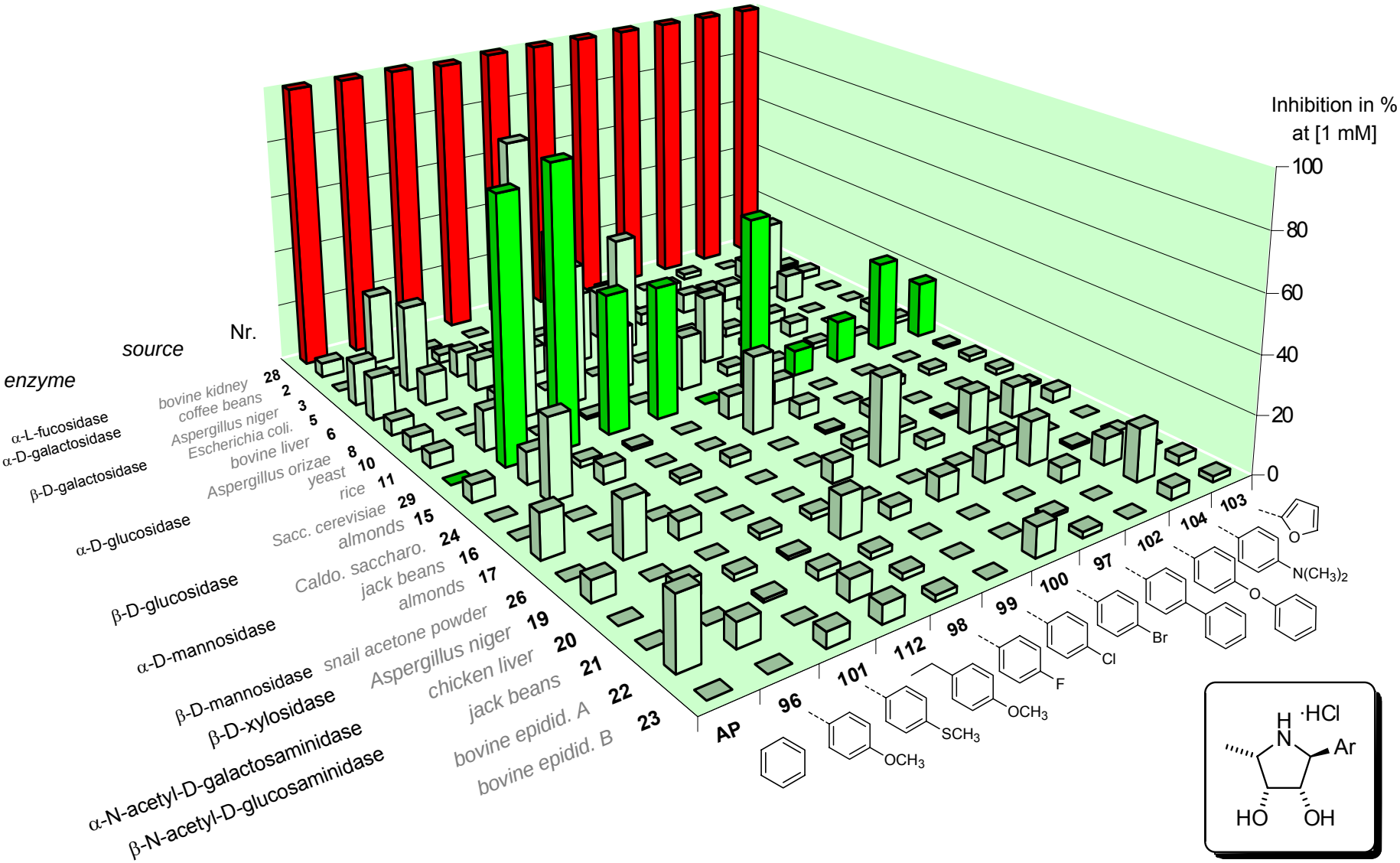

Diagram 67: Inhibition potency of all inhibition candidates against *bovine kidney* α-L-fucosidase

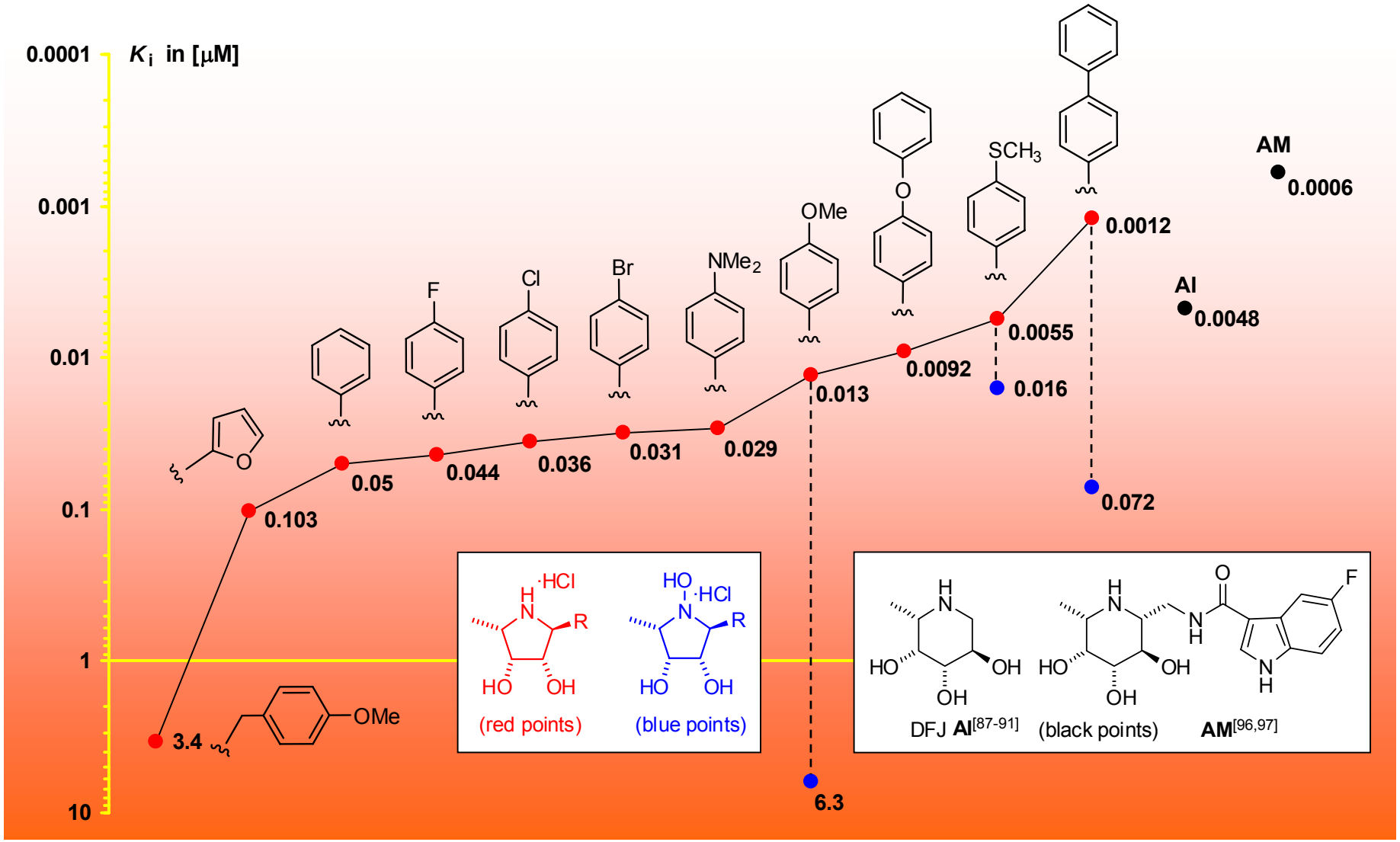

6.5.3 Discussion of structure-activity relationships

As shown above in the preceeding Tables 14-18, comprehensive glycosidase inhibition essays with up to 28 commercially available glycosidases were carried out. Gratifyingly, the results showed (apart for the *tert.*-butyl-substituted pyrrolidine diol **110·HBr**, see below) a selective inhibition of *bovine kidney* fucosidase at 1 mM inhibitor concentration. Essentially, none of the other enzymes under scrutiny were inhibited, as the selected data in the graphics clearly show (Diagrams 66 and 67). However, some isolated cross-inhibition of the *bier yeast* α-glucosidase (maltase) was observed, most notably by the *p*-thioanisyl, *p*-fluorophenyl, and *p*-methoxyphenyl-pyrrolidinediols, **101·HCl** (90 %), **98·HCl** (49 %) and **96·HCl** (61 %), respectively. In terms of the values obtained for the inhibition of α-L-fucosidase from *bovine kidney*, a brief account of plausible structure-activity conclusions can be drawn as follows:

(a) The presence of large, flat aromatic side chains was clearly preferred by α-L-fucosidase rather than for sterically voluminous, non-aromatic side chains; flexibility in the side chains is also not tolerated well. For instance, the *tert*-butyl-substituted pyrrolidine hydrobromide **110·HBr** was bereft of any useful enzyme inhibition (K_i = 1.24 mM), hinting that the voluminous *tert.*-butyl moiety may compromise the formation of a stable-enzyme inhibitor complex. The inhibition potency of this substance is even lower than the parent pyrrolidine of this class, the L-*lxyo*-configured diol **AN** from Bierer.[2] Similarly, the *p*-methoxybenzyl unit at C-2 in pyrrolidine diol **112·HBr** led to a weaker inhibitor than **AN** bearing no substituent at C-2. This suggests that the orientation of the flexible benzyl units, through inclusion of the methylene spacer, was not conducive for a “good fit” within the aglycon site. This contrasts to the case of the aminocyclopentantriols from Reymond and co-workers[403-406] (Section 6.4.1.2) when the same tactic was employed.

(b) Potent inhibition of α-L-fucosidase was obtained for the remaining pyrrolidine diol hydrochlorides with the aromatic moieties attached directly to C-2, as can be seen clearly in Diagram 67, from the 2-furyl-candidate **103·HCl** and thereafter, where IC_{50} values from 0.36 to 0.012 μM were measured. In comparison, the IC_{50} values of the fucosidase inhibitors from Bierer (cf. Thesis, lit.[2]) – bearing “non-aromatic” side chains directly attached to C-2 – were distinctly higher (e.g. IC_{50}: 22 μM for 2-R = CH_2NH_2 to 0.90 μM for 2-R = 2,3-dihydroxypropyl; hydrochloride salts; *bovine kidney*). The results further cement the findings that the aglycon subsite of α-L-fucosidase prefers a flat, hydrophobic sidechain to a hydrophilic one. Further, it is pleasing to

observe the enzyme's tolerance to new substrates augmented with *O*-methyl and *N*-dimethyl linkages at the *para*-position of the aromatic substituent. For example, in terms of the spread of K_i-values from 0.044 to 0.031 μM, a comparable interplay between the enzyme and the halogenated inhibitors **98**-**100·HCl** is found, which highlights a remarkable indifference of the enzyme to the lipophiliciy of the halogen substituent.

(c) A significant improvement in the binding constant to K_i = 0.0055 μM in the *p*-thioanisyl-substituted inhibitor (**101·HCl**), compared its methoxy counterpart, i.e. **96·HCl** (K_i = 0.025 μM) was a surprising result. This could be an indication of a specific H-bond interaction between one (or more) enzyme residues with the inhibitor.

(d) The exchange of *O*-methyl (**96·HCl**; K_i = 0.013 μM) for *O*-phenyl (i.e. **102·HCl**; K_i = 0.0092 μM) brought improvements in binding of the inhibitor to the enzyme. This demonstrates again the "hydrophobic effect". Omitting the oxy-bridge, however, lowered to K_i even further to 0.0012 μM for the "biphenyl"-derivative – overtaking the "parent" imino analogue of the natural substrate (i.e. DFJ **AI**; K_i = 0.0048 μM, cf. lit.[87-91]) in the process. This sets a new low for fucosidase inhibiton in this "structural class" as far as we are aware of! The inhibitors **97·HCl** and **102·HCl** are likened as being "*pseudo*-trisaccharides", since it can be argued that the extended side chain is capable of mimicing the hydrophobic pyranose core of the neighbouring +1/+2 monosaccharide subsites at the aglycon.

(e) Going from the "parent" L-*lyxo*-configured pyrrolidine diol **AN**[2] to the α-L-*lyxo* "biphenyl"-inhibitor **102·HCl** constitutes a ca. 60-fold improvement in inhibition potency. This contrasts to the Wong's series of elaborated 2-(amidomethyl)-aryl piperidines, such as to the best-case derivative **AM** for the *bovine kidney* source (Diagram 62, Section 6.4.1.3). As was shown, here only a ca. 10-fold enhancement over binding of its respective "parent" inhibitor, the piperidine DFJ **AI**, was achieved, despite the large increase in molecular complexity. Caution against a critical comparison is necessary, because the parent compounds of each class are obviously dissimilar transition state analogues; further, the side chains employed in Wong's work and from this Thesis essentially non-related.

(f) The inhibitory potency of pyrrolidines of type **AN** is attributed to their lower steric demand and a better resemblance of "half-chair" furanose structures at the transition

state (cf. discussion in Section 6.3). Obviously, the great leverage in "inhibitory gains" for the pyrrolidine diol inhibitors in this work catagorises them as being "mixed-type" inhibitors. Based on the inhibitors with "phenyl"(**AP**) und "biphenyl" (**97·HCl**) side chains, a change in K_i of ca. 1.6 logarithmic units equates to a lowering of the binding free energy ($\Delta G°$) of 9.3 kJ/mol (2.3 kcal/mol). This drop in $\Delta G°$ can be reconciled by the disruption of structured H-bonding with ordered water in the enzyme's active site following the docking of the lipophilic side chain. The water molecules which are squeezed out at this point result in increased disorder. Setting these water molecules in motion will have a positive effect on the entropy or *translational entropy*, thus the binding free energy is decreased, resulting in the lower K_i values observed.[28] This "liberation" of bound water molecules is illustrated in Diagram 68:

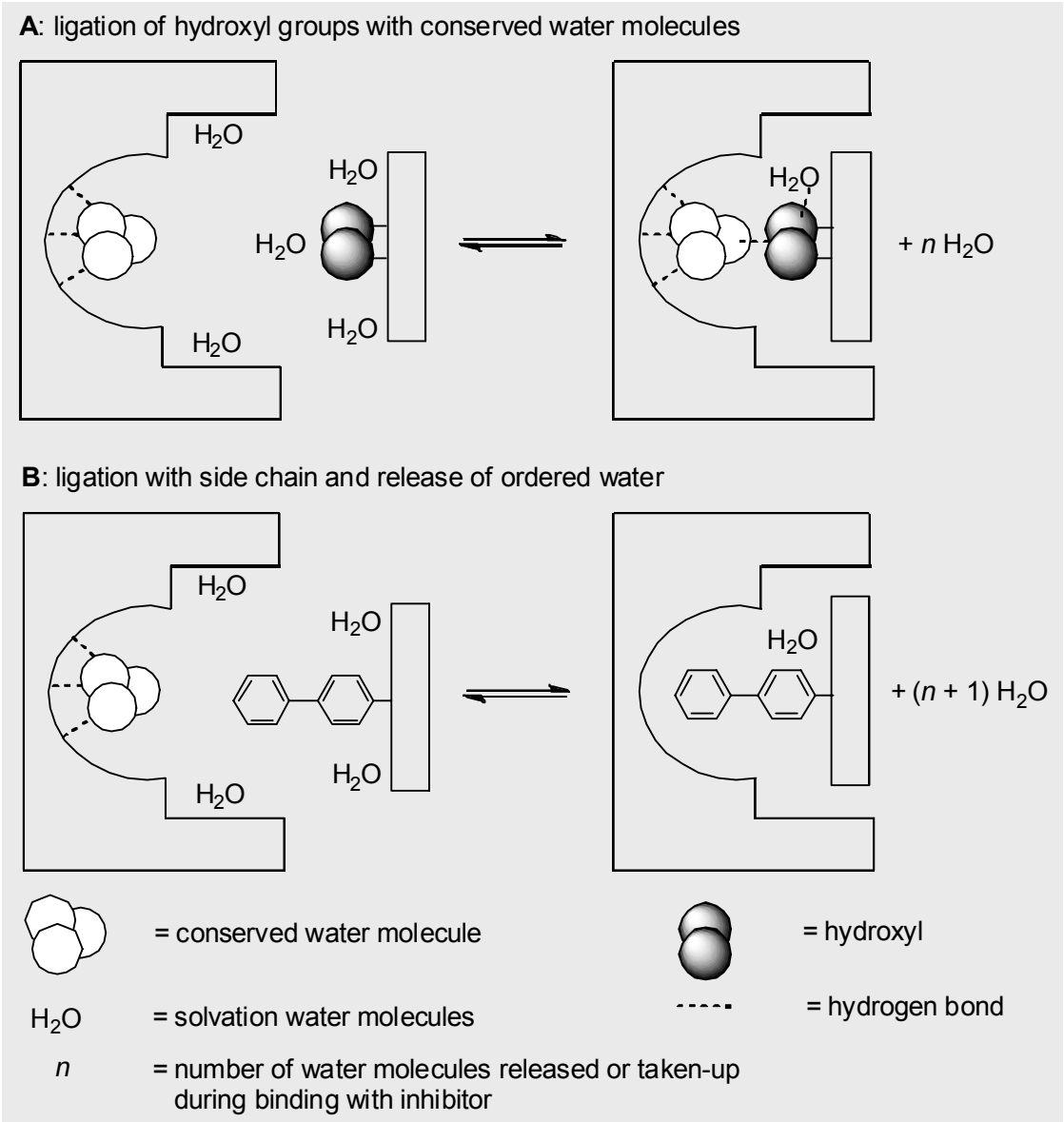

Diagram 68: The release of water from the active site upon side chain ligation

(g) For all pyrrolidine triols (**83**, **85·HCl** & **84·HCl**) a significant reduction in binding strength was found in comparison to the respective pyrrolidine diols. We initially thought that the N-OH moiety would be able to engineer further "binding interactions" with residues in the catalytic site. This turned out to be an incorrect assumption. With the inhibitor-enyzme complex, the catalytic acid, it is assumed (cf. Sections 6.2 and 6.3), can protonate the inhibitor giving an ion-pair and a source of attractive "electrostatic interactions". The inclusion of the N-OH moiety may reduce the pK_a of the inhibitor to a level of insufficient basicity to be protonated effectively by the catalytic acid. To reiterate, the pK_a value is simply the equilibrium constant for ionization. A rule of thumb from the Henderson-Hasselbalch equation is that for each unit difference in pH – pK_a, the tendancy of a basic ring moiety to accept a proton decreases tenfold. The lower limit, according to Legler[1] is around pK_a ≈ 4, since mathematically, assuming that an enzymatic test will be carried out at pH ≈ 7, the pH – pK_a ≈ 3, or [base]/[acid] = 1/1000, or % unionized/% ionized = 99.9/0.1. In this Thesis, the enzymatic tests were carried out at the pH optimum of the fucosidase (pH 6) and *not* at the pH optimum of the inhibitor. It would be interesting to investigate the dependence of 1/K_i on pH in accessing the ionisation state of these "N-OH inhibitors" over a wider range of pH values. Another point is that the N-OH substituent may impair interactions of the endocyclic –NH- group with the catalytic acid/base if standing *pseudo-equitorially* (?) on the same side. Remember, α-L-fucosidase catalyses the hydrolysis with retension of configuration and so a close distance of ≤ 3.0 Å is necessary between catalytic acid/base with the inhibitor – as discussed in detail in Section 6.1. This is a valid argument because the microenvironment of the ionisable group will affect the pK_a value also.

(h) Since the fucosidase inhibition constant of the "biphenyl" substituted deoxyfuconojirimycin derivative **115·HCl** stands alone, it is difficult to analyse this loss of activity in any valid context. One possible reason could be the change in ring conformation of the inhibitor: this L-*fuco*-C-glycoside is not $^1C_4$ in solution (usual for the α-L-fucopyranosides) but rather predominately $^4C_1$, for reasons dicussed earlier in relation to the rotational stability of the bulky "biphenyl" unit (cf. Section 5.1.8, p. 125). It is known, for example, from the crystal structure of *Thermotoga maritima* α-L-fucosidase that the exocyclic C-6 methyl group is enclosed in hydrophobic contact to largely conserved phenylalanine and tyrosine residues; important seems to be also the axial orientation of 4-OH, which is stabilised by histidine residues.[374] Modelling studies, according to Dashnau and co-workers,[423] reveal that a shift in hydroxyl

position from equatorial to axial may have significant effects on local water networks and the energetic cost of desolvation. A change in ring conformation may hence negatively perturb these interactions and interfere with the essential residues for catalysis in the proximity of the active site.

7 Summary

7.1 Bromocyclisations and Synthesis of Fucosidase Inhibitors

The main themes of this PhD thesis entailed the synthesis of new candidates for glycosidase inhibition assays. Glycosidases catalyze the degradation (i.e. hydrolytic cleavage or transfer) of glycosidic bonds. The synthesis of suitable, selective inhibitors of glycosidases may be a tool to stop detrimental or disease-related cell processes and may be of therapeutic value. In particular, this work focused on the synthesis of α-L-fucosidase inhibitors. Known inhibitors were taken for orientation: e.g. deoxyfuconojirimycin (DFJ, **AI**), which is a direct imino-analogue of the natural substrate (cf. α-L-fucoside), or the related one-carbon less 'L-*lyxo*' configured pyrrolidine **AN**, itself a selective, albeit less potent, competitive inhibitor of α-L-fucosidase. Noteworthy is that the 2-substiution at the pyrrolidine ring led to the discovery of a new lead compound **AP**, as described previously by Bierer and Jäger (Diagram 69).[2]

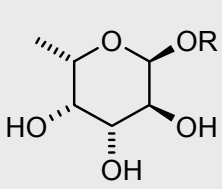

α-L-FUCOSIDE

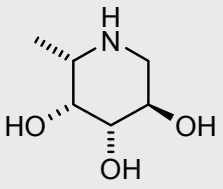

AI 'DFJ'[88-91]

K_i = 0.0048 μM b. k.

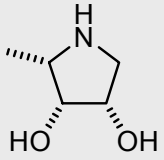

AN 'L-*lyxo*'[2]

0.70 μM b. e.

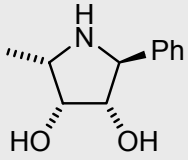

AP[2]

0.05 μM b. k.

Enzyme source: b. k. bovine kidney; b. e. bovine epididymis

Diagram 69: Iminopolyol fucosidase inhibitors relevant to this work

The route to these pyrrolidines relied on the halogen-induced cyclisation of unsaturated hydroxylamines. This reaction gives access to cyclic nitrones which are a class of synthetically versatile compounds. Starting from D-ribose, the unsaturated *erythro* pentenose oxime **4** is made in four efficient steps. In the presence of bromine, under neutral conditions, a bromocyclisation could be induced to afford two diastereomeric cyclic nitrones **5** and **6** in a

very respectable 64 % yield. Note that the desired L-*lyxo*-nitrone **5**, in which the configuration of the three of the four contingent stereocentres matches those in the natural substrate L-fucose, was obtained as the major diastereoisomer (Scheme 61).

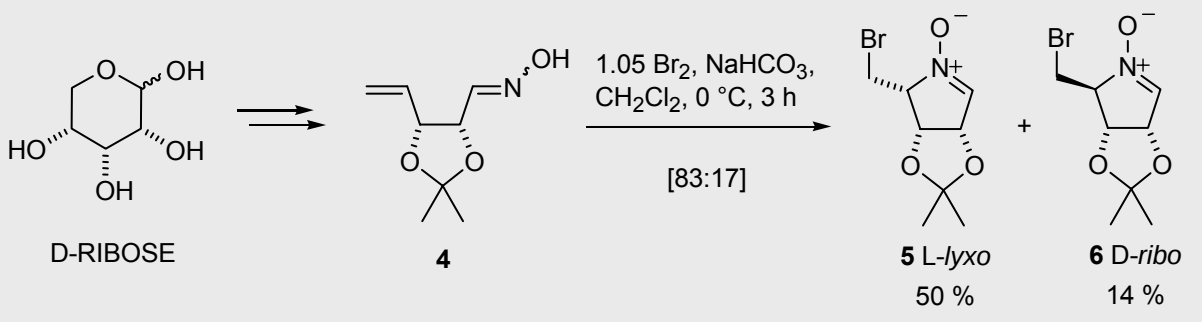

Scheme 61: The bromocyclisation of the D-ribose-derived pentenose oxime to yield the key L-*lyxo* nitrone **5** as the main product (cf. lit.[2])

With the L-*lyxo*-nitrone **5**, the addition of Grignard reagents furnished tetra-substituted pyrrolidines in high diastereoselectivity. A two-step reduction sequence and cleavage of the isopropylidene protecting group followed, to rapidly produce a library of polyhydroxylated pyrrolidines bearing several *para*-substituted aromatic side-chains (Scheme 62).

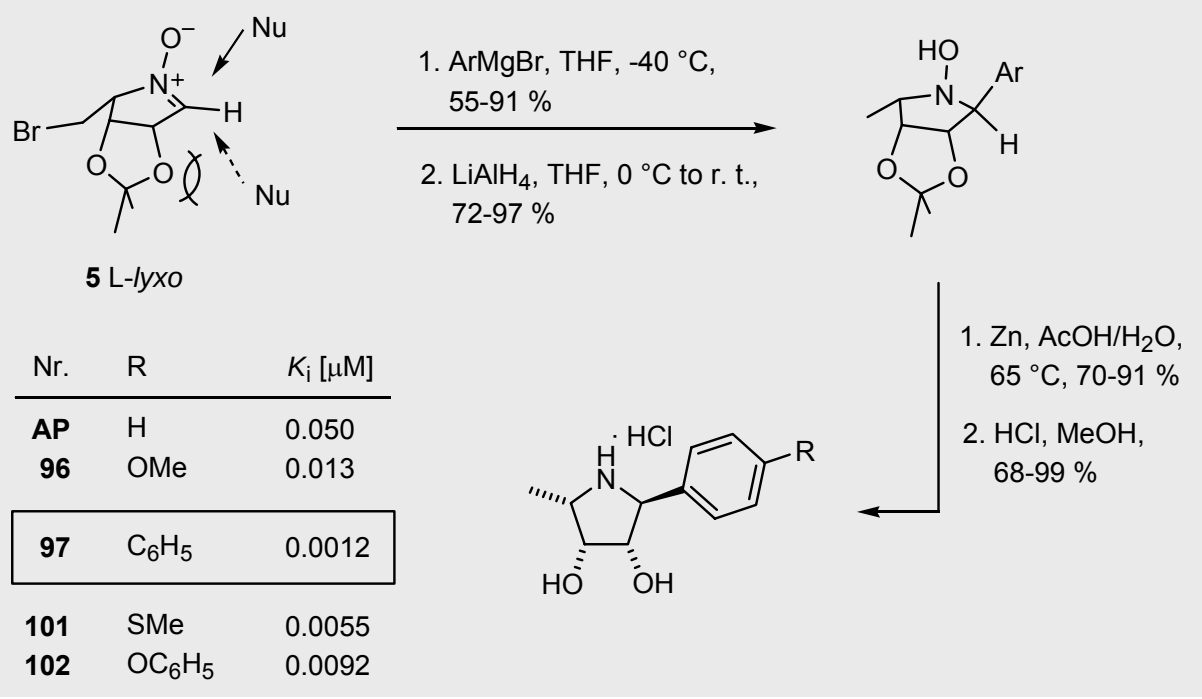

Nr.	R	K_i [μM]
AP	H	0.050
96	OMe	0.013
97	C_6H_5	0.0012
101	SMe	0.0055
102	OC_6H_5	0.0092

Scheme 62: The expedient route to the pyrrolidine diols bearing extended aromatic sidechains with potent fucosidase inhibition (cf. lit.[2])

The strategy of introducing substituents at the *para*-position of the phenyl substituent in **AP** paid dividends, leading to new candidates with considerably better inhibition potencies. In fact, a ca. 50 fold increase in α-L-fucosidase activity (against bovine kidney) could be achieved in the case of the biphenyl-substituted derivative, pyrrolidine **97·HCl** (K_i = 0.0012 μM, *bovine kidney*). Compared to the Bierer's[2] lead compound **AP** (K_i = 0.050 μM, *bovine kidney*), it is one of the strongest fucosidase inhibitors known to date (cf. Section 6.5).

In light of these astonishing improvements in inhibition potency, the second task was to synthesise piperidine analogues, i.e. 2-substituted derivatives of the potent α-L-fucosidase inhibitor, DFJ **AI**. This required the synthesis of key L-*fuco*-configured nitrone **28**, obtained in 8 steps from D-lyxose, along with a diastereoisomer, the D-*altro*-nitrone **29** (Scheme 63).

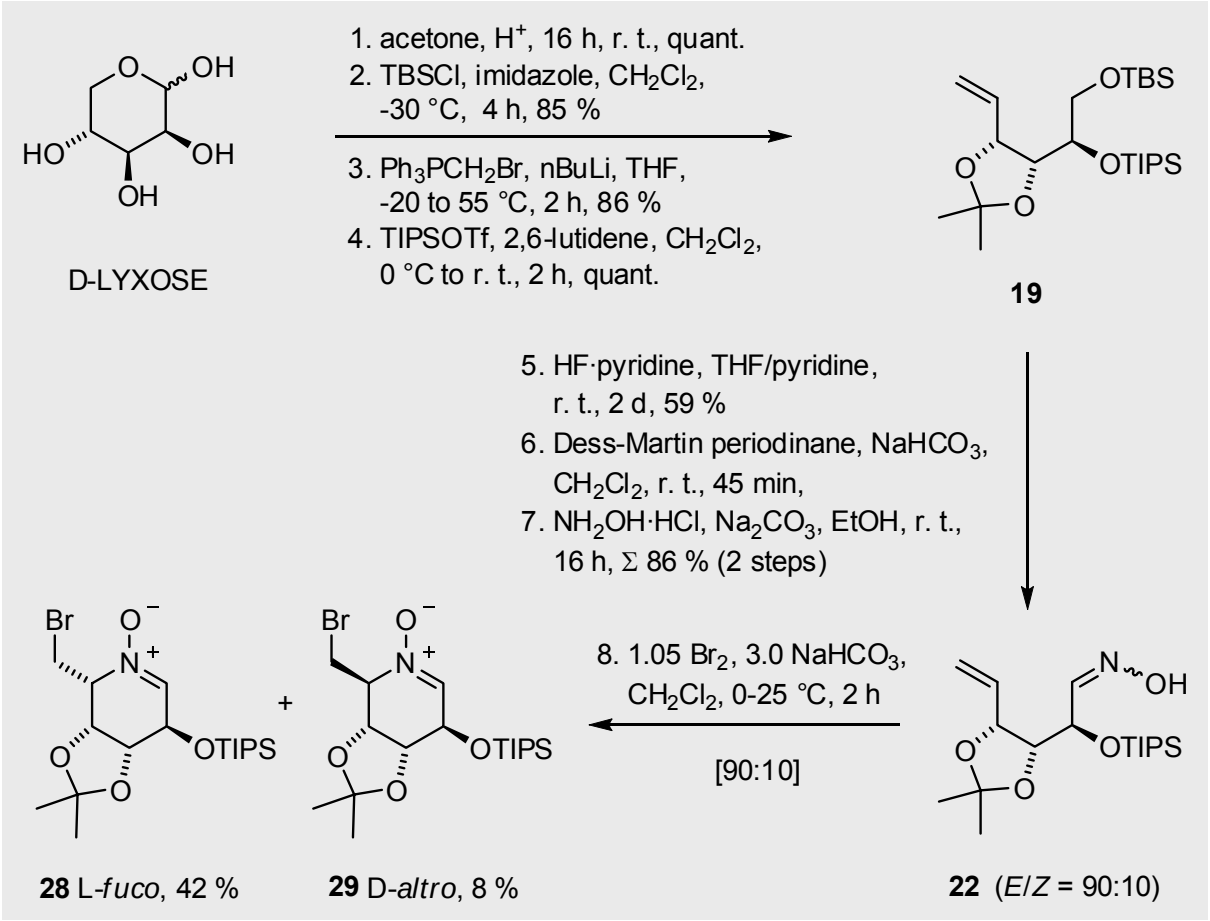

Scheme 63: Route to the D-lyxose-derived hexenose oxime **22** and subsequent bromocyclisation to afford the key L-*fuco*-nitrone **28** as the main component

The L-*fuco*-configured nitrone **28**, this time with all of the stereocentres of the natural substrate in place, was transformed in four additional steps into the deoxyfuconojirimycin-*C*-glycoside derivative **115·HCl** (in total 12 steps from D-lyxose, Σ 4.4 %, Scheme 64).

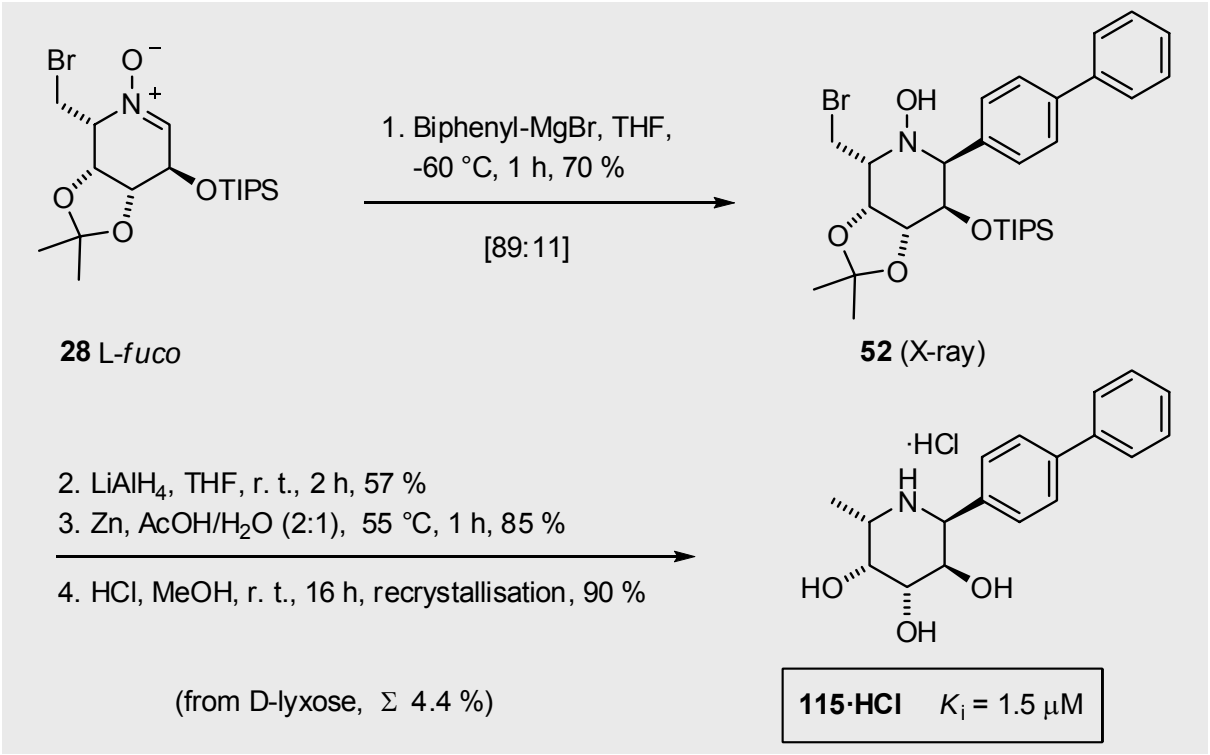

Scheme 64: Synthesis of the deoxyfuconojirimycin *C*-glycoside derivative **115·HCl**

Unfortunately, in comparison to the inhibitors featured above, this piperidine derivative lacked the fucosidase inhibition potency of its pyrrolidine counterparts, being a factor of ca. 1000 weaker in terms of the K_i values. However, further studies are underway to investigate this surprising result.

7.2 Oxidation of *N*-Hydroxypyrrolidines

Another aspect of this Thesis concerned the regioisomeric selectivity of the oxidation of tri- and tetra-substituted *N*-hydroxypyrrolidines and, to a lesser extent, the subsequent reactions of the new nitrones that were created. The results can be summarised as follows:

(a) The reactions employing manganese dioxide as oxidant were quicker than those which employed mercury(II) oxide, though the regioselectivities obtained in both cases were more or less identical.

(b) For the reaction of the 2-methyl-*N*-hydroxypyrrolidines **31** and **33**, the formation of the respective ketonitrones was favoured over the respective aldonitrones. This was in accordance with the literature findings and with basic thermodynamic and kinetic considerations (cf. discussions from Section 4.2 onwards).

(c) For the 2-methyl-substituted *N*-hydroxypyrrolidines **31** and **33**, only negligible differences were observed in oxidation regioselectivity for (i) the extraction of a *trans*-standing 2-H (with respect to the neighbouring acetonide protecting group) in comparison to (ii) the extraction of a *cis*-standing 2-H (with respect to the neighbouring acetonide protecting group), irrespective of the oxidant used. Thus, steric hindrance was not a significant factor at the site of hydrogen extraction:

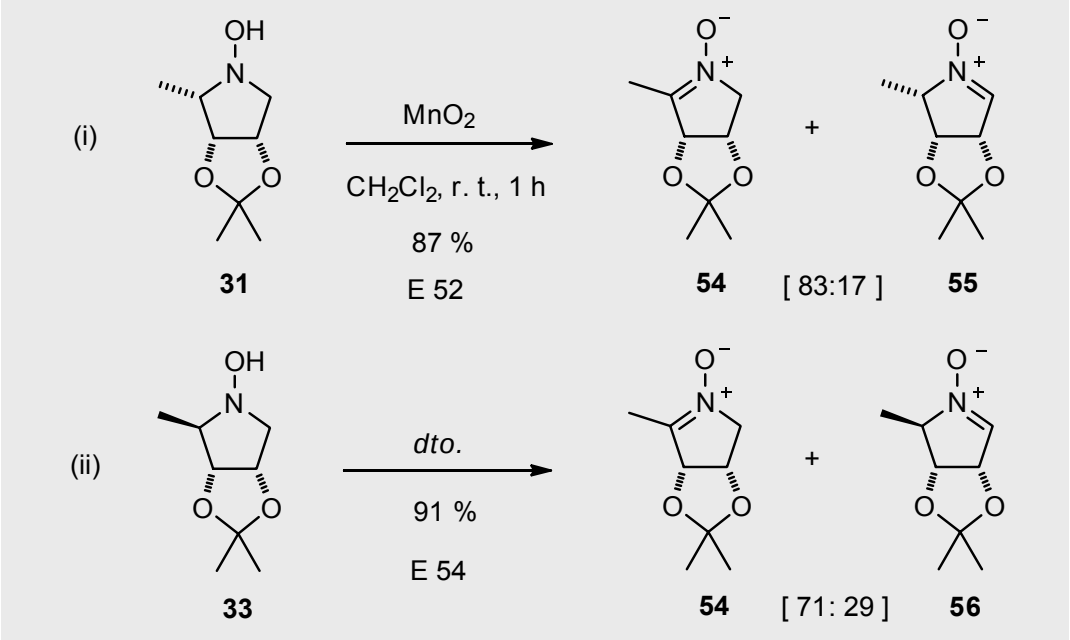

(d) On the other hand, the stereoelectronic effect was shown to be able to influence the extent of the regioisomeric outcome of the oxidation. This was studied with the 2-bromomethyl-*N*-hydroxypyrrolidines, that is, the (iii) L-*lyxo*- and (iv) D-*ribo*-substrates **30** and **32**, respectively, as the following scheme demonstrates:

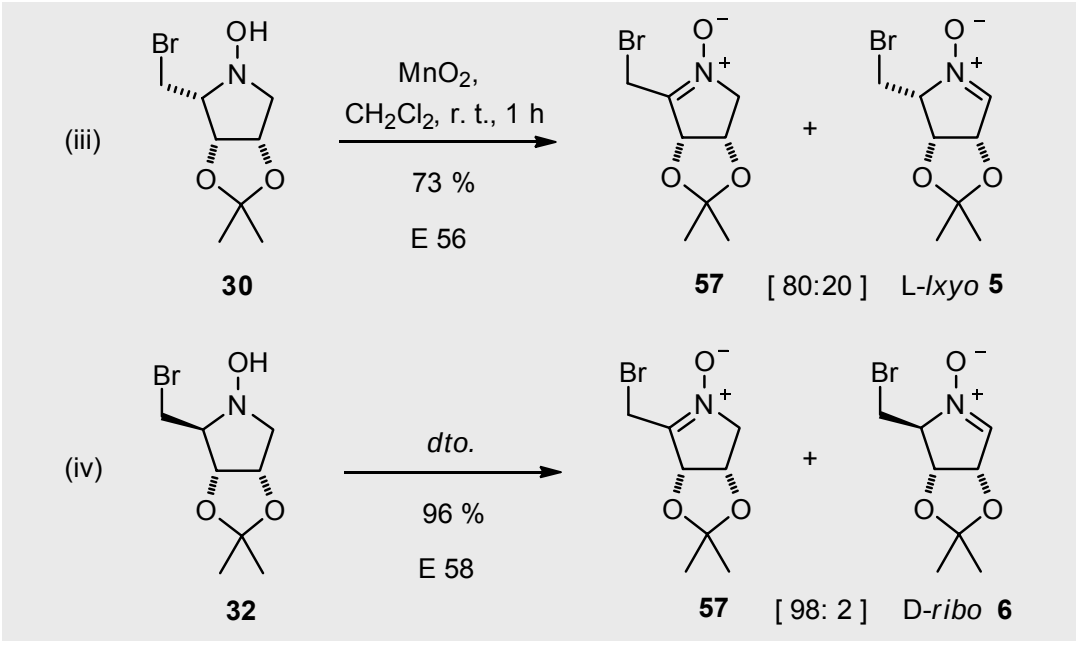

Essentially, a large enhancement in regioisomeric selectivity was found for the oxidation of the D-*ribo* derivative compared to the L-*lyxo* substrate, i.e. for D-*ribo* **32**, r. r.. = 98:2, whereas for L-*lxyo* **30**, r. r.. = 80:20. This suggests that the barrier to the abstraction of the 2-H atom in the D-*ribo* compound **32** was in relative terms approx. 1.50 kcal/mol lower than for the other diastereoisomer. The stereoelectronic effects which explain this relate to the disposition of the bromomethyl group with respect to the neighbouring proton on C-2. To summarise briefly, in D-*ribo* **32**, the bromine atom is standing *anti-periplanar* to 2-H. In this case, there is a possibility for overlap between the bonding $\sigma_{C—H}$ and anti-bonding $\sigma^*_{C—Br}$ orbitals, which can be visualised as follows:

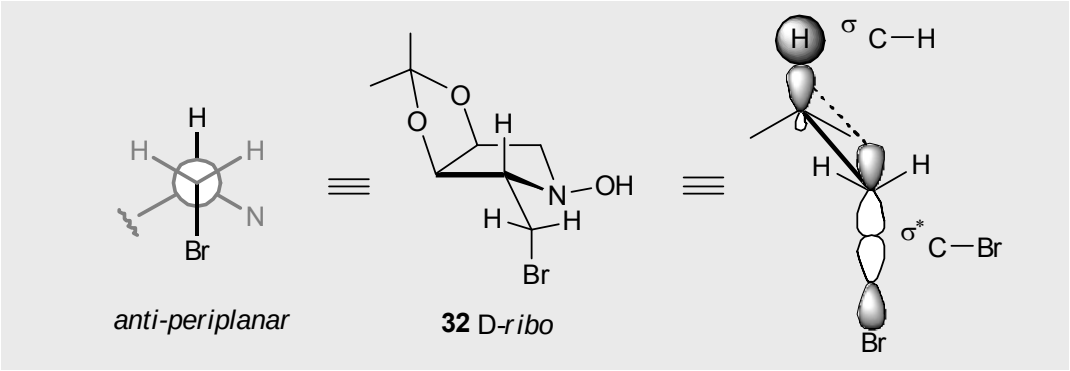

What this boils down to is that there is a hyperconjugative stabilisation of the incipient negative charge/unpaired electron developing during the extraction of the hydrogen in question. This means that the corresponding *anti* C-H bond is favourably cleaved (cf. Section 4.2.2 and lit.[303,308b,313]). For the L-*lyxo*-configured pyrrolidine **30**, the bromomethyl group is *syn-clinally* disposed to 2-H according to detailed NMR analysis and thus there are no, or rather, diminished "hyperconjugative" interactions available.

(e) The oxidation of the 5-anisyl-2-bromomethyl-substituted *N*-hydroxypyrrolidine **41** (v) was also studied in order to investigate the degree of product formation favouring the conjugated nitrone, in this case the nitrone **EU**, as follows:

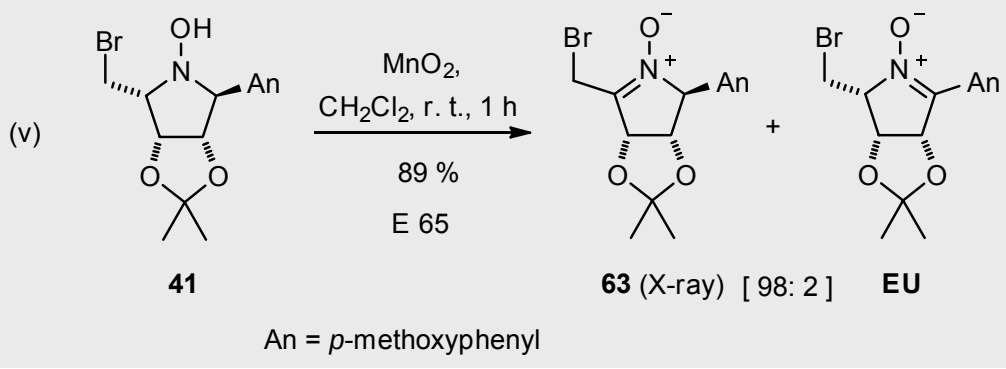

However, the results show that the oxidation was regioselective to the other side, to provide the unconjugated bromomethyl-ketonitrone **63**. Again, the outcome of this oxidation reflected the stereoelectronic effects, which favoured the extraction of the hydrogen standing *trans* or pseudo *anti-periplanar* to a neighbouring alkoxy substituent. In this instance, this turned out to be 2-H next to the alkoxy unit at C-3. The bromomethyl group in substrate **41** is *syn-clinal* dispositioned and, as discussed above and in Section 4.2.2, does not assist in aiding proton abstraction. An X-ray structure could be obtained from the bromomethyl-ketonitrone **63** to provide additional structural proof (cf. Section 9.8).

7.3 Outlook

The most salient aspects of this dissertation work have been summarised above. Of course, there are some prominent questions that come to mind when deciding where to go next. It is probably of little intellectual value to be mind-set on churning out dozens of additional pyrrolidine inhibitors in search of fucosidase inhibitory gains. As an alternative, more potential exists perhaps in the development of cyclic nitrones in the six-membered series, be it those of D-*manno*, D-*galacto*, D-*gluco* or, as initiated in this work, L-*fuco* configuration. Several endeavours have been started in these directions already, particularly by Mr. F. Wallasch[121] and Mrs. J. Heller.[122] However, the yields of the bromocyclisations leading to six-membered nitrones need to be improved. There are many possible avenues for improvement and one would be to investigate the nature of the protecting group(s). In this thesis, the triisopropylsilyl-protected oximes upon bromocyclisation returned much better yields compared to their *tert*-butyldimethylsilyl-protected counterparts. This should be extended to *tert*-butyldiphenylsilyl-protected oximes also, as follows:

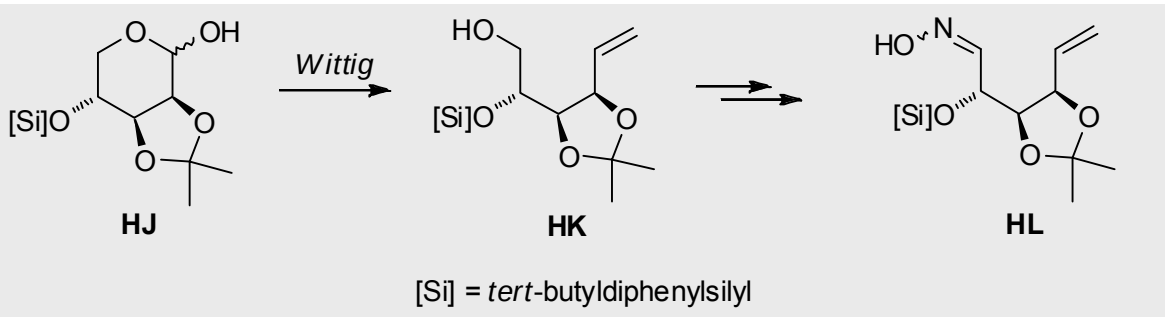

HJ **HK** **HL**

[Si] = *tert*-butyldiphenylsilyl

Scheme 65: The suggested synthesis of a rather bulky *tert*-butyldiphenylsilyl-protected oxime **HL** as a substrate for the bromocyclisation

As alluded to in Scheme 65, the synthesis of this oxime should proceed *via* the pyranose derivative **HJ** and Wittig olefination to provide primary alcohol **HK**, followed by oxidation and oximation in the usual way. This especially bulky silyl group should not undergo migration to the neighbouring alcohol position, as was observed in the reaction of the corresponding *tert*-butyldimethylsilyl-protected half-acetal **10** (Section 2.2.2.3).

The treatment of bromomethyl-ketonitrones of type **HL** with silver salts (usually silver tetrafluoroborate) leads to the generation of vinylnitrosonium ions (cf. reaction of bromomethyl-ketonitrones in Section. 4.4.1, p. 103). In principle, the only criterion to the silver salt taken is that the anionic component should be non-nucleophilic. Therefore, a range of silver salts should be investigated and tested. One interesting reaction would be to treat the vinyl nitrosonium salts with aqueous potassium cyanide. This should lead to the β-cyanohydrins of type **HM** (cf. Holzapfel and co-workers, lit.[336b]). It may be possible to transform these structures into interesting bicyclic "omuralide-like" systems **HN** – a structural type that has recently been investigated by Dr. Feng Li[188a] in the group of Prof. Jäger (Scheme 66).

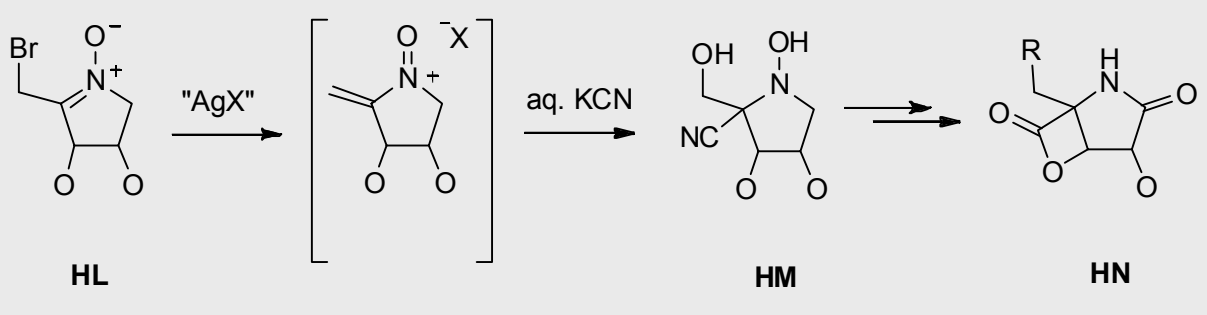

Scheme 66: Possible synthesis of biologically interesting bicyclic β-lactones from vinylnitrosonium ion intermediates.

8 Experimental

8.1 General

Work practices

The experiments are numbered consecutively. In the schemes and the tables, the experiment number is abbreviated simply to 'E', to save space. Codes are given to describe the experimenter responsible for carrying out the reaction; the number next to them refers to the corresponding journal entry. The following codes are used: LR (Leo Redcliffe), YG (Yana Galeyeva, Research Student, Feb.-March, 2003); SH (Sandra Heislbetz, Research Student, Feb.-April. 2004); FJS (Fransico Javier Sayago, PhD Research Associate, Stuttgart-Seville, July-Sept., 2003 and July-Sept., 2004); NM (Niall McCourt, ERASMUS Exchange Student from Edinburgh, Scotland, Dec. 2003-July 2004). If several compounds were prepared according to an analogous procedure, a Typical Laboratory Procedure was followed, abbreviated to 'TLP'. In this case, the experiment scale, yields etc. are to be found for each experiment individually.

Chemicals and solvents

The chemicals used were either bought directly from the institute's chemical store, "*Chemikalienausgabe*", or sourced commercially (Fluka, Aldrich, Merck-Schuchardt, Acros etc.). The drying of solvents was done according to standard procedure.[424] D-(—)-Ribose (Aldrich) and D-(—)-lyxose (Fluka) were used as starting materials. Hydroxylamine was made from the corresponding hydrochloride (Fluka). Grignard Reagents were either used directly as pre-prepared solutions in THF or diethyl ether from Aldrich, or made from magnesium and the corresponding organohalogen compound. The following organolithium, sodium, and potassium compounds were used: n-BuLi (Merck), FurylLi (synthesised from furan and n-BuLi according to lit.[4a]), NaHMDS (Fluka), LiHMDS (Fluka), potassium *tert*-butylate (Fluka). The zinc which had been activated by washing the zinc powder with 3 N

hydrochloric acid, water, MeOH and diethyl ether, followed by thorough drying (10^{-5} mbar, P_4O_{10}). Samarium metal (99.9 %) was taken as a powder (40 mesh) from Arcos Organics. Diiodoethane was bought from Aldrich and purified before use as follows: Dissolved in diethyl ether and washed with a saturated solution of sodium thiosulfate, water, dried over $MgSO_4$, then dried further overnight under vacuum (P_4O_{10}, 10^{-2} mbar). The colourless solid obtained is best used within a few days. The hydrogenation catalysts were supplied by Riedel-de Häën (10 % Pd/active carbon).

Catalytic hydrogenation

Catalytic hydrogenation was conducted using a shaking apparatus from Parr Instruments, Moline, Illinois, USA. Either 250 or 500 mL thick-walled hydrogenation flasks were used for these reactions. The separation of the hydrogenation catalyst was done by using a universal centrifuge apparatus from Hettich.

8.1.1 Separation und purification

Thin layer chromatography (TLC)

For TLC analysis, silica gel $60F_{254}$ covered aluminium plates from Merck were used. Detection was carried out using a UV lamp at 254 nm. Alternatively, the TLC plate was visualised by dipping into a solution of 2.1 g phosphomolybdic acid, 1.0 g cerium(IV) sulfate, 31 mL conc. H_2SO_4 und 470 mL water followed by heating with a heat gun.[425]

Column chromatography

Silica gel, particle diameter 40-63 μm, (Merck) was used. The amount of stationary phase used as well as the size (width x length) of the glass column and the solvent(s) applied is indicated for each experiment.

Medium pressure liquid chromatography (MPLC)

For MPLC separations, a dosis pump FL 1 with pulsation modulator Lewa MPD 3 was used. Injection manifold and column were provided by members of the Jäger group and were prepared according to a procedure from G. Helmchen und B. Glatz.[426] Detection was done

with a UV/VIS-spectrometer (Latek VIS L6 PR AEP, at 250 nm) and a differential refractometer (Knauer), coupled with a Knauer L 250 E line writer. Columns used were of the following: type B (30 cm x 3 cm, flow 30-35 mL/min at 10-12 bar, ground value: 5000) und type C (47 cm x 5 cm, flow 40-60 mL/min at 10-12 bar, ground value: 11700).

High pressure liquid chromatography (HPLC)

The setup consisted of a dosis pump (RSD 2249), mixing chamber and UV/VIS-spectrometer (RSD 2140) from LKB Pharmacia. For separation, columns of the type LiChrosorb Si 60 (Merck) were used. The storage and representation of the chromatograms were done using the program Wavescan EG, Version 1.02 (LKB Pharmacia).

Purification using ion exchange resins

Several polyhydroxylated pyrrolidines were purified using acidic ion exchange resins. For this, Dowex 50WX8 from Fluka was taken (strongly acidic, H^+ form, 200-400 mesh). For each experiment requiring purification by ion exchange, the amount of resin is given. Only columns with ca. 1 cm diameter fitted with a glass plug were used. Activation of the acidic resin was done as follows: the resin is taken up in water and stirred briefly with a glass rod, then poured into the column in one go and allowed to settle. The resin is then washed in the followed order with (each 50 mL) H_2O, 1 N NH_3, H_2O, 1 N HCl, H_2O (until neutral pH) and finally MeOH. The crude product is dissolved in MeOH and added in one go to the column. The inpurities were washed out with MeOH followed by H_2O. At no point should the column be allowed to run dry. The pyrrolidines are eluted with 1 N or 2 N NH_3 (see experiment for amounts used). The progress of the elution, i.e. the detection of the pyrrolidine, can be visualised by spotting a TLC plate, allowing the solvent to evaporate and dipping the plate into a ninhydrin solution, followed by heating with a heat gun (gives red-spots). After the elution is complete, the solvents are removed at 30 °C/10 mbar to produce the spectroscopically pure amine compound.

8.1.2 Analytic

Melting points

Melting points were determined on a heating block apparatus Fisher-Johns 4017 and are not corrected.

Optical rotation

The optical rotations were determined using a polarimeter with thermostat control from Perkin-Elmer (241 MC). The calculation of the optical rotation was done by measuring at the sodium D-line (589 nm) and extrapolated with values determined 546 nm and 578 nm according to the Drude-equation.[427]

$$[\alpha]_D^T = \frac{[\alpha]_{578}^T \times 3.199}{4.199 - \frac{[\alpha]_{578}^T}{[\alpha]_{546}^T}} \qquad [\alpha]_D^T = \frac{\alpha \times 100}{c \times d}$$

α: measured rotation c: concentration in g/100 cm^3

d: cell length in dm λ: wave length in nm

T: temperature in °C

Solvents used were CH_2Cl_2, $CHCl_3$ or MeOH (each of p.a. quality).

Elemental analysis

Elemental analyses were carried out at the Institut für Organische Chemie der Universität Stuttgart.

Mass spectrometry

Mass spectrometry was performed at the Institut für Organische Chemie der Universität Stuttgart using a Varian MAT 711, Finnigan MAT 95 or 'micrOTOF$_Q$' Brukner Daltonics (for electron spray ionisation) spectrometer. The applied method of sample ionisation is indicated for each individual experiment. High-resolution mass spectroscopy (HRMS) was recorded using either the Finnigan MAT 95 or 'micrOTOF$_Q$' machine. For liquid chromatography-mass spectroscopy ('LC-MS') measurements, an Agilent Technologies Series 1200 HPLC system, fitted with an Ascentis C18, reverse phase ('RP') HPLC column (5 cm x 2.1 mm, 3 μm) was used. RP-HPLC was carried out using a gradient elution with water/acetonitrile.

Infrared spectroscopy

IR spectra were recorded on a Perkin-Elmer 283 IR spectrometer and on a Bruker IFS 28 FT-IR-spectrometer. The positions of the absorption bands $\tilde{\nu}$ are given in cm^{-1}. The intensity of the absorptions is described as follows: vs (very strong), s (strong), m (medium), and w (weak).

Atomic spin spectroscopy

The ^{1}H and ^{13}C NMR spectra as well as H,H und C,H correlation spectra were recorded on the following machines: Bruker AC 250 (resonating frequency 250.1 and 62.9 MHz), Bruker ARX 300 (300.1 and 75.5 MHz), Bruker ARX 500 (500.1 and 125.8 MHz). All deuterated solvents used to prepare samples for measurement were sourced from Aldrich (and are indicated in brackets). Tetramethylsilane (TMS) was the internal standard (δ = 0.00 ppm). All recordings were made, if not otherwise indicated, at 25 °C (298 K). The nature of the chemical shifts is in ppm and is based on the δ-scale. The analysis of the spectra was done to 1st order approximation.[184,220,284] Signals are designated according to their splitting pattern as follows: s (singlet), d (doublet), t (triplet), q (quartet), m (multiplet), b (broad signal). Coupling constants *J* are in Hertz (Hz). Geminal coupling is indicated by ^{2}J. Long range couplings are denoted ^{4}J or ^{5}J. The labelling of the hydrogen atoms is common to the labelling of the carbon atoms. Diastereotopic protons are labelled A and B; the proton at highest field shift is designated H_A. With terminal unsubstituted olefins, the labels H_E and H_Z are used. The relative position of ^{13}C absorptions was determined by ^{13}C broadband decoupling experiments. The determination of diastereoisomeric ratios was – if not otherwise indicated – taken from the ^{13}C NMR spectum by measuring the intensities of separated signal pairs with similar relaxation times.[184,263d]

X-Ray structure analyses

The crystal structure analyses were determined using a Nicolet P 3 refractometer with a graphite monochromator using the Mo-K_α radiation. The structure was elucidated by the direct method using the programme SHELXS-86.[428] For refinements to the structure against F^2, the programme SHELXL-93 was used.[429] For the graphical presentation of the structures, programmes ORTEP II[430] and FRIEDA[431] were taken.

8.2 Experiments Relating to Chapter 2

8.2.1 Preparation of cyclic nitrones from D-ribose

Experiment 1 (FJS 1)

Methyl 2,3-*O*-isopropylidene-β-D-ribofuranoside (1)

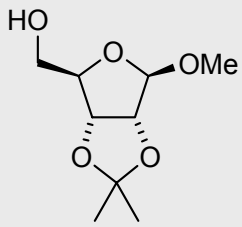

1

According to lit.[156] 17.80 g (0.118 mol) D-ribose (Aldrich) in abs. acetone (81 mL), 2,2-dimethoxypropane (36 mL) and abs. methanol (77 mL) were stirred together in an ice-bath. Over the course of 4 h, HCl gas was bubbled through the mixture periodically every 30 min. During this time, the suspension became a clear yellow solution, slowly turning more orange over time. After 8 h, TLC analysis had shown that the starting material was no longer present and the reaction was neutralised with pyridine (pH 5). The solvent was removed under vacuum using a rotary evaporator (30 °C/ 20 mbar) and the dark yellow oil obtained was taken up in 180 mL water and an equal amount of diethyl ether. The phases were separated; the aqueous phase was extracted with 3 x 50 mL diethyl ether and the combined organic phases were dried with $MgSO_4$. After filtration, the solvent was removed at atmospheric pressure (40 °C) on the rotary evaporator, and the resulting yellow oil was distilled using a "Kugelrohr" device (90 °C, 0.2 mbar). This afforded the ribofuranoside **1** (21.80 g, 0.107 mol, 90 %, lit.[156] 95 %) as an analytically pure, colourless oil.

$[\alpha]_D^{20}$ = –74 (*c* = 2.0, CH_2Cl_2); lit.[156] $[\alpha]_D^{20}$ = –80 (*c* = 2.1, $CHCl_3$)

$C_9H_{16}O_5$	calc.	C	52.93	H	7.90
(204.2)	found	C	52.74	H	7.83

IR (film): $\tilde{\nu}$ = 3451 (bs, OH), 2988 (s), 2940 (s), 2836 (m), 1651 (w), 1458 (m), 1374 (s), 1273 (m), 1240 (s), 1211 (s), 1161 (s), 1093 (s), 1044 (s), 1009 (s), 962 (m), 870 (s) cm^{-1}.

^{1}H NMR ($CDCl_3$, 250.1 MHz): δ = 1.30, 1.56 [2 s, 3 H each, $C(CH_3)_2$], 3.27 ("dd", $J_{5A,OH}$ = 3.5, $J_{5B,OH}$ = 9.1 Hz, 1 H, OH), 3.42 (s, 3 H, OCH_3), 3.60-3.65 (m, 2 H, 5-H_A, 5-H_B), 4.20-4.25 (m, 1 H, 4-H), 4.45 (d, $J_{2,3}$ = 5.9 Hz, 1 H, –3-H), 4.65 (d, $J_{2,3}$ = 5.9 Hz, 1 H, 2-H), 4.82 (d, $J_{1,2}$ = 1.5 Hz, 1 H, 1-H).

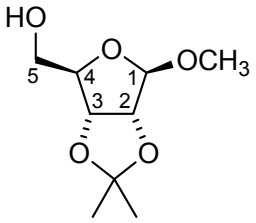

1

^{13}C NMR ($CDCl_3$, 75.5 MHz): δ = 24.6, 26.3 [2 q, C($\underline{C}H_3$)$_2$], 55.4 (q, OCH_3), 63.9 (t, C-5), 81.4 (d, C-2), 85.7 (d, C-3), 88.3 (d, C-4), 109.9 (d, C-1), 112.0 [s, $\underline{C}(CH_3)_2$].

Spectroscopic and analytical data were in accordance with literature values.[156]

Experiment 2 (LR 9)

Methyl 5-deoxy-5-iodo-2,3-*O*-isopropylidene-β-D-ribofuranoside (2)

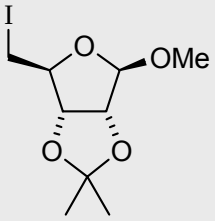

2

In accordance with lit.[2,4] the ribofuranoside **1** (20.01 g, 0.098 mol) was placed in absol. toluene (600 mL) with imidazole (17.36 g, 0.255 mol, Fluka) and triphenylphosphine (30.95 g, 0.118 mol, Fluka). The suspension was heated to 80 °C at which point iodine (29.95 g, 0.118 mol) was added. The mixture was strongly stirred for 3 h at 80 °C then allowed to cool. The supernatant was poured away and the reaction solvent removed on the rotary evaporator (40 °C/80 mbar). The crude product was subjected to flash column chromatography (SiO_2, 400 g, 8 cm x 22 cm, PE/EE = 90:10) which gave the compound **2** (25.13 g, 0.080 mol, 82 %, lit.[2] 90 %) as an analytically pure, colourless oil.

$[\alpha]_D^{20}$ = –55 (*c* = 1.1, CH_2Cl_2); lit.[2,4] $[\alpha]_D^{20}$ = –69 (*c* = 2.1, CH_2Cl_2)

$C_9H_{15}IO_4$	calc.	C	34.41	H	4.81	I	40.40
(314.1)	found	C	34.45	H	4.85	I	40.51

IR (film): $\tilde{\nu}$ = 2988 (s), 2936 (s), 2833 (m), 1457 (w), 1373 (w), 1272 (s), 1239 (s), 1211 (s), 1194 (s), 1161 (s), 1106 (vs), 1067 (vs), 1018 (vs), 982 (w), 956 (s), 925 (w), 869 (vs) cm $^{-1}$.

^{1}H NMR (250.1 MHz, $CDCl_3$) δ = 1.33, 1.48 [2 s, 3 H each, $C(CH_3)_2$], 3.15 (t, $J_{4,5B}$ = $^2J_{5A,5B}$ = 10.0 Hz, 1 H, 5-H_A), 3.26-3.32 (dd, $J_{4,5B}$ = 6.1, $^2J_{5A,5B}$ = 10.0 Hz, 1 H, 5-H_B), 3.37 (s, 3 H, OCH_3), 4.43-4.47 (ddd, $J_{3,4}$ = 0.7, $J_{4,5A}$ = 10.0, $J_{4,5B}$ = 6.1 Hz, 1 H, 4-H), 4.63 (d, $J_{2,3}$ = 5.9 Hz, 1 H, 2-H), 4.77 (d, $J_{2,3}$ = 5.9 Hz, 1 H, 3-H), 5.05 (s, 1 H, 1-H).

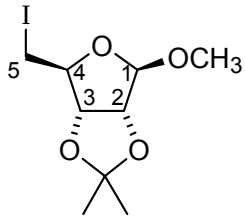

2

^{13}C NMR ($CDCl_3$, 75.5 MHz): δ = 6.7 (t, C-5), 25.0, 26.4 [2 q, $C(\underline{C}H_3)_2$], 55.2 (q, OCH_3), 83.0 (d, C-2), 85.3 (d, C-3), 87.4 (d, C-4), 109.6 (d, C-1), 112.6 [s, $\underline{C}(CH_3)_2$].

Spectroscopic and analytical data were in accordance with literature values.[2,4]

Experiment 3 (LR 27)

4,5-Dideoxy-2,3-*O*-isopropylidene-D-*erythro*-4-pentenose (3)

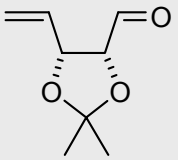

3

Following lit.[2,4], to an oven-dried flask under nitrogen was added the iodofuranoside **2** 10.08 g (32.1 mmol) in 130 mL abs. THF. The solution was cooled –78 °C (acetone/dry ice) and 30 mL (48.0 mmol, 1.5 Eq.) of a 1.6 M solution of n-butyllithium in hexane (Merck) was added dropwise over a period of 10 min. The solution was stirred at –78 °C for 2 h and afterwards quenched with excess solid NH_4Cl (3.3 g). The suspension was allowed to warm to –40 °C and treated with water (20 mL). The aqueous layer was extracted with 3 x 60 mL methylene chloride and dried over $MgSO_4$. The solvent was then removed carefully under vacuum (due to the volatile nature of the product) at 30 °C/50 mbar. The product obtained (ca. 5.0 g) was used immediately for the next step due to the risk of decomposition.

^{1}H NMR (250.1 MHz, $CDCl_3$): δ = 1.45, 1.62 [2 s, 6 H, $C(CH_3)_2$], 4.42 (dd, $J_{1,2}$ = 3.1, $J_{2,3}$ = 7.5 Hz, 1 H, 2-H), 4.86 (dd, $J_{2,3}$ = 7.5, $J_{3,4}$ = 6.8 Hz, 1 H, 3-H), 5.33 (dm, $J_{4,5E}$ = 10.3 Hz, 1 H, 5-H_E), 5.47 (dm, $J_{4,5Z}$ = 17.1 Hz, 1 H, 5-H_Z), 5.77 (ddd, $J_{3,4}$ = 6.8, $J_{4,5Z}$ = 17.1, $J_{4,5E}$ = 10.3 Hz, 1 H, 4-H), 9.56 (d, $J_{1,2}$ = 3.1 Hz, 1 H, 1-H).

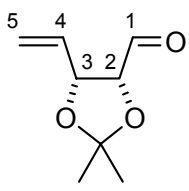

3

The ^{1}H NMR data were in accordance with literature values.[2,4]

Experiment 4 (LR 28)

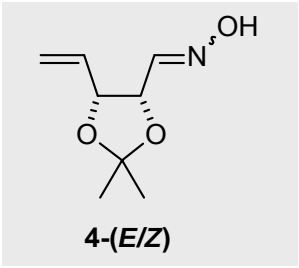

4-(*E*/*Z*)

4,5-Dideoxy-2,3-*O*-isopropylidene-D-*erythro*-4-pentenose-oxime (4-*E*/*Z*)

According to lit.[2], hydroxylamine hydrochloride (4.00 g, 57.6 mmol) was placed in 20 mL water with sodium carbonate (3.05 g, 28.8 mmol). After the ensuing reaction had subsided, the pentenose **3** (amount: see E 3) was taken up in ethanol (19 mL) and added dropwise to the hydroxylamine solution. The solution was stirred overnight at room temp. The layers were then parted and the organic layer was extracted with 3 x 40 mL methylene chloride and dried over $MgSO_4$. The solvents were removed under vacuum (30 °C/13 mbar) to afford a yellow oil that was purified using flash column chromatography (SiO_2, 150 g, 4.5 cm x 20 cm, PE/EE = 80:20). This gave the (*E*/*Z*)-oxime **4** (*E*:*Z* = 2:1;^{13}C NMR spectrum), 4.50 g (26.3 mmol, 89 %; lit.[2] 90 %) as an analytically pure oil that slowly solidified on standing.

Data of oxime (*Z*)-4

M. p. 89-90 °C

$[\alpha]_D^{20}$ = 215 (*c* = 0.50, CH_2Cl_2); lit.[2] $[\alpha]_D^{20}$ = 216 (*c* = 0.545, CH_2Cl_2)

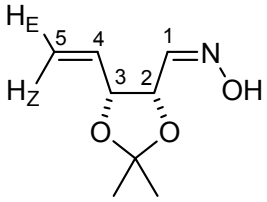

4-*Z*

$C_8H_{13}NO_3$	calc.	C	56.13	H	7.65	N	8.18
(171.2)	found	C	56.25	H	7.68	N	8.01

IR (KBr): $\tilde{\nu}$ = 3210 (bs, OH), 3080 (s), 3020 (s), 2970 (s), 1660 (w), 1455 (m), 1425 (m), 1380 (s), 1360 (s),1295 (s), 1245 (s), 1205 (s), 1145 (s), 1040 (vs), 975 (s), 935 (s), 905 (s), 890 (s), 867 (s), 799 (m) cm^{-1}.

^{1}H NMR ($CDCl_3$, 250.1 MHz): δ = 1.40, 1.55 [2 s, 3 H each, $C(CH_3)_2$], 4.84 ("tt", $J_{2,3}$ = $J_{3,4}$ = 6.7, $^4J_{3,5E}$ = $^4J_{3,5Z}$ = 1.2 Hz, 1 H, 3-H), 5.21 (ddd, $^4J_{3,5E}$ = 1.2, $J_{4,5E}$ = 10.3, $^2J_{5E,5Z}$ = 1.8 Hz, 1 H, 5-H_E), 5.31 (dd, $J_{1,2}$ = 5.2, $J_{2,3}$ = 6.7 Hz, 1 H, 2-H), 5.36 (ddd, $^4J_{3,5Z}$ = 1.2, $J_{4,5E}$ = 17.0, $^2J_{5E,5Z}$ = 1.8 Hz, 1 H, 5-H_Z), 5.77 (ddd, $J_{3,4}$ = 6.7, $J_{4,5E}$ = 10.3, $J_{4,5Z}$ = 17.0 Hz, 1 H, 4-H), 6.82 (d, $J_{1,2}$ = 5.2 Hz, 1 H, 1-H), 8.68 (s, 1 H, OH).

^{13}C NMR ($CDCl_3$, 75.5 MHz): δ = 25.2, 27.6 [2 q, $C(\underline{C}H_3)_2$], 72.8 (d, C-2), 78.5, (d, C-3), 109.6 [s, $\underline{C}(CH_3)_2$], 118.1 (t, C-5), 133.2 (d, C-4), 150.2 (d, C-1).

Data of oxime (*E*)-**4**

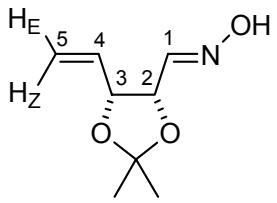

4-*E*

M. p. 48-52 °C

$[\alpha]_D^{20}$ = –49 (*c* = 0.50, CH_2Cl_2); lit.[2] $[\alpha]_D^{20}$ = –49 (*c* = 0.51, CH_2Cl_2)

$C_8H_{13}NO_3$	calc.	C	56.13	H	7.65	N 8.18
(171.2)	found	C	55.80	H	7.70	N 8.02

IR (KBr): $\tilde{\nu}$ = 3375 (bs, OH), 3097 (s), 2989 (s), 2938 (s), 1872 (w), 1647 (w), 1457 (m), 1429 (m), 1376 (s), 1343 (s),1246 (s), 1218 (s), 1165 (s), 1124 (w), 1053 (s), 991 (m), 934 (s), 867 (s), 890 (s), 798 (m) cm^{-1}.

^{1}H NMR ($CDCl_3$, 250.1 MHz): δ = 1.35, 1.47 [2 s, 3 H each, $C(CH_3)_2$], 4.62 (dd, $J_{1,2}$ = 7.7, $J_{2,3}$ = 6.6 Hz, 1 H, 2-H), 4.68 ("tt", $J_{2,3}$ = $J_{3,4}$ = 6.6, $^4J_{3,5E}$ = $^4J_{3,5Z}$ = 1.0 Hz, 1 H, 3-H), 5.24 (ddd, $^4J_{3,5E}$ = 1.0, $J_{4,5E}$ = 10.4, $^2J_{5E,5Z}$ = 1.6 Hz, 1 H, 5-H_E), 5.34 (ddd, $^4J_{3,5Z}$ = 1.0, $J_{4,5Z}$ = 17.1, $^2J_{5E,5Z}$ = 1.6 Hz, 1 H, 5-H_Z), 5.69 (ddd, $J_{3,4}$ = 6.6, $J_{4,5E}$ = 10.4, $J_{4,5Z}$ = 17.1 Hz, 1 H, 4-H), 7.24 (d, $J_{1,2}$ = 7.7 Hz, 1 H, 1-H), 8.27 (s, 1 H, OH).

^{13}C NMR ($CDCl_3$, 75.5 MHz) δ = 25.4, 27.9 [2 q, $C(\underline{C}H_3)_2$], 75.9 (d, C-2), 79.1, (d, C-3), 110.1 [s, $\underline{C}(CH_3)_2$], 119.4 (t, C-5), 132.2 (d, C-4), 148.9 (d, C-1).

Spectroscopic and analytical data in accordance with literature values.[2]

Experiment 5 (FJS 10; LR 59)

(2*R*,3*R*,4*S*)-2-Bromomethyl-3,4-dihydroxy-3,4-*O*-isopropylidene-3,4-dihydro-2*H*-pyrrole-1-oxide (5) (L-*lyxo*)

and (2*S*,3*R*,4*S*)-isomer (6) (D-*ribo*)

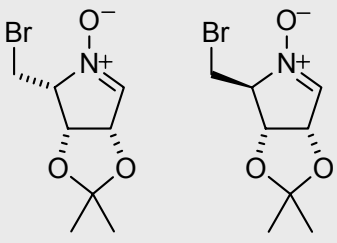

5 L-*lyxo** **6** D-*ribo*

Under the exclusion of light,[2] 2.00 g (11.68 mmol) of the oxime **4** was dissolved in 70 mL abs. methylene chloride and 2.943 g (35.04 mmol, 3.0 Eq.) sodium hydrogencarbonate was added. The suspension was cooled to 0 °C and, with the aid of a finely-ground glass dropping precision funnel, bromine (1.96 g, 12.24 mmol, 1.05 Eq.) in 47 mL abs. CH_2Cl_2 was added dropwise over 3 h. The suspension was warmed up to room temp. and stirred further

for 1 h. The supernatant was decanted off and washed consecutively with 3 mL of dilute $Na_2S_2O_3$-solution, 3 mL of saturated. $NaHCO_3$ and 3 mL saturated NH_4Cl solution. The combined aqueous layers were extracted with 2 x 50 mL methylene chloride. The combined organic layers then were dried ($MgSO_4$) and the solvent removed on the rotary evaporator (30 °C/20 mbar). The resulting light-yellow oil (^{1}H NMR: d. r. 17:83 for **5**:**6**) was purified and the diastereoisomers were separated using column chromatography (SiO_2, 150 g, 4 cm x 22 cm). Elution with PE/EE (30:70; then 10:90) afforded 0.375 g (1.50 mmol, 13 %; lit.[2] 14 %) D-*ribo* nitrone **6** as a pale yellow solid (analytically pure, m. p. 105 °C; X-ray structure, cf. lit.[182]) and 1.450 g (5.80 mmol, 50 %; lit.[2] 66 %) L-*lyxo* **5** as a colourless solid (analytically pure, m. p. 132 °C; for the X-ray structure, cf. Section 9.1 and lit.[186]).

Data of L-*lyxo*-nitrone **5**

$[\alpha]_D^{20}$ = 106 (*c* = 5.00, CH_2Cl_2); lit.[2] $[\alpha]_D^{20}$ = 104 (*c* = 0.715, CH_2Cl_2)

$C_8H_{12}BrNO_3$	calc.	C	38.42	H	4.79	N	5.60	Br	31.94
(250.1)	found	C	38.61	H	4.83	N	5.52	Br	31.85

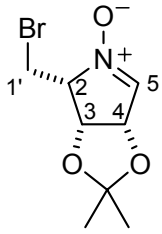

5 L-*lyxo*

IR (KBr): $\tilde{\nu}$ = 3020 (w), 2860 (m), 2820 (m), 1560 (vs, C=N), 1440 (w), 1370 (s), 1360 (s), 1340 (m),1290 (m), 1270 (s), 1220 (s), 1200 (s), 1050 (s), 940 (w), 900 (m), 850 (s), 840 (s), 780 (m), 680 (w), 600 (m), 550 (m) cm^{-1}.

^{1}H NMR ($CDCl_3$, 500.1 MHz): δ = 1.43, 1.46 [2 s, 3 H each, $C(CH_3)_2$], 3.65 (dd, $J_{2,1'A}$ = 11.4, $^2J_{1'A,1'B}$ = 9.7 Hz, 1 H, 1'-H_A), 4.08 (dd, $J_{2,1'B}$ = 3.6, $^2J_{1'A,1'B}$ = 9.6 Hz, 1 H, 1'-H_B), 4.3 (m, 1 H, 5-H), 5.05 (dd, $J_{2,3}$ = 4.8, $J_{3,4}$ = 6.1 Hz, 1 H, 3 H), 5.30 (dd, $J_{3,4}$ = 6.1, $J_{4,5}$ = 2.0 Hz, 1 H, 4-H), 6.95 (d, $J_{4,5}$ = 2.0 Hz, 1 H, 5-H).

^{13}C NMR ($CDCl_3$, 125.8 MHz): δ = 23.9 (t, C-1'), 25.6, 27.1 [2 q, $C(\underline{C}H_3)_2$], 74.3 (d, C-3), 75.4 (d, C-2), 77.2 (d, C-4), 112.6 [s, $\underline{C}(CH_3)_2$], 132.3 (d, C-5).

Data of D-*ribo*-nitrone **6**

$[\alpha]_D^{20}$ = 30 (*c* = 5.1, CH_2Cl_2); lit.[2] $[\alpha]_D^{20}$ = 26 (*c* = 0.50, CH_2Cl_2)

$C_8H_{12}BrNO_3$	calc.	C	38.42	H	4.79	N	5.60	Br	31.94
(250.1)	found	C	38.30	H	4.80	N	5.47	Br	32.37

IR (KBr): $\tilde{\nu}$ = 3020 (w), 3000 (w), 2860 (m), 2920 (m), 1570 (vs, C=N), 1410 (w), 1340 (s), 1290 (w), 1250 (m), 1200 (s),1140 (w), 1110 (s), 1050 (s), 1030 (s), 950 (w), 930 (w), 910 (w), 890 (w), 770 (m), 680 (m), 640 (m), 530 (m) cm^{-1}.

^1H NMR ($CDCl_3$, 500 MHz): δ = 1.39, 1.46 [2 s, 3 H each, $C(CH_3)_2$], 3.75 (ddd, $^4J_{4,1'A}$ = 0.8 Hz, $J_{2,1'A}$ = 2.9, $^2J_{1'A,1'B}$ = 11.3 Hz, 1 H, 1'-H_A), 4.09 (dd, $J_{2,1'B}$ = 3.5, $^2J_{1'A,1'B}$ = 11.3 Hz, 1 H, 1'-H_B), 4.3 (m, 1 H, 2-H), 4.80 (dd, $J_{2,3}$ = 1.3, $J_{3,4}$ = 6.5 Hz, 1 H, 4 H), 5.28 (dd, $J_{3,4}$ = 6.5, $J_{4,5}$ = 1.7 Hz, 1 H, 3-H), 7.02 (d, $J_{4,5}$ = 1.7 Hz, 1 H, 5-H).

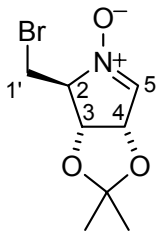

6 D-*ribo*

^{13}C NMR ($CDCl_3$, 125.1 MHz): δ = 26.1, 27.2 [2 q, $C(\underline{C}H_3)_2$], 30.0 (t, C-1'), 77.9 (d, C-3), 78.5 (d, C-4), 78.7 (d, C-2), 112.3 [s, $\underline{C}(CH_3)_2$], 133.5 (d, C-5).

Spectroscopic and analytical data of both **5** and **6** were in accordance with literature values.[2]

8.2.2 Preparation of cyclic nitrones from D-lyxose

Experiment 6 (LR 296)

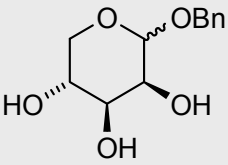

7

Benzyl α-D-lyxopyranoside (7)

According to a procedure given by Keck et al.,[208] D-lyxose (3.00 g, 0.019 mol) was placed in benzyl alcohol (9.60 g, 0.088 mol, 4.5 Eq.) and *para*-toluenesulfonic acid monohydrate (180 mg, 0.95 mmol, 0.05 Eq.) was added. The suspension was stirred at 60 °C for 48 h. TLC control showed the disappearance of starting material and the clear solution was cooled to 0 °C and liophilised with diethyl ether (100 mL). The precipitated crude product was filtered off, the filtrate concentrated on the rotary evaporator, and the liophilisation procedure repeated again. The combined precipitates were dried (P_40_{10}, 10^{-3} mbar) to afford 3.13 g (13.0 mmol, 68 %) of **7** as a spectroscopically pure, colourless solid (^{13}C NMR: α/β = 83:17). The filtrate, which contained mainly benzyl alcohol, was subjected to column chromatography (SiO_2, 60 g, 2.5 cm x 20 cm, eluant: CH_2Cl_2/MeOH = 90:10) to yield a further 0.82 g (3.4 mmol, 18 %; Σ 86 %; lit.[208] 81 %) of the benzyl pyranoside **7** as a colourless solid (m. p. 143-146 °C; lit.[208] 144 °C) with deviating elemental analysis (^{13}C NMR: α/β = 95:5).

$[\alpha]_D^{20}$ = 78 (*c* = 0.60, CH_3OH; α/β = 95:5); lit.[208] $[\alpha]_D^{20}$ = 83 (*c* = 3.10, CH_3OH) (>98:2)

$C_{12}H_{16}O_5$	calc.	C	59.99	H	6.71
(240.3)	found	C	58.08	H	6.49

MS (CI, positive-ion, carrier gas: CH_4, 435 K) *m*/*z* (%) = 241.1 (5) $[M+H]^+$, 223.1 (7) $[-H_2O]$, 209.1 (4), 205.1 (12), 187.1 (2), 175.1 (2), 163.1 (20), 133.0 (28), 131.0 (10), 115.0 (5), 103.0 (8), 91.0 (100) $[C_7H_7]^+$, 89.0 (7), 73.0 (13), 65.0 (9), 43.0 (6).
HRMS (CI, positive-ion, carrier gas: CH_4, 435 K) calc. for $C_{12}H_{16}O_5$+H: 241.1077; found 241.1071.

IR (neat): $\tilde{\nu}$ = 3367 (bs, OH), 3324 (bs, OH), 3060 (w), 3033 (w), 2945 (w), 2900 (w), 1606 (w), 1498 (w), 1453 (w), 1373 (w), 1356 (w), 1295 (m), 1240 (w), 1207 (w), 1139 (m), 1101 (w), 1084 (w), 1057 (w), 1016 (w), 998 (m), 954 (w), 856 (w), 765 (w), 736 (m), 679 (w) cm^{-1}.

^{1}H NMR (CD_3OD, 500.1 MHz): δ = 3.51 (dd, $J_{4,5A}$ = 9.4, $^2J_{5A,5B}$ = 11.0 Hz,1 H, 5-H_A), 3.67 (m, 1 H, 5-H_B), 3.70 (m, 1 H, 4-H), 3.79-3.81 (m, 1 H, 2-H), 3.81-3.84 (m, 1 H, 3-H), 4.50 (d, $^2J_{1'A,1'B}$ = 11.9 Hz, 1 H, 1'-H_A), 4.72 (d, $^2J_{1'A,1'B}$ = 11.9 Hz, 1 H, 1'-H_B), 4.75 (d, $J_{1,2}$ = 2.6 Hz, 1 H, 1-H), 7.25-7.40 (m, 5 H, C_6H_5).

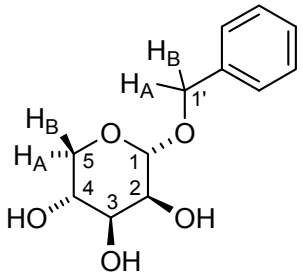

7

^{1}H NMR (DMSO-d_6 500.1 MHz): δ = 3.35 (dd, $J_{4,5A}$ = 8.9, $^2J_{5A,5B}$ = 10.9 Hz,1 H, 5-H_A), 3.67 (dd, $J_{3,4}$ = 3.4, $J_{4,5A}$ = 8.3 Hz, 1 H, 4-H), 3.54 (dd, $J_{4,5B}$ = 4.8 H, $^2J_{5A,5B}$ = 10.9 Hz, 1 H, 5-H_B), 3.59-3.63 (m, 2 H, 2-H, 3-H), 4.43 (d, $^2J_{1'A,1'B}$ = 12.1 Hz, 1 H, 1'-H_A), 4.63-4.64 ("d", $J_{1,2}$ = 2.9 Hz, and d, $^2J_{1'A,1'B}$ = 13.0 Hz, together 2 H, 1 H, 1'-H_B) 7.25-7.40 (m, 5 H, $C_6\underline{H}_5$).

^{13}C NMR ($CDCl_3$, 125.7 MHz): δ = 64.3 (t, C-5), 68.5 (d, C-3), 70.2 (t, 1'-C), 71.8 (d, C-2), 72.8 (d, C-4), 101.1 (d, C-1), 129.1, 129.4, 139.0 (C_6H_5).

Spectroscopic and analytical data were in accordance with literature values.[208]

Experiment 7 (LR 298)

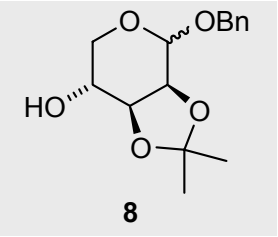

8

Benzyl 2,3-O-isopropylidene-D-lyxopyranoside (8)

To a suspension of the benzyl α-D-lyxopyranoside **7** (2.93 g, 0.012 mmol, α/β = 95:5) and acetone (200 mL) was added a catalytic amount of *para*-toluenesulfonic acid monohydrate (12 mg) at room temperature. After 1 h stirring, the flask contents had dissolved completely and were stirred for a further 16 h. The reaction was quenched with saturated $NaHCO_3$ solution (30 mL). The aqueous phase was extracted with diethyl ether (3 x 30 mL) and the combined organic phases were washed with saturated NaCl solution (2 x 15 mL), dried ($MgSO_4$), and concentrated on the rotary evaporator. Purification using column chromatography (SiO_2, 50 g, 4 cm x 15 cm, eluant: PE/EE = 6:4) produced the acetonide-protected lyxopyranoside **8** (2.43 g, 8.67 mmol, 71 %, lit.[208] 90 %) as an analytically pure, colourless solid (m. p. 62 °C; lit.[208] 66-68 °C; ^{13}C NMR: α/β = 88:12).

$[\alpha]_D^{20}$ = 89 (*c* = 3.10, CH_2Cl_2), lit.[208] $[\alpha]_D^{20}$ = 86 (*c* = 3.10, CH_2Cl_2)

$C_{15}H_{20}O_5$	calc.	C	64.27	H	7.19
(280.3)	found	C	64.43	H	7.09

IR (neat): $\tilde{\nu}$ = 3421 (bs, OH), 3032 (w), 2966 (w), 2931 (m), 2900 (w), 2864 (w), 1465 (w), 1454 (w), 1377 (m), 1304 (w), 1243 (m), 1220 (m), 1166 (w), 1138 (w), 1106 (w), 1088 (w), 1072 (s), 1058 (s), 994 (m), 965 (w), 952 (w), 861 (m), 792 (w), 767 (w), 731 (w), 693 (w), 672 (w) cm^{-1}.

^1H NMR ($CDCl_3$, 500.1 MHz): δ = 1.34, 1.46 [2 s, 3 H each, $C(C\underline{H}_3)_2$], 3.10 (bs, 1 H, OH), 3.75 (dd, = $J_{4,5A}$ = 6.5, $J_{5A,5B}$ = 12.3 Hz, 1 H, 5-H_A), 3.80-3.85 (m, 1 H, 3-H), 4.58 (d, $^2J_{1'A,1'B}$ = 11.8 Hz, 1 H, 1'-H_A), 4.87 (d, $^2J_{1'A,1'B}$ = 11.8 Hz, and d, $J_{1,2}$ = 2.5 Hz, together 2 H, 1-H, 1'-H_B), 7.25-7.40 (m, 5 H, C_6H_5).

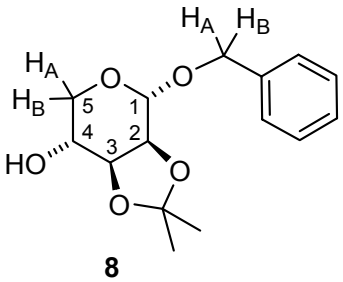

8

^{13}C NMR ($CDCl_3$, 75.5 MHz): δ = 25.6, 27.5 [2 q, $C(\underline{C}H_3)_2$], 63.0 (t, C-5), 67.4 (d, C-4), 69.8 (t, 1'-C), 74.5 (d, C-2), 76.3 (d, C-3), 97.3 (d, C-1), 109.5 [s, $\underline{C}(CH_3)_2$], 128.1, 128.2, 128.5 (3 d, *o*-, *m*-, *p*-C of C_6H_5), 136.5 (s, *i*-C of C_6H_5).

Spectroscopic and analytical data in accordance with literature values.[208]

Experiment 8 (LR 263, 299)

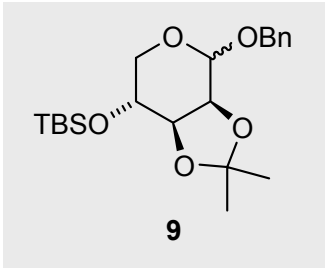

9

Benzyl 5-*tert*-butyldimethylsilyl-2,3-*O*-isopropylidene-D-lyxopyranoside (9)

A solution of the D-lyxopyranoside **8** (2.36 g, 8.41 mmol), *tert*-butyldimethylsilyl chloride (2.53 g, 13.00 mmol) and imidazole (1.145 g, 16.80 mmol) in 9 mL *N*,*N*-dimethylformamide was stirred at room temp. for 3 h. The suspension was concentrated on the rotary evaporator (30 °C, 10 mbar) and subjected to column chromatography (SiO_2, 50 g, 2.5 cm x 22 cm, elution PE:EE = 95:5) to yield the silyl ether **9** (3.13 g, 7.93 mmol, 94 %; lit.[208] 95 %) as an analytically pure, colourless oil (^{13}C NMR: α/β = 90:10).

$[\alpha]_D^{20}$ = 44 (*c* = 0.55, $CHCl_3$);

lit.[208] $[\alpha]_D^{20}$ = 41.2 (*c* = 3.40, $CHCl_3$)

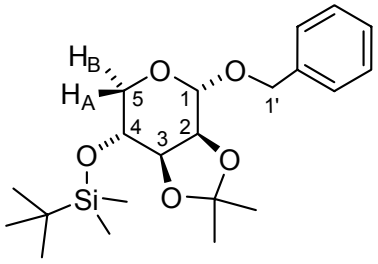

9 ($^1C_4$)

$C_{21}H_{34}O_5Si$	calc.	C	63.92	H	8.68
(394.6)	found	C	64.00	H	8.64

IR (neat): $\tilde{\nu}$ = 2953 (m), 2930 (m), 2900 (w), 2857 (w), 1493 (w), 1459 (m), 1370 (m), 1237 (m), 1220 (m), 1172 (w), 1119 (m), 1091 (m), 1073 (s), 1058 (m), 1009 (m), 970 (m), 954 (m), 926 (w), 894 (w), 833 (s), 781 (s), 762 (w), 733 (w), 713 (w), 610 (m), 579 (m) cm^{-1}.

^{1}H NMR ($CDCl_3$, 300.1 MHz): δ = 0.09, 0.12 [2 s, 3 H each, $Si(CH_3)_2$], 0.89 [s, 9 H, $C(CH_3)_3$], 1.34, 1.49 [2 s, 3 H each, $C(CH_3)_2$], 3.50 (dd, $J_{4,5A}$ = 5.5, $^2J_{5A,5B}$ = 11.4 Hz, 1 H, 5-H_A), 3.54 (dd, $J_{4,5B}$ = 9.6, $^2J_{5A,5B}$ = 11.4 Hz, 5-H_B), 3.79 (m, 1 H, 4-H), 4.05 (m, 1 H, 3-H), 4.13 (dd, $J_{1,2}$ = 1.5, $J_{2,3}$ = 5.6 Hz, 1 H, 2-H), 4.50 (d, $^2J_{1'A,1'B}$ = 11.8 Hz, 1 H, 1'-H_A), 4.73 (d, $^2J_{1'A,1'B}$ = 11.8 Hz, 1 H, 1'-H_B), 4.95 (d, $J_{1,2}$ = 1.5 Hz, 1 H, 1-H), 7.3-7.5 (m, 5 H, C_6H_5).

^{13}C NMR ($CDCl_3$, 75.5 MHz): δ = -4.8, -4.6 [2 q, $Si(\underline{C}H_3)_2$], 18.0 [s, $\underline{C}(CH_3)_3$], 26.4, 28.1 [2 q, $C(\underline{C}H_3)_2$], 25.8 [s, $C(C\underline{H}_3)_3$], 61.4 (t, C-1'), 69.1 (t, C-5), 69.6 (d, C-4), 75.6 (d, C-2), 78.8 (d, C-3), 96.8 (d, C-1), 108.9 [s, $\underline{C}(CH_3)_2$], 127.9, 128.2, 128.3, 128.4, 128.5 (5 d, *o*-, *m*-, *p*-C of C_6H_5), 137.1 (s, *i*-C of C_6H_5).

Spectroscopic and analytical data in accordance with literature values.[208]

Experiment 9 (LR 300)

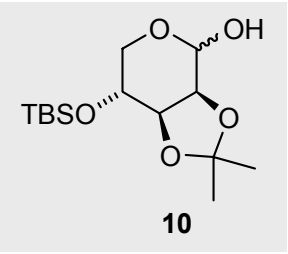

10

4-O-*tert*-Butyldimethylsilyl-2,3-*O*-isopropylidene-D-lyxopyranose (10)

A 250 mL, oven-dried three necked flask was fitted with a low temperature condenser (i.e. with liquid nitrogen trap), and flushed with argon. The benzyl glycoside **9** (4.20 g, 10.0 mmol) and 120 mL abs. THF were added and the solution was cooled to between -40 and -30 °C (acetone/CO_2). The condenser was filled with liquid nitrogen and ammonia gas was condensed (ca. 50 mL) into the reaction vessel. To this clear, colourless solution was then added portionwise freshly cut lithium metal (ca. 0.73 g, excess), which caused the solution to become immediately dark blue. After 30 min, TLC analysis indicated the absence of starting material and the reaction was quenched with ammonium chloride (5 g), and left to warm to room temp. over 2 h. The suspension was taken up in diethyl ether (100 mL) and washed with saturated $NaHCO_3$ solution (25 mL). The organic layer was dried ($MgSO_4$) and the solvent removed under reduced pressure (30 °C/ 10 mbar) to afford the crude product **10** (2.50 g, 8.2 mmol, 83 %, lit.[208] "100 %") as a spectroscopically pure, colourless solid (^{13}C NMR: α/β = 78:22), used without any further purification for the next step. For analytical purposeses, a small sample was subjected to column chromatography (SiO_2, 40 g, 4 cm x 13 cm, eluant: PE/EE = 8:2) to yield the hemi-acetal **10** as an analytically pure, colourless solid (m. p. 92-94 °C; lit.[208] 92-94 °C).

$[\alpha]_D^{20}$ = –15 (*c* = 0.95, $CHCl_3$); lit.[208] $[\alpha]_D^{20}$ = –13.5 (*c* = 1.35, $CHCl_3$)

$C_{14}H_{28}O_5Si$	calc.	C	55.23	H	9.27
(304.5)	found	C	55.33	H	9.24

IR (neat): $\tilde{\nu}$ = 3388 (bs), 2927 (m), 2882 (w), 2854 (w), 1459 (w), 1390 (w), 1374 (w), 1265 (w), 1248 (m), 1220 (m), 1164 (w), 1117 (m), 1088 (w), 1069 (m), 1040 (w), 1010 (w), 974 (w), 958 (w), 924 (w), 895 (w), 835 (w), 777 (m), 748 (w), 669 (m), 640 (w) cm^{-1}.

^1H NMR ($CDCl_3$, 300.1 MHz): δ = 0.12, 0.14 [2 s, 3 H each, $Si(C\underline{H}_3)_2$], 0.91 [s, 9 H, $C(CH_3)_3$], 1.36, 1.51 [2 s, 3 H each, $C(C\underline{H}_3)_2$], 3.74-3.80 (ddd, $^4J_{3,5A}$ = 0.8, $J_{4,5A}$ = 5.8, $^2J_{5A,5B}$ = 11.8 Hz, 1 H, 5-H_A), 3.85 ("d", $^2J_{5A,5B}$ = 11.7 Hz, and m, together 2 H, 5-H_B, 4-H), 3.98 (bs, 1 H, OH), 4.17 (m, 1 H, 3-H), 4.23 (dd, $J_{1,2}$ = 1.9, $J_{2,3}$ = 6.4 Hz, 1 H, 2-H), 5.15 (dd, $J_{1,2}$ = 1.9, $J_{1,OH}$ = 7.7 Hz, 1 H, 1-H).

^{13}C NMR ($CDCl_3$, 75.5 MHz): δ = -4.9, -4.7 [2 q, Si($\underline{C}H_3)_2$], 18.0 [s, $\underline{C}(CH_3)_3$], 25.3, 27.2 [2 q, C($\underline{C}H_3)_2$], 25.7 [s, C($C\underline{H}_3)_3$], 62.8 (t, C-5), 68.5 (d, C-4), 75.4 (d, C-2), 75.5 (d, C-3), 92.2 (d, C-1), 109.3 [s, $\underline{C}(CH_3)_2$].

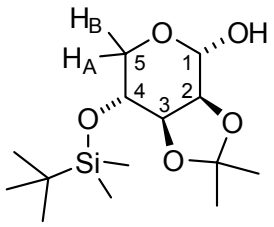

10 ($^4C_1$)

Spectroscopic and analytical data were in accordance with literature values.[208]

Wittig reaction of D-lyxopyranose **10** and 1,2-O-silyl migration

Experiment 10 (LR 316)

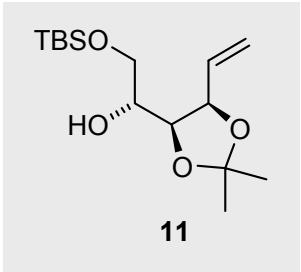

11

6-*O*-*tert*-Butyldimethylsilyl-3,4-*O*-isopropylidene-D-*arabino*-5-hexenitol (11)

In analogy to lit.[209], methyltriphenylphosphonium bromide (3.46 g, 9.70 mmol, 2.5 Eq.) was placed in 30 mL pa. THF, cooled to -10 °C and LiHMDS (8.5 mL, 8.56 mmol, 2.2 Eq., 1.0 M soln in THF) was added dropwise over 10 min. The mixture was stirred and allowed to warm to room temp. and stirred a further 45 min until the flask contents had completely dissolved. The deep-orange solution was then cooled to -20 °C and a solution of lyxopyranose **10** (1.18 g, 3.88 mmol) in 5 mL THF was added in one go. The orange colour disappeared rapidly on addition and the suspension was warmed to room temp. followed by heating at 50 °C for 1 h. The TLC analysis indicated the disappearance of starting material and the reaction was quenched with ice (ca. 50 g). The layers were separated; the aqueous layer was washed with methylene chloride (3 x 30 mL) and the combined organic layers were washed with saturated NaCl solution (20 mL), dried ($MgSO_4$) and concentrated under reduced pressure to yield the crude product as a yellow oil. Purification using column chromatography (SiO_2, 50 g, 3 cm x 15 cm, eluant: PE:EE = 8:2) provided the 1-*O*-silylated hexenitol **11** (0.943 g, 3.12 mmol, 80 %) as the unexpected main product as an analytically pure, colourless oil, and 0.120 g (0.394 mmol, 10 %) of recovered **10**.

$[\alpha]_D^{20}$ = –21 (*c* = 1.00, CH_2Cl_2)

$C_{15}H_{30}O_4Si$	calc.	C	59.56	H	10.00
(302.5)	found	C	59.76	H	9.96

IR (neat): $\tilde{\nu}$ = 3666 (bs, OH), 2985 (w), 2952 (m), 2929 (w), 2857 (w), 1463 (w), 1380 (m), 1253 (s), 1212 (w), 1164 (w), 1164 (s), 1114 (m), 1075 (w), 1003 (w), 836 (s) 632 (s) cm^{-1}.

^{1}H NMR ($CDCl_3$, 300.1 MHz): δ = 0.037, 0.047 [2 s, 3 H each, Si(C$\underline{H}_3$)$_2$], 0.081, 0.090 [2 s, 3 H each, Si(C$\underline{H}_3$)$_2$], 0.885, 0.895 [2 s, together 9 H, C(C$\underline{H}_3$)$_3$], 1.35, 1.49 [2 s, 3 H each, C(CH_3)$_2$], 3.59 (m, 2 H, 1-H_A, 1-H_B), 3.74 (m, 1 H, 2-H), 4.24 (dd, $J_{2,3}$ = 3.4, $J_{3,4}$ = 7.0 Hz, 1 H, 3-H), 4.60 ('t', $J_{3,4}$ = 7.0 Hz, 1 H, 4-H), 5.29 (dq, $J_{4,6E}$ = 0.8, $^2J_{6E,6Z}$ = 1.8, $J_{5,6E}$ = 10.0 Hz, 1 H, 6-H_E), 5.35 (dq, $J_{4,6Z}$ = 0.9, $^2J_{6E,6Z}$ = 1.6, $J_{5,6Z}$ = 17.2 Hz, 1 H, 6-H_Z), 5.80 (ddd, $J_{4,5}$ = 7.0, $J_{5,6E}$ = 10.0, $J_{5,6Z}$ = 17.2 Hz, 1 H, 5-H).

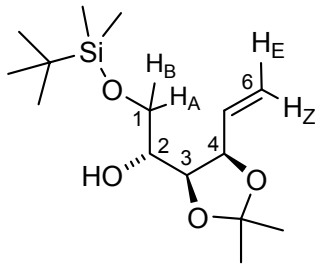

11

^{1}H NMR (DMSO-d_6, 300.1 MHz): δ = 0.03 [s, 6 H, Si(C$\underline{H}_3$)$_2$], 0.87 [s, 9 H, C(CH_3)$_3$], 1.28, 1.41 [2 s, 3 H each, C(CH_3)$_2$], 3.40 (m, 1 H, 2-H), 3.47-3.55 (m, 2 H, 1-H_A, 1-H_B), 4.10 (dd, $J_{2,3}$ = 4.2, $J_{3,4}$ = 6.8 Hz, 1 H, 3-H), 4.47 (d, 1 H, $J_{2,OH}$ = 6.0 Hz, 1 H, OH), 4.60 ('dd', $J_{4,6E}$ = 0.8, $J_{4,6Z}$ = 0.9, $J_{3,4}$ = 6.9, $J_{4,5}$ = 8.1 Hz, 1 H, 4-H), 5.19 (ddd, $J_{4,6E}$ = 0.8, $^2J_{6E,6Z}$ = 2.0, $J_{5,6E}$ = 10.2 Hz, 1 H, 6-H_E), 5.28 (ddd, $J_{4,6Z}$ = 0.9, $^2J_{6E,6Z}$ = 2.0, $J_{5,6Z}$ = 17.2 Hz, 1 H, 6-H_Z), 5.80 (ddd, $J_{4,5}$ = 8.1, $J_{5,6E}$ = 10.2, $J_{5,6Z}$ = 17.2 Hz, 1 H, 5-H).

^{13}C NMR ($CDCl_3$, 75.5 MHz): δ = -5.4 [q, Si($\underline{C}H_3$)$_2$], 18.3 [s, $\underline{C}$(CH_3)$_3$], 24.9, 27.2 [2 q, C($\underline{C}H_3$)$_2$], 25.9 [s, C($\underline{C}H_3$)$_3$], 64.2 (t, C-1), 69.9 (d, C-2), 77.1 (d, C-3), 79.2 (d, C-4), 108.7 [s, $\underline{C}$(CH_3)$_2$], 119.4 (t, C-6), 134.5 (d, C-5).

^{13}C NMR (DMSO-d_6, 75.5 MHz): δ = -5.3, -5.2 [2 q, Si($\underline{C}H_3$)$_2$], 18.0 [s, $\underline{C}$(CH_3)$_3$], 25.3, 27.2 [2 q, C($\underline{C}H_3$)$_2$], 25.8 [s, C($\underline{C}H_3$)$_3$], 64.4 (t, C-1), 69.4 (d, C-2), 77.4 (d, C-3), 78.4 (d, C-4), 107.6 [s, $\underline{C}$(CH_3)$_2$], 118.3 (t, C-6), 135.7 (d, C-5).

Experiment 11 (LR 275)

(3*R*,4*R*)-1-*O*-*tert*-Butyldimethylsilyl-3,4-*O*-isopropylidene-5-hexene-2-one oxime triol (*E*/*Z*-12)

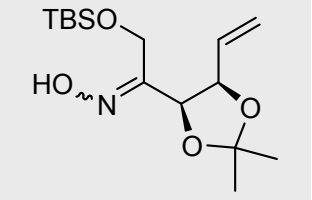

12-(*E*/*Z*)

The secondary alcohol **11** (304 mg, 1.01 mmol) was placed in methylene chloride (5 mL). *N*-methylmorpholine-*N*-oxide (473 mg, 4.04 mmol, 4.0 Eq.) and ca. molecular sieves 4 Å (200

mg) was added. The mixture was stirred at room temp. and *tetra*-n-propylammonium perruthenate(VII) (53 mg, 0.152 mmol, 0.15 Eq.) was added. After 4 h, the black suspension was filtered over a plug of silica gel (SiO_2, 1.5 cm x 4 cm); the plug was washed with ca. 150 mL of methylene chloride. The solvent was removed under reduced pressure (30 °C/10 mbar) to yield a yellow oil that was used directly for the next step, as follows: The ketone obtained (ca. 303 mg, ca. 1.01 mmol, "100 %") was taken up in pyridine (2 mL) and hydroxylamine hydrochloride (139 mg, 2.00 mmol, 2 Eq.) was added. The solution was stirred at room temp. overnight after which time TLC analysis indicated two new product spots at R_f 0.54 and R_f 0.40 (eluant: PE:EE = 8:2). Pyridine was removed under reduced pressure (10 mbar) and the yellow oil obtained was subjected to column chromatography (50 g SiO_2, 1.5 cm x 27 cm, eluant: PE:EE = 8:2) to afford 84 mg (0.266 mmol, 26 %) of the (*Z*)-configured oxime **12**, as an analytically pure, colourless solid (m. p. 55-57 °C) and 0.158 g (0.501 mmol, 50 %; Σ 76 %) of the (*E*)-configured oxime **12** as a colourless oil with slightly deviating elemental analysis.

Data of (*E*)-oxime **12**

$[\alpha]_D^{20}$ = 23 (*c* = 1.00, $CHCl_3$)

$C_{15}H_{29}O_4NSi$	calc.	C	57.11	H	9.26	N	4.44
(315.5)	found	C	57.28	H	9.31	N	4.28

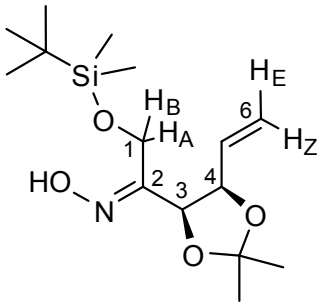

12-(*E*)

IR (neat): $\tilde{\nu}$ = 3246 (bs, OH), 2929 (m), 2857 (w), 1471 (w), 1380 (m), 1251 (m), 1214 (m), 1164 (m), 1103 (m), 1040 (s), 1008 (w), 935 (w), 835 (s), 775 (m), 678 (m), 597 (w) cm^{-1}.

^{1}H NMR ($CDCl_3$, 300.1 MHz): δ = 0.08 [s, 3 H, Si(C$\underline{H}_3$)$_2$], 0.09 [s, 3 H, Si(C$\underline{H}_3$)$_2$], 0.92 [s, 9 H, C(CH_3)$_3$], 1.41, 1.56 [2 s, 3 H each, C(CH_3)$_2$], 4.37 (d, $^2J_{1A,1B}$ = 16.5 Hz, 1 H, 1-H_A), 4.63 (d, $^2J_{1A,1B}$ = 16.5 Hz, 1 H, 1-H_B), 4.78 (dd, $J_{3,4}$ = 6.7, $J_{4,5}$ = 7.0 Hz, 1 H, 4-H), 5.15 (d, $J_{3,4}$ = 6.5 Hz, 1 H, 3-H), 5.20 (dd, $^2J_{6E,6Z}$ = 0.8, $J_{5,6E}$ = 10.3 Hz, 1 H, 6-H_E), 5.31 (dd, $^2J_{6E,6Z}$ = 0.8, $J_{5,6Z}$ = 17.1 Hz, 1 H, 6-H_E), 5.80 (ddd, $J_{4,5}$ = 7.0, $J_{5,6E}$ = 10.3, $J_{5,6Z}$ = 17.1 Hz, 1 H, 5-H), 9.55 (bs, 1 H, OH).

^{13}C NMR ($CDCl_3$, 75.5 MHz): δ = -5.8, -5.7 [2 q, Si($\underline{C}H_3$)$_2$], 18.2 [s, $\underline{C}$(CH_3)$_3$], 25.1, 27.5 [2 q, C($\underline{C}H_3$)$_2$], 25.8 [s, C($\underline{C}H_3$)$_3$], 58.6 (t, C-1), 76.4 (d, C-3), 79.4 (d, C-4), 109.0 [s, $\underline{C}$(CH_3)$_2$], 118.2 (t, C-6), 134.8 (d, C-5).

Data of (*Z*)-oxime **12**

$[\alpha]_D^{20}$ = 119 (*c* = 0.960, $CHCl_3$)

$C_{15}H_{29}O_4NSi$	calc.	C	57.11	H	9.26	N	4.44
(315.5)	found	C	58.01	H	9.43	N	4.51

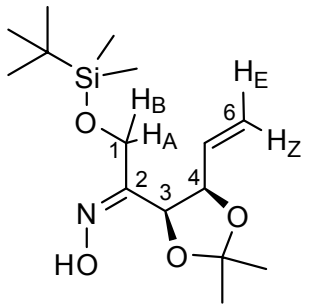

12-(*Z*)

IR (neat): $\tilde{\nu}$ = 3220 (bs, OH), 2928 (m), 2886 (w), 2856 (w), 1462 (w), 1373 (m), 1252 (m), 1213 (m), 1164 (w), 1113 (m), 1045 (w), 1007 (w), 927 (w), 876 (w), 836 (s), 777 (s), 668 (m), 623 (m), 604 (w), 590 (w), 579 (w), 556 (w) cm^{-1}.

^{1}H NMR ($CDCl_3$, 300.1 MHz): δ = 0.07 [s, 6 H, Si($C\underline{H}_3$)$_2$], 0.90 [s, 9 H, C($C\underline{H}_3$)$_3$], 1.37, 1.52 [2 s, 3 H each, C($C\underline{H}_3$)$_2$], 4.26 (d, $^2J_{1A,1B}$ = 15.5 Hz, 1 H, 1-H_A), 4.39 (d, $^2J_{1A,1B}$ = 15.5 Hz, 1 H, 1-H_B), 4.93 (dd, $J_{3,4}$ = , $J_{4,5}$ = 7.2 Hz, 1 H, 4-H), 5.12 (dt, $^2J_{6E,6Z}$ = $J_{4,6E}$ = 1.5, $J_{5,6E}$ = 10.5 Hz, 1 H, 6-H_E), 5.31-5.37 (m, together 2 H, 3-H, 6-H_Z), 5.80 (ddd, $J_{5,6E}$ = 10.4, $J_{5,6Z}$ = 16.9 Hz, 1 H, 5-H), 9.96 (bs, 1 H, OH).

^{13}C NMR ($CDCl_3$, 75.5 MHz): δ = -5.4 [q, Si($\underline{C}H_3$)2], 18.5 [s, $\underline{C}(CH_3)_3$], 24.6, 27.1 [2 q, C($\underline{C}H_3$)$_2$], 25.8 [s, C($\underline{C}H_3$)$_3$], 61.3 (t, C-1), 74.8 (d, C-3), 77.3 (d, C-4), 109.7 [s, $\underline{C}(CH_3)_2$], 117.1 (t, C-6), 134.2 (d, C-5).

Signal correlations were established with the help of H,H- and C,H-COSY.

Experiment 12 (LR 327; 382)

2,3-*O*-Isopropylidene-D-lyxofuranose (13)

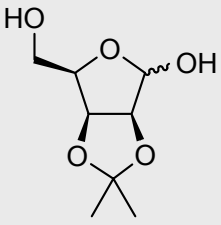

13

Using lit.[223] as a guideline, D-lyxose (3.00 g, 19.0 mmol, Aldrich) was added to 120 mL of acetone (pa. quality). The suspension was treated with 0.2 mL conc. H_2SO_4 at room temp. and stirred for 16 h. After this time, the pale-yellow solution was treated with ca. 8 g Na_2CO_3 and stirred for 5 h until the solution decolourised. The solid was filtered off, and the solvent removed on the rotary evaporator (10 mbar, 20 °C). Note: at higher temperatures (>35 °C),

the product showed signs of decomposition, i.e. turned dark-brown. After intensive drying (P_4O_{10}, 10^{-3} mbar), the furanose **13** was obtained as a spectroscopically pure, colourless oil (3.60 g, "100 %", 18.9 mmol) which was used directly for the next step. For analytical purposes, a small sample was subjected to column chromatography (SiO_2, 20 g, 2.5 cm x 10 cm, eluant: EE 100 %) to obtain the analytically pure furanose **13** (^{13}C NMR: α/β = 88:12).

$[\alpha]_D^{20}$ = 33 (*c* = 1.26, CH_2Cl_2) (α/β = 88:12)

$C_8H_{14}O_5$	calc.	C	50.52	H	7.42
(190.2)	found	C	50.70	H	7.44

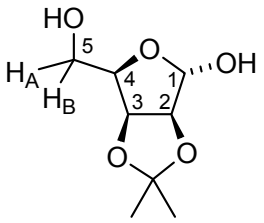

13

IR (neat): $\tilde{\nu}$ = 3396 (bs, OH), 2983 (m), 2939 (m), 1633 (w), 1457 (w), 1374 (s), 1209 (m), 1163 (s), 1067 (vs), 995 (w), 893 (m), 861 (m), 736 (w), 635 (m) cm^{-1}.

^{1}H NMR (CD_3OD, 500.1 MHz): α-anomer, δ = 1.29, 1.40 [2 s, 3 H each, $C(CH_3)_2$], 3.70 (dd, $J_{4,5A}$ = 7.0, $^2J_{5A,5B}$ = 10.8 Hz, 1 H, 5-H_A), 3.81 (dd, $J_{4,5B}$ = 5.0, $^2J_{5A,5B}$ = 10.8 Hz, 5-H_B), 4.17 (m, 1 H, 4-H), 4.53 (d, $J_{2,3}$ = 5.9 Hz, 1 H, 3-H), 4.74 (dd, $J_{1,2}$ = 3.6, $J_{2,3}$ = 5.9 Hz, 1 H, 2-H), 5.21 (s, 1 H, 1-H).

^{13}C NMR (CD_3OD, 75.5 MHz): α-anomer, δ = 25.0, 26.4 [2 q, $C(\underline{C}H_3)_2$], 61.3 (t, C-5), 81.2 (d, C-4), 81.6 (d, C-2), 87.3 (d, C-3), 102.2 (d, C-1). 113.5 [s, $\underline{C}(CH_3)_2$].

Spectroscopic and analytical data were in accordance with literature values.[223]

Experiment 13 (LR 317; 386)

5-O-*tert*-Butyldimethylsilyl-2,3-*O*-isopropylidene-D-lyxofuranose (14)

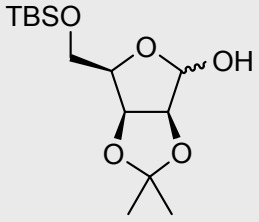

14

In analogy to lit.[224a] D-lyxofuranose **13** (6.666 g, 35.0 mmol) and imidazole (4.740 g, 69.7 mmol, 2.0 Eq.) were dissolved in methylene chloride (40 mL) under nitrogen. The temperature was reduced to -40 °C and *tert*-butyldimethylsilyl chloride (5.467 g, 36.4 mmol, 1.1 Eq.) in 6 mL CH_2Cl_2 was added dropwise over 1 h. Note: the temperature should stay below -30 °C in order to avoid the competing formation of the 1,5-di-*O*-silylated co-product.

After 4 h, the temperature was raised to -10 °C and quenched with water (10 mL). The layers were separated and the aqueous phase was washed with CH_2Cl_2 (3 x 10 mL); the combined organic layers were washed with saturated NaCl solution (5 mL), dried ($MgSO_4$), and concentrated on the rotary evaporator (10 mbar, 20 °C). The crude product was filtered over a short column of silica gel (SiO_2, 5.5 cm x 5 cm, eluant: PE/EE = 9:1) to yield the silyl ether **14** (9.086 g, 29.8 mmol, 85 %; ^{13}C NMR: α/β = 85:15) as an analytically pure, colourless oil.

$[\alpha]_D^{20}$ = 7.3 (*c* = 0.75, CH_2Cl_2)

$C_{14}H_{28}O_5Si$	calc.	C	55.23	H	9.27
(304.5)	found	C	55.12	H	9.36

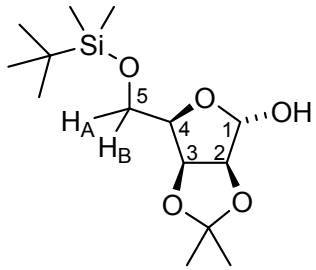

14

IR (neat): $\tilde{\nu}$ = 3422 (bs, OH), 2931 (m), 2884 (m), 2856 (m), 1471 (w), 1372 (m), 1252 (m), 1208 (m), 1290 (m), 1089 (s), 1050 (s), 1016 (w), 1001 (w), 834 (s), 776 (m), 664 (w) cm^{-1}.

^1H NMR ($CDCl_3$, 300.1 MHz): δ = 0.15 [s, 6 H, $Si(CH_3)_2$], 0.93 [s, 9 H, $C(CH_3)_3$], 1.30, 1.50 [2 s, 3 H each, $C(CH_3)_2$], 3.47 (bs, 1 H, OH), 3.83 (dd, $J_{4,5A}$ = 7.0, $^2J_{5A,5B}$ = 10.8 Hz, 1 H, 5-H_A), 3.93 (dd, $J_{4,5B}$ = 5.0, $^2J_{5A,5B}$ = 10.8 Hz, 5-H_B), 4.25 (m, 1 H, 4-H), 4.60 (d, $J_{2,3}$ = 5.9 Hz, 1 H, 3-H), 4.74 (dd, $J_{1,2}$ = 3.6, $J_{2,3}$ = 5.9 Hz, 1 H, 2-H), 5.40 (s, 1 H, 1-H).

^{13}C NMR ($CDCl_3$, 75.5 MHz): δ = -5.3, -5.4 [2 q, $Si(\underline{C}H_3)_2$], 18.5 [s, $\underline{C}(CH_3)_3$], 24.9, 26.0 [2 q, $C(\underline{C}H_3)_2$], 61.6 (t, C-5), 79.8 (d, C-4), 80.9 (d, C-2), 85.5 (d, C-3), 101.2 (d, C-1). 112.4 [s, $\underline{C}(CH_3)_2$].

Wittig reaction of the hemi-acetal **14** and 1,2-O-silyl migration to give **11** and **15**

Experiment 14 (LR 433)

1-*O*-*tert*-Butyldimethylsilyl-3,4-*O*-isopropylidene-D-*arabino*-5-hexenitol (11)

2-*O*-*tert*-Butyldimethylsilyl-3,4-*O*-isopropylidene-D-*arabino*-5-hexenitol (15)

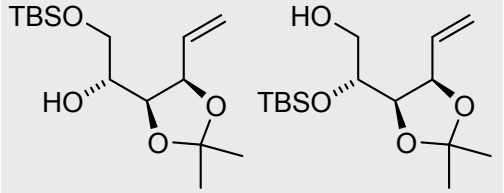

11 **15**

To a three-necked 2 L-flask fitted with a reflux condenser, argon ballon, thermometer (quickfit), and dropping funnel were added methyltriphenylphosphonium bromide (52.02 g,

0.1456 mol, 4.0 Eq.) and 600 mL pa. THF. The suspension was cooled over 20 min to -20 °C (acetone/dry ice) and nBuLi (91 mL, 0.1456 mmol, 1.6 M soln., hexanes, 4.0 Eq.) was added dropwise over 10 min. The cooling bath was removed and the suspension was left to warm to room temp. over 90 min. After this time, a homogeneous deep-orange solution was observed, which was cooled to -20 °C and treated portionwise with the hemi-acetal **14** (11.086 g, 0.0364 mol) in THF (100 mL). The now pale-yellow suspension was warmed to room temp. over 20 min and heated to 50-55 °C for 1 h. Heating was switched off and left with stirring overnight. Ice (100 g) was added with strong stirring followed by diethyl ether (100 mL); the phases were parted and the aqueous phase was washed with diethyl ether (3 x 200 mL). The combined organic layers were washed with saturated NaCl solution (2 x 100 mL), dried ($MgSO_4$) and concentrated on the rotary evaporator (25 °C/atmospheric normal pressure). The crude product was taken up in diethyl ether (100 mL) and placed in ice for 1 h. The triphenylphosphine oxide that precipitated was filtered off over celite (10 g, 1.5 cm x 7 cm). Diethyl ether was removed under reduced pressure and the orange oil obtained was purified using column chromatography (SiO_2, 70 g, 4.5 cm x 14 cm; eluant: PE/EE = 85:15) to afford the expected 1-*O*-silylated hexenitol **11** (9.498 g, 31.4 mmol, 86 %) and 2-*O*-silylated hexenitol **15** (1.107 g, 3.66 mmol, 10 %), both as analytically pure, colourless oils.

Data of the 1-*O*-silylated hexenitol **11**

$[\alpha]_D^{20}$ = –21.5 (*c* = 1.00, CH_2Cl_2)

$C_{15}H_{30}O_4Si$	calc.	C	59.56	H	10.00
(302.5)	found	C	59.64	H	9.98

Spectroscopic data were in accordance to those from Experiment 10.

Data of the 2-*O*-silylated hexenitol **15**

$[\alpha]_D^{20}$ = 27 (*c* = 0.25, CH_2Cl_2)

$C_{15}H_{30}O_4Si$	calc.	C	59.56	H	10.00
(302.5)	found	C	59.34	H	9.87

IR (neat): $\tilde{\nu}$ = 3500 (bs, OH), 2984 (m), 2930 (s), 2856 (m), 1472 (m), 1370 (m), 1253 (s), 1219 (m), 1037 (m), 928 (w), 836 (m), 780 (m) 688 (w), 669 (w), 646 (w), 619 (s) cm^{-1}.

^{1}H NMR ($CDCl_3$, 300.1 MHz): δ = 0.10 [s, 6 H, $Si(CH_3)_2$], 0.90 [s, 9 H, $C(CH_3)_3$], 1.35, 1.50 [2 s, 3 H each, $C(CH_3)_2$], 2.13 (dd, $J_{1A,OH}$ = 7.4, $J_{1B,OH}$ = 5.4 Hz, 1 H, 1-OH), 3.50 ('ddd', $^2J_{1A,1B}$ = 11.5, $J_{1A,OH}$ = 7.4, $J_{1A,2}$ = 4.4 Hz, 1 H, 1-H_A), 3.61 (ddd, $^2J_{1A,1B}$ = 11.5, $J_{1B,OH}$ = 5.4, $J_{1B,2}$ = 3.6 Hz, 1 H, 1-H_B), 3.78 (ddd, $J_{1A,2}$ = 4.4, $J_{1B,2}$ = 3.6, $J_{2,3}$ = 8.3 Hz, 1 H, 2-H), 4.20 (dd, $J_{2,3}$ = 8.3, $J_{3,4}$ = 6.0 Hz, 1 H, 3-H), 4.45 (dd, $J_{3,4}$ = 6.0, $J_{4,5}$ = 8.7 Hz, 1 H, 4-H), 5.25 (ddd, $J_{4,6E}$ = 0.7, $^2J_{6E,6Z}$ = 1.5, $J_{5,6E}$ = 10.2 Hz, 1 H, 6-H_E), 5.35 (ddd, $J_{4,6Z}$ = 0.9, $J_{5,6Z}$ = 17.2, $^2J_{6E,6Z}$ = 1.5 Hz, 1 H, 6-H_Z), 5.80 (ddd, $J_{4,5}$ = 8.8, $J_{5,6E}$ = 10.2, $J_{5,6Z}$ = 17.2 Hz, 1 H, 5-H).

^{13}C NMR ($CDCl_3$, 75.5 MHz): δ = -4.8, -4.2 [2 q, $Si(CH_3)_2$], 18.3 [s, $C(CH_3)_3$], 25.4, 28.0 [2 q, $C(CH_3)_2$], 25.9 [s, $C(CH_3)_3$], 63.5 (t, C-1), 71.8 (d, C-2), 78.7 (d, C-3), 78.8 (d, C-4), 108.5 [s, $C(CH_3)_2$], 119.2 (t, C-6), 134.5 (d, C-5).

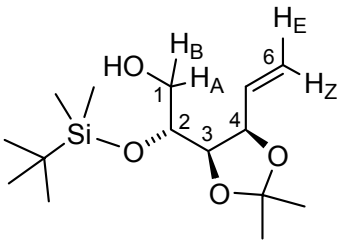

15

^{1}H NMR (DMSO-d_6, 500.1 MHz): δ = 0.06 [s, 6 H, $Si(CH_3)_2$], 0.87 [s, 9 H, $C(CH_3)_3$], 1.27, 1.40 [2 s, 3 H each, $C(CH_3)_2$], 3.25-3.40 (m, 2 H, 1-H_A, 1-H_B), 3.55 (ddd, $J_{1A,2}$ = 5.7, $J_{1B,2}$ = 4.6, $J_{2,3}$ = 10.3 Hz, 1 H, 2-H), 4.02 (t, $J_{3,4}$ = 6.3, 1 H, 3-H), 4.43 ('tqt', $J_{3,4}$ = 6.3, $J_{4,5}$ = 8.8, $J_{4,6E}$ = $J_{4,6Z}$ = ~ 0.9 Hz, 1 H, 4-H), 4.56 ('dd', $J_{1A,OH}$ = 5.3, $J_{1B,OH}$ = 5.7 Hz, 1 H, 1-OH), 5.15 (ddd, $J_{4,6E}$ = 0.9, $J_{5,6E}$ = 10.3, $^2J_{6E,6Z}$ = 2.0 Hz, 1 H, 6-H_E), 5.22 (ddd, $J_{4,6Z}$ = 1.0, $J_{5,6Z}$ = 17.2, $^2J_{6E,6Z}$ = 2.0 Hz, 1 H, 6-H_Z), 5.81 (ddd, $J_{4,5}$ = 8.8, $J_{5,6E}$ = 10.3, $J_{5,6Z}$ = 17.2 Hz, 1 H, 5-H).

^{13}C NMR (DMSO-d_6, 75.5 MHz): δ = -4.5, -4.3 [2 q, $Si(CH_3)_2$], 18.0 [s, $C(CH_3)_3$], 25.4, 27.5 [2 q, $C(CH_3)_2$], 25.8 [s, $C(CH_3)_3$], 62.5 (t, C-1), 72.5 (d, C-2), 77.8 (d, C-4), 78.2 (d, C-3), 107.2 [s, $C(CH_3)_2$], 118.1 (t, C-6), 135.2 (d, C-5).

Signal correlations were established with the help of H,H- and C,H-COSY.

Experiment 15 (LR 363)

1,2-Di-*O*-*tert*-Butyldimethylsilyl-3,4-*O*-isopropylidene-D-*arabino*-5-hexenitol (16)

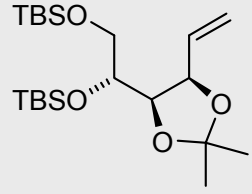

16

Based on lit.[225], compound **11** (4.523 g, 14.9 mmol) and 2,6-lutidine (3.190 g, 29.8 mmol, 2 Eq.) were placed in methylene chloride (15 mL) and cooled to 0 °C. *tert*-Butyldimethylsilyl

trifluoromethanesulfonate (5.138 g, 19.4 mmol, 1.3 Eq., Acros 98 %) was added dropwise over 5 min. The solution was allowed to warm to room temp. over 2 h and concentrated under reduced pressure (25 °C/10 mbar). The oil was filtered through a pad of silica gel (SiO_2, 30 g, 4 cm x 4 cm) and washed with ca. 250 mL methylene chloride. The solvents were removed on the rotary evaporator (25 °C/10 mbar) to afford the title compound **16** (6.089 g, 14.6 mmol, 98 %) as a spectroscopically pure substance used immediately for the next step.

^{1}H NMR ($CDCl_3$, 300.1 MHz): δ = 0.037, 0.047 [2 s, 3 H each, $Si(CH_3)_2$], 0.081, 0.090 [2 s, 3 H each, $Si(CH_3)_2$], 0.885, 0.895 [2 s, together 9 H, $C(CH_3)_3$], 1.35, 1.49 [2 s, 3 H each, $C(CH_3)_2$], 3.57-3.64 (dd, $^2J_{1A,1B}$ = 11.7, $J_{1A,2}$ = 4.9 Hz, overlapping with dd, $^2J_{1A,1B}$ = 11.7, $J_{1B,2}$ = 4.9 Hz, together 2 H, 1-H_A, 1-H_B), 3.74 (dt, $J_{1A,2}$ = $J_{1B,2}$ = 4.9, $J_{2,3}$ = 8.3 Hz, 1 H, 2-H), 4.15 (dd, $J_{2,3}$ = 7.1, $J_{3,4}$ = 6.2 Hz, 1 H, 3-H), 4.47 (m, 1 H, 4-H), 5.22 (ddd, $J_{4,6E}$ = 0.9, $J_{5,6E}$ = 10.2, $^2J_{6E,6Z}$ = 1.6 Hz, 1 H, 6-H_E), 5.35 (ddd, $J_{4,6Z}$ = 1.0, $J_{5,6Z}$ = 17.2, $^2J_{6E,6Z}$ = 1.7 Hz, 1 H, 6-H_Z), 5.80 (ddd, $J_{4,5}$ = 8.0, $J_{5,6E}$ = 10.2, $J_{5,6Z}$ = 17.2 Hz, 1 H, 5-H).

^{13}C NMR ($CDCl_3$, 75.5 MHz): δ = -5.25, -5.22 [2 q, $Si(CH_3)_2$], -4.29, -4.21 [2 q, $Si(CH_3)_2$] 18.51, 18.54 [2 s, $SiC(CH_3)_3$], 25.6, 28.0 [2 q, $C(CH_3)_2$], 26.1 [s, $C(CH_3)_3$], 65.1 (t, C-1), 72.9 (d, C-2), 79.0 (d, C-4), 79.2 (d, C-3), 108.2 [s, $C(CH_3)_2$], 118.4 (t, C-6), 137.3 (d, C-5).

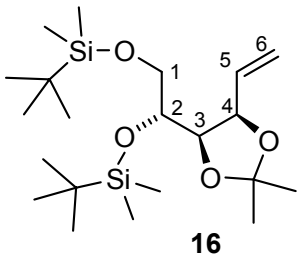

16

Signal correlations were established with the help of H,H- and C,H-COSY.

Experiment 16 (LR 364)

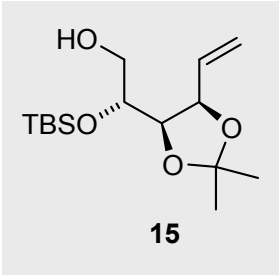

15

2-*O*-*tert*-Butyldimethylsilyl-3,4-*O*-isopropylidene-D-*arabino*-5-hexenitol (15)

Using lit.[226a] as a guideline, the 1,2-di-*O*-TBS-protected hexenitol **16** (3.43 g, 8.24 mmol) was placed in a polyethylene bottle and 12 mL THF and 4 mL pyridine were added at room temperature. To this solution was added dropwise over 5 min HF·pyridine (1.0 mL, ca. 41.2 mmol, approx. 5 Eq. 70 % HF solution, Fluka). The bottle was screwed shut and stirred at room temp. with regular monitoring by TLC analysis which indicated the appearance of a

new spot at the bottom, and the gradual appearance of a new base-line spot. After ca. 30 h, a saturated solution of $NaHCO_3$ was added (ca. 30 mL) and stirred for a further few hours. The layers were parted; the aqueous layer was washed with ethyl acetate (4 x 40 mL) and the combined organic layers were washed with saturated NH_4Cl solution (30 mL). The organic layers were dried ($MgSO_4$) and subjected to column chromatography (SiO_2, 75 g, 3 cm x 13 cm, elution PE:EE = 9:1), to provide the primary alcohol **15** (1.370 g, 4.53 mmol, 55 %) and 340 mg (8.16 mmol, 10 %) of recovered starting material, **16**.

Data of the 2-*O*-silylated hexenitol **15**

$[\alpha]_D^{20}$ = 27 (*c* = 0.25, CH_2Cl_2)

$C_{15}H_{30}O_4Si$	calc.	C	59.56	H	10.00
(302.5)	found	C	59.51	H	9.94

The spectroscopic properites of alcohol **15** were identical with those in Experiment 14 above.

Experiment 17 (LR 365)

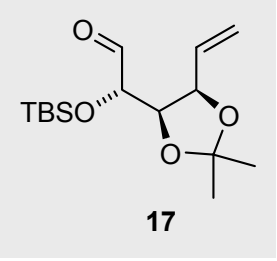

17

2-*O*-*tert*-Butyldimethylsilyl-3,4-*O*-isopropylidene-D-*arabino*-5-hexenose (17)

The primary alcohol **15** (640 mg, 2.13 mmol) was placed in methylene chloride (4 mL) and N-methyl-morpholine N-oxide (499 mg, 4.26 mmol, 2.0 Eq.) and ca. 100 mg of 4 Å molecular sieve was added. The mixture was stirred at room temp. and moments later *tetra*-n-propylammonium perruthenate(VII) (38 mg, 0.107 mmol, 0.05 Eq.) was added in one portion (cf. lit.[216]). After 1.5 h, the black suspension was filtered over a plug of silica gel (SiO_2, 15 g, 1.5 cm x 4 cm); the silica gel plug was washed with ca. 150 mL methylene chloride. The solvent was removed under reduced pressure (30 °C/10 mbar) to yield the hexenose **17** (ca. 640 mg, 2.13 mmol, “100 %”) as spectroscopically pure, lightly-coloured oil that was used directly for the next step without any further purification.

^{1}H NMR ($CDCl_3$, 500.1 MHz): δ = 0.10 [s, 6 H, $Si(CH_3)_2$], 0.93 [s, 9 H, $C(CH_3)_3$], 1.37, 1.53 [2 s, 3 H each, $C(CH_3)_2$], 4.08 (dd, $J_{1,2}$ = 0.9, $J_{2,3}$ = 5.3 Hz, 1 H, 2-H), 4.34 (dd, $J_{2,3}$ = 5.3, $J_{3,4}$ = 6.8 Hz, 1 H, 3-H), 4.74 (tt, $J_{3,4}$ = $J_{4,5}$ = 6.8, $J_{4,6E}$ ≈ $J_{4,6Z}$ = 1.4 Hz, 1 H, 4-H), 5.23 (dt, $J_{4,6E}$ ≈

$^2J_{6E,6Z}$ = 1.4, $J_{5,6E}$ = 10.5 Hz, 1 H, 6-H_E), 5.37 (dt, $J_{4,6Z} \approx {}^2J_{6E,6Z}$ = 1.4, $J_{5,6Z}$ = 17.2 Hz, 1 H, 6-H_Z), 5.94 (ddd, $J_{4,5}$ = 6.8, $J_{5,6E}$ = 10.5, $J_{5,6Z}$ = 17.2 Hz, 1 H, 5-H), 9.68 (d, $J_{1,2}$ = 0.9 Hz, 1 H, 1-H).

^{13}C NMR ($CDCl_3$, 125.7 MHz): δ = -4.8, -4.5 [2 q, $Si(CH_3)_2$], 18.2 [s, $C(CH_3)_3$], 25.1, 27.0 [2 q, $C(CH_3)_2$], 25.8 [s, $C(CH_3)_3$], 77.2 (d, C-2), 78.4 (d, C-4), 79.0 (d, C-3), 109.1 [s, $C(CH_3)_2$], 118.8 (t, C-6), 133.7 (d, C-5), 201.8 (d, C-1).

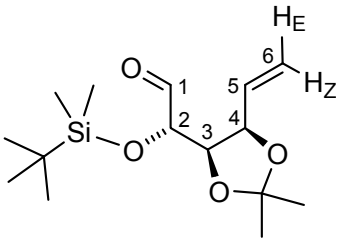

17

Experiment 18 (LR 366)

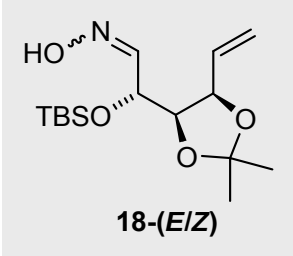

18-(*E*/*Z*)

2-*O*-*tert*-Butyldimethylsilyl-3,4-*O*-isopropylidene-D-*arabino*-5-hexenose oxime (*E*/*Z*-18)

Hydroxylamine hydrochloride (294 mg, 4.23 mmol, 2 Eq.) was placed in 2 mL water and sodium carbonate (224 mg, 2.115 mmol, 1 Eq.) was added. The aldehyde **17** (634 mg, 2.12 mmol) was taken up in ethanol (4 mL) and added dropwise over 5 min at room temperature. The solution was stirred for 2 h whereupon TLC analysis (PE/EE = 85:15) indicated the formation of a new spot at the bottom and no starting material. The layers were separated; the aqueous layer was washed with CH_2Cl_2 (3 x 20 mL) and the combined organic layers were dried ($MgSO_4$) and concentrated on the rotary evaporator. The yellow oil obtained was purified using flash column chromatrography (SiO_2, 90 g, 3 x 15 cm; PE/EE = 85:15) to yield the title compound **18** (457 mg, 1.45 mmol, Σ 68 %, 2 steps) as an analytically pure, colourless oil as a 90:10 mixture of *E*/*Z* isomers (according to ^{1}H NMR).

$[\alpha]_D^{20}$ = –20 (*c* = 0.13, CH_2Cl_2) (*E*/*Z* = 90:10)

lit.[99] (*ent*-(*E*)-**18**) $[\alpha]_D^{20}$ = 25 (*c* = 1.04, $CHCl_3$)

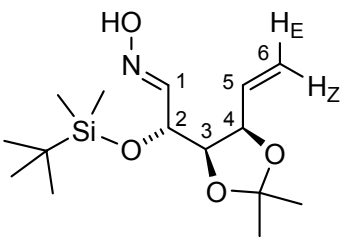

18-(*E*)

$C_{15}H_{29}NO_4Si$	calc.	C	57.11	H	9.26	N	4.44
(315.5)	found	C	57.11	H	9.37	N	4.29

IR (neat): $\tilde{\nu}$ = 3375 (bs, OH), 2930 (w), 2857 (w), 1462 (w), 1371 (m), 1252 (s), 1215 (s), 1135 (m), 1063 (s), 991 (w), 929 (s), 875 (w), 835 (vs), 776 (s), 671 (w) cm^{-1}.

^1H NMR ($CDCl_3$, 500.1 MHz, *E*/*Z* = 90:10 mixture), (*E*)-oxime: δ = 0.08, 0.12 [2 s, 3 H each, $Si(CH_3)_2$], 0.89 [s, 9 H, $C(CH_3)_3$], 1.37, 1.50 [2 s, 3 H each, $C(CH_3)_2$], 4.22 (dd, $J_{2,3}$ = 5.6, $J_{3,4}$ = 6.5 Hz, 1 H, 3-H), 4.29 (dd, $J_{1,2}$ = 7.0, $J_{2,3}$ = 5.6 Hz, 1 H, 2-H), 4.65 (tt, $J_{3,4} \approx J_{4,5}$ = 6.9, $J_{4,6E} \approx J_{4,6Z}$ = 1.2 Hz, 1 H, 4-H), 5.24 (dt, $J_{4,6E} \approx {}^2J_{6E,6Z}$ = 1.4, $J_{5,6E}$ = 10.4 Hz, 1 H, 6-H_E), 5.35 (dt, $J_{4,6Z} \approx {}^2J_{6E,6Z}$ = 1.4, $J_{5,6Z}$ = 17.3 Hz, 1 H, 6-H_Z), 6.00 (ddd, $J_{4,5}$ = 7.0, $J_{5,6E}$ = 10.4, $J_{5,6Z}$ = 17.3 Hz, 1 H, 5-H), 7.40 (d, $J_{1,2}$ = 7.0 Hz, 1 H, 1-H).

^1H NMR ($CDCl_3$, 500.1 MHz, *E*/*Z* = 90:10 mixture), (*Z*)-oxime: δ = 4.92 (dd, $J_{1,2}$ = 6.5, $J_{2,3}$ = 3.4 Hz, 2-H), 7.40 (d, $J_{1,2}$ = 6.4 Hz, 1-H) [other signals were not assigned, due to overlap with the (*E*)-oxime].

^{13}C NMR ($CDCl_3$, 125.7 MHz, *E*/*Z* = 90:10 mixture), (*E*)-oxime: δ = -4.8, -4.5 [2 q, $Si(CH_3)_2$], 18.2 [s, $C(CH_3)_3$], 25.4, 27.0 [2 q, $C(CH_3)_2$], 25.8 [s, $C(CH_3)_3$], 70.3 (d, C-3), 78.6 (d, C-4), 80.1 (d, C-2), 109.0 [s, $C(CH_3)_2$], 118.3 (t, C-6), 133.8 (d, C-5), 150.8 (d, C-1).

^{13}C NMR ($CDCl_3$, 125.7 MHz, *E*/*Z* = 90:10 mixture), (*Z*)-oxime: δ = 64.6 (d, C-2) [note: C-2 is shifted upfield due to the "*γ-gauche effect*", cf. Section 2.2.2.3], 152.6 (d, C-1) [other signals were not assigned, due to overlap with the (*E*)-oxime].

Experiment 19 (LR 367)

1-*O*-*tert*-Butyldimethylsilyl-3,4-*O*-isopropylidene-2-*O*-triisopropylsilyl-D-*arabino*-5-hexenitol (19)

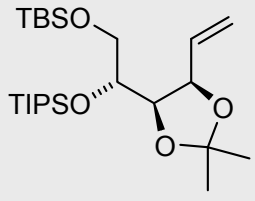

19

Using lit.[227a] as a guideline, the secondary alcohol **11** (4.12 g, 13.6 mmol) and 2,6-lutidine (2.91 g, 27.2 mmol, 2 Eq.) were placed in CH_2Cl_2 (15 mL) and cooled to 0 °C. Triisopropylsilyl trifluoromethanesulfonate (5.51 g, 18.0 mmol, 1.3 Eq., Acros 98 %) was added dropwise over 5 min. The solution was then stirred at room temp. for 2 h and concentrated under vacuum pressure (25 °C/10 mbar). The oil was filtered through a pad of silica gel (SiO_2, 30 g, 4 cm x 4 cm) and the silica gel was washed with ca. 250 mL CH_2Cl_2.

The solvents were removed on the rotary evaporator (25 °C/10 mbar) to afford the title compound **19** (6.627 g, 14.4 mmol, "106 %") as a spectroscopically pure substance, used immediately for the next step.

^{1}H NMR ($CDCl_3$, 500.1 MHz): δ = 0.030, 0.039 [2 s, 3 H each, $Si(CH_3)_2$], 0.882 [s, 9 H, $C(CH_3)_3$], 1.05-1.08 {s and m, together 21 H, $Si[CH(CH_3)_2]_3$, $Si[CH(CH_3)_2]_3$} 1.35, 1.48 [2 s, 3 H each, $C(CH_3)_2$], 3.58-3.68 (dd, $^2J_{1A,1B}$ = 10.3, $J_{1A,2}$ = 4.4 Hz, overlapping with dd, $^2J_{1A,1B}$ = 10.3, $J_{1B,2}$ = 4.6 Hz, together 2 H, 1-H_A, 1-H_B), 3.74 ('dt', $J_{1A,2}$ = 4.4, $J_{1B,2}$ = 4.6, $J_{2,3}$ = 7.3 Hz, 1 H, 2-H), 4.19 (dd, $J_{2,3}$ = 7.3, $J_{3,4}$ = 6.1 Hz, 1 H, 3-H), 4.48 (m, 1 H, 4-H), 5.21 (ddd, $J_{4,6E}$ = 0.9, $J_{5,6E}$ = 10.2, $^2J_{6E,6Z}$ = 1.8 Hz, 1 H, 6-H_E), 5.27 (ddd, $J_{4,6Z}$ = 1.0, $J_{5,6Z}$ = 17.2, $^2J_{6E,6Z}$ = 1.8 Hz, 1 H, 6-H_Z), 5.95 (ddd, $J_{4,5}$ = 8.0, $J_{5,6E}$ = 10.2, $J_{5,6Z}$ = 17.2 Hz, 1 H, 5-H).

^{13}C NMR ($CDCl_3$, 75.5 MHz): δ = -5.39, -5.32 [2 q, $Si(CH_3)_2$], 12.8 {q, $Si[CH(CH_3)_2]_3$}, 18.3 {s, $Si[CH(CH_3)_2]_3$}, 25.5, 26.1 [2 q, $C(CH_3)_2$], 26.0 [s, $SiC(CH_3)_3$], 65.5 (t, C-1), 73.0 (d, C-2), 78.9 (d, C-3), 79.6 (d, C-4), 108.1 [s, $C(CH_3)_2$], 118.2 (t, C-6), 135.5 (d, C-5).

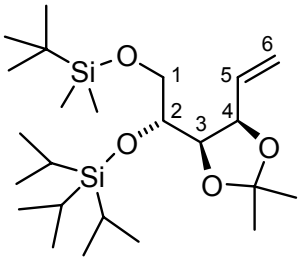

19

Experiment 20 (LR 368)

3,4-*O*-Isopropylidene 2-*O*-triisopropylsilyl-D-*arabino*-5-hexenitol (20)

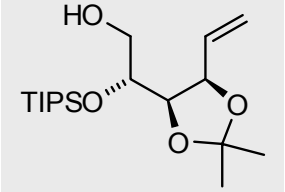

20

Taking lit.[226a] as a guide, the 1,2-di-*O*-TBS-protected hexenitol **19** (4.405 g, 9.60 mmol) was placed in a polyethylene bottle and 12 mL THF and 4 mL pyridine was added at room temperature. To this solution, HF·pyridine (1.3 mL, ca. 48.0 mmol, 5 Eq., 70 % HF solution, Fluka) was added dropwise over 5 min. The bottle was screwed shut, stirred, and monitored regularly by TLC analysis for 2 d. Then, a saturated solution of $NaHCO_3$ was added (ca. 30 mL) and stirred for a further few hours. The layers were parted; the aqueous layer was washed with ethyl acetate (4 x 40 mL) and the combined organic layers were washed with saturated NH_4Cl solution (30 mL). The organic layers were dried ($MgSO_4$) and subjected to column chromatography (SiO_2, 75 g, 3 cm x 13 cm, eluant PE:EE = 9:1), to provide the

primary alcohol **20** (1.950 g, 5.66 mmol, 59 %) as a colourless, analytically pure oil and 1.035 g (0.226 mmol, 24 %) of recovered starting material, **19**.

$[\alpha]_D^{20}$ = 26 (*c* = 0.205, CH_2Cl_2)

$C_{18}H_{36}O_4Si$	calc.	C	62.75	H	10.56
(344.6)	found	C	62.62	H	10.51

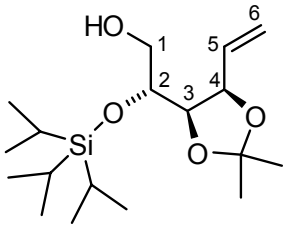

20

IR (neat): $\tilde{\nu}$ = 3463 (bs, OH), 2940 (s), 2865 (s), 1463 (m), 1427 (m), 1379 (m), 1244 (m), 1217 (s), 1142 (w), 1114 (s), 1038 (vs), 994 (m), 961 (m), 926 (m), 880 (vs), 827 (m), 740 (s), 676 (vs) cm^{-1}.

^{1}H NMR ($CDCl_3$, 500.1 MHz): δ = 1.01-1.08 {m, 18 H, $Si[CH(CH_3)_2]_3$}, 1.10-1.17 {m, 3 H, $Si[CH(CH_3)_2]_3$}, 1.35, 1.49 [2 s, 3 H each, $C(CH_3)_2$], 2.15 (bs, 1 H, OH), 3.52 (dd, $^2J_{1A,1B}$ = 11.5, $J_{1A,2}$ = 3.5 Hz, 1 H, 1-H_A), 3.67 (dd, $^2J_{1A,1B}$ = 11.5, $J_{1B,2}$ = 3.7 Hz, 1 H, 1-H_B), 3.93 (dt, $J_{1A,2} \approx J_{1B,2}$ = 3.6, $J_{2,3}$ = 8.6 Hz, 1 H, 2-H), 4.28 (dd, $J_{2,3}$ = 8.6, $J_{3,4}$ = 5.9 Hz, 1 H, 3-H), 4.46 ('dd', $J_{3,4}$ = 5.9, $J_{4,5}$ = 8.8 Hz, 1 H, 4-H), 5.24 (ddd, $J_{4,6E}$ = 0.7, $J_{5,6E}$ = 10.2, $^2J_{6E,6Z}$ = 1.5 Hz, 1 H, 6-H_E), 5.29 (ddd, $J_{4,6Z}$ = 0.8, $J_{5,6Z}$ = 17.2, $^2J_{6E,6Z}$ = 1.5 Hz, 1 H, 6-H_Z), 5.83 (ddd, $J_{4,5}$ = 8.8, $J_{5,6E}$ = 10.2, $J_{5,6Z}$ = 17.2 Hz, 1 H, 5-H).

^{13}C NMR ($CDCl_3$, 125.7 MHz): δ = 12.5 {q, $Si[CH(CH_3)_2]_3$}, 18.1 {d, $Si[CH(CH_3)_2]_3$}, 25.4, 28.1 [2 s, $C(CH_3)_3$], 63.6 (t, C-1), 71.8 (d, C-2), 78.7 (d, C-3), 78.8 (d, C-4), 108.6 [s, $C(CH_3)_2$], 119.2 (t, C-6), 134.6 (d, C-5).

Signal correlations were established with the help of H,H- and C,H-COSY.

Experiment 21 (LR 369)

3,4-*O*-Isopropylidene-2-*O*-triisopropylsilyl-3,4-*O*-isopropylidene-D-*arabino*-5-hexenose (21)

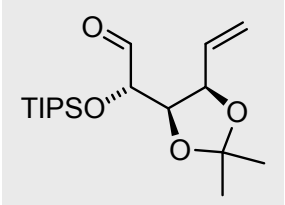

21

Using lit.[230c] as a guideline, the TIPS-protected alcohol **20** (1.858 g, 5.39 mmol) and $NaHCO_3$ (1.358 g, 16.2 mmol, 3 Eq.) were placed in CH_2Cl_2 and Dess Martin periodinane

(3.429 g, 8.09 mmol, 1.5 Eq.) was added portionwise at room temperature. TLC analysis indicated rapid product formation (new spot at the top) and after 45 min the reaction was finished. The suspension was filtered over a pad of silica gel (SiO_2, 40 g, 4 cm x 4 cm) followed by washing of the silica pad with 200 mL CH_2Cl_2. Removal of all solvents under vacuum (10 mbar/30 °C) led to the recovery of a spectroscopically pure aldehyde, compound **21** (1.833 g, 5.35 mmol, "99 %"), used directly for the next step without further purification.

^{1}H NMR ($CDCl_3$, 300.1 MHz): δ = 1.01-1.14 {m, 18 H, Si[CH(CH_3)$_2$]$_3$, overlapping with m, 3 H, Si[CH(CH_3)$_2$]$_3$}, 1.38, 1.52 [2 s, 3 H each, C(CH_3)$_2$], 4.26 (dd, $J_{1,2}$ = 1.2, $J_{2,3}$ = 6.0 Hz, 1 H, 2-H), 4.37 (dd, $J_{2,3}$ = 6.0, $J_{3,4}$ = 6.4 Hz, 1 H, 3-H), 4.75 (tt, $J_{3,4}$ = $J_{4,5}$ = 6.4, $J_{4,6Z}$ = $J_{4,6E}$ = 1.5 Hz, 1 H, 4-H), 5.23 (dt, $J_{4,6E}$ = $^2J_{6E,6Z}$ = 1.5, $J_{5,6E}$ = 10.5 Hz, 1 H, 6-H_E), 5.38 (dt, $J_{4,6Z}$ = $^2J_{6E,6Z}$ = 1.5, $J_{5,6Z}$ = 17.0 Hz, 1 H, 6-H_Z), 5.97 ('ddd', $J_{4,5}$ = 6.4, $J_{5,6E}$ = 10.5, $J_{5,6Z}$ = 17.0 Hz, 1 H, 5-H), 9.75 (d, $J_{1,2}$ = 1.2 Hz, 1 H, 1-H).

^{13}C NMR ($CDCl_3$, 75.5MHz): δ = 12.4 {q, Si[CH(CH_3)$_2$]$_3$}, 18.0 {d, Si[CH(CH_3)$_2$]$_3$}, 25.0, 26.9 [2 s, C(CH_3)$_2$], 77.5 (d, C-2), 78.2 (d, C-3), 79.3 (d, C-4), 109.1 [s, C(CH_3)$_2$], 118.6 (t, C-6), 133.5 (d, C-5), 201.4 (d, C-1).

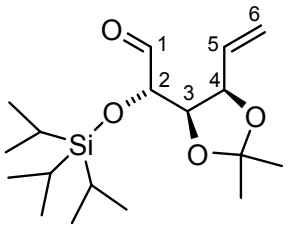

21

Experiment 22 (LR 370)

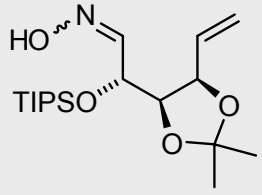

22-(*E*/*Z*)

3,4-*O*-Isopropylidene-2-*O*-triisopropylsilyl-D-*arabino*-5-hexenose oxime (22-*E*/*Z*)

Hydroxylamine hydrochloride (744 mg, 10.70 mmol, 2 Eq.) was placed in 5 mL and water and sodium carbonate (567 mg, 5.35 mmol, 1 Eq.) were added. After the ensuing reaction had subsided, the hexenose **21**, taken up in ethanol (4 mL), was added dropwise over 5 min at room temperature. The solution was stirred for 2 h whereupon TLC analysis (PE/EE = 85:15) indcated the formation of a new spot at the bottom and no more starting material. The layers were separated; the aqueous layer was washed with CH_2Cl_2 (3 x 30 mL) and the combined organic layers were dried ($MgSO_4$) and concentrated on the rotary evaporator. The yellow oil obtained was purified using flash column chromatrography (SiO_2, 90 g, 3 x 15 cm;

PE/EE = 85:15), to yield the oxime **22** (1.649 g, 4.62 mmol, Σ 86 %, 2 steps) as an analytically pure, colourless oil (90:10 mixture of *E*/*Z* isomers, according to ^{1}H NMR).

$[\alpha]_D^{20}$ = –9.5 (*c* = 0.095, CH_2Cl_2) (*E*:*Z* = 90:10)

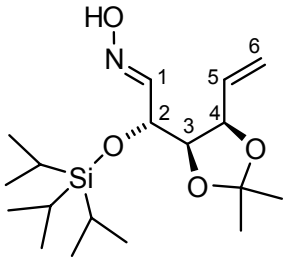

22-(*E*)

$C_{18}H_{35}NO_4Si$	calc.	C	60.46	H	9.87	N	3.92
(357.6)	found	C	60.54	H	9.78	N	3.84

IR (neat): $\tilde{\nu}$ = 3390 (bs, OH), 2942 (m), 2892 (m), 2866 (m), 1462 (m), 1380 (m), 1370 (m), 1253 (m), 1215 (m), 1136 (m), 1105 (m), 1062 (s), 1015 (m), 990 (m), 926 (s), 878 (vs), 827 (m), 780 (w), 751 (w), 679 (s) cm^{-1}.

^{1}H NMR ($CDCl_3$, 300.1 MHz, mixture of *E*/*Z* = 90:10), (*E*)-oxime: δ = 1.05-1.11 {m, 18 H, $Si[CH(CH_3)_2]_3$, overlapping with m, 3 H, $Si[CH(CH_3)_2]_3$}, 1.26, 1.35 [2 s, 3 H each, $C(CH_3)_2$], 4.27 (dd, $J_{2,3}$= 5.8, $J_{3,4}$ = 6.4 Hz, 1 H, 3-H), 4.42 (dd, $J_{1,2}$ = 7.4, $J_{2,3}$ = 5.8 Hz, 1 H, 2-H), 4.67 (tt, $J_{3,4}$ = $J_{4,5}$ = 6.4, $J_{4,6E}$ = $J_{4,6Z}$ = 1.3 Hz, 1 H, 4-H), 5.23 (dt, $J_{4,6E}$ = $^2J_{6E,6Z}$ = 1.3, $J_{5,6E}$ = 10.5 Hz, 1 H, 6-H_E), 5.36 (dt, $J_{4,6Z}$ = $^2J_{6E,6Z}$ = 1.3, $J_{5,6Z}$ = 17.1 Hz, 1 H, 6-H_Z), 6.05 ('ddd', $J_{4,5}$ = 6.4, $J_{5,6E}$ = 10.5, $J_{5,6Z}$ = 17.1 Hz, 1 H, 5-H), 7.43 (d, $J_{1,2}$ = 7.4 Hz, 1 H, 1-H).

^{13}C NMR ($CDCl_3$, 75.5 MHz, mixture of *E*/*Z* = 90:10), (*E*)-oxime: δ = 12.3 {q, $Si[CH(CH_3)_2]_3$}, 18.0 {d, $Si[CH(CH_3)_2]_3$}, 25.4, 27.2 [2 s, $C(CH_3)_3$], 70.8 (d, C-3), 78.5 (d, C-4), 80.1 (d, C-2), 109.1 [s, $C(CH_3)_2$], 118.0 (t, C-6), 133.7 (d, C-5), 150.6 (d, C-1).

Note: a small sample of the (*Z*)-oxime could be separated; the NMR data are as follows:

^{1}H NMR ($CDCl_3$, 300.1 MHz), (*Z*)-oxime: δ = 1.05-1.11 {m, 18 H, $Si[CH(CH_3)_2]_3$, overlapping with m, 3 H, $Si[CH(CH_3)_2]_3$}, 1.37, 1.52 [2 s, 3 H each, $C(CH_3)_2$], 4.31 (dd, $J_{2,3}$= 4.1, $J_{3,4}$ = 6.8 Hz, 1 H, 3-H), 4.68 (tt, $J_{3,4}$ = $J_{4,5}$ = 6.9, $J_{4,6E}$ = $J_{4,6Z}$ = 1.2 Hz, 1 H, 4-H), 5.19 (dd, $J_{1,2}$ = 6.9, $J_{2,3}$ = 4.1 Hz, 1 H, 2-H), 5.26 (dt, $J_{4,6E}$ = $^2J_{6E,6Z}$ = 1.4, $J_{5,6E}$ = 10.5 Hz, 1 H, 6-H_E), 5.40 (dt, $J_{4,6Z}$ = $^2J_{6E,6Z}$ = 1.5, $J_{5,6Z}$ = 17.3 Hz, 1 H, 6-H_Z), 6.15 ('ddd', $J_{4,5}$ = 6.9, $J_{5,6E}$ = 10.5, $J_{5,6Z}$ = 17.3 Hz, 1 H, 5-H), 6.89 (d, $J_{1,2}$ = 6.9 Hz, 1 H, 1-H).

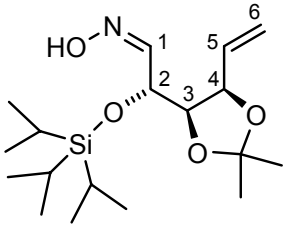

22-(*Z*)

^{13}C NMR ($CDCl_3$, 75.5MHz), (*Z*)-oxime: δ = 12.3 {q, Si[CH(CH_3)$_2$]$_3$}, 18.0 {d, Si[CH(CH_3)$_2$]$_3$}, 25.2, 26.7 [2 s, C(CH_3)$_3$], 65.1 (d, C-2), 78.8 (d, C-4), 80.1 (d, C-3), 109.1 [s, C(CH_3)$_2$], 118.4 (t, C-6), 133.9 (d, C-5), 151.8 (d, C-1).

Experiment 23 (LR 307; 394)

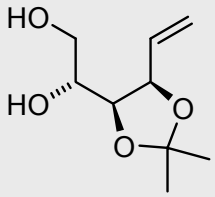

23

3,4-*O*-Isopropylidene-D-*arabino*-5-hexenitol (23)

The 5-*O*-*tert*-butyldimethylsilyl-protected hexenitol **11** (0.110 g, 0.364 mmol) was placed in 4 mL THF at room temp. and treated with tetrabutylammonium fluoride (1.1 mL, 1.09 mmol, 3 Eq., Fluka, 1 M soln. in THF) dropwise over 5 min. The solution was stirred at room temp. for 2 h and then concentrated on the rotary evaporator (30 °C/ 10 mbar). The brown oil obtained was subjected to column chromatography (SiO_2, 40 g, 1.5 cm x 17 cm, eluant: PE/EE = 1:9) to afford the diol **23** (0.061 g, 0.324 mmol, 89 %) as a spectroscopically pure, colourless oil, with slightly deviating elemental analysis.

$[\alpha]_D^{20}$ = 2 (*c* = 1.06, CH_2Cl_2)

$C_9H_{16}O_4$	calc.	C	57.43	H	8.57
(188.2)	found	C	56.82	H	8.58

IR (neat): $\tilde{\nu}$ = 3462 (bs, OH), 2985 (s), 2937 (m), 1642 (w), 1558 (w), 1457 (w), 1380 (s), 1248 (m), 1215 (s), 1166 (w), 1035 (s), 932 (w), 877 (m), 701 (s), 655 (s) cm^{-1}.

^{1}H NMR (CD_2Cl_2, 300.1 MHz): δ = 1.30, 1.46 [2 s, 3 H each, C(CH_3)$_2$], 2.05 (dd, $J_{1A,OH}$ = 5.0, $J_{1B,OH}$ = 7.0 Hz, 1 H, 1-OH), 2.38 (d, $J_{2,OH}$ = 5.7 Hz, 1 H, 2-OH), 3.40-3.51 (m, 2 H, 1-H$_A$, 1-H$_B$), 3.51-3.60 (m, 1 H, 2-H), 4.10 (dd, $J_{2,3}$ = 4.2, $J_{3,4}$ = 6.9 Hz, 1 H, 3-H), 4.55 ("tqt", $J_{3,4}$ = 6.9, $J_{4,5}$ = 7.9, $J_{4,6E}$ = $J_{4,6Z}$ = ~1.0 Hz, 1 H, 4-H), 5.22 (ddd, $J_{4,6E}$ = 0.9, $J_{5,6E}$ = 10.3, $^2J_{6E,6Z}$ = 1.7 Hz, 1 H, 6-H$_E$), 5.35 (ddd, $J_{4,6Z}$ = 1.0, $J_{5,6Z}$ = 17.2, $^2J_{6E,6Z}$ = 1.7 Hz, 1 H, 6-H$_Z$), 5.96 (ddd, $J_{4,5}$ = 7.9, $J_{5,6E}$ = 10.2, $J_{5,6Z}$ = 17.2 Hz, 1 H, 5-H).

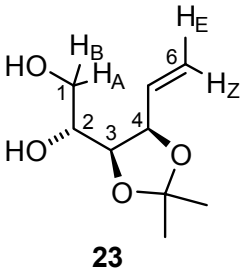

23

^{1}H NMR (DMSO-d_6, 500.1 MHz): δ = 1.29, 1.42 [2 s, 3 H each, C(CH_3)$_2$], 3.33-3.50 (m, 3 H, 1-H_A, 1-H_B, 2-H), 4.10 (dd, $J_{2,3}$ = 4.7, $J_{3,4}$ = 6.7, 1 H, 3-H), 4.42 (d, $J_{2,OH}$ = 5.8 Hz, 1 H, 2-OH), 4.51 ('tqt', $J_{3,4}$ = 6.7, $J_{4,5}$ = 8.1, $J_{4,6E}$ = $J_{4,6Z}$ = ~1.0 Hz, 1 H, 4-H), 4.67 ("t", $J_{1A,OH}$ ≈ $J_{1B,OH}$ = 5.7 Hz, 1 H, 1-OH), 5.19 (ddd, $J_{4,6E}$ = 0.8, $J_{5,6E}$ = 10.2, $^2J_{6E,6Z}$ = 2.0 Hz, 1 H, 6-H_E), 5.28 (ddd, $J_{4,6Z}$ = 0.9, $J_{5,6Z}$ = 17.2, $^2J_{6E,6Z}$ = 2.0 Hz, 1 H, 6-H_Z), 5.96 (ddd, $J_{4,5}$ = 8.1, $J_{5,6E}$ = 10.2, $J_{5,6Z}$ = 17.2 Hz, 1 H, 5-H).

^{13}C NMR (CD_2Cl_2, 75.5 MHz): δ = 25.0, 27.3 [2 q, C(CH_3)$_2$], 64.6 (t, C-1), 70.2 (d, C-2), 78.2 (d, C-3), 79.4 (d, C-4), 109.1 [s, C(CH_3)$_2$], 119.5 (t, C-6), 134.5 (d, C-5).

^{13}C NMR (DMSO-d_6, 125.5 MHz): δ = 25.4, 27.3 [2 q, C(CH_3)$_2$], 62.7 (t, C-1), 69.8 (d, C-2), 77.7 (d, C-3), 78.4 (d, C-4), 107.5 [s, C(CH_3)$_2$], 118.3 (t, C-6), 135.6 (d, C-5).

Experiment 24 (LR 311; 396)

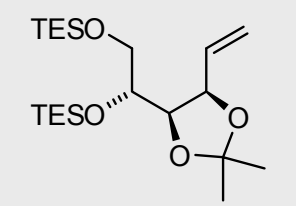

24

3,4-*O*-Isopropylidene-1,2-Di-*O*-triethylsilyl-D-*arabino*-5-hexenitol (24)

The diol **23** (167 mg, 0.887 mmol) was taken up in 6 mL pyridine under argon (balloon). Triethylsilyl chloride (389 mg, 2.58 mmol, 2.9 Eq., Fluka) was added dropwise at room temperature. The initially cloudy-white suspension was stirred overnight. Diethyl ether (5 mL) und water (1 mL) were added and the phases were separated; the aqueous phase was extracted with CH_2Cl_2 (3 x 10 mL). The combined organic layers were dried ($MgSO_4$) and concentrated under vacuum (30 °C/10 mbar). Following column chromatography (SiO_2, 40 g, eluant: PE/EE = 98:2), the silylated diol **24** (320 mg, 0.768 mmol, 86 %) was isolated as a spectroscopically pure, colourless oil, analytically almost pure.

$[\alpha]_D^{20}$ = 2.4 (*c* = 0.45, CH_2Cl_2)

$C_{21}H_{44}O_4Si_2$	calc.	C	60.52	H	10.64
(416.7)	found	C	59.90	H	10.47

IR (neat): $\tilde{\nu}$ = 2954 (s), 2911 (m), 2876 (s), 1459 (m), 1414 (m), 1378 (m), 1240 (s), 1216 (m), 1152 (s), 1097 (s), 1041 (m), 1006 (m), 926 (w), 871 (w), 789 (w), 743 (s), 670 (w), 661 (w), 638 (w) cm^{-1}.

^{1}H NMR ($CDCl_3$, 500.1 MHz): δ = 0.50 [m, together 12 H, 2 $Si(CH_2CH_3)_3$], 0.95 [m, together 18 H, 2 $Si(CH_2CH_3)_3$], 1.28, 1.42 [2 s, 3 H each, $C(CH_3)_2$], 3.57 (s, 1 H, 1-H_A,), 3.58 (s, 1 H, 1-H_B) 3.73 ('dt', $J_{1A,2}$ = 5.2, $J_{1B,2}$ = 6.3 $J_{2,3}$ = 1.0 Hz, 1 H, 2-H), 4.50 ('tqt', $J_{3,4}$ = 6.3, $J_{4,5}$ = 8.1, $J_{4,6E}$ = 0.9 Hz, 1 H, 4-H), 5.25 (ddd, $J_{4,6E}$ = 0.9, $J_{5,6E}$ = 10.3, $^2J_{6E,6Z}$ = 1.7 Hz, 1 H, 6-H_E), 5.35 (ddd, $J_{4,6Z}$ = 1.0, $J_{5,6Z}$ = 17.2, $^2J_{6E,6Z}$ = 1.7 Hz, 1 H, 6-H_Z), 5.96 (ddd, $J_{4,5}$ = 8.1, $J_{5,6E}$ = 10.2, $J_{5,6Z}$ = 17.2 Hz, 1 H, 5-H).

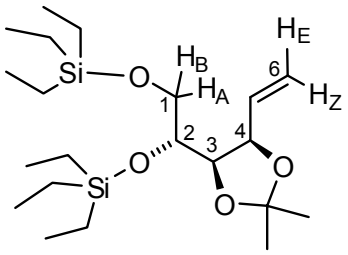

24

^{13}C NMR ($CDCl_3$, 125.5 MHz): δ = 4.3, 5.2 [2 t, 2 $Si(CH_2CH_3)_3$], 6.7, 6.9 [2 q, 2 $Si(CH_2CH_3)_3$], 24.9, 27.2 [2 q, $C(CH_3)_2$], 64.6 (t, C-1), 72.4 (d, C-2), 79.01 (d, C-3), 79.05 (d, C-4), 108.3 [s, $C(CH_3)_2$], 118.4 (t, C-6), 135.1 (d, C-5).

Experiment 25 (LR 397)

1-*O*-*tert*-Butyldimethylsilyl-2,3-*O*-isopropylidene-D-*arabino*-5-hexenitol (25)

(4*S*,5*R*)-6-(*tert*-Butyldimethylsilyloxy)-4,5-dihydroxy-4,5-O-isopropylidene-1-hexene-3-one (26)

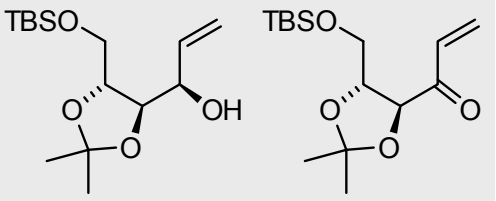

25 **26**

The 3,4-*O*-isopropylidene 1-*O*-silyl compound **11** (100 mg, 0.331 mmol) was placed in CD_2Cl_2 (3 mL) and a catalytic amount (ca. 1-2 mg) *para*-toluenesulfonic acid was added. A condenser was fitted and the solution was heated at reflux. After ca. 4 h, a ratio of **11**:**25** = 24:76 was reached according to ^{1}H NMR. Sodium hydrogencarbonate (83 mg, 0.993 mmol, 3 Eq.) was added followed quickly by addition of Dess-Martin periodinane (210 mg, 0.496 mmol, 1.5 Eq.). The suspension was stirred at room temp. and the reaction status checked regularly by TLC analysis. After ca. 20 min, the alcohol **25** had disappeared, whereas traces of compound **11** remained and the appearance of a new intense top-spot for the unsaturated ketone **26** was observed. The supension was filtered over a small plug of silica gel to remove undissolved matter, followed by washing with ca. 100 mL CH_2Cl_2. The crude product was concentrated under vacuum (30 °C/10 mbar) and purified by column chromatography (SiO_2, 30 g, 2.5 cm x 8 cm, eluant: PE/EE = 90:10) to give the unsaturated ketone **26** (60 mg, 0.200 mmol, 60 %) as a colourless, analytically pure oil.

NMR data of substance **25** (mixture of regioisomers **11**:**25** = [24:76])

^{1}H NMR ($CDCl_3$, 300.1 MHz): δ = 0.10 [s, $Si(CH_3)_2$, overlapping with $Si(CH_3)_2$ of **11**], 0.90 [s, $C(CH_3)_3$, overlapping with $C(CH_3)_3$ of **11**], 1.36, 1.38 [2 s, $C(CH_3)_2$, overlapping with $C(CH_3)_2$ of **11**], 2.70 (bs, OH), 3.69 (dd, $^2J_{1A,1B}$ = 10.5, $J_{1A,2}$ = 5.8 Hz, 1-H_A), 3.75-3.82 (m, 1-H_B, 2-H), 3.94 (dd, $J_{2,3}$ = 4.3, $J_{3,4}$ = 5.6 Hz, 3-H), 4.19 ('tt', $J_{3,4}$ = $J_{4,5}$ = 5.6, $J_{4,6E}$ = 1.5 Hz, 4-H), 5.20 (dd, $J_{4,6E}$ = 1.5, $J_{5,6E}$ = 10.6, $^2J_{6E,6Z}$ = 1.8 Hz, 6-H_E), 5.35 (t, $J_{5,6Z}$ = 17.2, $^2J_{6E,6Z}$ = 1.8 Hz, 6-H_Z, overlapping with 6-H_Z of **11**), 5.90 (ddd, $J_{4,5}$ = 5.6, $J_{5,6E}$ = 10.6, $J_{5,6Z}$ = 16.0 Hz, 5-H).

^{13}C NMR ($CDCl_3$, 75.5 MHz): δ = -5.6 [2 q, $Si(CH_3)_2$, overlapping with $Si(CH_3)_2$ of **11**], 18.3 [s, $C(CH_3)_3$], 24.9, 26.8 [2 q, $C(CH_3)_2$], 25.7 [s, $SiC(CH_3)_3$, overlapping with $SiC(CH_3)_3$ of **11**], 64.3 (t, C-1), 70.0 (d, C-2), 78.8 (d, C-4), 79.2 (d, C-3), 109.1 [s, $C(CH_3)_2$], 116.0 (t, C-6), 137.0 (d, C-5).

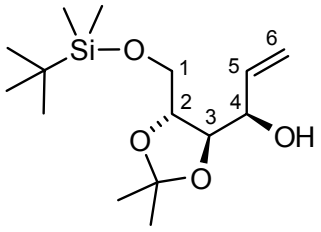

25

The data of the starting material, 3,4-*O*-isopropylidene derivate **11**, could also be identified.

Analytical data of the vinyl ketone **26**

$[\alpha]_D^{20}$ = – 17 (*c* = 0.365, CH_2Cl_2)

$C_{15}H_{28}O_4Si$	calc.	C	59.96	H	9.39
(300.5)	found	C	59.90	H	9.24

IR (neat): $\tilde{\nu}$ = 2988 (w), 2955 (m), 2930 (s), 2885 (w), 2857 (m), 1699 (s, C=O), 1611 (m), 1472 (m), 1462 (m), 1402 (m), 1381 (m), 1254 (s), 1214 (m), 1145 (m), 1096 (m), 983 (w), 955 (w), 836 (s), 814 (w), 778 (m), 727 (w), 674 (w), 654 (w), 636 (w) cm^{-1}.

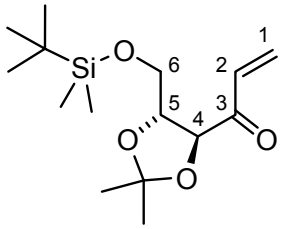

26

^{1}H NMR ($CDCl_3$, 300.1 MHz): δ = 0.10 [s, 6 H, $Si(CH_3)_2$], 0.90 [s, 9 H, $C(CH_3)_3$], 1.39, 1.46 [2 s, 3 H each, $C(CH_3)_2$], 3.76 (dd, $J_{5,6A}$ = 4.0, $^2J_{6A,6B}$ = 10.2 Hz, 1 H, 6-H_A), 3.87 (dd, $J_{5,6B}$ = 3.8, $^2J_{6A,6B}$ = 10.2 Hz, 1 H, 6-H_B), 4.12 (qu, $J_{4,5}$ = 7.2, $J_{5,6A}$ = 4.0, $J_{5,6B}$ = 3.8 Hz, 1 H, 5-H), 4.53 (d, $J_{4,5}$ = 7.2, 1 H, 4-H), 5.82 (dd, $^2J_{1E,1Z}$ = 1.6, $J_{1E,2}$ = 10.6 Hz, 1 H, 1-H_E), 6.44 (dd, $^2J_{1E,1Z}$ = 1.6, $J_{1Z,2}$ = 17.4 Hz, 1 H, 1-H_Z), 6.83 (dd, $J_{1E,2}$ = 10.6, $J_{1Z,2}$ = 17.4 Hz, 1 H, 2-H).

^{13}C NMR ($CDCl_3$, 75.5 MHz): δ = -5.4, -5.3 [2 q, $Si(CH_3)_2$], 18.4 [d, $SiC(CH_3)_3$], 25.7 [s, $SiC(CH_3)_3$], 26.3, 27.0 [2 q, $C(CH_3)_2$], 62.9 (t, C-6), 79.0 (d, C-5), 80.5 (d, C-4), 111.0 [s, $C(CH_3)_2$], 130.3 (t, C-1), 131.6 (d, C-2), 198.4 (q, C-3).

Experiment 26 (LR 398)

(2*R*,3*R*,4*R*,5*R*)-2-Bromomethyl-2,3,4,5-tetrahydro-3,4,5-trihydroxy-3,4-*O*-isopropylidene-5-*O*-triisopropylsilyl-pyridine-1-oxide (27) (L-*fuco*)

and (2*S*,3*R*,4*R*,5*R*)-isomer (CZ) (D-*altro*)

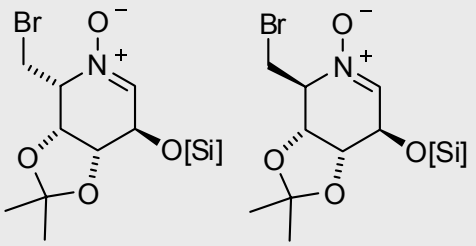

27 L-*fuco* **CZ** D-*altro*

[Si] = *tert*-butyldimethylsilyl (TBS)

To a two-necked 50 mL-flask fitted with a finely-ground glass precision dropping funnel (Ger. 'Dosiertropftrichters') was added 280 mg (0.889 mmol) of the TBS-protected D-*arabino* oxime **18**, dissolved in 5 mL CH_2Cl_2, and 224 mg (2.67 mmol, 3.0 Eq.) $NaHCO_3$. Bromine (149 mg, 0.937 mmol, 1.05 Eq.) was weighed carefully into 5 mL of CH_2Cl_2 and transferred to the dropping funnel. The mixture was cooled to 0 °C (ice/water) and the bromine solution was added dropwise over 1.5 h. The cooling bath was then removed and the reaction flask warmed to room temp. over 1 h. The supernatant was decanted off and washed consecutively with approx. 1 mL dilute $Na_2S_2O_3$, 1 mL saturated. $NaHCO_3$ and 1 mL saturated NH_4Cl solutions. The combined aqueous layers were extracted with 2 x 15 mL CH_2Cl_2. The combined organic layers were dried ($MgSO_4$) and concentrated on the rotary evaporator (25 °C/20 mbar). This provided several crude products as a dark-yellow oil (d. r. **27**:**CZ** = 90:10, ^{13}C NMR), according to TLC analysis. Attempted purification using column chromatography (SiO_2, 50 g, 2.5 cm x 20 cm, elution PE/EE 30:70, then 10:90) afforded 52.6 mg (0.134 mmol, 15 %) of L-*fuco*-nitrone **27** as a analytically pure, colourless oil and 5.3 mg (0.0134 mmol) of D-*altro*-nitrone **CZ** as a spectroscopically pure, colourless oil. The D-*altro* nitrone **CZ** was not fully characterised.

L-*fuco* nitrone **27**

$[\alpha]_D^{20}$ = –0.2 (*c* = 1.245, CH_2Cl_2)

MS (ESI, positive ion, 70 eV, 465 K) *m/z* (%) = 395 $[M+H]^+$ (50), 280 $[-SiC_6H_{15}]$ (65).
HRMS (ESI, positive ion): calc. for $C_{15}H_{28}BrNO_4Si$ +H: calc. 394.1044; found 394.1049.

$C_{15}H_{28}BrNO_4Si$	calc.	C	45.68	H	7.16	N	3.55	Br 20.26
(394.4)	found	C	45.86	H	7.18	N	3.49	Br 19.63

IR (neat): $\tilde{\nu}$ = 2928 (m), 2856 (m), 1564 (s), 1471 (m), 1382 (s), 1258 (s), 1210 (s), 1151 (m), 1073 (vs), 1020 (w), 977 (w), 953 (w), 923 (w), 879 (w), 834 (vs), 810 (w), 776 (vs), 683 (w), 666 (m), 586 (w) cm^{-1}.

^1H NMR (CD_2Cl_2, 500.1 MHz): δ = 0.08, 0.12 [2 s, 3 H each, $Si(CH_3)_2$], 0.90 [s, 9 H, $C(CH_3)_3$], 1.44 [s, 6 H, $C(CH_3)_2$], 3.80 (t, $^2J_{1'A,1'B}$ = $J_{2,1'A}$ = 10.4 Hz, 1 H, 1'-H_A), 4.36 (dd, $^2J_{1'A,1'B}$ = 10.4, $J_{2,1'B}$ = 4.6 Hz, 1 H, 1'-H_B), 4.51-4.55 ('dq', $J_{2,1'A}$ = 10.4, $J_{2,1'B}$ = 4.6, $J_{2,3} \approx {}^4J_{2,6}$ = 2.3 Hz, overlapping with 'ddd', J = 0.6, $J_{4,5}$ = 2.5, $J_{5,6}$ = 5.4 Hz, 2 H, 2-H, 5-H), 4.58 (ddd, $J_{3,4}$ = 7.2, $J_{4,5}$ = 2.5, $^4J_{4,6}$ = 1.2 Hz, 1 H, 4-H), 5.20 (dd, $J_{2,3}$ = 2.4, $J_{3,4}$ = 7.2 Hz, 1 H, 3-H), 7.19 (m, 1 H, 6-H).

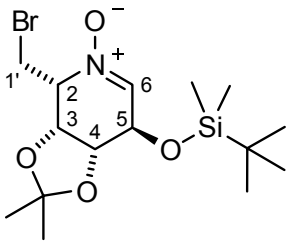

27 L-*fuco*

^{13}C NMR (CD_2Cl_2, 75.5 MHz): δ = -5.0, -4.7 [2 q, $Si(CH_3)_2$], 18.4 [s, $C(CH_3)_3$], 24.5, 26.4 [2 q, $C(CH_3)_2$], 25.8 [s, $C(CH_3)_3$], 26.8 (t, C-1'), 66.1 (d, C-5), 67.3 (d, C-2), 74.4 (d, C-3), 76.7 (d, C-4), 110.5 [s, $C(CH_3)_2$], 131.5 (d, C-6).

Experiment 27 (LR 399)

(2*R*,3*R*,4*R*,5*R*)-2-Bromomethyl-2,3,4,5-tetrahydro-3,4,5-trihydroxy-3,4-*O*-isopropylidene-5-*O*-triisopropylsilyl-pyridine-1-oxide (28) (L-*fuco*)

and (2*S*,3*R*,4*R*,5*R*)-isomer (29) (D-*altro*)

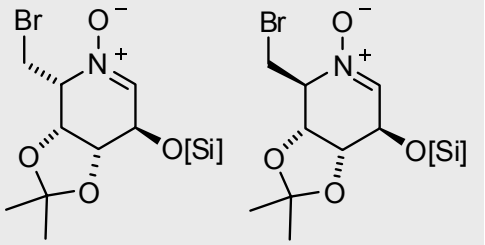

28 L-*fuco* **29** D-*altro*

[Si] = triisopropylsilyl (TIPS)

To a two-necked 100 mL-flask fitted with a finely-ground glass precision dropping funnel ('Dosiertropftrichters') was added 1.180 g (3.30 mmol) of the TIPS-protected oxime **22**,

dissolved in 20 mL CH_2Cl_2, followed by 0.832 g (9.90 mmol, 3.0 Eq.) $NaHCO_3$. Bromine (0.555 g, 3.47 mmol, 1.05 Eq.) was weighed into 35 mL of CH_2Cl_2 and transferred by a syringe to the dropping funnel. Meanwhile, the reaction vessel was cooled to 0 °C and the bromine solution was allowed to drop slowly into the suspension over 1.5 hours. The cooling bath was removed and the suspension warmed to room temp. over 1 h. The supernatant was decanted off and washed consecutively with 5 mL dilute $Na_2S_2O_3$, 5 mL saturated. $NaHCO_3$ and 5 mL saturated NH_4Cl solutions. The combined aqueous layers were extracted with CH_2Cl_2 (2 x 50 mL). The combined organic layers were then dried ($MgSO_4$) and the solvent removed on the rotary evaporator (25 °C/20 mbar). According to the ^{13}C NMR spectrum, the dark yellow oil had a d. r. 89:11 = **28**:**29**. However, TLC analysis indicated the formation of several other products as well as the presence of starting material. Purification using column chromatography (SiO_2, 150 g, 4 cm x 22 cm, elution with PE/EE 30:70 then 10:90) afforded 591 mg (1.35 mmol, 41 %) of L-*fuco*-nitrone **28** as a spectroscopically pure, colourless solid (m. p. 78-79 °C) and 115 mg (0.264 mmol, 9 %) of D-*altro*-nitrone **29** as a spectroscopically pure, colourless oil. In addition, 200 mg (0.559 mmol, 17 %) of the starting oxime **22** were recovered as a colourless, spectroscopic oil (note: data of oxime **22** were identified).

L-*fuco*-nitrone **28**

$[\alpha]_D^{20}$ = 8.9 (*c* = 0.225, CH_2Cl_2)

$C_{18}H_{34}BrNO_4Si$	calc.	C	49.53	H	7.85	N	3.21	Br	18.31
(436.5)	found	C	51.52	H	8.12	N	2.94	Br	17.12

MS (ESI, positive ion) *m/z* (%) = 436 $[M+H]^+$ (98).
HRMS (ESI, positive ion): for $C_{18}H_{34}BrNO_4Si$ +H: calc. 436.1513; found 436.1515 .

IR (neat): $\tilde{\nu}$ = 2923 (m), 2865 (m), 1565 (vs), 1461 (m), 1380 (s), 1342 (w), 1305 (w), 1266 (s), 1211 (w), 1166 (w), 1467 (w), 1111 (m), 1066 (vs), 1019 (w), 978 (m), 955 (m), 918 (m), 882 (s), 841 (s), 787 (s), 760 (w), 680 (vs), 644 (s), 652 (w) cm^{-1}.

^1H NMR (CD_2Cl_2, 500.1 MHz): δ = 0.85 {m, 21 H, $Si[CH(CH_3)_2]_3$ and $Si[CH(CH_3)_2]_3$}, 1.41, 1.64 [2 s, 3 H each, $C(CH_3)_2$], 3.70 (t, $^2J_{1'A,1'B} = J_{2,1'A}$ = 10.4 Hz, 1 H, 1'-H_A), 4.26 (dd, $^2J_{1'A,1'B}$ = 10.4, $J_{2,1'B}$ = 4.6 Hz, 1 H, 1'-H_B), 4.48 (dq, $J_{2,1'A}$ = 10.4, $J_{2,1'B}$ = 4.6, $J_{2,3}$ = 2.3 Hz, 1 H, 2-H), 4.51-4.54 ('ddd', *J* = 0.8, $J_{4,5}$ = 2.5 Hz, overlapping with 'ddd' $J_{4,5}$ = 2.5, $^4J_{4,6}$ = 1.2 Hz, together 2 H, 4-H, 5-H), 5.09 (ddd, *J* = 0.9 Hz, $J_{2,3}$ = 2.4, $J_{3,4}$ = 6.9 Hz, 1 H, 3-H), 7.20 ('ddd', $^4J_{2,6}$ = 2.5, $^4J_{4,6}$ = 1.4, $J_{5,6}$ = 5.0 Hz, 1 H, 6-H).

^{13}C NMR (CD_2Cl_2, 75.5 MHz): δ = 12.4 {q, Si[CH(CH_3)$_2$]$_3$}, 18.1 {d, Si[CH(CH_3)$_2$]$_3$}, 24.5, 26.2 [2 s, C(CH_3)$_3$], 26.8 (t, C-1'), 66.2 (d, C-5), 67.4 (d, C-2), 74.5 (d, C-3), 76.8 (d, C-4), 110.6 [s, C(CH_3)$_2$], 131.4 (d, C-6).

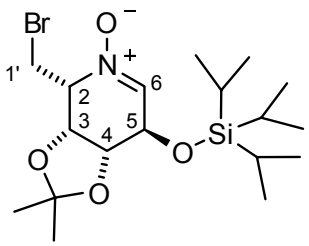

28 L-*fuco*

D-*altro*-nitrone **29**

$[\alpha]_D^{20}$ = –18 (*c* = 0.225, CH_2Cl_2)

MS (ESI, positive ion) *m/z* (%) = 436 $[M+H]^+$ (95).

HRMS (ESI, positive ion): calc. for $C_{18}H_{34}BrNO_4Si$ +H: calc. 436.1513; found 436.1518.

IR (neat): $\tilde{\nu}$ = 2924 (s), 2865 (m), 1578 (m), 1461 (m), 1382 (m), 1243 (w), 1212 (m), 1162 (w), 1056 (vs), 1014 (w), 996 (w), 953 (w), 908 (m), 881 (m), 838 (m), 778 (m), 681 (s), 598 (w), 573 (w) cm^{-1}.

^{1}H NMR ($CDCl_3$, 500.1 MHz): δ = 1.00-1.20 {m, 21 H, Si[CH(CH_3)$_2$]$_3$ and Si[CH(CH_3)$_2$]$_3$}, 1.36, 1.40 [2 s, 3 H each, C(CH_3)$_2$], 3.83 (dd, $^2J_{1'A,1'B}$ = 10.3, $J_{2,1'A}$ = 4.7 Hz, 1 H, 1'-H_A), 3.95 ('dd', $^2J_{1'A,1'B}$ = 10.3, $J_{2,1'B}$ = 9.7 Hz, 1 H, 1'-H_B), 4.17 (ddd, $J_{2,1'A}$ = 4.7, $J_{2,1'B}$ = 9.7, $J_{2,3}$ = 1.9 Hz, 1 H, 2 H), 4.44 (ddd, $J_{3,4}$ = 7.1, $J_{4,5}$ = 2.3, $^4J_{4,6}$ = 1.0 Hz, 1 H, 4-H), (dd, $J_{4,5}$ = 2.3, $J_{5,6}$ = 5.0 Hz, 1 H, 5-H), 4.97 (dd, $J_{2,3}$ = 1.9, $J_{3,4}$ = 7.1 Hz, 1 H, 3-H), 7.16 (dd, $^4J_{4,6}$ = 0.9, $J_{5,6}$ = 5.0 Hz, 1 H, 6-H).

^{13}C NMR ($CDCl_3$, 75.5 MHz): δ = 12.4 {q, Si[CH(CH_3)$_2$]$_3$}, 18.1 {d, Si[CH(CH_3)$_2$]$_3$}, 24.5, 26.6 [2 s, C(CH_3)$_3$], 29.6 (t, C-1'), 67.5 (d, C-5), 74.4 (d, C-2), 75.2 (d, C-3), 76.0 (d, C-4), 109.8 [s, C(CH_3)$_2$], 132.6 (d, C-6).

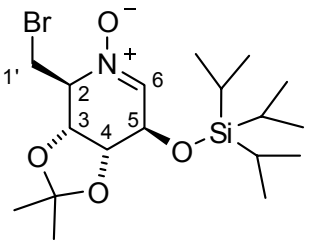

29 D-*altro*

8.3 Experiments Relating to Chapter 3

8.3.1 Chemioselective reduction of L-*lyxo*-nitrone 5 and D-*ribo*-nitrone 6

Experiment 28 (SHF 2)

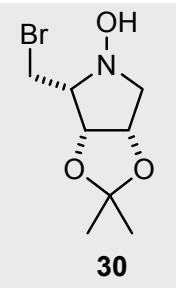

30

(2*R*,3*R*,4*S*)-2-Bromomethyl-1,3,4-trihydroxy-3,4-O-isopropy-lidene-pyrrolidine (30)

The L-*lyxo*-nitrone **5** (1.60 g, 6.40 mmol) was dissolved in 60 mL ethanol and 76 mg (1.92 mmol) $NaBH_4$ was added at 0 °C. After 1.5 h, 5 % citric acid solution (25 mL) was added and the layers were parted. The aqueous layer was extracted with methylene chloride (2 x 40 mL) and the combined organic layers were dried ($MgSO_4$) and concentrated under vacuum using the rotary evaporator (10 mbar; note: the temperature of the water bath should not exceed room temp. and venting should be done with argon). After column chromatography (SiO_2, 70 g, 2.5 cm x 12 cm, eluant: PE/EE = 70:30) 1.15 g (4.56 mmol, 71 %; lit.[2] 93 %) of the pyrrolidine **30** were obtained as an analytically pure, colourless solid (m. p. 90-92 °C; lit.[2] 93-94 °C).

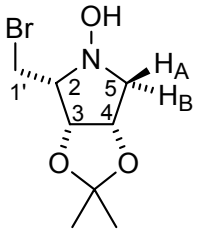

30

$[\alpha]_D^{20}$ = 101 (*c* = 1.00, CH_2Cl_2); lit.[2] $[\alpha]_D^{20}$ = 107 (*c* = 0.455, CH_2Cl_2)

$C_8H_{14}BrNO_3$	calc.	C	38.11	H	5.68	N	5.56	Br 31.69
(252.1)	found	C	38.25	H	5.60	N	5.60	Br 31.92

IR (neat): $\tilde{\nu}$ = 3170 (bs, OH), 2971 (m), 2945 (m), 1461 (m), 1374 (vs), 1287 (m), 1204 (s), 1164 (m), 1121 (m), 916 (m), 886 (w), 853 (s) cm^{-1}.

^{1}H NMR ($CDCl_3$, 500 MHz): δ = 1.30, 1.42 [2 s, 3 H each, $C(CH_3)_2$], 2.77 (dd, $J_{4,5A}$ = 4.5, $^2J_{5A,5B}$ = 11.0 Hz, 1 H, 5-H_A), 2.91 (m, 1 H, 2 H), 3.50 (d, $^2J_{5A,5B}$ = 10.9 Hz, 5-H_B), 3.55-3.62 (m, 2 H, 1'-H_A, 1'-H_B), 4.65 (dd, $J_{3,4}$ = 6.6, $J_{4,5A}$ = 4.50 Hz, 1 H, 4-H), 4.71 (dd, $J_{2,3}$ = 4.8, $J_{3,4}$ = 6.6 Hz, 1 H, 3-H), 7.8 (bs, 1 H, OH).

^{13}C NMR ($CDCl_3$, 62.9 MHz): δ = 24.1, 25.7 [2 q, $C(\underline{C}H_3)_2$], 26.8 (t, C-1'), 63.1 (d, C-5), 72.0 (d, C-2), 74.9 (d, C-4), 76.4 (d, C-3), 110.7 [s, $\underline{C}(CH_3)_2$].
Spectroscopic and analytical data were in accordance to those in lit.[2]

Experiment 30 (SHF 4)

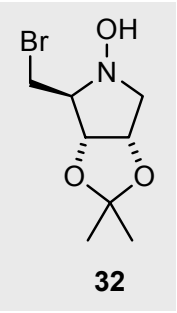

32

(2*S*,3*R*,4*S*)-2-Bromomethyl-1,3,4-trihydroxy-3,4-O-isopropylidene-pyrrolidine (32)

Following lit.[2] as a guide, the D-*ribo*-nitrone **6** (1.50 g, 5.99 mmol) was dissolved in 60 mL ethanol and $NaBH_4$ (0.730 g, 19.2 mmol, 3.0 Eq.) was added portionwise at 0 °C. The suspension was allowed to stir for 15 min and 5 % citric acid solution (25 mL) was added. After 10 min, the layers were separated and the organic phase was extracted with methylene chloride (4 x 25 mL). The combined organic layers were washed with saturated $NaHCO_3$ solution (2 x 10 mL), dried ($MgSO_4$) and the solvents were removed under vacuum (20 °C/10 mbar), taking care to flush the flask with argon when venting. This afforded 1.51 g of the crude product (orange oil), which was then purified by column chromatography (SiO_2, 50 g, 2.5 cm x 10 cm, PE/EE = 70:30) to furnish 1.210 g (4.80 mmol, 80 %) of pyrrolidine **32** as a colourless oil that slowly solidified on standing (m. p. 27-29 °C).

$[\alpha]_D^{20}$ = 12 (*c* = 1.00, CH_2Cl_2)

$C_8H_{14}BrNO_3$	calc.	C	38.11	H	5.60	N	5.56	Br	31.69
(252.1)	found	C	38.34	H	5.67	N	5.54	Br	31.66

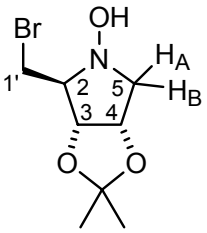

32

IR (neat): $\tilde{\nu}$ = 3236 (bs, OH), 2984 (w), 2935 (w), 2872 (w), 1463 (w), 1421 (w), 1375 (s), 1252 (m), 1206 (s), 1158 (m), 1094 (s), 1070 (s), 987 (w), 969 (w), 952 (w), 911 (w), 859 (s), 805 (w), 791 (w), 653 (s), 598 (s) cm^{-1}.

^{1}H NMR ($CDCl_3$, 500 MHz): δ = 1.30, 1.50 [2 s, 3 H each, $C(CH_3)_2$], 3.11 (dd, $J_{4,5A}$ = 4.2, $^2J_{5A,5B}$ = 11.0 Hz, 1 H, 5-H_A), 3.35 (m, 1 H, 2-H), 3.55 (m, 2 H, 1'-H_A, 1'-H_B), 3.72 (m, 1 H, 5-H_B), 4.55 (dd, $J_{3,4}$ = 6.8, $J_{4,5A}$ = 4.4 Hz, 1 H, 4-H), 4.71 (m,1 H, 3-H).

^{13}C NMR ($CDCl_3$, 62.9 MHz): δ = 24.9, 26.9 [2 q, $C(\underline{C}H_3)_2$], 30.3 (t, C-1'), 62.4 (d, C-5), 72.4 (d, C-2), 76.5 (d, C-4), 80.8 (d, C-3), 111.3 [s, $\underline{C}(CH_3)_2$].

Experiment 29 (SHF 1)

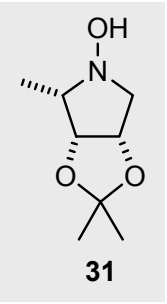

31

(2*S*,3*R*,4*S*)-1,3,4-Trihydroxy-3,4-O-isopropylidene-2-methyl-pyrrolidine (31)

To an oven-dried flask was added 0.400 g (11.3 mmol, 1.08 Eq.) lithium aluminium hydride and 80 mL abs. THF. At 0 °C, a solution of 2.60 g (10.4 mmol) L-*lyxo*-nitrone **5** in abs. 25 mL THF was added dropwise over 5 min. The temperature was raised to room temp. and stirred for a further 2 h. The suspension was hydrolysed by the slow addition (at 0 °C) of water (20 mL) and dilute sodium hydroxide solution (ca. 1 N, 0.4 mL). The layers were parted and the aqueous phase was extracted with diethyl ether (3 x 50 mL). The organic phases were combined, dried (MgSO4) and the solvent was removed on the rotary evaporator (30 °C/10 mbar). The crude product yielded was purified by column chromatography (SiO_2, 100 g, 4 cm x 16 cm, PE/EE = 50:50) to afford the title compound, the pyrrolidine **31** (1.20 g, 6.93 mmol, 67 %; lit.[2] 85 %), as a colourless, analytically pure solid (m.p: 113-114 °C; lit.[2] 113 °C).

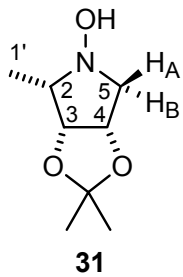

31

$[\alpha]_D^{20}$ = 58 (*c* = 1.01, CH_2Cl_2); $[\alpha]_D^{20}$ = 64 (*c* = 0.52, CH_2Cl_2) [lit.[2]]

$C_8H_{15}NO_3$	calc.	C	55.47	H	8.73	N	8.09
(173.2)	found	C	55.21	H	8.62	N	7.90

IR (film): $\tilde{\nu}$ = 3100 (bs, OH), 2963 (w), 2931 (w), 2844 (w), 1456 (m), 1376 (s), 1269 (w), 1305 (w), 1265 (w), 1202 (vs), 1170 (w),1133 (w), 1077 (w), 1060 (w), 1040 (w), 1003 (vs), 911 (w), 860 (s) cm^{-1}.

^{1}H NMR ($CDCl_3$, 500 MHz): δ = 1.28, 1.42 [2 s, 3 H each, $C(CH_3)$], 1.30 (d, $J_{2,1'}$ = 6.4 Hz, 3 H, 1'-H), 2.50 (dq, $J_{2,1'}$ = 6.4, $J_{2,3}$ = 4.9 Hz, 1 H, 2-H), 2.65 (dd, $J_{4,5A}$ = 4.8, $^2J_{5A,5B}$ = 10.5 Hz, 1 H, 1-H_A), 3.50 (d, $^2J_{5A,5B}$ = 10.5 Hz, 1 H, 1-H_B), 4.50 (dd, $J_{2,3}$ = 4.9, $J_{3,4}$ = 6.7 Hz, 1 H, 3-H), 4.61 (dd, $J_{3,4}$ = 6.7, $J_{4,5A}$ = 4.8 Hz, 1 H, 4 H).

^{13}C NMR ($CDCl_3$, 125 MHz): δ = 11.8 (q, C-1'), 24.0, 25.8 [2 q, $C(CH_3)_2$], 62.5 (d, C-5), 66.2 (d, C-2), 75.3 (C-4), 78.5 (C-3), 112.5 [s, $C(CH_3)_2$].

Spectroscopic and analytical data were in accordance to those found in lit.[2]

Experiment 31 (SHF 3)

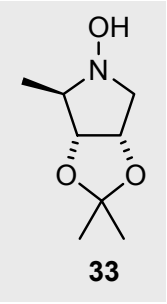

33

(2*R*,3*R*,4*S*)-1,3,4-Trihydroxy-3,4-O-isopropylidene-2-methyl-pyrrolidine (33)

The reaction scale and procedure is identical to that given in E 29 with one exception: Here, the reaction was stirred overnight, worked-up and purified, as described in E 29. This afforded the pyrrolidine **33** (1.29 g, 7.45 mmol, 72 %; lit.[2] 75 %) as a spectroscopically pure, colourless solid (m. p 43-45 °C; lit.[2] 50-51 °C).

$[\alpha]_D^{20}$ = 10 (*c* = 1.02, CH_2Cl_2); $[\alpha]_D^{20}$ = 5.2 (*c* = 0.50, CH_2Cl_2) [lit.[2]]

$C_8H_{15}NO_3$	calc.	C	55.47	H	8.73	N	8.09
(173.2)	found	C	54.96	H	8.45	N	7.80

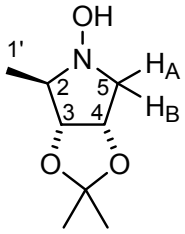

33

IR (film): $\tilde{\nu}$ = 3200 (bs, OH), 2935 (m), 2864 (m), 1455 (m), 1373 (vs), 1269 (w), 1205 (s), 1153 (m), 1080 (w), 1056 (m), 1020 (m), 975 (m), 858 (vs).

^{1}H NMR (C_6D_6, 500 MHz, 343 K) δ = 1.21 (d, $J_{2,1'}$ = 6.7 Hz, 3 H, 1'-H), 1.28, 1.59 [2 s, 3 H each, $C(CH_3)_2$], 3.23 (dd, $J_{4,5A}$ = 4.0, $^2J_{5A,5B}$ = 11.0 Hz, 1 H, 5-H_A), 3.30 (dq, $J_{2,1'}$ = 6.7, $J_{2,3}$ = 4.5 Hz, 1 H, 2-H), 3.38 (dd, $J_{4,5B}$ = 5.9, $^2J_{5A,5B}$ = 11.0 Hz, 1 H, 5-H_B), 4.15 (dd, $J_{2,3}$ = 4.5, $J_{3,4}$ = 7.0 Hz, 1 H, 3-H), 4.47 (ddd, $J_{3,4}$ = 7.0, $J_{4,5A}$ = 4.0 Hz, $J_{4,5B}$ = 5.9 Hz,1 H, 4 H), 5.90 (bs, 1 H, OH).

^{13}C NMR (C_6D_6, 125.8 MHz, 343 K): δ = 13.9 (q, C-1'), 25.1, 27.3 [2 q, $C(\underline{C}H_3)_2$], 62.6 (t, C-5), 68.2 (d, C-2), 77.3 (d, C-4), 84.5 (d, C-3), 112.9 [s, $\underline{C}(CH_3)_2$].

Spectroscopic and analytical data were in accordance to those found in lit.[2]

8.3.2 Addition of *C*-nucleophiles to L-*lyxo*-nitrone 5 and D-*ribo*-nitrone 6

Experiment 32 (LR 20, 204)

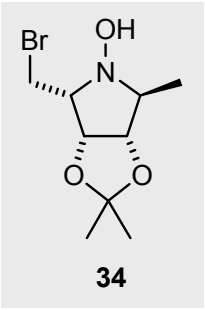

34

(2*R*,3*R*,4*S*,5*S*)-2-Bromomethyl-1,3,4-trihydroxy-3,4-*O*-isopropylidene-5-methyl-pyrrolidine (34)

To an oven-dried two-necked flask under argon was added the L-*lyxo*-nitrone **5** (900 mg, 3.59 mmol) in 25 mL abs. THF. The near colourless solution was cooled to -40 °C (dry ice/acetone) and a solution of methylmagnesium bromide (3.0 M solution in Et_2O, 3.40 mL, 10 mmol, 2.5 Eq., Aldrich) was added dropwise. Within 2 min a change from colourless to golden-yellow occurred which during the reaction gradually became darker in tone. After 2 h at 40 °C, the reaction was quenched through addition of a saturated solution of NH_4Cl (10 mL). The solution was warmed to room temp., the phases were separated, and the aqueous phase was extracted with methylene chloride (3 x 25 mL). The combined organic phases were dried ($MgSO_4$) and concentrated on the rotary evaporator (30 °C/ 10 mbar) (^{1}H NMR d. r. = 92:8). The crude product was purified using flash chromatography (SiO_2 30 g, 2.5 cm x 12 cm, PE/EE = 70:30) to afford the pyrrolidine **34** (873 mg, 1.08 mmol, 94 %; lit.[2] 90 %) as an analytically pure, colourless solid (m. p. 104 °C).

$[\alpha]_D^{20}$ = 98 (*c* = 0.98, $CHCl_3$); lit.[2] $[\alpha]_D^{20}$ = 106 (*c* = 0.535, CH_2Cl_2)

$C_9H_{16}BrNO_3$	calc.	C	40.62	H	6.06	N	5.26	Br	30.02
(266.1)	found	C	40.71	H	6.09	N	5.05	Br	29.60

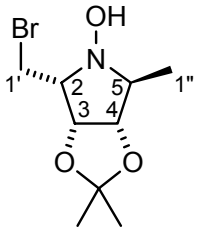

34

IR (neat): $\tilde{\nu}$ = 3194 (bs, OH), 2985 (w), 2931 (w), 1454 (w), 1373 (m), 1269 (w), 1234 (w), 1210 (s), 1164 (m), 1125 (w), 1048 (s), 978 (m), 933 (m), 861 (s) cm $^{-1}$.

^{1}H NMR ($CDCl_3$, 250.1 MHz): δ = 1.01 (d, $J_{5,1"}$ = 7.1 Hz, 1 H, 5-CH_3), 1.30, 1.42 [2 s, 3 H each, $C(CH_3)_2$], 3.30 (m, 1 H, 2-H), 3.55 (dd, $J_{2,1'A}$ = 4.0, $^2J_{1'A,1'B}$ = 9.0 Hz, 1 H, 1'-H_A), 3.57-3.62 (m, 2 H, 5-H, 1'-H_B), 4.38 (d, $J_{3,4}$ = 6.7 Hz, 1 H, 4-H), 4.68 (dd, $J_{2,3}$ = 5.1, $J_{3,4}$ = 6.7 Hz, 1 H, 3-H), 7.25 (bs, 1 H, OH).

^{13}C NMR ($CDCl_3$, 75.5 MHz): δ = 9.7 (q, C-1''), 24.1, 25.7 [2 q, $C(\underline{C}H_3)_2$], 27.8 (q, C-1'), 65.1 (d, C-5), 67.0 (d, C-2), 75.6 (d, C-3), 81.3 (d, C-4), 111.1 [s, $\underline{C}(CH_3)_2$].

Analytical and spectroscopic data were in agreement with literature values.[2]

Experiment 33 (LR 90)

(2*R*,3*R*,4*S*,5*S*)-2-Bromomethyl-1,3,4-trihydroxy-3,4-*O*-isopropylidene-5-propyl-pyrrolidine (35)

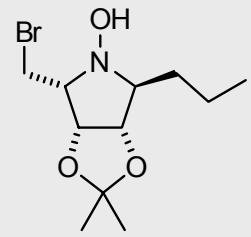

35

TLP 1: n-Propylmagnesium bromide; Typical Laboratory Procedure for the preparation of Grignard reagents from alkyl- and/or arylhalogenides with magnesium

To an oven-dried two-necked flask fitted with a reflux condenser was added magnesium turnings (140 mg, 5.70 mmol, 1.05 Eq.) under nitrogen. The flask was evacuated and heated with the heat-gun with stirring of the magnesium turnings. The flask was flushed with argon repeatedly for 3-4 times. After cooling, 3.5 mL THF was added to give a ca. 1.6 M solution of Grignard reagent). A crystal of iodine and 20 % of the total volume of n-propyl bromide (680 mg, 5.59 mmol, 2.0 Eq., Aldrich) was added dropwise. During the addition, the solution became warm and slightly opaque. The remaing n-propyl bromide was added at a rate so as to maintain a gently refluxing solution. The solution was then heated to 55 °C until no change to the amount of remaining magnesium turnings could be determined (max. 30 min). The resulting solution was then used immediately for addition to the L-*lyxo*-nitrone **5**, as described below.

TLP 2: n-Propylpyrrolidine 35; Typical Laboratory Procedure for the addition of Grignard Reagents to L-*lyxo*-nitrone 5

A second oven-dried flash under nitrogen was charged with the L-*lyxo*-nitrone **5** (700 mg, 2.79 mmol) and abs. THF (25 mL) and cooled to -40 °C (dry ice/acetone). n-Propyl-magnesium bromide solution from TLP 1 was added dropwise using a syringe which led to a golden-yellow solution. After 2 h, the colour had changed to orange/red and the reaction was quenched with a solution of saturated NH_4Cl (10 mL) and water (10 mL). The aqueous phase was extracted with CH_2Cl_2 (3 x 20 mL); the combined organic phases were washed with saturated NaCl solution (10 mL), dried ($MgSO_4$) and the solvent was removed on the rotary

evaporator (30 °C, 20 mbar) to yield the crude product of **35** (^{1}H NMR: d. r. = >95:5) which was purified using column chromatography (SiO_2, 40 g, 2.5 cm x 18 cm, PE/EE = 80:20) to afford the pyrrolidine **35** as an analytically almost pure, pale-yellow oil (520 mg, 1.83 mmol, 65 %).

$[\alpha]_D^{20}$ = 98 (*c* = 0.98, $CHCl_3$)

$C_{11}H_{20}BrNO_3$	calc.	C	44.91	H	6.85	N	4.76	Br	27.16
(294.2)	found	C	45.41	H	6.92	N	4.61	Br	26.44

IR (neat): $\tilde{\nu}$ = 3197 (bs, OH), 2958 (w), 2932 (w), 2871 (w), 1456 (w), 1374 (m), 1270 (s), 1207 (m), 1164 (m), 1125 (m), 1054 (s), 974 (m), 863 (m), 689 (m) cm^{-1}.

^{1}H and ^{13}C NMR data are contained in Tables 4-6 (p. 73-77).

Experiment 34 (LR 279)

(2*R*,3*R*,4*S*,5*S*)-2-Bromomethyl-1,3,4-trihydroxy-5-isopropyl-3,4-*O*-isopropylidene-pyrrolidine (36)

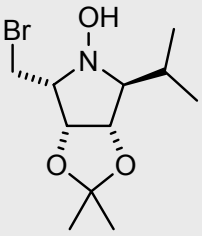

36

Isopropyl bromide (983 mg, 7.99 mmol), magnesium (200 mg, 8.18 mmol) and a crystal of iodine were combined according to TLP 1 and then added to the nitrone **5** (1.00 g, 3.99 mmol) using TLP 2 (–40 °C/2.5 h). The crude product, a dark yellow oil, was purified using column chromatography (SiO_2, 40 g, 2.5 cm x 18 cm, PE/EE = 80:20) to produce the pyrrolidine **36** (0.647 g, 2.2 mmol, 55 %) as an analytically pure, orange oil (stored at -18 °C).

$[\alpha]_D^{20}$ = 24 (*c* = 0.50, $CHCl_3$)

$C_{11}H_{20}BrNO_3$	calc.	C	44.91	H	6.85	N	4.76
(294.2)	found	C	45.21	H	6.81	N	4.70

IR (neat): $\tilde{\nu}$ = 3120 (bs, OH), 2962 (w), 2936 (w), 1609 (w), 1583 (w), 1462 (w), 1375 (m), 1209 (s), 1055 (s), 868 (m), 664 (m) cm^{-1}.

^{1}H and ^{13}C NMR data are contained in Tables 4-6 (p. 73-77).

Experiment 35 (LR 280)

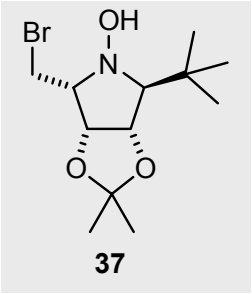

37

(2*R*,3*R*,4*S*,5*S*)-2-Bromomethyl-5-*tert*-butyl-1,3,4-trihydroxy-3,4-*O*-isopropylidene-pyrrolidine (37)

A solution of *tert*-butylmagnesium chloride (4.0 mL, 8.0 mmol, 2.0 M in THF, 2 Eq., Aldrich) was added to the nitrone **5** (1.00 g, 3.99 mmol) at –40 °C according to TLP 2. The heat-sensitive crude product (rotary evaporator: max. temp. 30 °C) was purified using column chromatography (SiO_2, 40 g, 2.5 cm x 21 cm, PE/EE = 80:20) to yield the pyrrolidine **37** (0.41 g, 1.3 mmol, 33 %) as an analytically pure, pale-yellow solid (m. p. 78 °C).

$[\alpha]_D^{20}$ = –6.0 (*c* = 1.0, $CHCl_3$)

$C_{12}H_{22}BrNO_3$	calc.	C	46.76	H	7.19	N	4.54	Br 25.92
(308.21)	found	C	46.93	H	7.13	N	4.52	Br 25.76

IR (neat): $\tilde{\nu}$ = 3120 (bs, OH), 2962 (w), 2936 (w), 1609 (w), 1583 (w), 1462 (w), 1375 (m), 1209 (s), 1055 (s), 868 (m), 664 (m), 632 (w), 611 (m), 601 (w), 591 (m) cm^{-1}.

^1H and ^{13}C NMR data are contained in Tables 4-6 (p. 73-77).

Experiment 36 (LR 117)

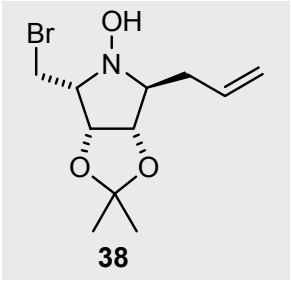

38

(2*R*,3*R*,4*S*,5*S*)-5-Allyl-2-bromomethyl-1,3,4-trihydroxy-3,4-*O*-isopropylidene-pyrrolidine (38)

An allylmagnesium bromide solution (7.6 mL, 7.6 mmol, 1.0 M in THF, 1.5 Eq., Aldrich) was added (see TLP 2) to the nitrone **5** (1.27 g, 5.08 mmol). Purification by column chromatography (SiO_2, 40 g, 2.5 cm x 20 cm, PE/EE = 80:20) afforded the pyrrolidine **38** (1.20 g, 4.1 mmol, 81 %; lit.[2] 90 %) as a colourless solid (m. p. 78-79 °C; lit.[2] 82-85 °C).

$[\alpha]_D^{20}$ = 58 (*c* = 1.00, $CHCl_3$); lit.[2] $[\alpha]_D^{20}$ = 72 (c = 0.49, CH_2Cl_2)

$C_{11}H_{18}BrNO_3$	calc.	C	45.22	H	6.21	N	4.79	Br	27.35
(292.2)	found	C	45.45	H	6.25	N	4.71	Br	27.02

IR (neat): $\tilde{\nu}$ = 3194 (bs, OH), 2979 (w), 2934 (w), 2882 (w), 1642 (w, C=C), 1456 (w), 1374 (m), 1207 (s), 1050 (s), 1031 (m), 918 (s) 861 (m), 694 (m) cm^{-1}.

^1H and ^{13}C NMR data are contained in Tables 4-6 (p. 73-77).

Experiment 37 (LR 143)

(2*R*,3*R*,4*S*,5*S*)-2-Bromomethyl-1,3,4-trihydroxy-3,4-*O*-isopropylidene-5-(4-pentenyl)-pyrrolidine (39)

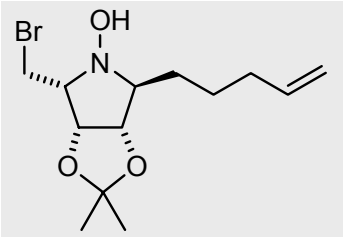

39

5-Bromopentene (1.240 g, 8.38 mmol, 1.5 Eq., Aldrich), magnesium (0.150 g, 8.66 mmol, 1.7 Eq.) and a crystal of iodine were combined according to TLP 1 and added to the nitrone **5** (1.40 g, 5.59 mmol) using TLP 2. The crude product was purified over silica gel (40 g, 2.5 cm x 20 cm, PE/EE = 80:20) to produce the pyrrolidine **39** (1.225 g, 3.83 mmol, 68 %) as an analytically pure, colourless solid (m. p. 50-52 °C) und 200 mg (0.80 mmol, 14 %) of the recovered nitrone **5**.

$[\alpha]_D^{20}$ = 75 (*c* = 1.03, $CHCl_3$)

$C_{13}H_{22}NO_3Br$	calc.	C	48.79	H	6.93	N	4.37	Br	24.97
(320.2)	found	C	48.60	H	6.88	N	4.31	Br	24.72

IR (KBr disc): $\tilde{\nu}$ = 3228 (bs, OH), 3078 (m), 2977 (w), 2929 (w), 1640 (w, C=C), 1456 (m), 1435 (m), 1376 (m), 1273 (s), 1207 (m), 1165 (m), 1122 (m), 1062 (s), 863 (s), 739 (m) cm^{-1}.

^1H and ^{13}C NMR data are contained in Tables 4-6 (p. 73-77).

Experiment 38 (LR 196)

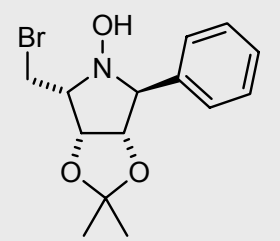

40

(2*R*,3*R*,4*S*,5*S*)-2-Bromomethyl-1,3,4-trihydroxy-3,4-*O*-isopropylidene-5-phenyl-pyrrolidine (40)

Bromobenzene (1.00 g, 6.39 mmol, 2.0 Eq.) and magnesium (150 mg, 6.40 mmol) were combined according to TLP 1 and added to the nitrone **5** (0.80 g, 3.20 mmol) using TLP 2. Crude product purification by column chromatography (SiO_2, 30 g, 2.5 cm x 12 cm, PE/EE = 80:20) provided the pyrrolidine **40** (752 mg, 2.29 mmol, 72 %; lit.[2] 91 %) as an analytically pure, colourless solid (m. p. 130-132 °C decomp.; lit.[2] 127-128 °C).

$[\alpha]_D^{20}$ = – 12 (*c* = 0.50, CH_2Cl_2); lit.[2] $[\alpha]_D^{20}$ = – 13 (c = 0.53, CH_2Cl_2)

$C_{14}H_{18}BrNO_3$	calc.	C	51.24	H	5.53	N	4.27	Br	24.35
(328.2)	found	C	51.34	H	5.56	N	4.27	Br	24.23

IR (neat): $\tilde{\nu}$ = 3097 (bs, OH), 2985 (w), 2937 (w), 2917 (w), 1498 (w), 1454 (w), 1379 (s), 1276 (s), 1209 (s), 1166 (m), 1105 (w), 1056 (s), 970 (w), 849 (m), 756 (s), 697 (s) cm^{-1}.

The spectroscopic and analytical data were in accordance with literature values.[2]
^1H and ^{13}C NMR data are contained in Tables 4-6 (p. 73-77).

Experiment 39 (LR 30)

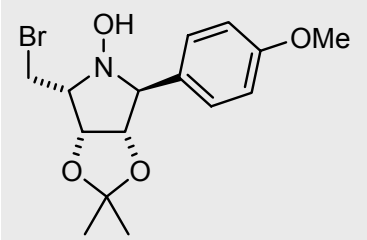

41

(2*R*,3*R*,4*S*,5*S*)-2-Bromomethyl-1,3,4-trihydroxy-3,4-*O*-isopropylidene-5-(4-methoxyphenyl)-pyrrolidine (41)

4-Methoxyphenylmagnesium bromide was prepared from 1.94 g (9.6 mmol) 4-bromoanisole and 240 mg (10.1 mmol) magnesium using TLP 1 and added to the L-*lyxo*-nitrone **5** (1.20 g, 4.8 mmol) using TLP 2. Column chromatography of the crude product (SiO_2, 40 g, 2.5 cm x 20 cm, PE/EE = 80:20) afforded the pyrrolidine **41** (1.49 g, 4.16 mmol, 87 %) as an

analytically pure, colourless solid (m. p. 146-147 °C). The structure of **41** was further confirmed by X-ray crystal structure analysis (data in Section 9.3).

$[\alpha]_D^{20}$ = –3 (*c* = 1.00, CH_2Cl_2)

$C_{15}H_{20}BrNO_4$	calc.	C	50.29	H	5.63	N	3.91	Br	22.31
(358.2)	found	C	50.37	H	5.65	N	3.85	Br	22.21

IR (neat): $\tilde{\nu}$ = 3253 (bs, OH), 3004 (m), 2931 (m), 2891 (m), 2829 (w), 1614 (s), 1514 (m), 1426 (s), 1378 (s), 1250 (s), 1210 (m), 1065 (s), 1034 (m), 1029 (m), 694 (m), 627 (m) cm^{-1}.

^1H and ^{13}C NMR data are contained in Tables 4-6 (p. 73-77).

Experiment 40 (LR 31, 138)

(2*R*,3*R*,4*S*,5*S*)-5-([1,1'-Biphenyl]-4-yl)-2-bromomethyl-1,3,4-trihydroxy-3,4-*O*-isopropylidene-pyrrolidine (42)

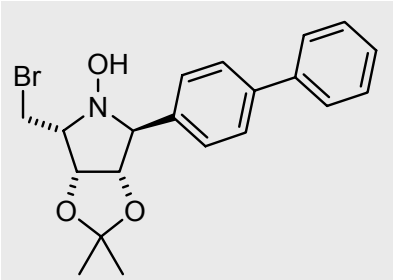

42

4-Bromobiphenyl (3.03 g, 13.0 mmol, Fluka, >99 %), magnesium (325 mg, 13.4 mmol), and a crystal of iodine in THF (9 mL) were combined according to TLP 1 and added to the nitrone **5** (1.63 g, 6.50 mmol) in 45 mL THF using TLP 2. Column chromatography of the crude product (SiO_2, 70 g, 2.5 cm x 25 cm, PE/EE = 80:20) provided the pyrrolidine **42** (2.10 g, 5.20 mmol, 80 %) as an analytically pure, colourless solid (m. p. 69 °C).

$[\alpha]_D^{20}$ = – 14 (*c* = 1.04, CH_2Cl_2)

$C_{20}H_{22}BrNO_3$	calc.	C	59.42	H	5.48	N	3.46	Br	19.76
(404.3)	found	C	59.71	H	5.58	N	3.22	Br	19.59

IR (neat): $\tilde{\nu}$ = 3219 (bs, OH), 3030 (m, -CH_2, st.), 2984 (m), 2930 (m), 2853 (m), 1604 (m), 1487 (s), 1376 (s), 1272 (s), 1210 (s), 1165 (m), 1063 (s), 974 (m), 840 (m), 757 (w), 685 (m), 622 (w), 604 (w), 577 (w) cm^{-1}.

^1H and ^{13}C NMR data are contained in Tables 4-6 (p. 73-77).

Experiment 41 (LR 213)

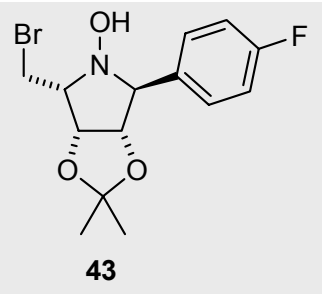

43

(2*R*,3*R*,4*S*,5*S*)-2-Bromomethyl-5-(4-fluorophenyl)-1,3,4-trihydroxy-3,4-*O*-isopropylidene-pyrrolidine (43)

1-Bromo-4-fluorobenzene (1.11 g, 6.38 mmol, Fluka, >98 %), magnesium (160 mg, 6.53 mmol), and a crystal of iodine in THF (4 mL) were combined according to TLP 1 and added to nitrone **5** (800 mg, 3.20 mmol) in 40 mL THF according to TLP 2. Column chromatography of the crude product (SiO_2, 70 g, 2.5 cm x 25 cm, PE/EE = 80:20) provided the pyrrolidine **43** (0.889 g, 2.57 mmol, 80 %) as a colourless solid (m. p. 113-115 °C, decomp.).

$[\alpha]_D^{20}$ = –8 (*c* = 1.00, $CHCl_3$)

$C_{14}H_{17}BrFNO_3$	calc.	C	48.57	H	4.95	N	4.05	Br	23.08
(346.2)	found	C	48.84	H	5.00	N	4.05	Br	22.99

IR (KBr): $\tilde{\nu}$ = 3194 (bs, OH), 2984 (w), 2935 (m), 1608 (s), 1512 (vs), 1457 (w), 1376 (s), 1282 (w), 1224 (m), 1207 (m), 1183 (m), 1060 (s), 1034 (w), 914 (w), 882 (w), 855 (w), 836 (s) cm^{-1}.

^1H and ^{13}C NMR data are contained in Tables 4-6 (p. 73-77).

Experiment 42 (LR 104, YG 9)

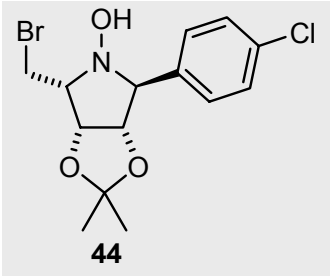

44

(2*R*,3*R*,4*S*,5*S*)-2-Bromomethyl-5-(4-chlorophenyl)-1,3,4-trihydroxy-3,4-*O*-isopropylidene-pyrrolidine (44)

1-Bromo-4-chlorobenzene (2.29 g, 12.0 mmol, Fluka, >98 %), magnesium (296 mg, 12.2 mmol), and a crystal of iodine in THF (7.5 mL) were combined according to TLP 1 and added to the L-*lyxo*-nitrone **5** (1.50 g, 6.00 mmol) in 40 mL THF according to TLP 2. After column chromatography of the crude product (SiO_2, 170 g, 6 cm x 17 cm, PE/EE = 90:10), the pyrrolidine **44** (1.97 g, 5.43 mmol, 91 %) was obtained as an analytically pure, colourless solid (m. p. 124-127 °C).

$[\alpha]_D^{20}$ = –15 (*c* = 1.10, CH_2Cl_2)

$C_{14}H_{17}BrClNO_3$	calc.	C	46.37	H	4.72	N	3.86
(362.7)	found	C	46.54	H	4.77	N	3.80

IR (KBr): $\tilde{\nu}$ = 3200 (bs, OH), 3098 (m), 2984 (m), 2932 (m), 2882 (m), 1660 (s), 1593 (m), 1492 (s), 1376 (s), 1277 (s), 1210 (s), 1160 (m), 1096 (s), 1021 (s), 975 (m), 925 (w), 885 (w), 830 (m), 793 (m), 743 (w) cm^{-1}.

^1H and ^{13}C NMR data are contained in Tables 4-6 (p. 73-77).

Experiment 43 (YG 13; LR 200)

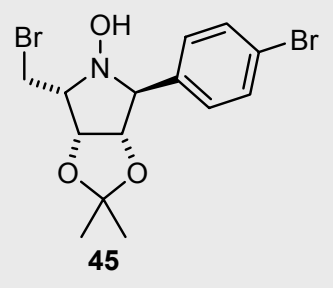

45

(2*R*,3*R*,4*S*,5*S*)-2-Bromomethyl-5-(4-bromophenyl)-1,3,4-trihydroxy-3,4-*O*-isopropylidene-pyrrolidine (45)

1,4-Dibromobenzene (1.50 g, 6.39 mmol, Fluka, >98 %), magnesium (155 mg, 6.40 mmol), and a crystal of iodine in THF (4.0 mL) were combined according to TLP 1 and added to the L-*lyxo*-nitrone **5** (800 mg, 3.20 mmol) in 30 mL THF according to TLP 2. After column chromatography of the crude material (SiO_2, 170 g, 6 cm x 17 cm, PE/EE = 90:10), the pyrrolidine **45** (55 %, 0.717 g, 1.76 mmol) was obtained as a spectroscopically pure, colourless solid (m. p. 135-138 °C). The crystals obtained from the purification were suitable for X-ray structure determination which provided additional structural proof (cf. Section 9.4).

$[\alpha]_D^{20}$ = –0.2 (*c* = 1.03, CH_2Cl_2)

$C_{14}H_{17}Br_2NO_3$	calc.	C	41.30	H	4.21	N	3.44	Br	39.26
(407.1)	found	C	42.41	H	4.35	N	3.40	Br	37.42
	Δ		+1.11						-1.84

IR (KBr): $\tilde{\nu}$ = 3219 (bs, OH), 3030 (m), 2984 (m), 2930 (m), 2853 (m), 1592 (m), 1489 (s), 1374 (s), 1281 (s), 1207 (s), 1164 (m), 1102 (m), 1070 (w), 1060 (s), 1010 (w), 975 (m), 915 840 (m), 757 (w), 697 (m) cm^{-1}.

^1H and ^{13}C NMR data are contained in Tables 4-6 (p. 73-77).

Experiment 44 (LR 50; SH 4)

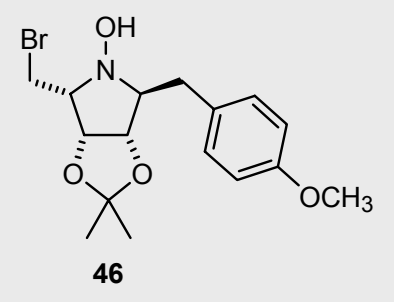

46

(2*R*,3*R*,4*S*,5*S*)-2-Bromomethyl-1,3,4-trihydroxy-3,4-*O*-isopropylidene-5-(4-methoxybenzyl)-pyrrolidine (46)

p-Methoxybenzyl chloride (0.92 g, 12.07 mmol), magnesium (300 mg, 12.38 mmol), and a crystal of iodine in THF (7.5 mL) were combined according to TLP 1 and added to the L-*lyxo*-nitrone **5** (1.51 g, 6.04 mmol) in 40 mL THF according to TLP 2. Column chromatography of the crude material (SiO_2, 60 g, 2.5 cm x 31 cm, PE/EE = 80:20) provided the pyrrolidine **46** as a colourless oil (2.01 g, 5.4 mmol, 89 %) which slowly solidified to give colourless crystals (m. p. 54-56 °C).

$[\alpha]_D^{20}$ = 76 (*c* = 1.04, $CHCl_3$)

$C_{16}H_{22}BrNO_4$	calc.	C	51.62	H	5.96	N	3.76	Br	21.46
(372.3)	found	C	51.57	H	5.94	N	3.60	Br	21.48

IR (neat): $\tilde{\nu}$ = 3216 (bs, OH), 3030 (m), 2988 (m), 2937 (m), 2835 (w, -OCH_3), 1611 (m), 1511 (s), 1453 (s), 1373 (m), 1245 (s), 1207 (m), 1054 (s), 1034 (m), 1003 (m), 871 (m), 811 (w), 647 (m), 616 (s) cm^{-1}.

^1H and ^{13}C NMR data are contained in Tables 4-6 (p. 73-77).

Experiment 45 (LR 45)

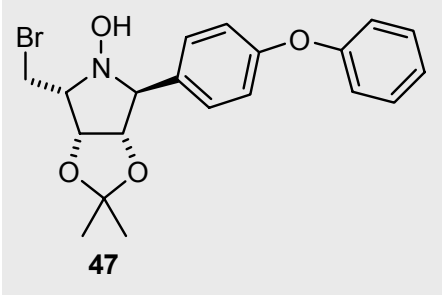

47

(2*R*,3*R*,4*S*,5*S*)-2-Bromomethyl-1,3,4-trihydroxy-3,4-*O*-isopropylidene-5-(4-phenoxyphenyl)-pyrrolidine (47)

p-Bromodiphenyl ether (1.28 g, 4.82 mmol), magnesium (120 mg, 5.14 mmol), and a crystal of iodine in THF (3.0 mL) were combined according to TLP 1 and added to the L-*lyxo*-nitrone **5** (0.402 g, 1.67 mmol) in 20 mL THF according to TLP 2. Column chromatography of the crude material (SiO_2, 40 g, 2 cm x 20 cm, PE/EE = 80:20) provided 0.500 g (1.19 mmol, 75

%) of the title compound **47** as an analytically pure, colourless solid (m. p. 100-104 °C, decomp.), whose structure was confirmed by X-ray analysis (cf. Section 9.5).

$[\alpha]_D^{20}$ = –10 (*c* = 1.00, CH_2Cl_2)

$C_{20}H_{22}BrNO_4$	calc.	C	57.15	H	5.28	N	3.33	Br	19.01
(420.3)	found	C	57.30	H	5.40	N	3.15	Br	18.67

IR (KBr): $\tilde{\nu}$ = 3210 (bs, OH), 3067 (m), 2984 (m), 2933 (m), 1734 (w), 1588 (m), 1517 (m), 1495 (s), 1377 (m), 1240 (s), 1203 (w), 1062 (s), 974 (w), 923 (w), 872 (w), 838 (w), 752 (m), 692 (w) cm^{-1}.

^1H and ^{13}C NMR data are contained in Tables 4-6 (p. 73-77).

Experiment 46 (LR 47; NM 8)

(2*R*,3*R*,4*S*,5*S*)-2-Bromomethyl-1,3,4-trihydroxy-3,4-*O*-isopropylidene-5-(4-methylthiophenyl)-pyrrolidine (48)

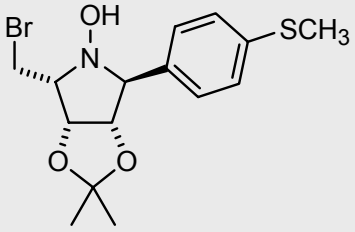

48

4-Bromothioanisole (0.81 g; 3.89 mmol; Aldrich, 97 %), magnesium (100 mg, 4.15 mmol), and a crystal of iodine in THF (2.5 mL) were combined according to TLP 1 and added to the nitrone **5** (0.32 g, 1.28 mmol) in 20 mL THF according to TLP 2. The crude product was purified over a silica gel column (SiO_2, 40 g, 2 cm x 20 cm, PE/EE = 80:20) to yield the pyrrolidine **48** (0.383 g, 1.02 mmol, 80 %) as an analytically pure, pale-yellow solid (m. p. 130 °C).

$[\alpha]_D^{20}$ = –11 (*c* = 0.99, $CHCl_3$)

$C_{15}H_{20}BrNO_3S$	calc.	C	48.13	H	5.39	N	3.74	S	8.57	Br	21.35
(374.3)	found	C	48.23	H	5.45	N	3.60	S	8.84	Br	21.32

IR (KBr): $\tilde{\nu}$ = 3255 (bs, OH), 2929 (m), 2881 (w), 1600 (w), 1494 (m), 1377 (m), 1277 (s), 1214 (m), 1062 (s), 973 (w), 925 (w), 856 (w), 826 (w), 572 (m) cm^{-1}.

^1H and ^{13}C NMR data are contained in Tables 4-6 (p. 73-77).

Experiment 47 (YG 15, NM 7)

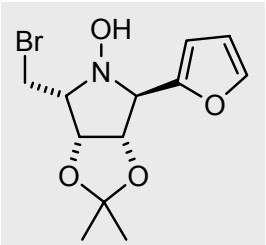

49

(2*R*,3*R*,4*S*,5*S*)-2-Bromomethyl-2-(2-furyl)-1,3,4-trihydroxy-3,4-*O*-isopropylidene-pyrrolidine (49)

To an oven-dried flask under nitrogen was added freshly distilled furan (1.4 mL, 19 mmol) in 50 mL abs. THF. The solution was cooled to -80 °C and 12 mL (19 mmol) of n-butyllithium (1.6 M in hexane) was added slowly dropwise. The reaction vessel was allowed to warm to 0 °C over 1.5 h. The reaction was once again cooled to -80 °C and a solution of the L-*lyxo*-nitrone **5** (1.60 g, 6.40 mmol) in 30 mL THF was added dropwise over 5 min. The reaction was stirred for 1.5 h at -80 °C, then quenched slowly with 15 mL of saturated NH_4Cl solution and warmed to 10 °C. The aqueous phases were extracted with 3 x 40 mL CH_2Cl_2 and the combined organic layers dried ($MgSO_4$). The solvent was removed on the rotary evaporator (30 °C/10 mbar). The crude product was purified using column chromatography (SiO_2, 90 g, 3.5 cm x 22 cm, PE/EE 80 : 20). This afforded the substituted 5-furyl-pyrrolidine **49** (1.62 g, 5.08 mmol, 80 %) as an analytically pure, colourless solid (m. p. 117 °C).

$[\alpha]_D^{20}$ = 39 (*c* = 0.98, $CHCl_3$)

$C_{12}H_{16}BrNO_4$	calc.	C	45.30	H	5.07	N	4.40	Br 25.11
(318.2)	found	C	45.47	H	5.09	N	4.41	Br 25.27

IR (neat): $\tilde{\nu}$ = 3111 (bs), 2979 (w), 2940 (w), 1500 (w), 1427 (w), 1375 (m), 1274 (w), 1207 (s), 1156 (m), 1125 (m), 1058 (s), 1035 (m), 1009 (w), 974 (m), 931 (m), 866 (s), 835 (m), 792 (w), 741 (m), 691 (w), 645 (w), 610 (w), 598 (s) cm^{-1}.

^1H and ^{13}C NMR data are contained in Tables 4-6 (p. 73-77).

Experiment 48 (LR 195)

(2*R*,3*R*,4*S*,5*S*)-2-Bromomethyl-5-(4-*N,N*-dimethylanilino)-1,3,4-trihydroxy-3,4-*O*-isopropylidene-pyrrolidine (50)

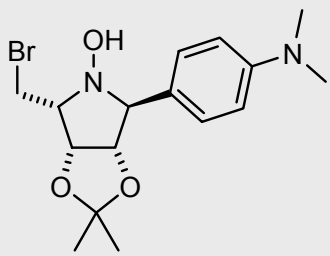

50

4-Bromo-*N*,*N*-dimethylaniline (1.28 g, 6.39 mmol; Lancaster, 97 %), magnesium (162 mg, 6.69 mmol), and a crystal of iodine in THF (2.5 mL) were combined according to TLP 1 and added to the L-*lyxo*-nitrone **5** (0.800 g, 3.19 mmol) in 40 mL THF according to TLP 2. Purification of the crude product by column chromatography (SiO_2, 60 g, 2.5 cm x 20 cm, PE/EE = 70:30) afforded the title α-L-*lyxo*-configured pyrroldine **50** (1.034 g, 2.78 mmol, 87 %) as an analytically pure, yellow solid (m. p. 131 °C).

$[\alpha]_D^{20}$ = –8 (*c* = 1.00, $CHCl_3$)

$C_{16}H_{23}BrN_2O_3$	calc.	C	51.76	H	6.24	N	7.55	Br 21.52
(371.3)	found	C	51.84	H	6.23	N	7.47	Br 21.49

IR (neat): $\tilde{\nu}$ = 3492 (bs, OH), 2977 (w), 2933 (w), 1610 (s), 1524 (s), 1364 (s), 1275 (w), 1205 (m), 1164 (m), 1059 (s), 1015 (w), 975 (m), 946 (m), 912 (w) cm^{-1}.

^1H and ^{13}C NMR data are contained in Tables 4-6 (p. 73-77).

Addition of Grignard reagent to the D-*ribo* nitrone **6**

Experiment 49 (LR 341)

(2*S*,3*R*,4*S*,5*S*)-2-Bromomethyl-5-(4-*N,N*-dimethylanilino)-1,3,4-trihydroxy-3,4-*O*-isopropylidene-pyrrolidine (51)

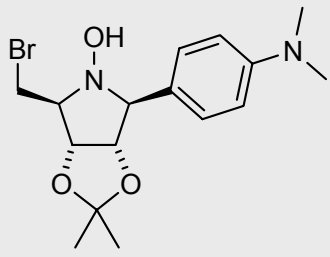

51

Experiment 49 was carried out in an identical way and scale to Experiment 48 (above; reaction of the other diastereoisomer). After column chromatographic purification of the crude product (SiO_2, 80 g, 3 cm x 25 cm, eluant: PE/EE = 80:20), the β-D-*ribo*-configured

pyrrolidine **51** (0.940 g, 2.53 mmol, 79 %) was obtained as an analytically pure, colourless solid (m. p. 133 °C). The configuration was confirmed by X-ray crystal structure analysis (data contained in Section 9.6).

$[\alpha]_D^{20}$ = –39 (*c* = 1.00, $CHCl_3$)

$C_{16}H_{23}BrN_2O_3$	calc.	C	51.76	H	6.24	N	7.55	Br 21.52
(371.3)	found	C	51.98	H	6.26	N	7.49	Br 21.32

IR (neat): $\tilde{\nu}$ = 3405 (bs, OH), 2981 (w), 2932 (m), 2859 (m), 2805 (w), 1613 (s), 1522 (s), 1484 (w), 1444 (w), 1374 (m), 1354 (m), 1300 (w), 1270 (w), 1249 (w), 1210 (m), 1187 (w), 1156 (w), 1128 (w), 1080 (s), 1025 (w), 972 (w), 936 (w), 906 (w), 865 (s), 811 (s), 738 (w), 680 (w), 647 (w), 628 (w), 588 (w) cm^{-1}.

^1H and ^{13}C NMR data are contained in Tables 4-6 (p. 73-77).

8.3.3 Nucleophilic addition to the TIPS-protected L-*fuco*-nitrone 28

Experiment 50 (LR 410)

(2*R*,3*R*,4*R*,5*R*,6*S*)-6-([1,1'-Biphenyl]-4-yl)-2-bromomethyl-3,4,5-trihydroxy-3,4-*O*-isopropylidene-5-triisopropylsilyloxypiperidine (52) (α-L-*fuco*)

and (2*R*,3*R*,4*R*,5*R*,6*R*)-isomer (53) (β-L-*fuco*)

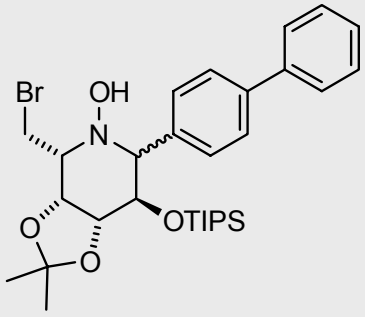

52/53

To a flask containing magnesium turnings (34 mg, 1.44 mmol, 2.1 Eq.) was added THF (2 mL) and a crystal of iodine. 4-Bromobiphenyl (319 mg, 1.37 mmol, 2 Eq.; Fluka, >99%) was taken up in THF (2 mL) and ca. 50 % of this solution was added dropwise to the flask containing magnesium. The reaction was warmed gently with a heat gun until the Grignard reaction became initiated (recognisable through opaque appearance of the solution). The rest of the 4-bromobiphenyl/THF solution was added over 5 min; the Grignard suspension was then kept refluxing gently for a further 20 min, then allowed to cool. Meanwhile, a second oven-dried flask was charged with the L-*fuco*-nitrone **28** in 6 mL THF, cooled to -60

°C and treated with the Grignard solution dropwise over 5 min. TLC control (eluant: PE:EE = 9:1) after 40 min showed the appearance of a new spot at the spot and consumption of starting material. Ammonium chloride (ca. 1 g) and water (5 mL) were added and the suspension was warmed to room temperature. The layers were separated and the aqueous layer was washed with ethyl acetate (4 x 30 mL); the combined organic layers were washed with saturated NaCl solution (15 mL), dried ($MgSO_4$), and concentrated under vacuum (25 °C/10 mbar) to yield crude product as a colourless oil (^{13}C NMR: d. r. = 92:8). Column chromatography (SiO_2, 70 g, 2.5 cm x 18 cm; eluant: PE/EE = 9:1), followed by MPLC purification (short column, 3 cm x 18 cm; PE/EE = 96:4, several injections; peak detection 252 nm) yielded 265 mg (0.449 mmol, 65 %) of the piperidine **52** as an analytically pure, colourless solid (m. p. 87-89 °C) and the piperidine **53** (19 mg, 0.0322 mmol, 5 %; Σ 70 %) as a colourless, spectroscopically pure oil. The structure of piperidine **52** was elucidated and confirmed by X-ray analysis (cf. Section 9.7).

Major diastereoisomer **52** (α-L-*fuco*)

$[\alpha]_D^{20}$ = –11 (*c* = 0.15, CH_2Cl_2)

$C_{30}H_{44}BrNO_4Si$	calc.	C	61.00	H	7.51	N	2.37	Br 13.53
(590.7)	found	C	60.15	H	7.63	N	2.14	Br 12.62

HRMS (ESI, positive ion): calc. for $C_{30}H_{44}BrNO_4$ + H: calc. 590.2296; found 590.2288.

IR (neat): $\tilde{\nu}$ = 3422 (w), 2939 (m, 2865 (m), 1600 (w), 1487 (m), 1461 (m), 1380 (m), 1243 (m), 1210 (m), 1114 (s), 1060 (s), 1008 (w), 972 (w), 915 (w), 880 (s), 838 (m), 805 (m), 763 (s), 738 (w), 861 (s) cm^{-1}.

^1H NMR ($CDCl_3$, 500.1 MHz): δ = 0.75-1.00 {m, together 21 H, $Si[CH(CH_3)_2]_3$ and $Si[CH(CH_3)_2]_3$}, 1.41, 1.64 [2 s, $C(CH_3)_2$], 3.78 (dd, $^2J_{1'A,1'B}$ = 9.7, $J_{2,1'A}$ = 7.7 Hz, 1 H, 1'-H_A), 3.97 (m, 1 H, 2-H), 4.03 (dd, $^2J_{1'A,1'B}$ = 9.7, $J_{2,1'B}$ = 6.6 Hz, 1 H, 1'-H_B), 4.18 ('t', $J_{4,5} \approx J_{5,6}$ = 2.7, 1 H, 5-H), 4.39 (dd, $J_{3,4}$ = 7.6, $J_{4,5}$ = 2.8 Hz, 1 H, 4-H), 4.55 (d, $J_{5,6}$ = 2.6 Hz, 1 H, 6-H), 4.72 (dd, $J_{2,3}$ = 1.4, $J_{3,4}$ = 7.6 Hz, 1 H, 3-H), 5.20 (bs, 1 H, OH), 7.30-7.60 (m, 9 H, C_6H_4 and C_6H_5).

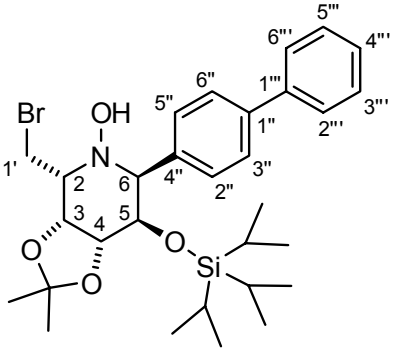

52

^{13}C NMR ($CDCl_3$ 125.8 MHz): δ = 12.6 {q, $Si[CH(CH_3)_2]_3$}, 17.9 {d, $Si[CH(CH_3)_2]_3$}, 23.9, 26.9 [2 s, $C(CH_3)_3$], 31.2 (t, C-1'), 59.6 (d, C-2), 67.9 (d, C-6), 73.5 (d, C-3), 73.6 (d, C-5), 76.1 (d, C-4), 110.0 [s, $C(CH_3)_2$], 126.9, 127.1, 127.14 (3 d, C-2'', C-6'', C-2''', C-4''', C-6'''; 5 signals expected, 3 found: some overlap of C_6H_4 and C_6H_5), 128.7, 128.74 (2 d, C-3'', C-5'', C-3''', C-5'''; 4 signals expected, 2 found: some overlap of C_6H_4 and C_6H_5), 139.3, 140.2, 141.4 (3 s, C-1'', C-4'', C-1''' of C_6H_4 and C_6H_5).

Minor diastereoisomer **53** (β-L-*fuco*)

$[\alpha]_D^{20}$ = –54 (*c* = 0.20, CH_2Cl_2)

HRMS (ESI, positive ion): calc. for $C_{30}H_{44}BrNO_4$ + H: calc. 590.2296; found 590.2300.

IR (neat): $\tilde{\nu}$ = 3501 (w), 2838 (m), 2864 (m), 1487 (w), 1461 (m), 1371 (m), 1244 (m), 1217 (m), 1132 (s), 1053 (m), 1015 (m), 929 (m), 880 (s), 835 (m), 676 (vs), 590 (s) cm^{-1}.

^{1}H NMR ($CDCl_3$, 500.1 MHz): δ = 0.75-1.00 {m, together 21 H, $Si[CH(CH_3)_2]_3$ and $Si[CH(CH_3)_2]_3$}, 1.40, 1.55 [2 s, $C(CH_3)_2$], 3.26 ('dt', $J_{2,1'A}$ = 10.5, $J_{2,1'B}$ = 3.5 Hz, 1 H, 2-H), 3.52 ('d', $J_{5,6}$ = 8.6 Hz, 1 H, 6-H), 3.71 (dd, $^2J_{1'A,1'B}$ = 9.3, $J_{2,1'A}$ = 10.5 Hz, 1 H, 1'-H_A), 4.02 (dd, $^2J_{1'A,1'B}$ = 9.3, $J_{2,1'B}$ = 3.6 Hz, 1 H, 1'-H_B), 4.06-4.10 (m, 2 H, 4-H, 5-H), 4.55 (bs, 1 H, OH), 4.72 ('q', $J_{2,3}$ = 3.2, $J_{3,4}$ = 5.1 Hz, 1 H, 3-H), 7.30-7.60 (m, 9 H, C_6H_4 and C_6H_5).

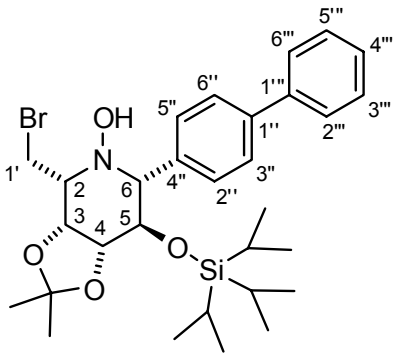

53

^{13}C NMR ($CDCl_3$ 125.8 MHz): δ = 12.7 {q, $Si[CH(CH_3)_2]_3$}, 18.05, 18.14 {2 d, $Si[CH(CH_3)_2]_3$}, 25.9, 28.0 [2 s, $C(CH_3)_3$], 30.1 (t, C-1'), 66.3 (d, C-2), 73.1 (d, C-3), 77.15 (d, C-5), 77.20 (d, C-6), 79.4 (d, C-4), 119.2 (s, $C(CH_3)_2$), 127.14, 127.17, 127.2 (3 d, C-2'', C-6'', C-2''', C-4''', C-6'''; 5 signals expected, 3 found: some overlap of C_6H_4 and C_6H_5), 128.8, 129.2 (2 d, C-3'', C-5'', C-3''', C-5'''; 4 signals expected, 2 found: some overlap of C_6H_4 and C_6H_5), 138.7, 140.8, 141.1 (3 s, C-1'', C-4'', C-1''' of C_6H_4 and C_6H_5).

Signal correlations were established with the help of H,H- and C,H-COSY.

For help in the assignment of the aromatic carbons, lit.[221,222,357] was consulted.

8.4 Experiments Relating to Chapter 4

8.4.1 Oxidation of 2-substituted *N*-hydroxypyrrolidines

Experiments 51, 52

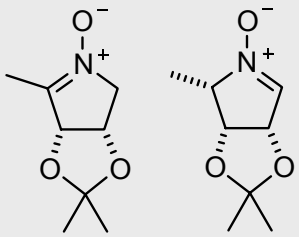

54 **55**

(3*S*,4*R*)-3,4-Dihydroxy-3,4-O-isopropylidene-5-methyl-3,4-dihydro-2*H*-pyrrole-1-oxide (54)

(2*S*,3*R*,4*S*)-3,4-Dihydroxy-3,4-O-isopropylidene-2-methyl-3,4-dihydro-2*H*-pyrrole-1-oxide (55)

Experiment 51 (LR 420)

The *N*-hydroxypyrrolidine **31** (300 mg, 1.73 mmol) was taken up in 5 mL CH_2Cl_2 and mercury(II) oxide (1.124 g, 5.19 mmol, 3 Eq.) was added in one portion. The orange suspension was stirred at 22 °C. After ca. 7 h, the suspension had turned orange-green and TLC analysis indicated no more starting material. The suspension was filtered over celite (2 cm x 5 cm) and washed with ca. 80 mL CH_2Cl_2. The HPLC analysis of the filtrate (CH_2Cl_2/MeOH = 95:5; at λ_{max} 242 nm) showed a r. r. of 79:21 for **54**:**55**. The filtrate was concentrated to give the crude product mixture (^{13}C NMR: r. r. **54**:**55** = 87:13), which was purified by MPLC (short column, 3 cm x 28 cm; CH_2Cl_2/MeOH = 94:6, several injections). This furnished the ketonitrone **54** (217 mg, 1.27 mmol, 73 %) as a crystalline, spectroscopically pure, colourless solid (m. p. 125-127 °C; lit.[4a] 125-127 °C) and the aldonitrone **55** (35 mg, 0.204 mmol, 12 %) as a spectroscopically pure, colourless oil that solidified on standing (m. p. 74-76 °C).

Data of the ketonitrone **54**

$[\alpha]_D^{20}$ = 21 (*c* = 0.50, CH_2Cl_2); lit.[4a] $[\alpha]_D^{20}$ = 20 (*c* = 0.61, CH_2Cl_2)

$C_8H_{13}NO_3$	calc.	C	56.13	H	7.65	N	8.18
(171.2)	found	C	56.52	H	7.75	N	7.86

The spectroscopic data of nitrone **54** were in accordance to those from lit.[4a] and Experiment 52, below.

Data of nitrone **55**

$[\alpha]_D^{20}$ = –15 (*c* = 0.116, CH_2Cl_2)

$C_8H_{13}NO_3$	calc.	C	56.13	H	7.65	N	8.18
(171.2)	found	C	55.44	H	7.62	N	7.67

MS (ESI, positive ion) *m/z* (%) = 194 $[M+Na]^+$ (95), 172 $[M+H]^+$ (100).
HRMS (ESI, positive ion): calc. for $C_8H_{13}NO_3$+H: calc. 172.0968; found 172.0968.

Spectroscopic data of nitrone **55** were in agreement to those in Experiment 52, below.

Experiment 52 (LR 421)

The N-hydroxypyrrolidine **31** (303 mg, 1.75 mmol) was placed in CH_2Cl_2 (6 mL) and cooled to 0 °C at which point manganese dioxide (219 mg, 2.30 mmol, 1.3. Eq. Fluka, techn. 90 %; 'oxidation active') was added with strong stirring. The ice bad was removed and after ca. 25 min, TLC analysis (PE/EE = 90:10) indicated no more starting material present. The suspension was filtered over celite (2 cm x 4 cm) and washed with CH_2Cl_2. The resulting light-yellow filtrate was analysed using HPLC (CH_2Cl_2/MeOH = 95 :5, peak integration at λ_{max} 242 nm) to reveal a regioisomer ratio of 78:22 for **54**:**55**. Removal of the solvents (^{13}C NMR: r. r. = 83:17 for **54**:**55**), followed by MPLC (short column, 3 cm x 28 cm; CH_2Cl_2/MeOH = 95:5, several injections) provided the ketonitrone **54** (225 mg, 1.31 mmol, 75 %) as an analytically pure, colourless solid (m. p. 125-127 °C; lit.[4a] 125-127 °C) and 37 mg (0.216 mmol, 12 %) of the L-*lyxo*-configured nitrone **55** as a colourless oil with slightly deviating elemental analysis that crystallised on standing (m. p. 74-76 °C).

Data of the ketonitrone **54**

$[\alpha]_D^{20}$ = 20 (*c* = 0.50, CH_2Cl_2); lit.[4a]: $[\alpha]_D^{20}$ = 20 (*c* = 0.61, CH_2Cl_2)

$C_8H_{13}NO_3$	calc.	C	56.13	H	7.65	N	8.18
(171.2)	found	C	56.06	H	7.54	N	8.13

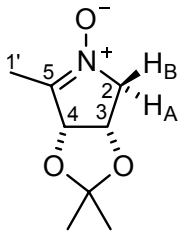

54

IR (neat): $\tilde{\nu}$ = 2987 (s), 1604 (s), 1421 (m), 1379 (m), 1341 (w), 1309 (w), 1211 (vs), 1154 (m), 1069 (s), 1053 (s), 1038 (vs), 908 (w), 868 (w), 839 (m), 787 (w), 718 (w), 682 (s) cm^{-1}.

^{1}H NMR ($CDCl_3$, 500.1 MHz): δ = 1.39-1.40 [2 s, 6 H, $C(CH_3)_2$], 2.08 (q, $^4J_{2A,1'}$ = 1.6, $^4J_{2B,1'}$ = 3.5 Hz, 3 H, 5-CH_3), 4.07 (doublet of sextets, $^2J_{2A,2B}$ = 14.9, $^4J_{2A,1'}$ = $J_{2A,3}$ = 1.6 Hz, 1 H, 2-H_A), 4.15 (doublet of sextets, $^2J_{2A,2B}$ = 14.9, $J_{2B,3}$ = 5.2 Hz, 1 H, 2-H_B), 4.82 ('dtd', $J_{2B,3}$ = 5.2, $J_{3,4}$ = 6.4 Hz, 1 H, 3-H), 5.20 (d, $J_{3,4}$ = 6.4 Hz, 1 H, 4-H).

^{13}C NMR ($CDCl_3$, 125.1 MHz): δ = 10.7 (q, C-1'), 26.1, 27.4 [2 q, $C(\underline{C}H_3)_2$], 67.6 (t, C-2), 71.9 (d, C-3), 82.8 (d, C-4), 112.3 [s, $\underline{C}(CH_3)_2$], 142.8 (s, C-5).

Analytical and spectroscopic data were in agreement with literature values.[4a]

Data of nitrone **55**

$[\alpha]_D^{20}$ = –14 (*c* = 0.48, CH_2Cl_2)

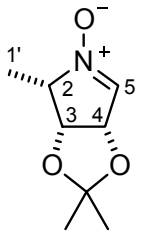

55

$C_8H_{13}NO_3$	calc.	C	56.13	H	7.65	N	8.18
(171.2)	found	C	56.04	H	7.80	N	7.46

MS (ESI, positive ion) *m/z* (%) = 194 $[M+Na]^+$ (100).

IR (neat): $\tilde{\nu}$ = 3104 (w), 2995 (m), 2947 (m), 1576 (vs), 1450 (m), 1375 (s), 1311 (w), 1260 (m), 1266 (w), 1204 (s), 1167 (m), 1148 (m), 1046 (vs), 1030 (vs), 924 (w), 866 (s), 851 (s), 816 (w), 782 (m), 679 (vs) cm^{-1}.

^{1}H NMR ($CDCl_3$, 500.1 MHz): δ = 1.40, 1.45 [2 s, 3 H each, $C(CH_3)_2$], 1.50 (d, $J_{2,1'}$ = 7.0 Hz, 3 H, 2-CH_3), 4.08 (dqu, $J_{2,1'}$ = 7.2, $J_{2,3}$ = 5.8, $^4J_{2,5}$ = $J_{4,5}$ = 1.6 Hz, 1 H, 2-H), 4.90 ('t', $J_{2,3}$ = 5.8 Hz, 1 H, 3-H), 5.29 (dd, $J_{3,4}$ = 6.3, $J_{4,5}$ = 1.6 Hz, 1 H, 4-H), 6.93 ('t', $^4J_{2,5}$ = $J_{4,5}$ = 1.6 Hz, 1 H, 5-H).

^{13}C NMR ($CDCl_3$, 125.1 MHz): δ = 11.4 (q, C-1'), 26.2, 27.5 [2 q, $C(\underline{C}H_3)_2$], 71.5 (d, C-2), 76.2 (d, C-3), 78.2 (d, C-4), 112.5 [s, $\underline{C}(CH_3)_2$], 131.6 (s, C-5).

Experiments 53, 54

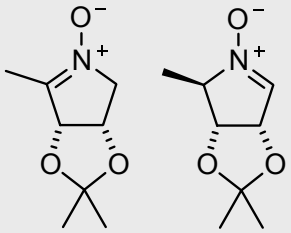

54 **56**

(3*S*,4*R*)-3,4-Dihydroxy-3,4-O-isopropylidene-5-methyl-3,4-dihydro-2*H*-pyrrole-1-oxide (54)

(2*R*,3*R*,4*S*)-3,4-Dihydroxy-3,4-O-isopropylidene-2-methyl-3,4-dihydro-2*H*-pyrrole-1-oxide (56)

Experiment 53 (LR 422)

Mercury(II) oxide (762 mg, 3.52 mmol, 3 Eq.) was added to the N-hydroxypyrrolidine **33** (203 mg, 1.17 mmol) in 5 mL CH_2Cl_2 and stirred at 22 °C for 7 h until the suspension became dark orange-green. At this point, TLC analysis had indicated the disappearance of starting material and the suspension was filtered over celite (2 cm x 5 cm) and washed with ca. 80 mL CH_2Cl_2. HPLC analysis of the filtrate (CH_2Cl_2/MeOH = 95:5; peak integration at λ_{max} 242 nm) indicated a r. r. of 67:33 for **54**:**56** (^{13}C NMR: r. r. **54**:**56** = 68:32). After solvent removal on the rotary evaporator (25 °C/10 mbar), MPLC separation of the crude product (short column, 3 cm x 28 cm; CH_2Cl_2/MeOH = 94:6, several injections) provided the nitrone **54** (109 mg, 0.637 mmol, 54 %; lit.[4a] 52 %) as an analytically pure, crystalline, colourless solid (m. p. 125-127 °C; lit.[4a] 125-127 °C) and the nitrone **56** (58 mg, 0.339 mmol, 29 %; lit.[4a] 25 %) as a colourless, hygroscopic, spectroscopically pure oil.

Data of the ketonitrone **54**

$[\alpha]_D^{20}$ = 20 (*c* = 0.43, CH_2Cl_2); lit.[4a]: $[\alpha]_D^{20}$ = 20 (*c* = 0.61, CH_2Cl_2)

$C_8H_{13}NO_3$	calc.	C	56.13	H	7.65	N	8.18
(171.2)	found	C	55.93	H	7.65	N	7.88

Spectroscopic data were in agreement with lit.[4a] and identical to those resulting from Experiments 51, 52 and 54 (below).

Data of the aldonitrone **56**

$[\alpha]_D^{20}$ = –32 (*c* = 0.24, CH_2Cl_2); lit.[4a]: $[\alpha]_D^{20}$ = –36 (*c* = 0.58, CH_2Cl_2)

$C_8H_{13}NO_3$	calc.	C	56.13	H	7.65	N	8.18
(171.2)	found	C	54.06	H	7.80	N	7.55
$C_8H_{13}NO_3 \cdot (H_2O)_{0.5}$:	calc.	C	53.32	H	7.83	N	7.77

MS (ESI, positive ion) *m/z* (%) = 194 $[M+Na]^+$ (100).
HRMS (ESI, positive ion): calc. for $C_8H_{13}NO_3$+H: calc. 172.0968; found 172.0972.

Spectroscopic data were in accordance to lit.[4a] and those in Experiment 54.

Experiment 54 (LR 423)

The D-*ribo*-configured pyrrolidine **33** (293 mg, 1.69 mmol) was placed in CH_2Cl_2 (6 mL) and manganese dioxide (212 mg, 2.20 mmol, 1.3. Eq., Fluka, techn. 90 %; 'oxidation active') was added at 0 °C with strong stirring. After addition, the ice bath was taken away. The TLC analysis (PE/EE = 90 :10) indicated complete consumption of starting material within ca. 1 h. The suspension was filtered over celite (2 cm x 4 cm) and washed with CH_2Cl_2 (80 mL). HPLC analysis of the filtrate (CH_2Cl_2/MeOH = 95:5, peak integration at λ_{max} 242 nm) indicated a r. r. of 71:29 for **54**:**56**. Following the removal of solvent on the rotary evaporator (25 °C/10 mbar) (^{13}C NMR: r. r. = 71:29 for **54**:**56**) and MPLC separation (short column, 3 cm x 28 cm; CH_2Cl_2/MeOH = 95:5, several injections), 205 mg (1.20 mmol, 71 %) of the nitrone **54** were isolated as a spectroscopically pure, colourless solid (m. p. 125-127 °C; lit.[4a] 125-127 °C) along with 57 mg (0.333 mmol, 20 %) of the D-*ribo*-configured nitrone **56** as a spectroscopically pure, hygroscopic colourless oil.

Data of the ketonitrone **54**

$[\alpha]_D^{20}$ = 20 (*c* = 0.43, CH_2Cl_2); lit.[4a]: $[\alpha]_D^{20}$ = 20 (*c* = 0.61, CH_2Cl_2)

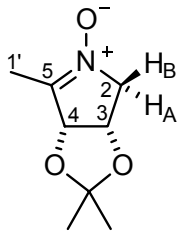

54

$C_8H_{13}NO_3$	calc.	C	56.13	H	7.65	N	8.18
(171.2)	found	C	56.73	H	7.83	N	7.77

MS (ESI, positive ion) *m/z* (%) = 194 $[M+Na]^+$ (100), 172 $[M+H]^+$ (30).
HRMS (ESI, positive ion): calc. for $C_8H_{13}NO_3$ + H: calc. 172.0968; found 172.0968.

IR (neat): $\tilde{\nu}$ = 2987 (s), 2935 (w), 1604 (s), 1461 (w), 1422 (m), 1389 (w), 1379 (m), 1341 (w), 1309 (w), 1288 (w), 1210 (vs), 1153 (m), 1084 (m), 1069 (m), 1053 (s), 1039 (vs), 908 (w), 868 (w), 839 (m), 788 (w), 717 (w) cm^{-1}.

^{1}H NMR ($CDCl_3$, 500.1 MHz): δ = 1.39-1.40 [2 s, peaks overlapping, together 6 H, $C(CH_3)_2$], 2.08 (q, $^4J_{2A,1'}$ = 1.6, $^4J_{2B,1'}$ = 3.5 Hz, 3 H, 1'-CH_3), 4.07 (doublet of sextets, $^2J_{2A,2B}$ = 14.9, $^4J_{2A,1'}$ = $J_{2A,3}$ = 1.6 Hz, 1 H, 2-H_A), 4.15 (doublet of sextets, $^2J_{2A,2B}$ = 14.9, $J_{2B,3}$ = 5.2 Hz, 1 H, 2-H_B), 4.82 ('dtd', $J_{2B,3}$ = 5.2, $J_{3,4}$ = 6.4 Hz, 1 H, 3-H), 5.20 (d, $J_{3,4}$ = 6.4 Hz, 1 H, 4-H).

^{13}C NMR ($CDCl_3$, 125.1 MHz): δ = 10.7 (q, C-1'), 26.1, 27.4 [2 q, $C(\underline{C}H_3)_2$], 67.6 (d, C-2), 71.9 (d, C-3), 82.8 (d, C-4), 112.3 [s, $\underline{C}(CH_3)_2$], 142.8 (d, C-5).

Analytical and spectroscopic data were in agreement with literature values.[4a]

Data of the aldonitrone **56**

$[\alpha]_D^{20}$ = –30 (*c* = 0.23, CH_2Cl_2); lit.[4a]: $[\alpha]_D^{20}$ = –36 (*c* = 0.58, CH_2Cl_2)

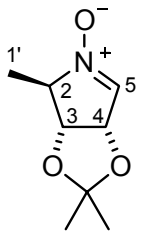

56

$C_8H_{13}NO_3$	calc.	C	56.13	H	7.65	N	8.18
(171.2)	found	C	52.64	H	8.11	N	7.11
$C_8H_{13}NO_3 \cdot (H_2O)_{0.5}$:	calc.	C	53.32	H	7.83	N	7.77

IR (neat): $\tilde{\nu}$ = 3398 (w), 2987 (m), 2935 (m), 1573 (vs), 1456 (w), 1375 (m), 1257 (s), 1207 (vs), 1158 (m), 1118 (w), 1043 (vs), 965 (w), 932 (w), 864 (s), 783 (w), 669 (s), 644 (s), 608 (s) cm^{-1}.

^{1}H NMR ($CDCl_3$, 500.1 MHz): δ = 1.37, 1.46 [2 s, 3 H each, $C(CH_3)_2$], 1.51 (d, $J_{2,1'}$ = 7.3 Hz, 3 H, 1'-CH_3), 4.12 (dq, $^4J_{2,5}$ = 1.0, $J_{2,1'}$ = 7.3 Hz, 1 H, 2-H), 4.61 (d, $J_{3,4}$ = 6.3 Hz, 1 H, 3-H), 5.29 (d, $J_{3,4}$ = 6.3 Hz, 1 H, 4-H), 6.83 (s, 1 H, 5-H).

^{13}C NMR ($CDCl_3$, 125.1 MHz): δ = 17.4 (q, C-1'), 26.2, 27.6 [2 q, $C(\underline{C}H_3)_2$], 75.6 (d, C-2), 78.5 (d, C-3), 80.4 (d, C-4), 112.5 [s, $\underline{C}(CH_3)_2$], 131.2 (s, C-5).

Analytical and spectroscopic data were in agreement to literature values.[4a]

Experiments 55, 56

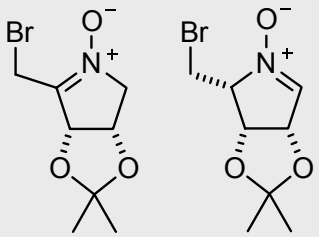

57 **5**

(3*S*,4*R*)-5-Bromomethyl-3,4-dihydroxy-3,4-*O*-isopropylidene-3,4-dihydro-2*H*-pyrrole-1-oxide (57)

(2*R*,3*R*,4*S*)-2-Bromomethyl-3,4-dihydroxy-3,4-*O*-isopropylidene-3,4-dihydro-2*H*-pyrrole-1-oxide (5)

Experiment 55 (LR 424)

The bromomethyl-N-hydroxypyrrolidine **30** (21 mg, 0.083 mmol) was placed in a one-necked flask and taken up in 2 mL CH_2Cl_2. Mercury(II) oxide (54 mg, 0.250 mmol, 3 Eq.) was added in one portion with vigorous stirring. The reaction was stirred at 22 °C overnight. After 16 h, the suspension had turned orange-green and TLC analysis indicated the disappearance of starting material. The suspension was filtered over celite (2 cm x 7 cm), and washed with ca. 80 mL CH_2Cl_2. The HPLC analysis (PE:EE = 85:15; peak integration at 262 nm) confirmed the disappearance of starting material and the appearance of two new products as well as a source of impurities/decomposition accompanying the solvent front. The solvents were removed under reduced pressure on the rotary evaporator (25 °C/20 mbar) to yield the crude product as a deep-orange oil. The ^{1}H and ^{13}C analyses were fraught with impurity/decomposition so that a meaningful determination of the regioisomeric ratio could not be done, and, furthermore, the products not be isolated.

Experiment 56 (LR 425)

Dichloromethane (3 mL) was added to bromomethyl-N-hydroxypyrrolidine **30** (80 mg, 0.317 mmol) and the solution cooled to 0 °C. Manganese dioxide (40 mg, 0.412 mmol, 1.3. Eq.; Fluka, Techn. 90 %; 'oxidation active') was added with strong stirring. The ice-bath was removed and the suspension warmed to room temperature. After 0.5 h, TLC analysis (PE/EE = 40:60) had indicated complete consumption of the starting material. The suspension was poured onto celite (2 cm x 4 cm) and washed with 30 mL CH_2Cl_2. HPLC analysis of the filtrate (PE/EE = 85:15) indicated formation of the L-*lyxo*-nitrone **5** (λ_{max} = 240 nm) and nitrone **57** (λ_{max} = 262 nm). The removal of the solvents (25 °C/10 mbar) (^{13}C NMR: r. r. = **57**:**5** = 80:20) followed by MPLC separation (short column, 3 cm x 28 cm; PE/EE = 85:15, several injections) yielded 49 mg of the ketonitrone **57** (0.196 mmol, 62 %) as an analytically pure, colourless solid (m. p. 100-102 °C, decomp.) and 9 mg of the L-*lyxo*-nitrone **5** (0.036

mmol, 11 %) as a spectroscopically pure, colourless solid (m. p. 132 °C; lit.[2]: 130-135 °C, decomp.) Note: compound **57** should be storred at -18 °C, since it decomposes gradually (i.e. 1 week) at room temperature.

Data of L-*lyxo*-nitrone **5**

$[\alpha]_D^{20}$ = 108 (*c* = 0.180, CH_2Cl_2); lit.[2]: $[\alpha]_D^{20}$ = 104 (*c* = 0.715, CH_2Cl_2)

$C_8H_{12}BrNO_3$	calc.	C	38.42	H	4.79	N	5.60	
(250.1)	found	C	38.86	H	5.17	N	5.39	

Spectroscopic data of L-*lyxo*-nitrone **5** were in accordance to lit.[2] and those in Experiment 5.

Data of nitrone **57**

$[\alpha]_D^{20}$ = –31 (*c* = 0.20, CH_2Cl_2)

$C_8H_{12}BrNO_3$	calc.	C	38.42	H	4.84	N	5.60	Br	31.95
(250.1)	found	C	38.60	H	4.92	N	5.47	Br	32.02

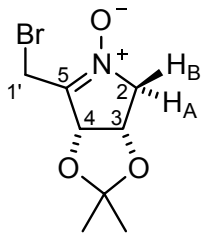

57

IR (neat): $\tilde{\nu}$ = 2988 (s), 2937 (m), 1580 (vs), 1435 (m), 1374 (m), 1266 (m), 1209 (vs), 1156 (w), 1125 (w), 1084 (s), 1051 (w), 1016 (w), 866 (w) cm^{-1}.

^{1}H NMR ($CDCl_3$, 500.1 MHz): δ = 1.40, 1.42 [2 s, 3 H each, $C(CH_3)_2$], 4.00 (d, $^2J_{1'A,1'B}$ = 10.5 Hz, 1 H, 1'-H_A), 4.11 (dqu, $^2J_{2A,2B}$ = 15.3, $J_{2A,3}$ = 1.5, $J_{2B,3}$ = 5.3 Hz, 1 H, 2-H_A), 4.22 (dd, $^2J_{2A,2B}$ = 15.3, $J_{2A,3}$ = 5.3 Hz, 1 H, 5-H_B), 4.51 (d, $^2J_{1'A,1'B}$ = 10.5 Hz, 1 H, 1'-H_B), 4.90 ('ddd', $J_{2A,3}$ = 1.5, $J_{2B,3}$ = 5.3, $J_{3,4}$ = 6.2 Hz, 1 H, 3-H), 5.45 (d, $J_{3,4}$ = 6.2 Hz, 1 H, 4-H).

^{13}C NMR ($CDCl_3$, 125.1 MHz): δ = 19.3 (t, C-1'), 26.0, 27.3 [2 q, $C(\underline{C}H_3)_2$], 68.4 (t, C-2), 71.7 (d, C-3), 80.1 (d, C-4), 112.9 [s, $\underline{C}(CH_3)_2$], 140.0 (s, C-5).

Signal correlations were established with the help of H,H- and C,H-COSY.

Experiments 57, 58

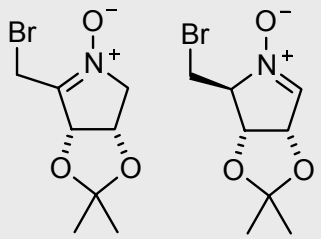

57 **6**

(3*S*,4*R*)-5-Bromomethyl-3,4-dihydroxy-3,4-*O*-isopropylidene-3,4-dihydro-2*H*-pyrrole-1-oxide (57)

(2*S*,3*R*,4*S*)-2-Bromomethyl-3,4-dihydroxy-3,4-*O*-isopropylidene-3,4-dihydro-2*H*-pyrrole-1-oxide (6)

Experiment 57 (LR 426)

The bromomethyl-*N*-hydroxypyrrolidine **32** (269 mg, 1.07 mmol) was placed in 5 mL CH_2Cl_2 and mercury(II) oxide (695 mg, 3.21 mmol, 3 Eq.) was added. The reaction was allowed to stir at 22 °C. After ca. 1 h, TLC analysis indicated a slow reaction; the reaction was left to stir overnight. After 20 h, the suspension became orange-green. TLC analysis indicated the disappearance of starting material and the suspension was filtered over celite (2 cm x 7 cm), followed by washing with ca. 80 mL CH_2Cl_2. HPLC analysis of the yellow filtrate (PE:EE = 15:85) indicated formation of a main product and several other impurities/decomposition products accompanying the solvent front. The solvents were removed under reduced pressure (20 mbar, 25 °C) to yield the reaction products as a deep-orange oil. The ^{1}H and ^{13}C analysis indicated substantial decomposition.

Experiment 58 (LR 427)

The bromomethyl-*N*-hydroxypyrrolidine **32** (217 mg, 0.860 mmol) was placed in 6 mL CH_2Cl_2, cooled to 0 °C and MnO_2 (107 mg, 1.128 mmol, 1.3. Eq.; Fluka, techn. 90 %; 'oxidation active') was added. The ice-bad was removed and warmed to r. t. (22 °C). After 0.5 h, TLC (PE/EE = 40:60) indicated complete disappearance of the pyrrolidine **32**. The suspension was filtered over celite (2 cm x 4 cm) and washed with 80 mL CH_2Cl_2. HPLC analysis of the filtrate (PE/EE = 15:85; detection at fish wavelengths 240 nm for nitrone **6** and 262 nm for **57**) revealed the near exclusive formation of the bromomethyl-ketonitrone **57** which was confirmed, after solvent removal (10 mbar, 25 °C) by ^{13}C NMR (r. r. **57**:**6** = >98:2). MPLC purification (short column, 3 cm x 28 cm; PE/EE = 15:85, detection at λ_{max} = 262 nm, several injections) afforded the ketonitrone **57** (200 mg, 0.800 mmol, 93 %) as a nearly analytically pure, colourless solid (m. p. 100-102 °C, decomp.) and 7 mg of the D-*ribo*-nitrone **6** (0.028 mmol, 3 %) as an orange oil that solidified on standing. The spectroscopic properties of the

D-*ribo*-nitrone **6** were in accordance to literature values.[2] Note: the nitrone **57** should be storred at -18 °C due to its propensity to decompose at room temperature.

Data of the ketonitrone **57**

$[\alpha]_D^{20}$ = –34 (*c* = 0.20, CH_2Cl_2)

$C_8H_{12}BrNO_3$	calc.	C	38.42	H	4.84	N	5.60	Br	31.95
(250.1)	found	C	38.77	H	4.95	N	5.61	Br	31.96

MS (ESI, positive) *m/z* (%) = 272 $[M+Na]^+$ (100).

The spectroscopic data of the nitrone **57** were in accordance to those obtained from Experiment 56.

8.4.2 Oxidation of 2,5-disubstituted *N*-hydroxypyrrolidines

Experiments 59, 60

(2*S*,3*S*,4*R*)-5-Bromomethyl-3,4-dihydroxy-3,4-*O*-isopropylidene-2-methyl-3,4-dihydro-2*H*-pyrrole-1-oxide (58)

(2*R*,3*R*,4*S*)-2-Bromomethyl-3,4-dihydroxy-3,4-*O*-isopropylidene-5-methyl-3,4-dihydro-2*H*-pyrrole-1-oxide (59)

(2*S*,3*S*,4*R*,2'*R*,3'*R*,4'*S*,5'*S*)-5-(2-Bromomethyl-3,4-dihydroxy-3,4-O-isopropylidene-5-methyl-pyrrolidin-1-yloxymethyl)-3,4-dihydroxy-3,4-O-isopropylidene-2-methyl-3,4-dihydro-2*H*-pyrrole-1-oxide (60)

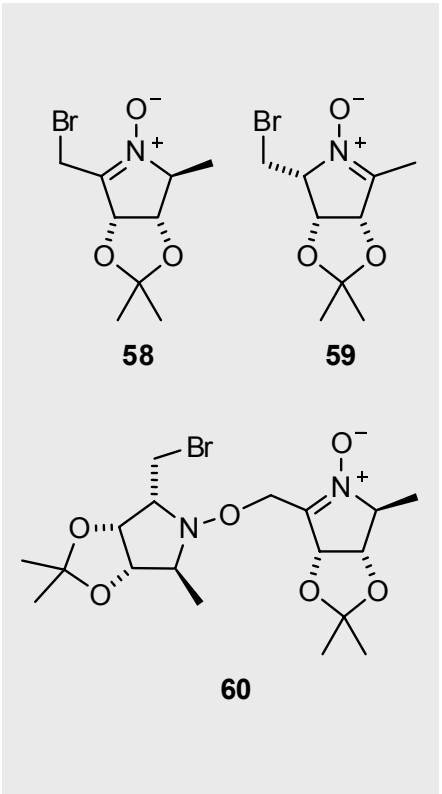

Experiment 59 (LR 428)

The 2-bromomethyl-5-methyl-*N*-hydroxypyrrolidine **34** (131 mg, 0.492 mmol) was taken up in 4 mL CH_2Cl_2 and mercury(II) oxide (320 mg, 1.49 mmol, 3 Eq.) was added. The initial TLC analysis indicated a slow reaction. After 16 h, TLC analysis showed product formation though incomplete consumption of starting material and other products. The suspension was filtered over celite (2 cm x 5 cm) and washed with ca. 80 mL CH_2Cl_2. The HPLC analysis of the filtrate (CH_2Cl_2/MeOH = 95:5) indicated the presence of the bromomethyl-ketonitrone **58** (λ_{max} = 260 nm) and the methyl-ketonitrone **59** (λ_{max} = 240 nm) as well as a new co-product. Due to impurities, the r. r. of the crude products could not be determined by ^{13}C NMR. MPLC purification (short column, 3 cm x 28 cm; CH_2Cl_2/MeOH = 98:2, several injections) provided the nitrone **58** (34 mg, 0.129 mmol, 26 %) as a spectroscopically pure, unstable colourless oil that darkenend rapidly on standing and the nitrone **59** (2 mg, 0.00757 mmol, 2 %) as a spectroscopically pure, colourless solid (m. p. 98-102 °C). The substitution co-product **60** was also isolated as a colourless, spectroscopically pure oil (17 mg, 0.0378 mmol, 15 %).

Data of the nitrone **58**

$[\alpha]_D^{20}$ = 113 (*c* = 0.040, CH_2Cl_2)

MS (EI, positive ion, 70 eV, 405 K) *m/z* (%) = 263 $[M+H]^+$ (18), 184 $[-Br]^+$ (100).

Spectroscopic data were comparable to those in Experiment 60, see below.

Data of the nitrone **59**

$[\alpha]_D^{20}$ = 88 (*c* = 0.105, CH_2Cl_2)

MS (EI, positive ion, 70 eV, 355 K) *m/z* (%) = 263 $[M+H]^+$ (40), 184 $[-Br]^+$ (85).

Spectroscopic data were in accordance to those in Experiment 60, see below.

Data of the bromine substitution product, the nitrone **60**

$[\alpha]_D^{20}$ = 23 (*c* = 0.100, CH_2Cl_2)

MS (EI, positive ion, 70 eV, 420 K) *m/z* (%) = 435 $[M+H, -CH_3]^+$ (8), 264 $[-C_8H_{13}NO_3]$ (100).

HRMS (ESI, positive ion): for $C_{18}H_{29}BrN_2O_6$+H calc. 449.1282; found 449.1293.

IR (neat): $\tilde{\nu}$ = 3197 (bs, OH), 2958 (w), 2932 (w), 2871 (w), 1601 (s), 1433 (w),1374 (m), 1270 (s), 1207 (m), 1164 (m), 1125 (m), 1127 (s), 1061 (vs), 977 (m), 932 (w), 889 (m), 862 (w), 862 (s), 738 (w), 703 (m), 667 (m), 642 (m), 588 (s) cm^{-1}.

^{1}H NMR ($CDCl_3$, 500.1 MHz): δ = 1.15 (d, $J_{5',5'\text{-Me}}$ = 7.1 Hz, 3 H, 5'-CH_3), 1.31, [s, 3 H, C(CH_3)], 1.37-1.38 [2 s, overlapping signals, together 6 H, C(CH_3) & C(CH_3)], 1.47 [s, 3 H, C(CH_3)], 1.50 (d, $J_{2,2\text{-Me}}$ = 8.3 Hz, 3 H, 2-CH_3), 3.36 (m, 1 H, 2'-H), 3.59 (dd, $^2J_{1''A,1''B}$ = 9.2, $J_{2',1''A}$ = 4.3 Hz, 1 H, 1'-H_A), 3.63-3.70 (d, $J_{5',5'\text{-Me}}$ = 7.1 Hz, and dd, $^2J_{1''A,1''B}$ = 9.1, $J_{2',1''B,}$ = 9.9 Hz, overlapping signals, together 2 H, 1'-H_B, 5'-H), 4.10 ('d', $J_{2,2\text{-Me}}$ = 7.3 Hz, 3 H, 2-CH_3), 4.31-4.39 (d, $J_{3',4'}$ = 6.8 Hz, overlapping signals with C$\underline{H}_A$H$_B$, together 2 H, 4'-H, C$\underline{H}_A$H$_B$), 4.51 (dd, $J_{2,3}$ = 0.9, $J_{3,4}$ = 6.2 Hz, 1 H, 3-H), 4.67 (dd, $J_{2',3'}$ = 5.3, $J_{3',4'}$ = 6.8 Hz, 1 H, 3'-H), 4.78 (d, $^2J_{AB}$ = 13.3 Hz, 1 H, CH$_A\underline{H}_B$), 5.4 (d, $J_{3,4}$ = 6.0 Hz, 1 H, 4-H).

^{13}C NMR ($CDCl_3$, 75.5 MHz): δ = 10.7 (q, 5'-CH_3), 16.9 (2-CH_3), 24.9, 25.9, 26.1, 27.2 [4 q, C($\underline{C}H_3$)$_2$], 28.1 (t, C-1''), 64.6 (d, C-5'), 67.2 (d, C-2'), 75.3 (d, C-3', overlap with d, C-2), 78.2 (d, C-3), 79.8 (d, C-4', overlap with d, C-4), 111.6, 112.0 [2 s, $\underline{C}$(CH_3)$_2$], 139.8 (s, C-5).

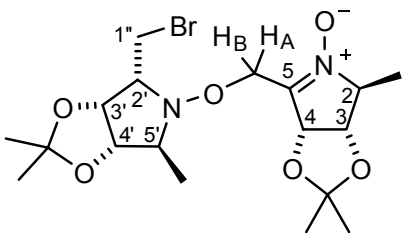

60

All signal correlations were established with the help of H,H- and C,H-COSY.

Experiment 60 (LR 429)

2-Bromomethyl-5-methyl-N-hydroxypyrrolidine **34** (136 mg, 0.511 mmol) was placed in CH_2Cl_2 (3 mL) and manganese dioxide (58 mg, 0.664 mmol, 1.3. Eq.; Fluka, techn. 90 %; 'oxidation active') was added at 0 °C. After addition, the ice bath was taken away. TLC analysis indicated complete consumption of starting material within 0.5 h. The suspension was filtered over celite (2 cm x 4 cm) and washed with CH_2Cl_2 (80 mL). Removal of solvents (10 mbar, 30 °C) led to the isolation of the crude product as a colourless solid (^{13}C NMR: r. r = 92:8 for **58**:**59**) which was separated by MPLC (short column, 3 cm x 28 cm; CH_2Cl_2/MeOH = 98:2, several injections) to yield the nitrone **58** (98 mg, 0.370 mmol, 73 %) as a spectroscopically pure, colourless oil that darkended rapidly and decomposed on standing, and the nitrone **59** (9 mg, 0.0341 mmol, 7 %) as a nearly colourless, spectroscopically pure solid (m. p. 98-102 °C).

Data of the nitrone **58**

$[\alpha]_D^{20}$ = 112 (*c* = 0.040, CH_2Cl_2)

$C_9H_{14}BrNO_3$	calc.	C	40.93	H	5.34	N	5.30	Br 30.25
(264.12)	found	C	41.30	H	5.51	N	5.27	Br 31.90

MS (ESI, positive ion, 70 eV, 415 K) *m/z* (%) = 263 $[M+H]^+$ (18), 184 $[-Br]^+$ (100).

IR (neat): $\tilde{\nu}$ = 2986 (w), 2932 (s), 2853 (w), 1601 (s), 1433 (w), 1392 (w), 1379 (m), 1339 (m), 1310 (w), 1252 (w), 1211 (vs), 1161 (w), 1145 (w), 1127 (s), 1061 (vs), 977 (m), 932 (w), 889 (m), 862 (w), 862 (s), 738 (w), 703 (m), 667 (m), 642 (m), 588 (s) cm^{-1}.

^{1}H NMR ($CDCl_3$, 500.1 MHz): δ = 1.39, 1.41 [2 s, 3 H each, $C(CH_3)_2$], 1.48 (d, $J_{2,1'}$ = 7.3 Hz, 3 H, 2-CH_3), 4.00 (dd, $^2J_{1''A,1''B}$ = 10.5, $^4J_{4,1''A}$ = 1.0 Hz, 1 H, 1''-H_A), 4.15 ('qq', $J_{2,1'}$ = 7.3, $J_{2,3}$ = 1.0 Hz, 1 H, 2-H), 4.50 (dd, $^2J_{1''A,1''B}$ = 10.5, $^4J_{4,1''B}$ = 0.7 Hz, 1 H, 1''-H_B), 4.55 (dd, $J_{2,3}$ = 1.0, $J_{3,4}$ = 6.3 Hz, 1 H, 3-H), 5.39 ('d', $J_{3,4}$ = 6.3 Hz, 1 H, 4-H).

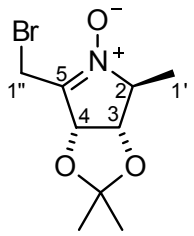

58

^{13}C NMR ($CDCl_3$, 125.1 MHz): δ = 16.5 (q, C-1'), 19.5 (t, C-1''), 25.8, 27.1 [2 q, C($\underline{C}H_3$)$_2$], 75.2 (d, C-2), 77.7 (d, C-3), 78.1 (d, C-4), 112.4 [s, $\underline{C}(CH_3)_2$], 138.7 (s, C-5).

Data of nitrone **59**

$[\alpha]_D^{20}$ = 85 (*c* = 0.095, CH_2Cl_2)

MS (ESI, positive ion) *m/z* (%) = 286 $[M+Na]^+$, 264 $[M+H]^+$.

HRMS (ESI, positive ion): calc. for $C_9H_{14}BrNO_3$+H: calc. 264.0230; found 264.0221.

IR (neat): $\tilde{\nu}$ = 3376 (w), 2986 (w), 2932 (m), 2853 (w), 1601 (s), 1433 (w), 1392 (m), 1379 (m), 1339 (w), 1310 (w), 1252 (m), 1212 (s), 1145 (w), 1127 (s), 1061 (vs), 977 (m), 932 (w), 914 (m), 889 (m), 862 (s), 786 (w). 703 (m), 667 (m), 642 (m) cm^{-1}.

^{1}H NMR ($CDCl_3$, 300.1 MHz): δ = 1.37, 1.44 [2 s, 3 H each, $C(CH_3)_2$], 2.09 (s, 3 H, 1''-CH_3), 3.62 (dd, $^2J_{1'A,1'B}$ = 9.5, $J_{2,1'A}$ = 11.4 Hz, 1 H, 1'-H_A), 4.15 (dd, $^2J_{1'A,1'B}$ = 9.5, $J_{2,1'B}$ = 3.4 Hz, 1 H, 1'-H_B), 4.32 (m, 1 H, 5-H), 4.96 (dd, $J_{3,4}$ = 5.8, $J_{4,5}$ = 4.8 Hz, 1 H, 4 H), 5.30 ('d', $J_{3,4}$ = 5.8 Hz, 1 H, 3-H).

^{13}C NMR ($CDCl_3$, 75.5 MHz): δ = 10.7 (q, C-1''), 24.4 (t, C-1'), 26.3, 27.2 [2 q, C($\underline{C}H_3)_2$], 72.8 (d, C-3), 75.2 (d, C-2), 80.1 (d, C-4), 112.5 [s, $\underline{C}(CH_3)_2$], 143.6 (s, C-5).

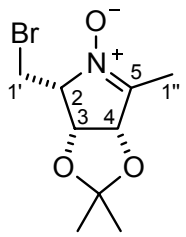

59

Experiments 61, 62

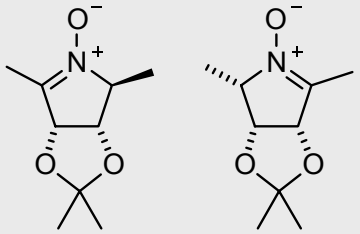

61 **62**

(2*S*,4*R*,3*S*)-3,4-Dihydroxy-3,4-*O*-isopropylidene-2,5-dimethyl-3,4-dihydro-2*H*-pyrrole-1-oxide (61)

(2*S*,3*R*,4*S*)-3,4-Dihydroxy-3,4-*O*-isopropylidene-2,5-dimethyl-3,4-dihydro-2*H*-pyrrole-1-oxide (62)

Experiment 61 (LR 430)

Mercury(II) oxide (409 mg, 1.89 mmol, 3 Eq.) was added to the 2,5-dimethyl-N-hydroxypyrrolidine **68** (118 mg, 0.631 mmol) in 3 mL CH_2Cl_2 at 22 °C and stirred for 4 h. The colour turned dark orange-green and TLC analysis confirmed the disappearance of starting material. The suspension was filtered over celite (2 cm x 7 cm), followed by washing with ca. 40 mL CH_2Cl_2. The HPLC analysis (CH_2Cl_2/MeOH = 96:4; peak integration at 241 nm) indicated a ratio of nitrones **61**:**62** of 92:8 (^{13}C NMR: r. r. **61**:**62** = 96:4). Purification by MPLC (short column, 3 cm x 28 cm; CH_2Cl_2/MeOH = 96:4, several injections) gave the nitrone **61** as a hygroscopic colourless oil (97 mg, 0.524 mmol, 83 %) and the nitrone **62** as a spectroscopically pure, near-colourless solid (4.8 mg, 0.027 mmol, 4 %; m. p. 78 °C).

Data of the nitrone **61**

$[\alpha]_D^{20}$ = 18 (*c* = 1.53, $CHCl_3$)

$C_9H_{15}NO_3$	calc.	C	58.36	H	8.16	N	7.56
(185.2)	found	C	55.72	H	8.30	N	7.04
$C_9H_{15}NO_3 \cdot (H_2O)_{0.5}$:	calc.	C	55.65	H	8.30	N	7.21

MS (ESI, positive ion) *m/z* (%) = 208 $[M+Na]^+$, 186 $[M+H]^+$.
HRMS (ESI, positive ion): calc. for $C_9H_{15}NO_3$+H: calc. 185.1125; found 186.1128.

IR (neat): $\tilde{\nu}$ = 3425 (bs, OH), 2987 (m), 2937 (m), 1606 (s), 1453 (m), 1375 (s), 1346 (w), 1207 (vs), 1156 (m), 1116 (w), 1083 (w), 1053 (vs), 968 (w), 918 (w), 866 (s), 723 (w), 671 (w), 622 (w), 602 (m), 586 (m) cm^{-1}.

^{1}H NMR ($CDCl_3$, 300.1 MHz): δ = 1.45 (s, 3 H, 1'-CH_3), 1.47, 1.49 [2 s, 3 H each, $C(CH_3)_2$], 2.07 (s, 3 H, 1''-CH_3), 4.10 ('qqu', $J_{2,3}$ = 1.3, $J_{2,1'}$ = 7.4 Hz, 1 H, 2-H), 4.51 (dd, $J_{2,3}$ = 1.3, $J_{3,4}$ = 6.2 Hz, 1 H, 3-H), 5.15 ('dt', $J_{3,4}$ = 6.2, $^4J_{3,1'}$ = 1.3 Hz, 1 H, 4-H).

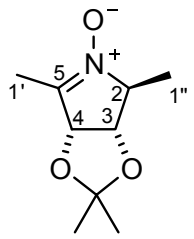

61

^{13}C NMR ($CDCl_3$, 75.5 MHz): δ = 10.6 (q, C-1''), 16.9 (q, C-1'), 26.0, 27.2 [2 q, $C(\underline{C}H_3)_2$], 74.5 (d, C-2), 78.1 (d, C-3), 80.9 (d, C-4), 112.0 [s, $\underline{C}(CH_3)_2$], 141.0 (s, C-5).

Data of the nitrone **62**

$[\alpha]_D^{20}$ = –9 (*c* = 0.096, $CHCl_3$)
MS (ESI, positive ion) *m/z* (%) = 208 $[M+Na]^+$, 186 $[M+H]^+$.
HRMS (ESI, positive ion): calc. for $C_9H_{15}NO_3$+H: calc. 185.1125; found 186.1125

IR (solid): $\tilde{\nu}$ = 3391 (bs, OH), 2989 (m), 2933 (m), 1605 (s), 1448 (m), 1396 (w), 1376 (m), 1345 (w), 1315 (w), 1298 (w), 1262 (m), 1207 (vs), 1165 (w), 1142 (m), 1119 (m), 1083 (w), 1050 (vs), 995 (m), 974 (m), 965 (m), 867 (s), 837 (w), 801 (m), 713 (m), 701 (m), 645 (w), 616 (m), 591 (w) cm^{-1}.

^{1}H NMR ($CDCl_3$, 300.1 MHz): δ = 1.37, 1.41 [2 s, 3 H each, $C(CH_3)_2$], 1.51 (d, $J_{2,1'}$ = 7.2 Hz, 3 H, 1'-CH_3), 2.09 (s, 3 H, 1''-CH_3), 4.10 (m, 1 H, 2-H), 4.79 ('q', $J_{2,3}$ = 1.0, $J_{3,4}$ = 6.2 Hz, 1 H, 3-H), 5.16 (m, 1 H, 4-H).

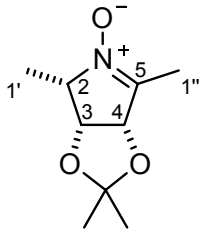

62

^{13}C NMR ($CDCl_3$, 75.5 MHz): δ = 10.6 (s, C-1''), 11.1 (q, C-1'), 26.1, 27.1 [2 q, $C(\underline{C}H_3)_2$], 70.3 (d, C-2), 74.3 (d, C-3), 80.8 (d, C-4), 111.8 [s, $\underline{C}(CH_3)_2$], 141.6 (s, C-5).

Experiment 62 (LR 431)

Manganese dioxide (124 mg, 1.24 mmol, 1.3 Eq. Fluka; techn. 90 %; 'oxidation active') was added to the 2,5-dimethyl-*N*-hydroxypyrrolidine **68** (178 mg, 0.951 mmol) in 3 mL CH_2Cl_2 at 0 °C. The reaction was warmed to r. t. and, according to TLC analysis, had gone to completion after ca. 20 min. The suspension was filtered over celite (1.5 cm x 6 cm) followed by washing with CH_2Cl_2 (ca. 40 mL). HPLC analysis of the filtrate showed a r. r. for **61**:**62** of 94:6 (^{13}C NMR: r. r. **61**:**62** = 96:4). After MPLC purification (short column, 3 cm x 28 cm; CH_2Cl_2/MeOH = 98:2, several injections), the nitrone **61** (147 mg, 0.794 mmol, 84 %) was furnished as an analytically pure, hygroscopic, colourless oil and the nitrone **62** (8 mg, 0.043 mmol, 5 %) as a spectroscopically pure, colourless solid (m. p. 78 °C).

Data of nitrone **61**

$[\alpha]_D^{20}$ = 21 (*c* = 0.288, $CHCl_3$)

$C_9H_{15}NO_3$	calc.	C	58.36	H	8.16	N	7.56
(185.2)	found	C	55.83	H	8.22	N	7.19
$C_9H_{15}NO_3 \cdot (H_2O)_{0.5}$:	calc.	C	55.65	H	8.30	N	7.21

Spectroscopic and analytical data were in agreement to those in Experiment 61 (above).

Data of nitrone **62**

$[\alpha]_D^{20}$ = –7 (*c* = 0.164, $CHCl_3$)

Spectroscopic and analytical data were in agreement those in Experiment 61, above.

Experiments 63, 64

(2*S*,3*R*,4*S*)-5-Bromomethyl-3,4-dihydroxy-3,4-*O*-isopropylidene-2-(4-methoxyphenyl)-3,4-dihydro-2*H*-pyrrole-1-oxide (63)

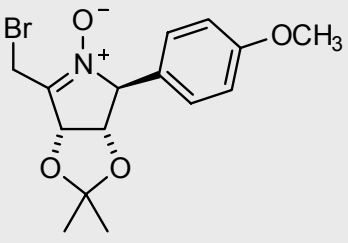

63

Experiment 63 (LR 432)

Mercury(II) oxide (285 mg, 1.320 mmol, 3 Eq.) was added to the bromomethyl-N-hydroxypyrrolidine **41** (157 mg, 0.439 mmol) in 5 mL CH_2Cl_2 at room temp. After 8 h, the suspension turned dark orange-green; TLC analysis indicated the disappearance of starting material. The suspension was filtered over celite (2 cm x 7 cm), followed by washing with ca. 40 mL CH_2Cl_2. HPLC analysis of the filtrate (CH_2Cl_2/MeOH = 98:2; peak detection at 275 nm) indicated formation of bromomethyl-ketonitrone **63** and other impurifications. The solvents were removed under reduced pressure (25 °C/20 mbar) to afford a near-colourless oil (^{13}C NMR: r. r. = 96:4) which was purified by MPLC (short column, 3 cm x 28 cm; CH_2Cl_2/MeOH = 99:1, several injections). This provided the nitrone **63** as a colourless solid (89 mg, 0.250 mmol, 56 %; m. p. 153-156 °C, decomp.) with slightly deviating bromine analysis.

$[\alpha]_D^{20}$ = –40 (*c* = 1.00, $CHCl_3$)

$C_{15}H_{18}BrNO_4$	calc.	C	50.58	H	5.09	N	3.93	Br 22.43
(356.2)	found	C	50.60	H	5.15	N	3.88	Br 21.47

The spectroscopic and analytical data were in agreement to those in Experiment 64 (below).

Experiment 64 (SHF 16)

Manganese dioxide (56 mg, 0.74 mmol, 1.3 Eq.) was added to 0.204 g (0.57 mmol) of the bromomethyl pyrrolidine **41** in CH_2Cl_2 (5 mL) at 0 °C. The suspension was warmed to r. t. for 0.5 h, after which point TLC analysis indicated that the reaction was complete. The suspension was filtered over celite (1.5 cm x 6 cm), washed with CH_2Cl_2 (ca. 40 mL) followed by removal of solvents on the rotary evaporator (25 °C/10 mbar). The crude product obtained (^{13}C NMR: r. r. = 98:2) was purified using column chromatography (SiO_2, 20 g, 2 cm x 10 cm, CH_2Cl_2/MeOH = 95:5) to produce the bromomethyl-ketonitrone **63** (0.181 g, 0.508 mmol, 89 %) as an analytically pure, colourless solid (m. p. 153-156 °C, decomp.). The crystals were of suitable quality for the preparation of a X-ray structure analysis (cf. Section 9.8).

$[\alpha]_D^{20}$ = –40 (*c* = 1.00, $CHCl_3$)

$C_{15}H_{18}BrNO_4$	calc.	C	50.58	H	5.09	N	3.93	Br 22.43
(356.2)	found	C	50.31	H	5.11	N	3.86	Br 22.43

IR (solid): $\tilde{\nu}$ = 2980 (s), 2943 (s), 2845 (s), 1612 (m), 1573 (s), 1518 (s), 1465 (w), 1448 (w), 1426 (w), 1377 (s), 1314 (w), 1301 (w), 1253 (s), 1198 (m), 1185 (m), 1152 (m), 1059 (m), 1027 (s), 875 (m), 820 (s) cm^{-1}.

^1H NMR ($CDCl_3$, 500.1 MHz): δ = 1.39, 1.46 [2 s, 3 H each, $C(CH_3)_2$], 3.80 (s, 3 H, OCH_3), 4.01 ("ddd", $^5J_{3,1'A}$ = 0.7, $^4J_{4,1'A}$ = 1.7, $^2J_{1'A,1'B}$ = 10.4 Hz, 1 H, 1'-H_A), 4.62 (d, $^2J_{1'A,1'B}$ = 10.4 Hz, 1 H, 1'-H_B), 4.70 (dd, $^5J_{3,1'A}$ = 0.6, $J_{3,4}$ = 6.0 Hz, 1 H, 3-H), 5.10 (s, 1 H, 2-H), 5.57 ("d", $J_{3,4}$ = 6.0 Hz, 1 H, 4-H), 6.94 ("dd", $J_{A,B}$ = $J_{A',B'}$ = 6.7 Hz, 2 H, A,A' of AA'BB'), 7.10 ("dd", $J_{A,B}$ = $J_{A',B'}$ = 6.6 Hz, 2 H, B,B' of AA'BB').

^{13}C NMR ($CDCl_3$, 125.1 MHz): δ = 18.9 (t, C-1'), 25.7, 27.1 [2 q, $C(\underline{C}H_3)_2$], 55.4 (q, OCH_3), 68.0 (d, C-2), 71.4 (d, C-3), 79.3 (d, C-4), 112.6 [s, $\underline{C}(CH_3)_2$], 114.0 (d, *m*-C), 114.8 (d, *m*-C), 126.1 (d, *o*-C), 128.4 (d, *o*-C), 130.3 (s, *i*-C), 140.7 (s, C-5), 160.2 (s, *p*-C).

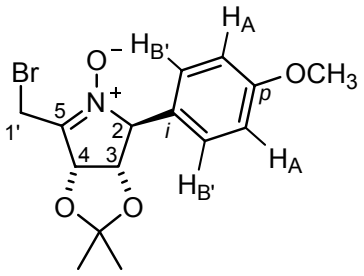

63

Experiments 65, 66

(2*S*,3*S*,4*R*)-3,4-Dihydroxy-3,4-*O*-isopropylidene-2-(4-methoxyphenyl)-5-methyl-2*H*-pyrrole-1-oxide (64)

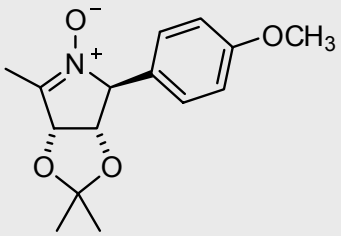

64

Experiment 65 (LR 433)

Mercury(II) oxide (48 mg, 0.225 mmol, 3 Eq.) was added at r. t. to 2-anisyl-5-methyl-*N*-hydroxypyrrolidine **71** (21 mg, 0.075 mmol) dissolved in 2 mL CH_2Cl_2. The reaction was allowed to stir for 8 h. The dark orange-green suspension was filtered over celite (2 cm x 7 cm), and washed with ca. 40 mL CH_2Cl_2. The HPLC analysis of the filtrate (CH_2Cl_2/MeOH = 98:2; peak integration at 265 nm) indicated formation of the methyl-ketonitrone **64** and some inpurifications. The solvents were removed under reduced pressure (25 °C/20 mbar) to yield a nearly colourless solid (^{13}C NMR: r. r. = 94:6). Purification by MPLC (short column, 3 cm x

28 cm; CH_2Cl_2/MeOH = 99:1, several injections) afforded the nitrone **64** as a colourless solid (18 mg, 0.065 mmol, 86 %; m. p. 122 °C) with slightly deviating elemental analysis.

$[\alpha]_D^{20}$ = –68 (*c* = 0.258, $CHCl_3$)

$C_{15}H_{19}NO_4$	calc.	C	64.97	H	6.91	N	5.05
(277.3)	found	C	64.49	H	6.91	N	4.91

Spectroscopic and analytical data were in agreement to those in Experiment 66 (see below).

Experiment 66 (LR 434)

Manganese dioxide (32 mg, 0.321 mmol, 1.3 Eq. Fluka; techn. 90 %; 'oxidation active') was added at 0 °C to the 2-anisyl-5-methyl-*N*-hydroxypyrrolidine **71** (69 mg, 2.47 mmol) in 3 mL CH_2Cl_2. The ice bath was removed after addition and 20 min later TLC analysis had indicated that the reaction was finished. The suspension was filtered over celite (1.5 cm x 6 cm) and washed with CH_2Cl_2 (ca. 40 mL). The HPLC analysis of the filtrate indicated near-exclusive formation of the nitrone **64**. Removal of solvents under reduced pressure on the rotary evaporator (25 °C/10 mbar) (^{13}C NMR: r. r. = 98:2) and MPLC purification (short column, 3 cm x 28 cm; CH_2Cl_2/MeOH = 98:2, several injections) furnished the nitrone **64** (64 mg, 0.231 mmol, 94 %) as an analytically pure, colourless solid (m. p. 122 °C).

$[\alpha]_D^{20}$ = –72 (*c* = 0.112, $CHCl_3$)

$C_{15}H_{19}NO_4$	calc.	C	64.97	H	6.91	N	5.05
(277.3)	found	C	64.74	H	6.83	N	5.00

IR (solid): $\tilde{\nu}$ = 2994 (m), 1596 (s), 1516 (s), 1465 (w), 1453 (m), 1372 (s), 1329 (w), 1311 (w), 1275 (m), 1233 (vs), 1178 (m), 1150 (m), 1116 (w), 1069 (vs), 1029 (vs), 955 (w), 855 (w), 869 (m), 843 (m), 843 (m), 816 (s), 784 (m), 754 (w), 727 (w), 684 (s) cm^{-1}.

^{1}H NMR ($CDCl_3$, 500.1 MHz): δ = 1.39, 1.44 [2 s, 3 H each, $C(CH_3)_2$], 2.17 (s, 3 H, 1'-CH_3), 3.80 (s, 3 H, OCH_3), 4.68 (dt, $J_{2,3}$ = 1.3, $J_{3,4}$ = 5.9 Hz, 1 H, 3-H), 5.11 (s,1 H, 2-H), 5.31 (d, $J_{3,4}$ = 5.9 Hz, 1 H, 4-H), 6.91 ("dd", $J_{A,B}$ = $J_{A',B'}$ = 8.8 Hz, 2 H, A,A' of AA'BB'), 7.11 ("dd", $J_{A,B}$ = $J_{A',B'}$ = 8.8 Hz, 2 H, B,B' of AA'BB').

^{13}C NMR ($CDCl_3$, 125.1 MHz): δ = 10.6 (q, C-1'), 26.1, 27.3 [2 q, C($\underline{C}H_3)_2$], 55.4 (q, OCH_3), 77.5 (d, C-2), 79.2 (d, C-3), 81.4 (d, C-4), 112.1 [s, $\underline{C}(CH_3)_2$], 114.5 (d, *m*-C), 114.6 (d, *m*-C), 116.0 (s, *i*-C), 126.5 (d, *o*-C), 128.2 (d, *o*-C), 140.1 (s, C-5), 160.0 (s, *p*-C).

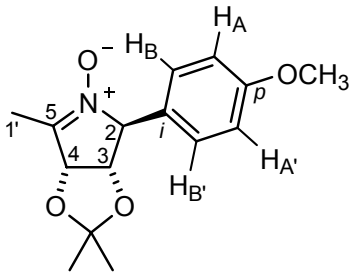

64

8.4.3 Reactions of the bromomethyl-ketonitrones 57 and 63

Experiment 67 (LR 369)

(3a*S*,4*S*,5*S*,6*S*)-3a-Bromomethyl-3,4-dihydroxy-4,5-*O*-isopropylidene-6-(4-methoxyphenyl)-methyl-pyrrolo[1,2-b]isoxalizidine-1,2-dimethylester (65)

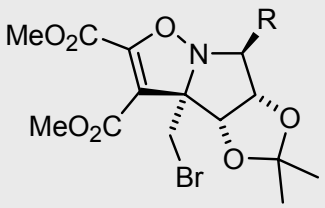

65

R = *p*-C_6H_4OMe

The bromomethylnitrone **63** (100.8 mg, 0.283 mmol) was placed in toluene (4 mL) and 200 mg (1.42 mmol, 5 Eq.) dimethyl acetylenedicarboxylate was added. The solution was heated to 75 °C for 6 h. The solvent was removed on the rotary evaporator (30 °C/10 mbar) and the near-colourless oil obtained (^{13}C NMR: d. r. = 80:10; d. r. = 85:15 from HPLC; detection at 275 nm) was filtered over a short column of silica gel (40 g) and washed with ca. 100 mL of hexan/EE (75:25). The diastereoisomers were separated using MPLC (eluant: PE/EE = 75:25) to obtain the main diastereoisomer, the 4-isoxazoline **65** (104 mg, 0.209 mmol, 74 %) as a colourless solid with slightly deviating elemental analysis, and a minor diastereoisomer (10 mg, 2.01 mmol, 7 %) as a spectroscopically pure, brown solid that, however, decomposed rapidly on standing at room temp. (according to ^{1}H and ^{13}C NMR spectra).

$[\alpha]_D^{20}$ = 138 (*c* = 0.285, CH_2Cl_2)

$C_{21}H_{24}BrNO_8$	calc.	C	50.61	H	4.85	N	2.81	Br	16.03
(498.3)	found	C	51.28	H	5.07	N	2.73	Br	16.25

IR (solid): $\tilde{\nu}$ = 2953 (m), 2943 (s), 1751 (C=O, s), 1715 (C=O, s), 1649 (m), 1613 (w), 1513 (s), 1436 (s), 1374 (m), 1297 (m), 1246 (m), 1211 (m), 1174 (w), 1156 (w), 1093 (w), 1064 (s), 1030 (m), 929 (w), 864 (m), 826 (m), 801 (m), 762 (w), 663 (m), 608 (m) cm^{-1}.

^{1}H NMR ($CDCl_3$, 300.1 MHz): δ = 1.37, 1.57 [2 s, 3 H each, $C(CH_3)_2$], 3.56 (d, $^2J_{A,B}$ = 10.5 Hz, 1 H of $C\underline{H}_A H_B Br$), 3.80 [2 s, 3 H each, 2 $C(O)O\underline{C}H_3$], 3.86 (s, OCH_3), 4.05 (d, $^2J_{A,B}$ = 10.5 Hz, 1 H of $C\underline{H}_A H_B Br$), 4.24 (d, $J_{5,6}$ = 7.6 Hz, 1 H, 6-H), 4.52 (dd, $J_{4,5}$ = 5.5, $J_{5,6}$ = 7.6 Hz, 1 H, 5-H), 4.79 (d, $J_{4,5}$ = 5.5 Hz, 1 H, 4-H), 6.92 ("dd", $J_{A,B} = J_{A',B'}$ = 6.7 Hz, 2 H, A,A' of AA'BB'), 7.45 ("dd", $J_{A,B} = J_{A',B'}$ = 6.7 Hz, 2 H, B,B' of A,A'BB').

^{13}C NMR ($CDCl_3$, 75.5 MHz): δ = 26.0, 27.8 [2 q, $C(\underline{C}H_3)_2$], 37.5 (t, CH_2Br), 52.1, 55.3 (2 q, of 2 $C(O)O\underline{C}H_3$), 53.3 (q, OCH_3), 76.5 (d, C-5), 80.1 (q, C-3a), 82.4 (d, C-4), 83.7 (d, C-5),108.6 (s, C-3), 113.7 [s, $\underline{C}(CH_3)_2$], 114.2 (d, *m*-C), 128.1 (s, *i*-C), 129.6 (d, *o*-C), 152.2 (s, C-2), 159.6 (s, *p*-C), 158.6, 162.4 (2 s, each of 2 $\underline{C}O_2CH_3$).

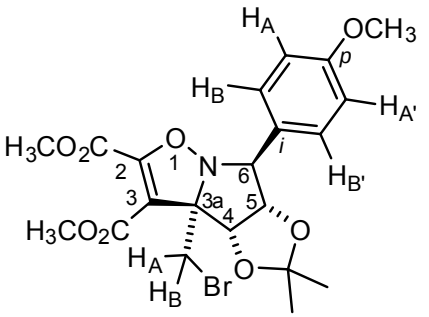

65

Assignment of the signals was done using a DEPT and C,H-COSY.

Experiment 68 (LR 435)

(1*R*,2*S*,4a*R*,8a*R*,9a*R*)-1,2-Dihydroxy-O-1,2-isopropylidene-octahydro-4-oxa-3a-aza-cyclopenta[b]napthalene-9a-carbonitrile (66)

and (1*R*,2*S*,4a*S*,8a*S*,9a*R*)-diastereoisomer (67)

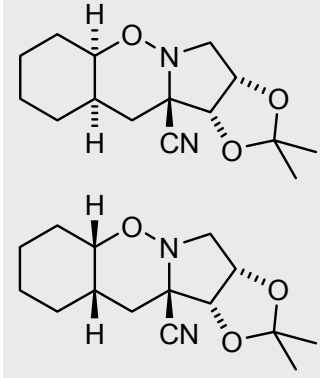

66

67

Using lit.[100] as a guideline, silver tetrafluoroborate (308 mg, 1.58 mmol, 1.05 Eq., Fluka) was added quickly to an oven-dried flask (wrapped in aluminum foil to prevent the influx of light) containing 1,2-dichloroethane (Fluka, p.a. over MS 4 Å) and cyclohexene (124 mg, 1.51 mmol, 1. Eq., Fluka, p.a.) at 0 °C. The bromomethylnitrone **57** (377 mg, 1.51 mmol, 1 Eq.) was taken up in 1 mL 1,2-dichloromethane and added dropwise over a period of 15 min. After several drops, silver bromide could be observed to precipitate out of solution as a colouless solid that became darker with time. After addition, TLC analysis indicated the disappearance of nitrone **57** and the appearance of several spots at the bottom, including two equally intense spots at R_f = 0.15 (EE 100 %). The reaction was warmed to r. t. and stirred for a further 90 min. After this point, TLC analysis indicated no major differences to the

reaction composition. The suspension was filtered over a glass-filter, attached to a shaking funnel and washed with 25 mL CH_2Cl_2. The filtrate was placed in an Erlymeyer flask and treated with ca. 0.8 g potassium cyanide dissolved in ca. 2 mL water and was strirred strongly for 20 min. The TLC analysis of the mixture indicated the disappearnce of all UV-active components and the appearance of two new close-running top-spots (R_f = 0.7, PE:EE = 80:20). The organic layer was separated and washed with water (5 mL) and saturated NaCl solution (5 mL), followed by drying ($MgSO_4$) and removal of solvents under vacuum (25 °C/10 mbar), to yield the crude products as a pale-yellow oil (127 mg). The ^{1}H NMR analysis indicated a 1:1 mixture of cycloadducts **66**/**67**, which were purified over a short flash column (SiO_2, 4 cm x 5 cm, PE 100 %, then PE:EE = 80:20) to yield the title compounds, **66** and **67** as an analytically pure oil (85 mg, 0.305 mmol, 20 %). The diastereoisomers were separated using column chromatography (SiO_2, 2 cm x 22 cm, PE 100 %, then PE:EE 90:10) to yield the 1,2-oxazine **66** (35 mg, 0.126 mmol, 8.3 %) as a colourless oil that solidified on standing (m. p. 88-91 °C), and the cycloadduct **67** (42 mg, 0.151 mmol, 10 %; Σ 18 %) as a crystalline colourless solid (m. p. 119-121 °C). From diastereoisomer **67**, a X-ray crystal structure determination was made to provide additional structural proof (cf. Section 9.9 for full data).

(Elemental analysis from a 1:1 mixture of **66**/**67**):

$C_{15}H_{22}N_2O_3$	calc.	C	64.73	H	7.97	N	10.06
(278.4)	found	C	64.42	H	7.98	N	9.83

Analytical data of **66**

$[\alpha]_D^{20}$ = –61 (*c* = 0.038, CH_2Cl_2)

MS (ESI, positive ion) *m/z* (%) = 301.1 $[M+Na]^+$, 279.2 $[M+H]^+$, 252.2 [M, -HCN]$^+$.
HRMS (ESI, positive ion): calc. for $C_{15}H_{22}N_2O_3$ + Na^+: calc. 301.1523; found 301.1514.

IR (neat): $\tilde{\nu}$ = 2939 (s), 2856 (m), 1447 (m), 1373 (m), 1329 (w), 1268 (w), 1241 (w), 1206 (vs), 1164 (w), 1100 (s), 1086 (m), 1045 (w), 1027 (m), 1005 (m), 986 (w), 972 (w), 942 (w), 926 (w), 906 (m), 888 (m), 857 (m), 820 (s), 800 (w), 766 (w), 723 (w), 633 (w), 643 (w) cm^{-1}.

^{1}H NMR ($CDCl_3$, 300.1 MHz): δ = 1.15 (m, 1 H, 7-H_A), 1.31 [s, 3 H, C(CH_3)], 1.39-1.54 [m, overlapping signals, together 7 H, 8-H_A, 7-H_B, 6-H_A, 5-H_A and C($C\underline{H}_3$)], 1.77-1.84 (m, overlapping signals and d, $^2J_{9A,9B}$ = 13.4 Hz, 3 H, 9-H_A, 8-H_B, 8a-H), 1.89-2.00 ('d', $^2J_{6A,6B}$ = 13.2 Hz, 1 H, 6-H_B), 2.20-2.41 (dq, $J_{4a,5B}$ = 3.7, $^2J_{5A,5B}$ = 13.3 Hz, and dd, $J_{8a,9B}$ = 6.2, $^2J_{9A,9B}$ =

13.6 Hz, together 2 H, 5-H_B, 9-H_B), 3.10 (dd, $J_{2,3A}$ = 4.8, $^2J_{3A,3B}$ = 10.2 Hz, 1 H, 3-H_A), 3.44 (d, $^2J_{3A,3B}$ = 10.2 Hz, 1 H, 3-H_B), 4.15 ('q', $J_{4a,5B}$ = 3.3 Hz, $J_{4a,8a}$ = 7.3 Hz, 1 H, 4a-H), 4.57 (d, $J_{1,2}$ = 6.5 Hz, 1 H, 1-H), 4.77 (dd, $J_{1,2}$ = 6.5, $J_{2,3A}$ = 4.8 Hz, 1 H, 2-H).

^{13}C NMR ($CDCl_3$, 75.5 MHz): δ = 20.9 (t, C-7), 25.6, 26.0 [2 q, C(<u>C</u>H_3)$_2$], 26.2 (t, C-8), 27.2 (t, C-5), 30.0 (t, C-6), 31.8 (t, C-9), 33.0 (d, C-8a), 56.7 (t, C-3), 64.0 (s, C-9a), 75.6 (d, C-2), 78.6 (d, C-4a), 81.3 (d, C-1), 113.2 [s, <u>C</u>$(CH_3)_2$], 119.6 (s, CN).

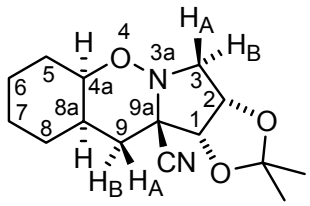

66

<u>Analytical data of **67**</u>

$[\alpha]_D^{20}$ = –93 (*c* = 0.028, CH_2Cl_2)

MS (ESI, positive ion) *m/z* (%) = 301.1 $[M+Na]^+$, 279.2 $[M+H]^+$, 252.2 $[-HCN]^+$.
HRMS (ESI, positive ion): calc. for $C_{15}H_{22}N_2O_3$+ Na^+: calc. 301.1523; found 301.1521.

IR (neat): $\tilde{\nu}$ = 2995 (w), 2932 (s), 2870 (w), 1451 (s), 1434 (w), 1376 (vs), 1346 (w), 1269 (s), 1238 (m), 1208 (vs), 1163 (w), 1143 (w), 1106 (vs), 1089 (vs), 1031 (s), 1000 (s), 993 (s), 927 (w), 918 (w), 889 (m), 873 (s), 853 (m), 798 (w), 780 (w), 719 (w), 684 (w), 661 (w) cm^{-1}.

^{1}H NMR ($CDCl_3$, 300.1 MHz): δ = 1.25-1.35 [m, overlapping signals, together 5 H, 6-H_A, 7-H_A and C(C<u>H</u>$_3$)], 1.40-1.50 [m, overlapping signals, together 5 H, 7-H_B, 8-H_A & C(C<u>H</u>$_3$)], 1.63-1.78 (m, overlapping signals, 5-H_A, 8-H_B and d, $^2J_{9A,9B}$ = 13.2 Hz, 1 H, 9-H_A), 1.79-1.85 (m, 1 H, 6-H_B), 2.15 ('dq', $J_{4a,5B} \approx J_{5B,6}$ = 3.8, $^2J_{5A,5B}$ = 13.2 Hz, 1 H, 5-H_B), 2.42-2.44 (m, 2 H, 8a-H, 9-H_B), 2.93 (dd, $J_{2,3A}$ = 4.9, $^2J_{3A,3B}$ = 10.4 Hz, 1 H, 3-H_A), 3.51 (d, $^2J_{3A,3B}$ = 10.4 Hz, 1 H, 3-H_B), 3.90 ('dt', $J_{4a,5B}$ = 3.3 Hz, $J_{4a,8a}$ = 4.3 Hz, 1 H, 4a-H), 4.67 (d, $J_{1,2}$ = 6.5 Hz, 1 H, 1-H), 4.79 (dd, $J_{1,2}$ = 6.5, $J_{2,3A}$ = 4.8 Hz, 1 H, 2-H).

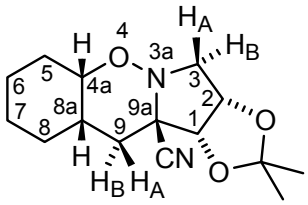

67

^{13}C NMR ($CDCl_3$, 75.5 MHz): δ = 20.4 (t, C-7), 25.0, 25.9 [2 q, C(<u>C</u>H_3)$_2$], 25.6 (t, C-8), 26.2 (t, C-5), 27.8 (t, C-9), 29.5 (t, C-6), 31.4 (d, C-8a), 57.2 (t, C-3), 69.1 (s, C-9a), 75.7 (d, C-2), 78.6 (d, C-4a), 81.0 (d, C-1), 113.1 [s, <u>C</u>$(CH_3)_2$], 119.8 (s, CN).

8.5 Experiments Relating to Chapter 5

8.5.1 Lithium aluminium reduction of the bromomethyl group

Experiment 69 (LR 241)

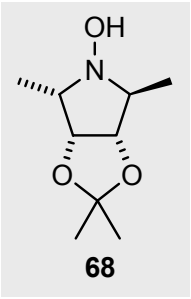

68

(2*S*,3*S*,4*R*,5*S*)-1,3,4-Trihydroxy-3,4-*O*-isopropylidene-2,5-dimethyl-pyrrolidine (68)

TLP 3: Typical Laboratory Procedure for chemoselective reduction of the bromomethyl group with lithium aluminium hydride

To a two-necked flask (50 mL) under nitrogen was added 2-bromomethyl-5-methyl-*N*-hydroxypyrrolidine **34** (306 mg, 1.15 mmol) and abs. THF (10 mL). At 0 °C, lithium aluminium hydride (73 mg, 1.95 mmol, 1.8 Eq.) was added portionwise. The reaction proceeded rapidly over the course of 1.5-2 h, whereupon TLC analysis showed that the reaction had to gone to completion. Hydrolysis followed at 0 °C through the dropwise addition of a 5 % solution of citric acid (2 mL), and water (5 mL). The suspension was placed in a separating funnel and the layers parted. The aqueous layer was extracted with methylene chloride (4 x 15 mL), and the combined organic layers were washed with 15 mL of a saturated $NaHCO_3$ solution and dried over $MgSO_4$. After removal of the solvents under vacuum (30 °C/20 mbar), the crude product was purified using column chromatography (SiO_2, 35 g, 2 cm x 15 cm, PE:EE = 70:30) to yield the 2-methyl-*N*-hydroxypyrrolidine **68** (0.180 g, 0.961 mmol, 84 %; lit.[2] 73 %) as an analytically pure, colourless solid (m. p. 27-29 °C; lit.[2] 58-59 °C).

$[\alpha]_D^{20}$ = 54 (*c* = 2.45, $CHCl_3$); lit.[2] $[\alpha]_D^{20}$ = 67 (*c* = 0.55, CH_2Cl_2)

$C_9H_{17}NO_3$	calc.	C	57.73	H	9.15	N	7.48
(187.2)	found	C	57.81	H	9.09	N	7.36

IR (film): $\tilde{\nu}$ = 3205 (bs, OH), 2975 (m), 2933 (m), 2873 (w), 1453 (m), 1372 (s), 1285 (w), 1266 (w), 1233 (w), 1207 (s), 1156 (s), 1118 (m), 1098 (w), 1055 (m), 1055 (s), 1008 (s), 999 (w), 964 (w), 918 (w), 873 (s), 821 (w), 759 (w), 663 (s), 639 (s) cm^{-1}.

Spectroscopic and analytical data were in accordance to that in lit.[2]

The ^{1}H and ^{13}C NMR spectroscopic data are presented in Tables 20-22 – see below.

Experiment 70 (LR 291)

(2*S*,3*S*,4*R*,5*S*)-1,3,4-Trihydroxy-2-isopropyl-3,4-*O*-isopropylidene-5-methyl-pyrrolidine (69)

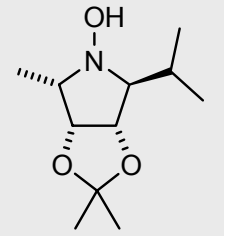

69

In line with TLP 3, the pyrrolidine **36** (325 mg, 1.105 mmol) was allowed to react with 74 mg (2.00 mmol, 1.8 Eq.) lithium aluminium hydride in 10 mL abs THF at 0 °C. After work-up and product isolation according to TLP 3, the crude product obtained was filtered over a small plug of silica gel and washed with methylene chloride (ca. 100 mL). This afforded the title compound, the 2-isopropyl-*N*-hydroxypyrrolidine **69** (0.157 g, 0.730 mmol, 66 %), as an analytically pure, colourless solid (m.p: 107 °C). An X-ray structure determination could be made to provide additional structural proof (cf. Section 9.10 for full data).

$[\alpha]_D^{20}$ = 8 (*c* = 0.19, $CHCl_3$)

$C_{11}H_{21}NO_3$	calc.	C	61.37	H	9.83	N	6.51
(215.2)	found	C	61.31	H	9.71	N	6.31

IR (neat): $\tilde{\nu}$ = 3225 (bs, OH), 2981 (w), 2954 (w), 2933 (m), 2873 (w), 1464 (m), 1372 (s), 1267 (m), 1233 (w), 1204 (m), 1161 (m), 1133 (w), 1108 (w), 1091 (m), 1062 (w), 1020 (m), 991 (w), 972 (w), 959 (m), 940 (w), 869 (s), 840 (w), 807 (w), 735 (w), 683 (w) cm^{-1}.

The ^{1}H and ^{13}C NMR spectroscopic data are presented in Tables 20-22 – see below.

Experiment 71 (LR 123, 277)

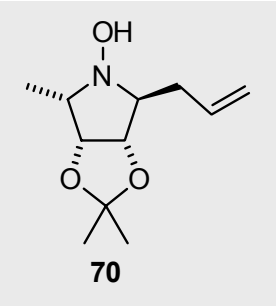

70

(2*S*,3*S*,4*R*,5*S*)-2-Allyl-1,3,4-trihydroxy-3,4-*O*-isopropylidene-5-methyl-pyrrolidine (70)

Using TLP 3 as an experimental guideline, 325 mg (1.11 mmol) of the pyrrolidine **38** was allowed to react with 74 mg (2.00 mmol, 1.8 Eq.) of lithium aluminium hydride in 15 mL abs. THF at 0 ºC. After 2 h, work-up as described in TLP 3 afforded the 2-allyl-substituted *N*-hydroxypyrrolidine as a spectroscopically pure oil (0.230 g, 1.08 mmol, '97 %'). This was filtered over a small plug of silica gel (40 g) and washed with ca. 100 mL PE/EE (7:3). After removal of the solvents on the rotary evaporator (25 °C/10 mbar), the title compound **70** was obtained (0.192 g, 0.90 mmol, 81 %) as an analytically pure, colourless oil, that slowly solidified on standing at 4 ºC (m. p. 75 ºC).

$[\alpha]_D^{20}$ = 13 (*c* = 0.96, $CHCl_3$)

$C_{11}H_{19}NO_3$	calc.	C	61.95	H	8.98	N	6.57
(213.3)	found	C	61.87	H	8.96	N	6.51

IR (neat): $\tilde{\nu}$ = 3200 (bs, OH), 3077 (w), 2977 (m), 2931 (m), 2870 (w), 2351 (w), 1641 (w), 1448 (w), 1373 (m), 1270 (w), 1238 (w), 1208 (m), 1169 (w), 1143 (w), 1119 (w), 1056 (m), 1005 (m), 962 (w), 915 (w), 870 (w), 821 (w), 776 (w) cm^{-1}.

The ^1H and ^{13}C NMR spectroscopic data are presented in Tables 20-22 – see below.

Notes concerning Experiments 73-81

There is a degree of close similarity in the structures concerned in the following series of reactions. Reductions were therefore carried out using TLP 3, as described above. A representative example is provided below for the reduction of the 4-methoxyphenyl-substituted pyrrolidine **41**. The ^{1}H and ^{13}C NMR data is presented in "standard notation" for the product, the pyrrolidine **71**. This is done to highlight the multiplicites, i.e. peak splittings, and should be seen as a typical example of what is yet to follow. The reaction parameters for Experiments 73-81 are presented in Table 19 for convenience below. The ^{1}H and ^{13}C NMR data follow thereafter in Tables 20-22.

Experiment 72 (FJS 13; LR 70)

(2*S*,3*S*,4*R*,5*S*)-1,3,4-Trihydroxy-3,4-*O*-isopropylidene-2-(4-methoxyphenyl)-5-methyl-pyrrolidine (71)

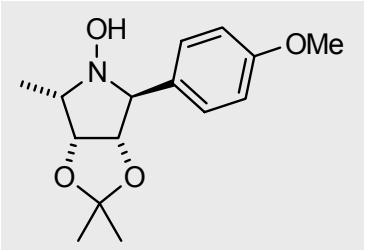

71

Following TLP 3, the bromomethyl-pyrrolidine **41** (580 mg, 1.62 mmol) was allowed to react with 92 mg (2.46 mmol, 1.5 Eq.) lithium aluminium hydride in 10 mL abs THF at 0 °C. After work-up and product isolation according to TLP 3, the crude product obtained was purified using column chromatography (SiO_2, 30 g, 2 cm x 15 cm, PE:EE = 70:30), which yielded the 2-anisyl-*N*-hydroxyppyrrolidine **71** (0.440 g, 1.58 mmol, 97 %) as a analytically pure, colourless solid (m. p. 119 °C).

$[\alpha]_D^{20}$ = 47 (*c* = 1.00, CH_2Cl_2)

$C_{15}H_{21}NO_4$	calc.	C	64.55	H	7.58	N	5.17
(279.3)	found	C	64.43	H	7.47	N	4.88

IR (neat): $\tilde{\nu}$ = 3240 (bs, OH), 2971 (m), 2930 (m), 2882 (w), 1610 (s), 1513 (m), 1452 (m), 1372 (m), 1269 (m), 1109 (w), 1057 (w), 1032 (w), 999 (m), 863 (m) cm^{-1}.

^{1}H NMR ($CDCl_3$, 300.1 MHz): δ = 1.24 (d, $J_{5,1'}$ = 6.3 Hz, 3 H, 1'-H), 1.37, 1.49 [2 s, 3 H each, $C(CH_3)_2$], 3.16 (m, 1 H, 5-H), 3.79 (s, 3 H, OCH_3), 4.38 (s, 1 H, 2-H), 4.61 (dd, $J_{3,4}$ = 6.5, $J_{4,5}$ = 5.0 Hz, H, 4-H), 4.81 (dd, $J_{2,3}$ = 1.0, $J_{3,4}$ = 6.5 Hz, 1 H, 3-H), 6.90 ("dd", $J_{A,B}$ = $J_{A',B'}$ = 8.7 Hz, 2 H, A,A' of AA'BB'), 7.10 ("dd", $J_{A,B}$ = $J_{A',B'}$ = 8.7 Hz, 2 H, B,B' of AA'BB'), 8.22 (bs, 1 H, OH).

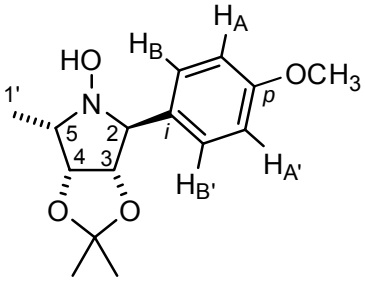

71

^{13}C NMR ($CDCl_3$, 75.5 MHz): δ = 11.6 (q, C-1'), 24.2, 25.9 [2 q, $C(\underline{C}H_3)_2$], 55.2 (q, OCH_3), 61.1 (d, C-5), 72.1 (d, C-2), 78.5 (d, C-4), 81.2 (d, C-3), 113.2 [q, $\underline{C}(CH_3)_2$], 109.7 (d, *m*-C), 126.8 (s, *i*-C), 131.1 (d, *o*-C), 159.3 (s, *p*-C).

Assignment of the signals was done using a DEPT and C,H-COSY.

Experiments 73-81

(2*S*,3*S*,4*R*,5*S*)-2-([1,1'-Biphenyl]-4-yl)-1,3,4-trihydroxy-3,4-*O*-isopropylidene-5-methyl-pyrrolidine (72)

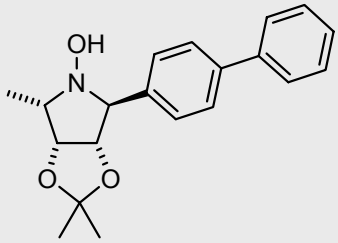

72

(2*S*,3*S*,4*R*,5*S*)-2-(4-Fluorophenyl)-1,3,4-trihydroxy-3,4-*O*-isopropylidene-5-methyl-pyrrolidine (73)

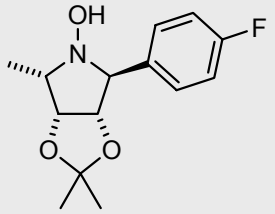

73

(2*S*,3*S*,4*R*,5*S*)-2-(4-Chlorophenyl)-1,3,4-trihydroxy-3,4-*O*-isopropylidene-5-methyl-pyrrolidine (74)

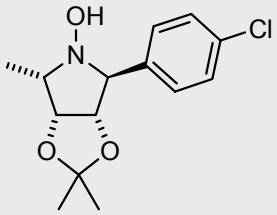

74

(2*S*,3*S*,4*R*,5*S*)-2-(4-Bromophenyl)-1,3,4-trihydroxy-3,4-*O*-isopropylidene-5-methyl-pyrrolidine (75)

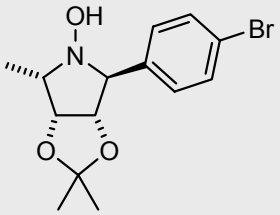

75

(2*S*,3*S*,4*R*,5*S*)-1,3,4-Trihydroxy-3,4-*O*-isopropylidene-5-methyl-2-(4-methylthiophenyl)-pyrrolidine (76)

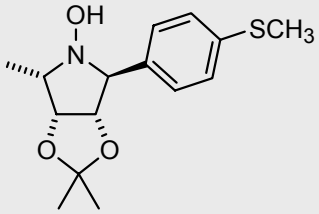

76

(2*S*,3*S*,4*R*,5*S*)-1,3,4-Trihydroxy-3,4-*O*-isopropylidene-2-(4-methoxybenzyl)-5-methyl-pyrrolidine (77)

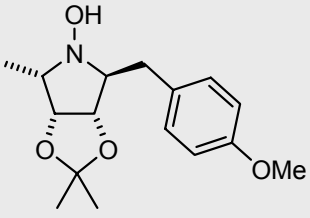

77

(2*S*,3*S*,4*R*,5*S*)-1,3,4-Trihydroxy-3,4-*O*-isopropylidene-5-methyl-2-(4-phenoxyphenyl)-pyrrolidine (78)

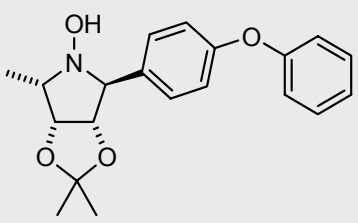

78

(2*S*,3*S*,4*R*,5*S*)-1,3,4-Trihydroxy-3,4-*O*-isopropylidene-5-methyl-2-(4-*N,N*-dimethylanilino)-pyrrolidine (79)

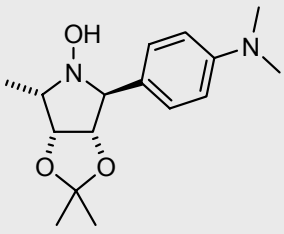

79

(2*S*,3*S*,4*R*,5*S*)-2-(2-Furyl)-1,3,4-trihydroxy-3,4-*O*-isopropylidene-5-methyl-pyrrolidine (80)

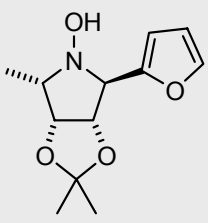

80

Table 19: Synthesis of 5-substituted-2-methyl-N-hydroxypyrrolidines **72**-**80** according to TLP 3

Product (R)[a] / Experiment Nr.	Nr.	Educt mg / mmol	$LiAlH_4$ mg / mmol	Product mg / %	M. p. °C	$[\alpha]_D^{20}$ (*c*, CH_2Cl_2)	Elemental analysis							
72 ("Biphenyl") E 73 (LR 152)	**42**	779 / 1.93	110 / 2.90	570 / 91[b]	89	58 (1.00)	$C_{20}H_{23}NO_3$ (325.4)	calc.	C	73.82	H	7.12	N	4.30
								found	C	73.99	H	7.19	N	4.38
73 (4-Fluorophenyl) E 74 (LR 265)	**43**	745 / 2.15	139 / 3.65	511 / 89	83-85	14 (0.65)	$C_{14}H_{18}NO_3F$ (267.3)	calc.	C	62.90	H	6.78	N	5.24
								found	C	62.90	H	6.78	N	5.16
74 (4-Chlorophenyl) E 75 (LR 144)	**44**	410 / 1.13	64 / 1.69	230 / 72	72-74	58 (0.35)	$C_{14}H_{18}NO_3Cl$ (283.8)[c]	calc.	C	59.26	H	6.39	N	4.94
								found	C	59.17	H	6.39	N	4.86
75 (4-Bromophenyl) E 76 (LR 270)	**45**	235 / 0.58	39 / 1.03	175 / 92	123-125[d]	9 (0.66)	$C_{14}H_{18}NO_3Br$ (328.2)[e]	calc.	C	51.23	H	5.53	N	4.27
								found	C	52.40	H	5.67	N	4.30
76 (4-Thioanisyl) E 77 (LR 55; NM 9)	**46**	696 / 1.86	112 / 2.95	490 / 89	110-111	59 (1.01)	$C_{15}H_{21}NO_3S$ (295.4)[f]	calc.	C	60.99	H	7.17	N	4.74
								found	C	61.02	H	7.19	N	4.78
77 (4-Methoxybenzyl) E 78 (SH 5)	**47**	400 / 1.07	61 / 1.61	280 / 89	-[g]	25 (1.05)	$C_{16}H_{23}NO_4$ (293.4)	calc.	C	65.51	H	7.90	N	4.77
								found	C	65.44	H	7.89	N	4.63
78 (4-Phenoxyphenyl) E 79 (LR 182)	**48**	577 / 1.37	78 / 2.05	429 / 91	54-56	40 (1.00)	$C_{20}H_{23}NO_4$ (341.4)	calc.	C	70.36	H	6.79	N	4.10
								found	C	70.40	H	6.82	N	3.92
79 (2-Furyl) E 80 (NM 10)	**49**	702 / 2.21	125 / 3.30	484 / 92[b]	82	71 (1.00)	$C_{12}H_{17}NO_4$ (239.3)	calc.	C	60.24	H	7.16	N	5.85
								found	C	60.35	H	7.18	N	5.73
80 (4-*N*,*N*-Dimethylanilino) E 81 (LR 239)	**50**	400 / 1.08	82 / 2.15	277 / 88	123-126	51 (0.59)	$C_{16}H_{24}N_2O_3$ (292.4)	calc.	C	65.73	H	8.27	N	9.58
								found	C	65.54	H	8.23	N	9.46

[a] 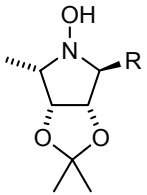

[b] The crude product obtained was analytically pure. [c] calc. Cl 12.49; found Cl 11.30. [d] Partial decomposition. [e] In spite of chromatography (i.e. flash silica gel or MPLC), the product remained ca. 90 % pure; correspondingly, the bromine content was not determined. [f] calc. S 10.85; found S 11.02 [g] Colourless oil.

Table 20: ^{1}H NMR Chemical shifts of the N-hydroxypyrrolidines **68**-**70**, **72**-**80** (δ [ppm], 300.1 MHz or 500.1 MHz, $CDCl_3$)

Nr.	2-H	3-H	4-H	5-H	1'-CH_3	$C(CH_3)_2$	*p*-C_6H_4 and/or other 5-R; OH
68	3.50	4.31	4.95	3.05	1.20-1.35[a]	1.20-1.35[a], 1.43	1.07 (2-CH_3)
69	3.35	4.47	4.61	2.96	1.14	1.25, 1.40	0.91 (CH_3), 0.96 (CH_3), 2.00 (C<u>H</u>$(CH_3)_2$)
70	3.40	4.41	4.48	3.05	1.28-1.29[a]	1.28-1.29[a], 1.44	1.85 (C<u>H</u>$_a$H$_b$), 2.85 (CH$_a$<u>H</u>$_b$), 5.14 (CH$_E$<u>H</u>$_Z$), 5.15 (C<u>H</u>$_E$H$_Z$), 5.81 (CH)
72	4.58	4.95	4.76	3.27	1.25	1.37, 1.51	6.20-6.90 [9 H, C_6H_4 and C_6H_5]
73	4.44	4.85	4.71	3.24	1.22	1.35, 1.50	7.09 [2 H, H_A,$H_{A'}$], 7.48 [2 H, H_B,$H_{B'}$]
74	4.35	4.80	4.61	3.10	1.15	1.25, 1.40	7.00 [2 H, H_A,$H_{A'}$], 7.20 [2 H, H_B,$H_{B'}$]
75	4.40	4.83	4.70	3.20	1.23	1.34, 1.49	7.09 [2 H, H_A,$H_{A'}$], 7.47 [2 H, H_B,$H_{B'}$]
76	4.35	4.80	4.61	3.10	1.15	1.25, 1.40	2.40 (-SCH_3), 6.95 [2 H, H_A,$H_{A'}$], 7.00 [2 H, H_B,$H_{B'}$], 7.80 (OH)
77	3.60	4.50	4.35	3.10	1.25	1.20, 1.38	2.15 (C<u>H</u>$_A$H$_B$), 3.30 (CH$_A$<u>H</u>$_B$), 3.72 (OCH_3), 6.80 [2 H, H_A,$H_{A'}$], 7.00 [2 H, H_B,$H_{B'}$]
78	4.46	4.89	4.70	3.31	1.25	1.34, 1.48	6.90-7.40 [9 H, C_6H_4 and C_6H_5]
79	4.40	4.75	4.62	3.23	1.19	1.24, 1.51	6.24 (3'-H), 6.28 (2'-H), 7.31 (4'-H), 8.0 (OH)
80	4.50	4.88	4.71	3.20	1.25	1.35, 1.51	2.95 [6 H, $N(CH_3)_2$], 6.70 [2 H, H_A,$H_{A'}$], 7.05 [2 H, H_B,$H_{B'}$]

[a] The overlap with other signals prevented exact determination of chemical shifts.

Table 21: Coupling constants of N-hydroxypyrrolidines **68**-**70**, **72**-**80** (J [Hz], $CDCl_3$)

Nr.	$J_{2,3}$	$J_{3,4}$	$J_{4,5}$	$J_{5,1'\text{-Me}}$	Others (2-R; AA'BB')
68	–	6.7	5.2	6.3	J(2-H,2-CH_3) = 7.1
69	3.1	6.9	5.6	6.9	J(2-H,CH) = 8.0
70	—	6.8	5.0	—[a]	J(2-H,C$\underline{H}_a$) = 3.7, J(2-H,C$\underline{H}_b$) = 11.2, J(C$\underline{H}_a$,CH) = 5.5, J(C$\underline{H}_b$,CH) = 4.0, J(C$\underline{H}$=C$H_E\underline{H}_Z$) = 17.8, J(C$\underline{H}$=C$\underline{H}_E\underline{H}_Z$) = 11.9, ^2J(C$\underline{H}_E\underline{H}_Z$) = 1.9
72	0.9	6.6	5.1	6.4	—
73	1.0	6.8	5.4	6.5	J(H_A,H_B) = J($H_{A'}$,$H_{B'}$) = 8.4
74	1.0	6.7	5.2	6.5	J(H_A,H_B) = J($H_{A'}$,$H_{B'}$) = 8.6
75	1.2	6.7	5.3	6.5	J(H_A,H_B) = J($H_{A'}$,$H_{B'}$) = 8.5
76	—	6.7	5.3	6.5	J(H_A,H_B) = J($H_{A'}$,$H_{B'}$) = 8.7
77	—	6.9	5.1	6.6	J(2-H,C$\underline{H}_a$,CH_b) = 3.6, J(2-H,CH_a,C$\underline{H}_b$) = 11.7, ^2J(C$\underline{H}_a$,C$\underline{H}_b$) = 14.1
78	1.0	6.8	5.4	6.5	—
79	—	6.6	5.2	6.5	J(3'-H,5'-H) = 1.5, J(4'-H, 5'-H) = 1.9, J(3'-H,4'-H) = 3.3
80	—	6.6	5.3	6.5	J(H_A,H_B) = J($H_{A'}$,$H_{B'}$) = 8.8

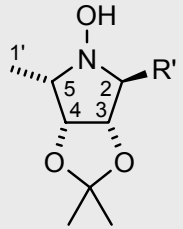

	R' =
68	CH_3
69	$C(CH_3)_2$
70	$CH_2CH{=}CH_2$

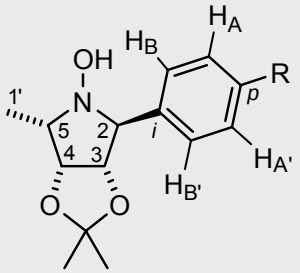

	R =
72	Ph
73	F
74	Cl
75	Br
76	SCH_3
78	OPh
80	$N(CH_3)_2$

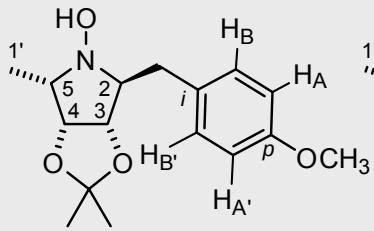

77

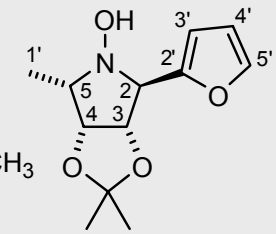

79

[a] Coupling constants could not be determined due to overlapping signals.

Table 22: ^{13}C NMR Chemical shifts of N-hydroxypyrrolidines **68-70, 72-80** (δ [ppm], $CDCl_3$, 62.9 or 125.8 MHz)

Nr.	C-2	C-3	C-4	C-5	5-CH_3	$C(CH_3)_2$	Other (2-R; Ar-C or *p*-C_6H_4)
68	64.1	81.7	78.1	60.2	12.0	24.1, 25.8, 110.5	9.6 (2-CH_3)
69	3.35	4.47	4.61	2.96	1.14	1.25, 1.40	0.91 (CH_3), 0.96 (CH_3), 2.00 ($C\underline{H}(CH_3)_2$)
70	68.5	79.4	77.7	61.5	12.2	24.2, 25.8	27.9 (CH_2), 117.5 (CH=$\underline{C}H_2$), 135.3 ($\underline{C}H$=CH_2)
72	73.0	81.0	79.0	61.9	11.9	24.6, 26.4, 111.8	127.2, 127.5, 127.8, 129.1, 130.6, 134.4, 141.2, 141.3 (8 d, 3 s for 12 C, some signals overlapping, C_6H_4 and C_6H_5)
73	72.0	81.3	78.4	61.4	11.4	24.2, 25.8, 111.5	114.8, 115.1 (2 d, *m*-C), 128.1 (s, *i*-C), 131.3 (d, *o*-C), 163.4 (s, *p*-C)
74	70.1	79.9	77.5	77.4	10.4	23.1, 24.8, 110.4	126.9, 127.0, (2 d, *m*-C), 127.1, 128.8 (2 d, *o*-C), 130.1 (s, *p*-C), 132.9 (s, *i*-C)
75	72.3	81.4	78.5	61.6	11.4	24.2, 25.9, 111.7	122.0 (s, *p*-C), 128.4 (s, *i*-C), 131.2 (d, *o*-C), 134.3 (d, *m*-C)
76	72.5	81.3	78.7	61.5	11.6	24.3, 26.0, 111.6	16.0 (SCH_3), 114.4 (d, *m*-C), 126.4 (s, *i*-C), 130.3 (d, *o*-C), 138.4 (s, *p*-C)
77	70.1	79.9	77.5	77.4	10.4	23.1, 24.8, 110.4	28.5 ($\underline{C}H_2C_6H_4$), 115.6 (d, *m*-C), 128.1 (s, *i*-C), 131.4 (d, *o*-C), 160.6 (s, *p*-C)
78	72.1	81.3	76.6	61.3	11.4	24.1, 25.8, 111.4	118.9, 119.1, 123.4, 129.7, 131.1, 156.8, 157.0 (8 d, 3 s of 12 C, some signals overlapping, C_6H_4, C_6H_5)
79	67.4	80.1	78.8	62.4	12.0	24.5, 26.0, 110.4	111.4 (2'), 111.6 (3'), 142.7 (4'), 150.4 (5')
80	72.4	78.7	81.7	61.5	11.5	24.3, 26.0, 112.0	40.5 [$N(\underline{C}H_3)_2$], 112.0 (d, *o*-C), 130.4 (2 d, 1 s, overlap of *i*-C, *m*-C) 150.2 (s, *p*-C)

IR Data

2-([1,1'-Biphenyl]-4-yl)-pyrrolidine **72**: (neat): $\tilde{\nu}$ = 3140 (bs, OH), 2978 (m), 2932 (m), 1599 (w), 1487 (s), 1449 (w), 1373 (s), 1267 (m), 1234 (s), 1207 (s), 1168 (m), 1059 (s), 1005 (s), 913 (m), 887 (m), 833 (w) cm^{-1}.

2-(4-Fluorophenyl)-pyrrolidine **73**: (neat): $\tilde{\nu}$ = 3309 (bs, OH), 2972 (m), 2502 (w), 2932 (w), 1606 (w), 1510 (m), 1449 (w), 1373 (m), 1281 (w), 1207 (m), 1183 (w), 1168 (w), 1144 (w), 1130 (w), 1009 (w), 1054 (m), 1007 (m), 889 (w), 867 (w), 852 (w), 832 (w), 792 (w), 778 (m), 602 (w) cm^{-1}.

2-(4-Chlorophenyl)-pyrrolidine **74**: (neat) $\tilde{\nu}$ = 3243 (bs, OH), 2982 (m), 2937 (m), 1695 (m), 1493 (s), 1375 (s), 1269 (m), 1208 (s), 1091 (w), 1059 (m), 1010 (s), 886 (w), 827 (m) cm^{-1}.

2-(4-Bromophenyl)-pyrrolidine **75**: (neat): $\tilde{\nu}$ = 3130 (bs, OH), 2983 (w), 2929 (m), 2873 (w), 1599 (w), 1591 (w), 1488 (m), 1450 (w), 1407 (w), 1374 (m), 1279 (w), 1232 (w), 1208 (s), 1165 (w), 1144 (w), 1131 (w), 1110 (w), 1059 (s), 1007 (s), 976 (w), 883 (m), 866 (w), 853 (w), 828 (w), 797 (w), 779 (w) cm^{-1}.

2-(4-Methylthiophenyl)-pyrrolidine **76**: (neat) $\tilde{\nu}$ = 3208 (bs, OH), 2972 (w), 2916 (m), 2984 (w), 2863 (w), 1599 (m), 1495 (m), 1430 (m), 1373 (m), 1281 (s), 1234 (w), 1208 (s), 1185 (w), 1166 (w), 1142 (w), 1059 (s), 1001 (s), 953 (m), 928 (m), 886 (w), 798 (w) cm^{-1}.

2-(4-Methoxybenzyl)-pyrrolidine **77**: (neat): $\tilde{\nu}$ = 3199 (bs, OH), 2986 (m), 2933 (m), 2835 (w), 1611 (m), 1583 (w), 1511 (s), 1453 (s), 1373 (m), 1245 (s), 1207 (m), 1176 (m), 1140 (m), 1054 (m), 1034 (m), 1003 (m), 870 (m), 810 (w) cm^{-1}.

2-(4-Phenoxyphenyl)-pyrrolidine **78**: (neat): $\tilde{\nu}$ = 3205 (bs, OH), 3038 (w), 2981 (w), 2932 (w), 1609 (m), 1506 (w), 1487 (w), 1372 (m), 1284 (s), 1204 (s), 1058 (s), 1005 (m), 869 (m), 750 (w) cm^{-1}.

2-(2-Furyl)-pyrrolidine **79**: (neat): ν = 3203 (bs, O-H), 2988 (w), 2934 (w), 2868 (w), 1497 (w), 1453 (m), 1384 (m), 1275 (w), 1211 (s), 1145 (m), 1056 (s), 1009 (m), 872 (m), 837 (m), 787 (w), 741 (m) cm^{-1}.

2-(4-*N,N*-Dimethylanilino)-pyrrolidine **80**: (neat): $\tilde{\nu}$ = 3200 (bs, OH), 2989 (w), 2974 (m), 2933 (w), 2865 (w), 1678 (w), 1614 (m), 1598 (m), 1562 (w), 1524 (w), 1483 (w), 1445 (w), 1358 (m), 1283 (w), 1257 (w), 1226 (m), 1161 (m), 1130 (w), 1060 (m), 1043 (m), 1005 (w), 945 (w), 928 (w), 804 (m), 779 (w), 765 (w), 716 (w), 693 (w), 669 (w), 645 (w) cm^{-1}.

Mass spectroscopy

2-(4-Chlorophenyl)-pyrrolidine **74**: (EI, 70 eV) *m/z* (%) = 283.2 $[M]^+$ (12), 266.2 (10), 207.1 (20), 166.2 (100), 139.1 (18), 131.1 (26), 125.0 (16), 102.1 (8), 71.1 (10), 59.1 (10), 43.0 (10), 28.0 (25).

2-(4-Bromophenyl)-pyrrolidine **75**: (EI, 70 eV) *m/z* (%) = 327.1 $[M]^+$ (14), 310.1 (12), 252.1 (12), 224.0 (10), 210.0 (100), 183.0 (16), 169.0 (16), 131.1 (36), 102.1 (19), 85.1 (8), 71.1 (14), 59.1 (17), 43.0 (19), 28.0 (8).

Reduction in the D-*ribo* series

Experiment 82 (LR 345)

(2*R*,3*S*,4*R*,5*S*)- 2-(4-*N*,*N*-Dimethylanilino)-1,3,4-trihydroxy-3,4-*O*-isopropylidene-5-methyl-pyrrolidine (81)

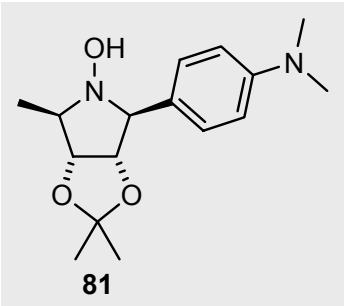

81

Scale: 0.300 g (0.81 mmol) *N*-hydroxypyrrolidine **51** / 15 mL THF
0.055 g (1.45 mmol, 1.8 Eq.) lithium aluminium hydride

The reaction was carried out in accordance to TLP 3. After 1 h, the reaction was stopped through the addition of 2 mL of a 5 % citric acid solution and water (5 mL) at 0 °C. The aqueous phase was extracted with methylene chloride (4 x 15 mL); the combined organic phases were then washed with ca. 25 mL saturated $NaHCO_3$ solution and dried ($MgSO_4$). Solvent was removed on the rotary evaporator (25 °C/10 mbar) and the crude product was purified using column chromatography (SiO_2, 25 g, 2 cm x 12 cm, eluant: PE:EE = 70:30). This resulted in the isolation of the title compound, β-D-*ribo* pyrrolidine **81** (0.213 g, 0.73 mmol, 90 %), as an analytically pure, colourless solid (m. p. 125 °C).

$[\alpha]_D^{20}$ = 5 (*c* = 1.05, $CHCl_3$)

$C_{16}H_{24}N_2O_3$	calc.	C	65.73	H	8.27	N	9.58
(292.4)	found	C	65.75	H	8.31	N	9.55

IR (neat): $\tilde{\nu}$ = 3423 (bs), 3222 (bs), 2979 (w), 2930 (w), 2802 (w), 1613 (s), 1566 (w), 1522 (s), 1479 (w), 1445 (m), 1370 (s), 1350 (s), 1268 (w), 1207 (m), 1162 (m), 1130 (w), 1079 (w), 1058 (s), 1004 (s), 984 (w), 946 (w), 929 (w), 884 (w), 864 (m), 813 (s), 779 (w), 756 (w), 643 (s) cm^{-1}.

^{1}H NMR ($CDCl_3$, 300.1 MHz): δ = 1.35 (d, $J_{5,1'}$ = 6.3 Hz, 3 H, 1'-H), 1.27, 1.56 [2 s, 3 H each, $C(CH_3)_2$], 2.94 [s, 6 H $N(CH_3)_2$], 3.05 (m, 1 H, 5-H), 3.81 (d, $J_{2,3}$ = 5.7 Hz, 1 H, 2-H), 4.16 (dd, $J_{3,4}$ = 7.3, $J_{4,5}$ = 6.0 Hz, 1 H, 4-H), 4.33 (dd, $J_{2,3}$ = 5.7, $J_{3,4}$ = 7.3 Hz, 1 H, 3-H), 4.51 (bs, 1 H, OH), 6.75 ("dd", $J_{A,B}$ = $J_{A',B'}$ = 8.8 Hz, 2 H, A,A' of AA'BB'), 7.10 ("dd", $J_{A,B}$ = $J_{A',B'}$ = 8.6 Hz, 2 H, B,B' of AA'BB').

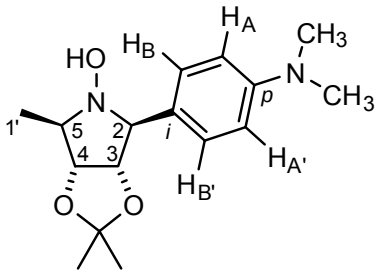

81

^{13}C NMR ($CDCl_3$, 125 MHz): δ = 16.9 (q, C-1'), 25.1, 27.2 [2 q, $C(\underline{C}H_3)_2$], 40.8 [$N(CH_3)_2$], 68.3 (q, OCH_3), 68.3 (d, C-5), 77.0 (d, C-2), 81.4 (d, C-4), 82.5 (d, C-3), 112.9 [q, $\underline{C}(CH_3)_2$], 113.4 (d, *o*-C), 127.5 (d, *m*-C), 128.5 (s, *i*-C), 150.4 (s, *p*-C).

Signal correlations were established with the help of H,H- and C,H-COSY.

8.5.2 Attempts at the concomitant reduction of C—Br and N—O bonds

Attempted catalytic reduction of 2-bromomethyl-5-phenyl-N-hydroxypyrrolidine **82**

Experiment 83 (LR 190)

(2*R*,3*S*,4*R*)-3,4-Dihydroxy-3,4-*O*-isopropylidene-5-methyl-2-phenyl-2*H*-pyrrole-1-oxide (82)

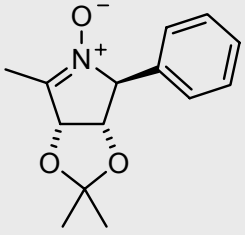

82

The pyrrolidine **82** (0.103 g, 0.314 mmol) was placed in 8 mL abs. MeOH and 66 mg (0.062 mmol, 0.2 Eq.) Pd-C (10 % Riedel-de Häën) and triethylamine (0.063 g, 0.62 mmol, 2.0 Eq.) were added. The mixture was hydrogenated at atmospheric pressure for 4 d, after which time TLC control indicated that the starting material had disappeared. The suspension was filtered over a small amount of celite and the solvents were removed on the rotary evaporator (30 °C/10 mbar). However, according to the ^{1}H and ^{13}C NMR spectra of the crude material, the obtained product looked like the formation of the cyclic nitrone **82**, and not of the expected pyrrolidine-hydrobromide salt . The crude product was purified by column chromatography (SiO_2, 30 g, 1.5 cm x 20 cm, PE:EE = 30:70, then EE 100 %) to yield the cyclic nitrone **82** as a spectroscopically pure, pale-yellow solid (40 mg, 0.162 mmol, 52 %; m. p. 126-130 °C). Following slow evaporation of the reaction solvent, crystals of suitable quality were obtained for X-ray crystal structure analysis (cf. Section 9.11 for complete data).

$[\alpha]_D^{20}$ = –14 (*c* = 0.24, $CHCl_3$)

$C_{14}H_{17}NO_3$	calc.	C	68.00	H	6.93	N	5.66
(247.1)	found	C	68.06	H	6.94	N	5.36

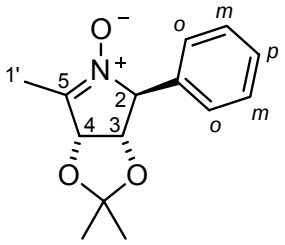

82

MS (EI, 70 eV, 350 K) *m/z* (%) = 248.1 $[M+H]^+$ (22), 247.1 $[M]^+$ (100), 173.1 (13), 172.1 (25), 161.1 (95), 105.1 (15), 104.0 (24), 103.0 (94), 90.0 (60), 87.0 (26), 59.1 (8), 43.0 (40).

IR (neat): $\tilde{\nu}$ = 2927 (m, CH_2), 1610 (s), 1501 (w), 1453 (2), 1379 (m, CH_3), 1368 (w), 1339 (w), 1257 (m), 1206 (w), 1156 (m), 1053 (s), 884 (m), 872 (m), 834 (w), 727 (m), 695 (s), 665 (m) cm^{-1}.

^{1}H NMR ($CDCl_3$, 500.1 MHz,): δ = 1.31, 1.37 [2 s, 3 H each, $C(CH_3)_2$], 1.46 (“s”, 3 H, 1’-CH_3), 4.67 (d, $J_{3,4}$ = 5.8 Hz, 1 H, 3-H), 5.03 (s, 1 H, 2-H), 5.49 (d, $J_{3,4}$ = 5.8 Hz, 1 H, 4-H), 7.2-7.5 (m, 5 H, C_6H_5).

^{13}C NMR ($CDCl_3$, 125 MHz): δ = 10.1 (q, C-1’), 26.2, 27.5 [2 q, $C(\underline{C}H_3)_2$], 80.4 (d, C-2), 82.7 (d, C-3), 84.1 (d, C-4), 113.4 [s, $\underline{C}(CH_3)_2$], 125.5, 128.3, (2 d, *o*-C), 128.4, 129.6 (2 d, *m*-C) 130.1 (s, *p*-C), 130.9 (s, *i*-C), 135.5 (s, C-5).

Attempted concomitant N—O and C—Br bond cleavage using nickel(II) chloride/sodium borohydride ("P2 nickel")[343-346]

Experiment 84 (LR 187)

(2*S*,3*S*,4*R*,5*S*)-3,4-Dihydroxy-3,4-*O*-isopropylidene-2-(4-methoxyphenyl)-5-methylpyrrolidine (86)

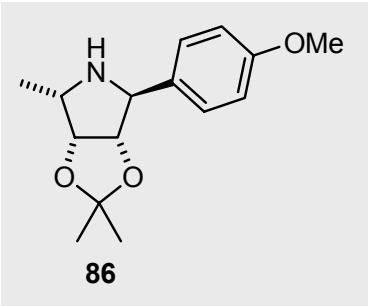

86

Following lit.[343] To a flask containing the bromomethyl-*N*-hydroxypyrrolidine **41** (0.140 g, 0.391 mmol) and 0.210 g (1.61 mmol, 4 Eq.) anhydrous (yellow) nickel chloride in 5 mL ethanol was added 0.180 g (4.85 mmol, 12 Eq.) of sodium borohydride. Upon addition, a spontaneous colour change was observed (yellow to black) indicating the formation of nickel boride. The reaction was stirred at room temp for 1 h, and the reaction solids were filtered over celite (2 cm x 5 cm) and washed with 20 mL methylene chloride. The filtrate was then concentrated on the rotary evaporator (20 °C/10 mbar) and taken up in water (5 mL), extracted with methylene chloride (3 x 15 mL) and dried over $MgSO_4$. The solvent was removed under vacuum (25 °C/10 mbar) to yield, according to TLC analysis, the title compound and at least two other unidentifiable side-products. The mixture was purified and separated by column chromatography (SiO_2, 40 g, 1.5 cm x 20 cm, PE/EE = 50:50) which afforded 47 mg (0.178 mmol, 45 %) of the cyclic amine **86** as a light-red, analytically pure oil that slowly solidified on standing (m. p. 106 °C).

$C_{15}H_{21}NO_3$	calc.	C	68.42	H	8.04	N	5.32
(263.3)	found	C	68.24	H	8.07	N	5.31

^1H and ^{13}C NMR spectroscopic data were in agreement to those found in Experiment 88.

Reduction by catalytic hydrogenation

Experiment 112 (LR 286)

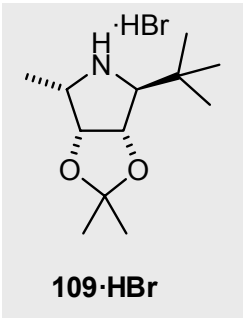

109·HBr

(2*S*,3*S*,4*R*,5*S*)-2-*tert*-Butyl-3,4-dihydroxy-3,4-*O*-isopropylidene-5-methyl-pyrrolidine hydrobromide (109·HBr)

To a 250 mL-hydrogenation flask under argon was added 0.082 g (0.12 mmol, 0.2 Eq.) palladium on carbon (10 % Riedel-de Häën), 7 mL abs. MeOH and 120 mg (0.39 mmol) of the 2-bromomethyl-substituted pyrrolidine **37**. The suspension was hydrogenated at 3 bar for 5 d. The catalyst was removed by filtration over celite (10 g). The filtrate was then concentrated on the rotary evaporator (40 °C/10 mbar) which afforded the title compound, the pyrrolidine hydrobromide **109·HBr**, as a spectroscopically pure, colourless solid (0.110 g, 0.37 mmol, 96 %). This was then recrystallised using the diffusion method with ($MeOH/Et_2O$ see Experiment 98 for details). Within 2 d, needle-like crystals formed. Isolation of the crystals yielded the pyrrolidine **109·HBr** (0.102 g, 0.346 mmol, 89 %) as a colourless solid (m. p. 200 °C, decomp.), with slightly deviating elemental analysis.

$[\alpha]_D^{20}$ = –33 (*c* = 0.32, CH_3OH)

$C_{12}H_{24}BrNO_2$	calc.	C	48.99	H	8.22	N	4.76	Br	27.16
(294.3)	found	C	48.47	H	8.09	N	4.61	Br	27.85

(EI, 70 eV) *m*/*z* (%) = 213.2 $[M]^+$ (6), 198.2 (6), 172.1 (2), 156.1 $[-C(CH_3)_3]^+$ (100), 140.1 (3), 126.1 (3), 113.1 (3), 82.0 (12), 57.0 (6).

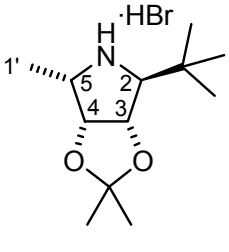

109·HBr

IR (neat) $\tilde{\nu}$ = 2963 (bs), 2868 (bs), 2771 (w), 2711 (w), 2514 (w), 2462 (w), 1580 (m), 1475 (w), 1383 (s), 1269 (w), 1214 (m), 1154 (m), 1127 (m), 1076 (s), 1036 (m), 1001 (m), 903 (w), 866 (s), 604 (w) cm^{-1}.

^1H NMR ($CDCl_3$, 300.1 MHz,): δ = 1.15 [s, 9 H, $C(C\underline{H}_3)_3$] 1.35 [s, 3 H, CH_3 of $C(CH_3)_2$], 1.66 [2 s, 6 H, overlapping signals, CH_3 of $C(CH_3)_2$, 1'-CH_3], 3.49 (d, $J_{2,3}$ = 2.8 Hz, 1 H, 2-H), 3.75 (m, 1 H, 5-H), 4.60 (m, 1 H, 4-H), 4.65 (dd, $J_{2,3}$ = 2.8, $J_{3,4}$ = 6.5 Hz, 1 H, 3-H).

^{13}C NMR ($CDCl_3$, 77.5 MHz): δ = 13.2 (q, C-1'), 25.2, 27.1 [2 q, C($\underline{C}H_3$)$_2$], 26.6 [q, C($\underline{C}H_3$)$_3$], 32.4 [s, $\underline{C}$(CH$_3$)$_3$], 59.0 (d, C-5), 74.7 (d, C-2), 80.2 (d, C-4), 81.0 (C-3), 113.4 [s, $\underline{C}$(CH$_3$)$_2$].

Experiment 114 (LR 181)

(2*S*,3*S*,4*R*,5*S*)-3,4-Dihydroxy-3,4-*O*-isopropylidene-2-(4-methoxybenzyl)-5-methyl-pyrrolidine hydrobromide (111·HBr)

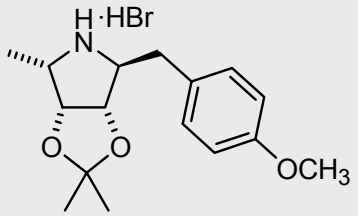

111·HBr

Under argon to a 250 mL-hydrogenation flask was added 0.128 g (0.12 mmol, 0.2 Eq., 10 % Riedel-de Häën) palladium on carbon, 7 mL methanol and the bromomethyl-*N*-hydroxypyrrolidine **46** (224 mg, 0.602 mmol). The suspension was hydrogenated at 3 bar for 4 d. The catalyst was removed by centrifugation. The filtrate was concentrated on the rotary evaporator (40 °C/20 mbar) which afforded the pyrrolidine hydrobromide **111·HBr** as a spectroscopically pure, colourless oil (203 mg, 0.54 mmol, 91 %). The hydrobromide salt was lyophilised (diethyl ether) and recrystallised from MeOH/Et_2O (diffusion method, cf. Experiment 98). After 2 d, the crystals were filtered off and dried (P_4O_{10}, 0.01 mbar) to yield the cyclic amine **111·HBr** as a colourless solid (187 mg, 0.51 mmol, 87 %, m. p. 212 °C) with slightly deviating elemental analysis.

$[\alpha]_D^{20}$ = –3.6 (*c* = 0.36, CH_3OH)

$C_{16}H_{24}BrNO_3$	calc.	C	53.64	H	6.75	N	3.91	Br	22.30
(358.3)	found	C	51.72	H	6.63	N	3.68	Br	22.03

MS (FAB positive ion, matrix: 3-nitrobenzyl alcohol) *m/z* (%) = 279.2 (18), 278.2 $[M+H]^+$ (100), 220.1 (5), 176.1 (3), 156.1 (9), 135.1 (8), 121.1 (16), 95.1 (12), 83.1 (12), 69.1 (18).

HRMS (FAB positive ion, matrix: 3-nitrobenzyl alcohol + PEG 200); calc. for $C_{16}H_{24}NO_3$+ H: 278.1756; found 278.1775.

IR (neat) $\tilde{\nu}$ = 2934 (bs), 2783 (m), 2644 (w), 2487 (w), 1706 (w), 1570 (m), 1569 (m), 1513 (s), 1454 (w), 1376 (m), 1302 (w), 1247 (m), 1210 (w), 1179 (w), 1165 (w), 1126 (w), 1110 (w), 1060 (m), 1032 (w), 1006 (w), 867 (m), 822 (m), 760 (w), 658 (m) cm^{-1}.

^{1}H NMR ($CDCl_3$, 500.1 MHz,): δ = 1.27, 1.50 [2 s, 3 H each, $C(CH_3)_2$], 1.45 (d, $J_{5,1''}$ = 6.7 Hz, 2 H, 1''-CH_3), 2.99 (dd, $J_{2,1'A}$ = 11.1, $^2J_{1'A,1'B}$ = 14.0 Hz, 1 H, 1'-H_A), 3.05 (dd, $J_{2,1'B}$ = 5.7, $^2J_{1'A,1'B}$ = 14.0 Hz, 1 H, 1'-H_B), 3.35 (s, 1 H, NH), 3.79 (s, 3 H, OCH_3), 3.90 (dd, $J_{2,1'A}$ = 11.1, $J_{2,1'B}$ = 5.7 Hz, 1 H, 2-H), 3.98 (dd, $J_{4,5}$ = 4.4, $J_{5,1''}$ = 6.7 Hz, 1 H, 5-H), 4.63 (dd, $J_{2,3}$ = 0.5, $J_{3,4}$ = 5.8 Hz, 1 H, 3-H), 4.82 (dd, $J_{2,3}$ = 5.8, $J_{4,5}$ = 4.4 Hz, 1 H, 4-H), 6.93 ("dd", $J_{A,B}$ = $J_{A',B'}$ = 8.8 Hz, 2 H, A,A' of AA'BB'), 7.27 ("dd", $J_{A,B}$ = $J_{A',B'}$ = 8.8 Hz, 2 H, B,B' of AA'BB').

^{13}C NMR ($CDCl_3$, 125.7 MHz): δ = 11.5 (q, C-1''), 23.8, 25.8 [2 q, $C(\underline{C}H_3)_2$], 34.2 (t, C-1'), 55.8 (q, OCH_3), 58.2 (d, C-5), 66.4 (d, C-2), 80.3 (d, C-4), 82.9 (C-3), 113.1 [s, $\underline{C}(CH_3)_2$], 115.6 (d, *m*-C), 128.1 (s, *i*-C), 131.4 (d, *o*-C), 160.6 (s, *p*-C).

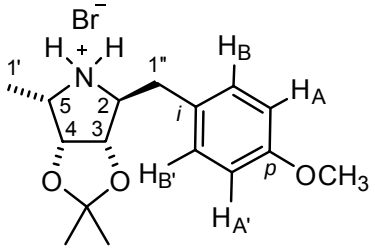

111·HBr

8.5.3 Reduction by catalytic hydrogenation

Experiment 112 (LR 286)

(2*S*,3*S*,4*R*,5*S*)-2-*tert*-Butyl-3,4-dihydroxy-3,4-*O*-isopropylidene-5-methyl-pyrrolidine hydrobromide (109·HBr)

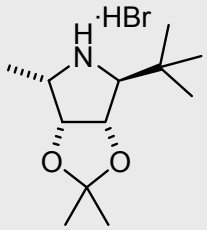

109·HBr

To a 250 mL-hydrogenation flask under argon was added 0.082 g (0.12 mmol, 0.2 Eq.) palladium on carbon (10 % Riedel-de Häën), 7 mL abs. MeOH and 120 mg (0.39 mmol) of the 2-bromomethyl-substituted pyrrolidine **37**. The suspension was hydrogenated at 3 bar for 5 d. The catalyst was removed by filtration over celite (10 g). The filtrate was then concentrated on the rotary evaporator (40 °C/10 mbar) which afforded the title compound, the pyrrolidine hydrobromide **109·HBr**, as a spectroscopically pure, colourless solid (0.110 g, 0.37 mmol, 96 %). This was then recrystallised using the diffusion method with ($MeOH/Et_2O$ see Experiment 98 for details). Within 2 d, needle-like crystals formed. Isolation of the crystals yielded the pyrrolidine **109·HBr** (0.102 g, 0.346 mmol, 89 %) as a colourless solid (m. p. 200 °C, decomp.), with slightly deviating elemental analysis.

$[\alpha]_D^{20}$ = –33 (*c* = 0.32, CH_3OH)

$C_{12}H_{24}BrNO_2$	calc.	C	48.99	H	8.22	N	4.76	Br	27.16
(294.3)	found	C	48.47	H	8.09	N	4.61	Br	27.85

(EI, 70 eV) *m*/*z* (%) = 213.2 $[M]^+$ (6), 198.2 (6), 172.1 (2), 156.1 $[-C(CH_3)_3]^+$ (100), 140.1 (3), 126.1 (3), 113.1 (3), 82.0 (12), 57.0 (6).

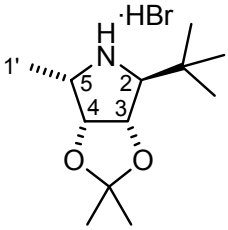

109·HBr

IR (neat) $\tilde{\nu}$ = 2963 (bs), 2868 (bs), 2771 (w), 2711 (w), 2514 (w), 2462 (w), 1580 (m), 1475 (w), 1383 (s), 1269 (w), 1214 (m), 1154 (m), 1127 (m), 1076 (s), 1036 (m), 1001 (m), 903 (w), 866 (s), 604 (w) cm^{-1}.

^1H NMR ($CDCl_3$, 300.1 MHz,): δ = 1.15 [s, 9 H, $C(C\underline{H}_3)_3$] 1.35 [s, 3 H, CH_3 of $C(CH_3)_2$], 1.66 [2 s, 6 H, overlapping signals, CH_3 of $C(CH_3)_2$, 1'-CH_3], 3.49 (d, $J_{2,3}$ = 2.8 Hz, 1 H, 2-H), 3.75 (m, 1 H, 5-H), 4.60 (m, 1 H, 4-H), 4.65 (dd, $J_{2,3}$ = 2.8, $J_{3,4}$ = 6.5 Hz, 1 H, 3-H).

^{13}C NMR ($CDCl_3$, 77.5 MHz): δ = 13.2 (q, C-1'), 25.2, 27.1 [2 q, $C(\underline{C}H_3)_2$], 26.6 [q, $C(\underline{C}H_3)_3$], 32.4 [s, $\underline{C}(CH_3)_3$], 59.0 (d, C-5), 74.7 (d, C-2), 80.2 (d, C-4), 81.0 (C-3), 113.4 [s, $\underline{C}(CH_3)_2$].

Experiment 114 (LR 181)

(2*S*,3*S*,4*R*,5*S*)-3,4-Dihydroxy-3,4-*O*-isopropylidene-2-(4-methoxybenzyl)-5-methyl-pyrrolidine hydrobromide (111·HBr)

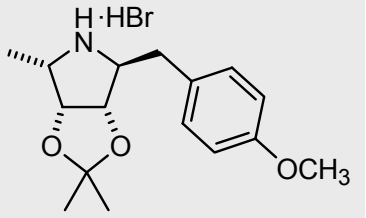

111·HBr

Under argon to a 250 mL-hydrogenation flask was added 0.128 g (0.12 mmol, 0.2 Eq., 10 % Riedel-de Häën) palladium on carbon, 7 mL methanol and the bromomethyl-*N*-hydroxypyrrolidine **46** (224 mg, 0.602 mmol). The suspension was hydrogenated at 3 bar for 4 d. The catalyst was removed by centrifugation. The filtrate was concentrated on the rotary evaporator (40 °C/20 mbar) which afforded the pyrrolidine hydrobromide **111·HBr** as a spectroscopically pure, colourless oil (203 mg, 0.54 mmol, 91 %). The hydrobromide salt was lyophilised (diethyl ether) and recrystallised from MeOH/Et_2O (diffusion method, cf. Experiment 98). After 2 d, the crystals were filtered off and dried (P_4O_{10}, 0.01 mbar) to yield

the cyclic amine **111·HBr** as a colourless solid (187 mg, 0.51 mmol, 87 %, m. p. 212 °C) with slightly deviating elemental analysis.

$[\alpha]_D^{20}$ = –3.6 (*c* = 0.36, CH_3OH)

$C_{16}H_{24}BrNO_3$	calc.	C	53.64	H	6.75	N	3.91	Br	22.30
(358.3)	found	C	51.72	H	6.63	N	3.68	Br	22.03

MS (FAB positive ion, matrix: 3-nitrobenzyl alcohol) *m/z* (%) = 279.2 (18), 278.2 $[M+H]^+$ (100), 220.1 (5), 176.1 (3), 156.1 (9), 135.1 (8), 121.1 (16), 95.1 (12), 83.1 (12), 69.1 (18).

HRMS (FAB positive ion, matrix: 3-nitrobenzyl alcohol + PEG 200); calc. for $C_{16}H_{24}NO_3$+ H: 278.1756; found 278.1775.

IR (neat) $\tilde{\nu}$ = 2934 (bs), 2783 (m), 2644 (w), 2487 (w), 1706 (w), 1570 (m), 1569 (m), 1513 (s), 1454 (w), 1376 (m), 1302 (w), 1247 (m), 1210 (w), 1179 (w), 1165 (w), 1126 (w), 1110 (w), 1060 (m), 1032 (w), 1006 (w), 867 (m), 822 (m), 760 (w), 658 (m) cm^{-1}.

^{1}H NMR ($CDCl_3$, 500.1 MHz,): δ = 1.27, 1.50 [2 s, 3 H each, $C(CH_3)_2$], 1.45 (d, $J_{5,1''}$ = 6.7 Hz, 2 H, 1''-CH_3), 2.99 (dd, $J_{2,1'A}$ = 11.1, $^2J_{1'A,1'B}$ = 14.0 Hz, 1 H, 1'-H_A), 3.05 (dd, $J_{2,1'B}$ = 5.7, $^2J_{1'A,1'B}$ = 14.0 Hz, 1 H, 1'-H_B), 3.35 (s, 1 H, NH), 3.79 (s, 3 H, OCH_3), 3.90 (dd, $J_{2,1'A}$ = 11.1, $J_{2,1'B}$ = 5.7 Hz, 1 H, 2-H), 3.98 (dd, $J_{4,5}$ = 4.4, $J_{5,1''}$ = 6.7 Hz, 1 H, 5-H), 4.63 (dd, $J_{2,3}$ = 0.5, $J_{3,4}$ = 5.8 Hz, 1 H, 3-H), 4.82 (dd, $J_{2,3}$ = 5.8, $J_{4,5}$ = 4.4 Hz, 1 H, 4-H), 6.93 ("dd", $J_{A,B}$ = $J_{A',B'}$ = 8.8 Hz, 2 H, A,A' of AA'BB'), 7.27 ("dd", $J_{A,B}$ = $J_{A',B'}$ = 8.8 Hz, 2 H, B,B' of AA'BB').

^{13}C NMR ($CDCl_3$, 125.7 MHz): δ = 11.5 (q, C-1''), 23.8, 25.8 [2 q, $C(\underline{C}H_3)_2$], 34.2 (t, C-1'), 55.8 (q, OCH_3), 58.2 (d, C-5), 66.4 (d, C-2), 80.3 (d, C-4), 82.9 (C-3), 113.1 [s, $\underline{C}(CH_3)_2$], 115.6 (d, *m*-C), 128.1 (s, *i*-C), 131.4 (d, *o*-C), 160.6 (s, *p*-C).

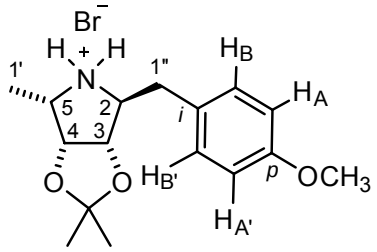

111·HBr

8.5.4 N—O bond cleavage of the *N*-hydroxypyrrolidines using zinc

Experiment 88 (FJS 23)

(2*S*,3*S*,4*R*,5*S*)-3,4-Dihydroxy-3,4-*O*-isopropylidene-2-(4-methoxyphenyl)-5-methyl-pyrrolidine (86)

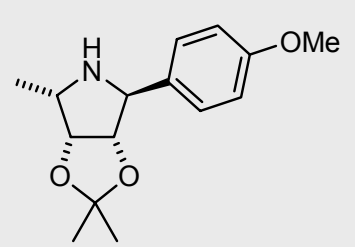

86

TLP 4: Typical Laboratory Procedure for the N—O bond reduction of *N*-Hydroxypyrrolidines using zinc

To the *N*-hydroxypyrrolidine **71** (0.288 g, 1.03 mmol) was added a 2:1 mixture of glacial acetic acid/water (6.0 mL/3.0 mL) and a 20-fold excess of zinc dust (1.37 g, 21 mmol). The suspension was heated to 65 °C. The TLC analysis indicated the appearance of a new, slow-moving spot at the bottom and, typically within 2 h, the complete disappearance of starting material. The reaction mixture was allowed to cool and taken up in methanol. The remaining unreacted zinc powder was removed by filtration over celite (10 g, glass filter, 1.5 cm x 5 cm) and washed with adequate amounts of methanol (ca. 20 mL). The filtrate was concentrated on the rotary evaporator (25 °C, 10 mbar). Care should be taken to firstly ventilate the rotary evaporator with argon (balloon) before removing the flask. The red oil that resulted was taken up in 5-10 mL water and made basic (pH 9-10) through the addition of a 3 N NaOH solution and strong stirring. To the colourless suspension obtained was added 5 mL saturated NH_4Cl solution followed by thorough extraction with ethyl acetate (4 x 20 mL). The combined organic phases were washed with saturated NaCl solution (5 mL), dried ($MgSO_4$) and the solvent was removed under vacuum (25 °C, 10 mbar, argon!). The crude product was purified by column chromatography (SiO_2, 40 g, 2 cm x 18 cm, PE:EE = 20:80) to afford the cyclic amine **86** (0.230 g, 0.87 mmol, 85 %) as an analytically pure, red oil that slowly solidified at +4 °C (m. p. 106 °C) on standing.

$[\alpha]_D^{20}$ = 1.0 (*c* = 0.810, CH_3OH)

$C_{15}H_{21}NO_3$	calc.	C	68.02	H	8.04	N	5.32
(263.3)	found	C	68.24	H	8.07	N	5.31

MS (EI, 70 eV) *m/z* (%) = 263.2 $[M]^+$, 248.1 (4), 205.1 (8), 190.1 (4), 188.1 (9), 164.1 (10), 163.1 (100), 148.1 (7), 135.0 (22), 105.0 (3), 91.1 (4), 43.0 (6), 28.0 (6), 18.1 (10).

IR (neat): $\tilde{\nu}$ = 3203 (bs, NH) 2976 (m), 2933 (m), 2834 (w), 1583 (w), 1513 (s), 1456 (m), 1372 (m), 1347 (w), 1292 (w), 1208 (m), 1190 (m), 1160 (w), 1180 (w), 1170 (w), 1145 (w), 1091 (w), 1045 (m), 1011 (w), 990 (w), 841 (w). 805 (w), 760 (w) cm^{-1}.

^1H NMR ($CDCl_3$, 500.1 MHz): δ = 1.16 (d, $J_{5,1'}$ = 6.6 Hz, 3 H, 1'-H), 1.38, 1.56 [2 s, 3 H each, $C(CH_3)_2$], 2.40 (bs, 1 H, NH), 3.11 (m, 1 H, 5-H), 3.81 (s, OCH_3), 4.20 (s, 1 H, 2-H), 4.52 (dd, $J_{3,4}$ = 6.0, $J_{4,5}$ = 5.0 Hz, 1 H, 4-H), 4.90 (d, $J_{3,4}$ = 5.5 Hz, 1 H, 3-H), 6.8 ("dd", $J_{A,B}$ = $J_{A',B'}$ = 8.8 Hz, 2 H, A,A' of AA'BB'), 7.2 ("dd", $J_{A,B}$ = $J_{A',B'}$ = 8.8 Hz, 2 H, B,B' of AA'BB').

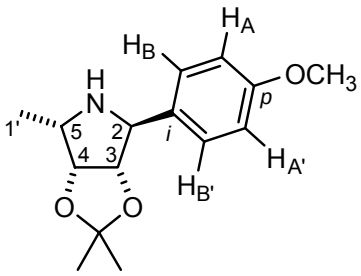

86

^{13}C NMR ($CDCl_3$, 125.1 MHz): δ = 13.4 (q, C-1'), 24.0, 26.0 [2 q, $C(CH_3)_2$], 54.2 (q, OCH_3), 55.6 (d, C-5), 65.1 (d, C-2), 82.5 (d, C-4), 87.8 (d, C-3), 109.8 [q, $C(CH_3)_2$], 112.8 (d, *m*-C), 126.8 (s, *i*-C), 131.1 (d, *o*-C), 157.4 (s, *p*-C).

Experiments 89-95

(2*S*,3*S*,4*R*,5*S*)-2-([1,1'-Biphenyl]-4-yl)-3,4-dihydroxy-3,4-*O*-isopropylidene-5-methyl-pyrrolidine (87)

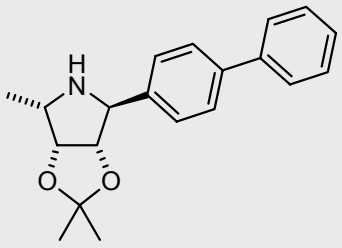

87

(2*S*,3*S*,4*R*,5*S*)-2-(4-Fluorophenyl)-3,4-dihydroxy-3,4-*O*-isopropylidene-5-methyl-pyrrolidine (88)

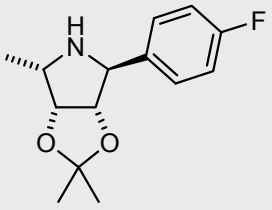

88

(2*S*,3*S*,4*R*,5*S*)-2-(4-Chlorophenyl)-3,4-dihydroxy-3,4-*O*-isopropylidene-5-methyl-pyrrolidine (89)

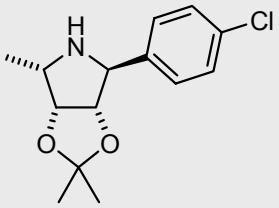

89

(2*S*,3*S*,4*R*,5*S*)-2-(4-Bromophenyl)-3,4-dihydroxy-3,4-*O*-isopropylidene-5-methyl-pyrrolidine (90)

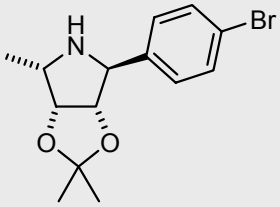

90

(2*S*,3*S*,4*R*,5*S*)-3,4-Dihydroxy-3,4-*O*-isopropylidene-5-methyl-2-(4-methylthiophenyl)-pyrrolidine (91)

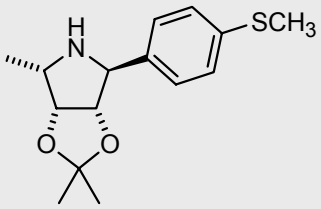

91

(2*S*,3*S*,4*R*,5*S*)-3,4-Dihydroxy-3,4-*O*-isopropylidene-5-methyl-2-(4-phenoxyphenyl)-pyrrolidine (92)

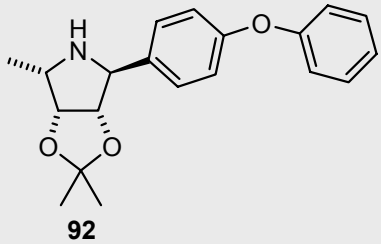

92

(2*S*,3*S*,4*R*,5*S*)-2-(2-Furyl)-3,4-dihydroxy-3,4-*O*-isopropylidene-5-methyl-pyrrolidine (93)

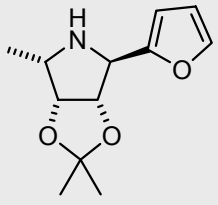

93

Table 23: Reduction of the N-hydroxypyrrolidines **72**-**78** using zinc according to TLP 4

Product (R)[a] / Experiment (E) Nr.	Nr.	Educt mg / mmol	Zn; AcOH/H_2O[b] g / mmol / mL	Product mg / %	$[\alpha]_D^{20}$ (c, CH_2Cl_2)	Elemental analysis							
86 ([1,1'-Biphenyl]-4-yl)	**72**	210 / 0.65	0.842 / 1.29 / 9	170 / 85[c]	–13 (1.00)	$C_{20}H_{23}NO_2$	calc.	C	77.60	H	7.49	N	4.52
E 89 (LR 98)						(309.4)	found	C	77.55	H	7.53	N	4.54
87 (4-Fluorophenyl)	**73**	444 / 1.66	2.158 / 33.00 / 10	340 / 81	24 (1.00)	$C_{14}H_{18}FNO_2$	calc.	C	66.91	H	7.22	N	5.67
E 90 (LR 332)						(251.3)	found	C	67.10	H	7.37	N	5.52
88 (4-Chlorophenyl)	**74**	580 / 2.04	2.616 / 40.00 / 27	400 / 73	9 (1.01)[d]	$C_{14}H_{18}ClNO_2$	calc.	C	62.80	H	6.78	N	5.23
E 91 (LR 111)						(267.8)[e]	found	C	62.65	H	6.79	N	5.11
89 (4-Bromophenyl)	**75**	40 / 0.12	0.159 / 0.24 / 4	34 / 91[f]	–2 (0.01)	$C_{14}H_{18}BrNO_2$	calc.	C	53.86	H	5.81	N	4.49
E 92 (LR 258)						(312.2)[g]	found	C	54.22	H	5.89	N	4.45
90 (4-Methylthiophenyl)	**76**	110 / 0.37	0.392 / 6.00 / 22	90 / 87	59 (1.01)	$C_{15}H_{21}NO_2S$	calc.	C	64.48	H	7.58	N	5.01
E 93 (NM 28)						(279.4)[h]	found	C	64.41	H	7.63	N	4.82
91 (4-Phenoxyphenyl)	**77**	44 / 0.1288	0.168 / 2.57 / 2.1	40 / 96[f]	3 (0.61)[d]	$C_{20}H_{23}NO_3$	calc.	C	73.82	H	7.12	N	4.30
E 94 (LR 242)						(325.4)	found	C	73.79	H	7.12	N	4.27
92 (2-Furyl)	**78**	160 / 0.669	0.876 / 13.4 / 21	105 / 70	7 (0.99)[d]	$C_{12}H_{17}NO_3$	calc.	C	64.55	H	7.67	N	6.27
E 95 (NM 15, 29)						(223.3)	found	C	64.43	H	7.72	N	6.04

[a] 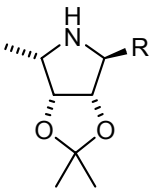

[b] Volume (mL) refers to a glacial acetic acid/water ratio of 2:1. [c] The crude product isolated was of analytical purity. [d] Measured in CHCl3. [e] calc. Cl 13.24; found Cl 13.50. [f] Yield is based on isolated crude product; used directly for the next step. [g] Owing to limited product amount, no further purification (e.g. MPLC, crystallisation) was undertaken; bromine content not determined, used directly for the next step. [h] calc. S 11.48; found S 11.22.

Table 24: ^{1}H NMR Chemical shifts of pyrrolidines **87**–**93** (δ [ppm], 300.1 MHz or 500.1 MHz, $CDCl_3$)

Nr.	2-H	3-H	4-H	5-H	1'-CH_3	$C(CH_3)_2$	NH	*p*-C_6H_4 or other 2-R
87	4.38	4.92	4.50	3.15	1.25	1.35, 1.52	2.40	7.30-7.60 [9 H, C_6H_4 and C_6H_5][a]
88	4.28	4.85	4.49	3.05	1.24	1.35, 1.53	2.33	7.00 [2 H, H_A, $H_{A'}$], 7.45 [2 H, H_B, $H_{B'}$]
89	4.20	4.75	4.40	2.95	1.15	1.26, 1.45	2.25	7.15 [2 H, H_A, $H_{A'}$], 7.26 [2 H, H_B, $H_{B'}$]
90	4.25	4.82	4.47	3.10	1.25	1.34, 1.53	2.37	7.30 [2 H, H_A, $H_{A'}$], 7.44 [2 H, H_B, $H_{B'}$]
91[b]	4.28	4.85	4.47	3.06	1.25	1.34, 1.52	2.54	2.45 (-SCH_3), 7.22 [2 H, H_A, $H_{A'}$], 7.33 [2 H, H_B, $H_{B'}$]
92	4.30	4.90	4.51	3.11	1.25	1.35, 1.53	2.50	7.15-7.50 [9 H, C_6H_4 and C_6H_5][a]
93	4.29	4.94	4.62	3.18	1.23	1.35, 1.52	2.35	6.17 (4'-H), 6.30 (3'-H), 7.35 (2'-H)

[a] Multiplet. [b] Measured on 250.1 MHz spectrometer

Table 25: Coupling constants of pyrrolidines **87**–**93** (*J* [Hz], $CDCl_3$)

Nr.	$J_{2,3}$	$J_{3,4}$	$J_{4,5}$	$J_{5,1'\text{-Me}}$	Other (2-R; AA',BB')
87	—	5.4	5.2	6.3	—[a]
88	0.6	5.3	4.3	6.6	—[a]
89	—	4.8	4.4	6.7	$J(H_A,H_B) = J(H_{A'},H_{B'}) = 7.1$
90	0.5	5.4	4.0	6.6	$J(H_A,H_B) = J(H_{A'},H_{B'}) = 8.7$
91	—	5.4	5.0	6.6	$J(H_A,H_B) = J(H_{A'},H_{B'}) = 8.5$
92	—	5.0	4.5	6.5	—[a]
93	—	5.5	4.5	6.5	*J*(3'-H,5'-H) = 1.5, *J*(4'-H,5'-H) = 1.9, *J*(3'-H,4'-H) = 3.2

[a] Multiplet

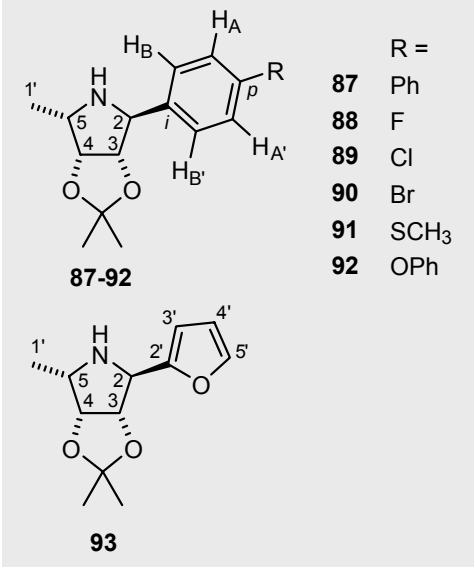

Table 26 : ^{13}C NMR Chemical shifts of pyrrolidines **87**–**93** (δ [ppm], $CDCl_3$, 62.9, 75.4 or 125.8 MHz)

Nr.	C-2	C-3	C-4	C-5	5-CH_3	$C(CH_3)_2$	*p*-C_6H_4 or Ar-C	Others
87	66.8	89.2	83.7	57.0	13.6	24.2, 26.3, 110.0	127.2, 127.3, 127.4, 139.3, 139.8, 141.0 [8 d, 3 s of 12 C, some signals overlapping, C_6H_4 and C_6H_5]	
88	66.3	89.0	83.6	56.5	13.5	24.1, 26.1, 110.1	115.0, 115.3 (2 d, *m*-C), 128.2 (s, *i*-C), 135.7 (d, *o*-C), 160.1, 163.3 (2 s, *p*-C)	
89	65.2	88.0	82.5	55.7	12.3	23.0, 25.0, 109.9	127.0 (s, *i*-C),[a] 127.4 (d, *m*-C),[a] 131.3 (d, *o*-C), 137.5 (s, *p*-C)	
90	66.8	89.1	83.7	56.9	13.5	24.1, 26.1, 111.0	126.6, 126.7 (2 s, *i*-C), 128.4, 128.5 (2 d, *o*-C), 131.5 (d, *m*-C), 139.2 (s, *p*-C)	
91	66.4	88.9	83.6	56.8	13.5	24.1, 26.1, 110.8	126.9 (s, *i*-C), 127.6 (d, *m*-C), 129.0 (d, *o*-C), 137.1 (s, *p*-C)	16.0 (SCH_3)
92	66.4	89.0	83.7	56.7	13.5	24.8, 26.1, 110.9	118.7, 118.8, 123.1, 128.1, 129.7, 134.9, 155.9, 157.3 [8 d, 3 s of 12 C, some signals overlapping, C_6H_4 and C_6H_5]	
93	62.1	85.7	83.1	56.9	11.5	24.1, 26.1, 110.4		110.1 (2'-C) 111.0 (3'-C), 142.0 (4'-C), 153.6 (5'-C)

[a] Assignments possibly switched

IR Data

2-([1,1'-Biphenyl]-4-yl)-pyrrolidine **87**: (neat): $\tilde{\nu}$ = 3203 (bs, NH), 2981 (w), 2933 (w), 1487 (m), 1379 (s), 1371 (m), 1341 (m), 1301 (w), 1265 (w), 1063 (s), 1005 (m), 862 (m), 841 (w), 745 (m), 682 (m) cm^{-1}.

2-(4-Fluorophenyl)-pyrrolidine **88**: (neat): $\tilde{\nu}$ = 3250 (s, NH), 2980 (m), 2933 (m), 2168 (w), 2078 (w), 2031 (w), 1993 (w), 1606 (w), 1508 (s), 1455 (w), 1379 (m), 1269 (w), 1214 (s), 1146 (w), 1091 (w), 1050 (m), 1008 (m), 877 (w), 844 (w), 765 (w), 708 (w), 679 (w) cm^{-1}.

2-(4-Chlorophenyl)-pyrrolidine **89**: (neat) $\tilde{\nu}$ = 3309 (s, NH), 2977(m), 2932 (w), 2932 (w), 1595 (w), 1488 (w), 1378 (s), 1267 (m), 1206 (s), 1089 (s), 1055 (s), 1007 (m), 874 (m) cm^{-1}.

2-(4-Bromophenyl)-pyrrolidine **90**: (neat): $\tilde{\nu}$ = 2976 (m), 2932 (m), 1591 (w), 1486 (s), 1454 (w), 1395 (s), 1379 (s), 1347 (w), 1295 (w), 1267 (s), 1208 (w), 1164 (w), 1145 (s), 1121 (w), 1091 (m), 1071 (m), 1049 (s), 1007 (s), 960 (w), 914 (w), 875 (s), 842 (w), 772 (w), 691 (w), 662 (w), 643 (w) cm^{-1}.

2-(4-Thiomethylphenyl)-pyrrolidine **91**: (neat): $\tilde{\nu}$ = 2973 (m), 293 (w), 2238 (w, SCH3), 1492 (m), 1436 (m), 1379 (s), 1374 (m), 1269 (m), 1208 (s), 1165 (w), 1146 (w), 1048 (m), 877 (w), 778 (w), 670 (w) cm^{-1}.

2-(4-Phenoxyphenyl)-pyrrolidine **92**: (neat): $\tilde{\nu}$ = 3330 (s, NH), 2976 (m), 2931 (w), 1589 (w), 1504 (m), 1488 (w), 1378 (s), 1234 (vs), 1208 (m), 1165 (w), 1145 (m), 1090 (m), 1048 (m), 1007 (m), 873 (m), 846 (w), 751 (w), 692 (w), 632 (m) cm^{-1}.

2-(2-Furyl)-pyrrolidine **93**: (neat): $\tilde{\nu}$ = 2973 (m, CH2), 2935 (w), 1509 (w), 1459 (w), 1427 (w), 1377 (m), 1348 (w), 1315 (w), 1270 (m), 1250 (w), 1208 (s), 1165 (w), 1146 (m), 1123 (w), 1089 (w), 1050 (s), 952 (w), 912 (m), 874 (s), 853 (m), 805 (m), 758 (m), 740 (s) cm^{-1}.

Mass spectrometry

2-(4-Bromophenyl)-pyrrolidine **90**: (EI, 70 eV) m/z (%) = 313.0 $[M]^+$ (4), 253.0 (6), 238.0 (12), 211.0 (100), 183.9 (10), 168.9 (4), 132.1 (16), 102.1 (4), 85.0 (4), 43.0 (10).

8.5.5 N—O bond cleavage of *N*-hydroxypyrrolidines with samarium diiodide

Experiment 96 (LR 334)

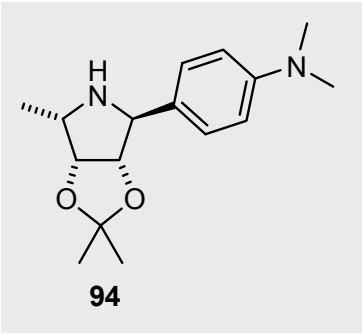

94

(2*S*,3*S*,4*R*,5*S*)-3,4-Dihydroxy-2-(*p*-*N*,*N*-dimethylanilino)-3,4-*O*-isopropylidene-5-methyl-pyrrolidine (94)

THF (abs.) 14 mL was added to a three-necked flask and degassed by bubbling argon through the solution for 4 min. Samarium powder (220 mg, 1.46 mmol, 3.5 Eq.) was added quickly followed by 411 mg (1.56 mmol, 3.5 Eq.) of freshly purified diiodoethane (see notes at beginning of Experimental chapter). Within 10 min, the solution developed a Prussian-blue colour, accompanied by the liberation of ethene gas. The suspension was stirred at room temp. for a further ca. 90 min. During this time, a second (Schlenk) flask was charged with the pyrrolidine **80** (100 mg, 0.342 mmol) and 4 mL degassed (important!) THF. The freshly prepared samarium diiodide solution (14 mL, ca. 3.5 Eq.) was added dropwise to pyrrolidine **80**. The reaction was complete after 10 min according to TLC analysis. A colour change from dark-blue to light-green was observed. Sodium thiosulfate solution (5 mL) was added and the phases were parted. The aqueous phase was extracted with CH_2Cl_2 (3 x 15 mL) and dried ($MgSO_4$). After removal of the solvents on the rotary evaporator (25 °C/10 mbar), the cyclic amine **94** was obtained (75 mg, 2.68 mmol, 79 %) as an analytically pure, colourless solid (m. p. 56 °C).

$[\alpha]_D^{20}$ = –2 (*c* = 0.355, $CHCl_3$)

$C_{16}H_{24}N_2O_2$	calc.	C	69.53	H	8.75	N	10.14
(276.4)	found	C	69.31	H	8.76	N	9.84

IR (neat): $\tilde{\nu}$ = 2974 (m), 2932 (w), 2909 (w), 1615 (s), 1565 (w), 1522 (s), 1481 (w), 1448 (m), 1379 (s), 1370 (s), 1357 (s), 1295 (w), 1268 (m), 1235 (w), 1024 (m), 1185 (m), 1166 (m), 1143 (m), 1085 (m), 1038 (s), 999 (s), 955 (w), 926 (w), 912 (w), 873 (m), 859 (m), 840 (w), 817 (w), 798 (w), 779 (m), 750 (m), 699 (w), 658 (w) cm^{-1}.

^{1}H NMR ($CDCl_3$, 500.1 MHz,): δ = 1.22 (d, $J_{5,1'}$ = 6.6 Hz, 3 H, 1'-CH_3), 1.35, 1.52 [2 s, 3 H each, $C(CH_3)_2$], 2.49 (bs, 1 H, NH), 2.91 [s, 6 H, $N(CH_3)_2$], 3.06-3.16 (m, 1 H, 5-H), 4.49 (dd, $J_{3,4}$ = 5.9, $J_{4,5}$ = 4.2 Hz, 1 H, 4-H), 4.89 (dd, $J_{2,3}$ = 0.5, $J_{3,4}$ = 5.9 Hz, 1 H, 3-H), 6.71 ("dd", $J_{A,B} = J_{A',B'}$ = 8.9 Hz, 2 Hz, A,A' of AA'BB'), 7.10 ("dd", $J_{A,B} = J_{A',B'}$ = 8.7 Hz, 2 H, B,B' of AA'BB').

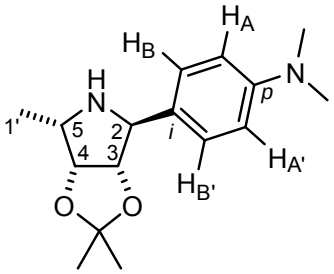

94

^{13}C NMR ($CDCl_3$, 62.9 MHz): δ = 13.5 (q, C-1'), 24.1, 26.1 [2 q, $C(\underline{C}H_3)_2$], 40.7 [2 q, $N(CH_3)_2$], 56.5 (d, C-5), 66.1 (d, C-2), 83.5 (d, C-3), 88.7 (d, C-4), 110.7 [s, $\underline{C}(CH_3)_2$], 112.6 (d, *m*-C), 127.5 (s, *i*-C), 127.7 (d, *o*-C), 149.5 (s, *p*-C).

Experiment 97 (LR 354)

(2*S*,3*S*,4*R*,5*R*)-3,4-Dihydroxy-2-(*p*-*N*,*N*-dimethylanilino)-3,4-*O*-isopropylidene-5-methyl-pyrrolidine (95)

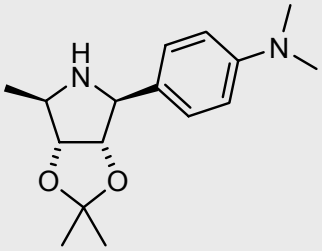

95

The required samarium diiodide solution was prepared freshly according to the procedure given above (Experiment 96) using the following amounts: samarium metal (339 mg, 2.26 mmol, 10.6 Eq.), diiodoethane (636 mg, 2.26 mmol, 10.6 Eq.) in 22 mL abs. THF. The β-D-*ribo*-N-hydroxypyrrolidine **81** was meanwhile placed in a (Schlenk) flask in THF (6 mL) and water was added (0.12 mL). This aqueous THF solution was carefully degassed by passing argon through it for several minutes. The freshly prepared samarium diiodide solution (2.2 mL, ca. 1.0 Eq.) was added dropwise. In comparison to the reaction of its diastereoisomer, i.e. the α-L-*lyxo*-pyrrolidine **80**, the deep-blue colour persisted. Regular TLC analysis after each additional equivalent of added samarium diiodide indicated a much slower reaction. Over the course of 3 h, a total of 5 Eq. samarium diiodide was added and the reaction subsequently stirred overnight. The reaction was quenched with sodium thiosulfate solution and worked up as described above in Experiment 96. After column chromatography, the cyclic amine **95** was obtained, albeit as a spectroscopically pure, orange oil (513 mg, 1.86 mmol, 82 %).

$[\alpha]_D^{20}$ = –28 (*c* = 0.560, $CHCl_3$)

$C_{16}H_{24}N_2O_2$	calc.	C	69.53	H	8.75	N	10.14
(276.4)	found	C	67.50	H	8.70	N	9.83

IR (neat): $\tilde{\nu}$ = 3329 (w), 2981 (m), 2929 (m), 2805 (m), 2655 (w), 2493 (m), 1615 (s), 1566 (w), 1521 (s), 1480 (w), 1453 (w), 1417 (w), 1369 (m), 1345 (m), 1270 (w), 1208 (s), 1158 (m), 1127 (w), 1068 (s), 967 (w), 946 (m), 867 (s), 811 (s), 617 (w), 586 (w), 562 (w) cm^{-1}.

^1H NMR ($CDCl_3$, 300.1 MHz): δ = 1.27 (d, $J_{5,1'}$ = 6.5 Hz, 3 H, 1'-CH_3), 1.31, 1.56 [2 s, 3 H each, $C(CH_3)_2$], 2.91 [s, 6 H, $N(CH_3)_2$], 3.33 (ddd, $J_{4,5}$ = 5.5, $J_{5,1'}$ = 6.6 Hz, 1 H, 5-H), 4.10 (bs, 1 H, NH), 4.14 (d, $J_{2,3}$ = 5.4 Hz, 2-H), 4.29 (dd, $J_{3,4}$ = 7.2, $J_{4,5}$ = 5.4 Hz, 1 H, 4-H), 4.60 (dd, $J_{2,3}$ = 5.4, $J_{3,4}$ = 7.2 Hz, 1 H, 3-H), 6.71 ("dd", $J_{A,B}$ = $J_{A',B'}$ = 8.9 Hz, 2 H, A,A' of AA'BB'), 7.10 ("dd", $J_{A,B}$ = $J_{A',B'}$ = 8.8 Hz, 2 H, B,B' of AA'BB').

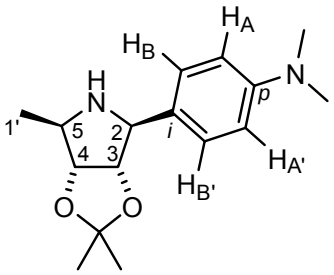

95

^{13}C NMR ($CDCl_3$, 62.9 MHz): δ = 18.3 (q, C-1'), 25.3, 27.4 [2 q, $C(\underline{C}H_3)_2$], 40.7 [2 q, $N(CH_3)_2$], 60.1 (d, C-5), 67.5 (d, C-2), 86.0 (d, C-4), 86.6 (d, C-3), 112.7 [s, $\underline{C}(CH_3)_2$], 114.4 (d, *m*-C), 127.1 (s, *i*-C), 127.9 (d, *o*-C), 150.3 (s, *p*-C).

8.5.6 Synthesis of pyrrolidinetriols

Experiment 85 (FJS 22)

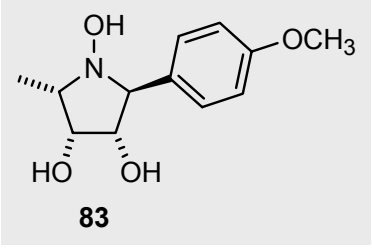

83

(2*S*,3*S*,4*R*,5*S*)-1,3,4-Trihydroxy-2-(4-methoxyphenyl)-5-methylpyrrolidine (83)

The *N*-hydroxypyrolidine **71** (200 mg, 0.716 mmol) dissolved in MeOH (8 mL) was cooled to 0 °C and concentrated hydrochloric acid (0.9 mL) was added. Stirring overnight followed by TLC analysis confirmed the disappearance of starting material and the emergence of a new spot at the baseline. The solvents were removed on the rotary evaporator (25 °C/10 mbar);

the last traces of water were removed azeotropically with toluene, then finally at high vacuum (10^{-3} mbar, P_4O_{10}). This afforded the crude product which was purified using ion-exchange resin (4 g, Dowex 50 WX8, Fluka, strong acid; H^+-form, 200-400 mesh). Liberation of the free amine was achieved by eluting with 1 N ammonia (60 mL). The removal of the solvents and drying (0.001 mbar, P_4O_{10}) yielded the pyrrolidine triol **83** (160 mg, 0.669 mmol, 93 %) as an analytically pure, colourless solid (m. p. 103-105 °C).

$[\alpha]_D^{20}$ = 0.6 (*c* = 0.96, CH_3OH)

$C_{12}H_{17}NO_4$	calc.	C	60.24	H	7.16	N	5.85
(239.3)	found	C	60.07	H	7.21	N	5.65

MS (EI, 70 eV, 380 K): *m/z* (%) = 239.1 (25) $[M]^+$, 223.1 (4), 192 (5), 162.1 (100), 121.1 (14), 108.0 (40), 91.1 (6), 77.1 (8), 66.0 (3), 43.0 (13), 28.0 (5), 18.1 (71).

IR (neat): $\tilde{\nu}$ = 3441 (bs, OH), 3350 (bs, OH), 2975 (m), 2830 (m), 1614 (m), 1578 (w), 1513 (w), 1466 (w), 1387 (w), 1364 (m), 1303 (w), 1221 (s), 1210 (m), 1180 (m), 1149 (w), 1045 (w), 1000 (m), 975 (w), 924 (w), 880 (w), 795 (m) cm^{-1}.

The ^1H and ^{13}C NMR data are contained in Tables 27-29, p. 310-312.

Experiment 86 (LR 108)

(2*S*,3*S*,4*R*,5*S*)-2-([1,1'-Biphenyl]-4-yl)-1,3,4-trihydroxy-5-methylpyrrolidine hydrochloride (84·HCl)

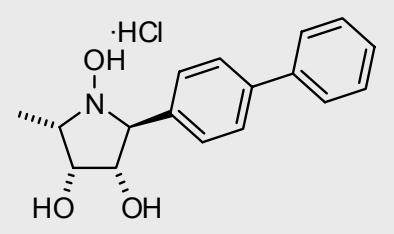

84 ·HCl

Concentrated hydrochloric acid (0.7 mL) was added dropwise to the *N*-hydroxypyyrolidine **72** (196 mg, 0.602 mmol) at 0 °C in methanol (8 mL). Stirring overnight followed by TLC analysis confirmed the disappearance of starting material and the emergence of a new spot at the baseline. The reaction solvents were removed on the rotary evaporator (25 °C/10 mbar); the last traces of water were removed azeotropically with toluene, then finally at high vacuum (10^{-3} mbar, P_4O_{10}). Recrystallisation followed (diffusion method, cf. Experiment 98) using MeOH/Et_2O. After ca. 2 d, and after filtration (small Büchner funnel) and washing with minimal amounts of diethyl ether (3-5 mL), *N*-hydroxypyrrolidine hydrochloride **84·HCl** was

obtained (110 mg, 0.342 mmol, 57 %) as analytically pure, colourless needles (m. p. 213-215 °C, decomp.), which were unfortunately unsuitable for X-ray structure determination. Concentration of the filtrate yielded a further 66 mg (0.205 mmol, 34 %, Σ 91 %) of pyrrolidine **84·HCl**, albeit as a spectroscopically pure, light-red resin.

$[\alpha]_D^{20}$ = –40 (*c* = 0.75, CH_3OH)

$C_{17}H_{20}ClNO_3$	calc.	C	63.45	H	6.26	N	4.35	Cl	11.02
(321.8)	found	C	63.56	H	6.33	N	4.32	Cl	10.74

IR (neat): $\tilde{\nu}$ = 3358 (bs, OH), 3150 (w, NH), 2954 (m, CH_2), 2624 (bs), 1448 (m), 1409 (m), 1287 (w), 1246 (w), 1191 (w), 1162 (m), 1120 (m), 1063 (w), 1004 (m), 944 (w), 915 (w), 764 (w), 836 (w) cm^{-1}.

The ^1H and ^{13}C NMR data are contained in Tables 27-29, p. 310-312.

Experiment 87 (NM 15)

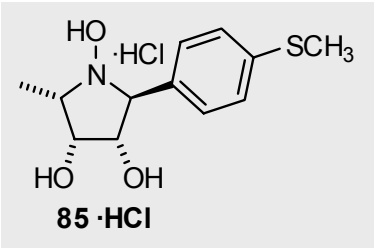

85 ·HCl

(2*S*,3*S*,4*R*,5*S*)-1,3,4-Trihydroxy-5-methyl-2-(4-methylthiophenyl)-pyrrolidine hydrochloride (85·HCl)

After treating the *N*-hydroxypyrrolidine **76** (231 mg, 0.782 mmol) with methanol (9 mL) and concentrated HCl (1.0 mL) as set out above (cf. E 86), the crude product was isolated as a dark-brown solid after removal of solvents and drying (cf. E 86, same conditions). Recrystallisation by the diffusion method ($MeOH/Et_2O$) followed. After 2 d, the analytically pure thioanisyl-substituted triol **85·HCl** precipitated as colourless, needle-like crystals (48.9 mg, 0.1679 mmol, 21 %, m. p. 151 °C). Attempts to isolate additional material by several more repeated recrystallisations of the filtrate were unsuccessful.

$[\alpha]_D^{20}$ = –29 (*c* = 1.00, CH_3OH)

$C_{12}H_{18}ClNO_3S$	calc.	C	49.38	H	6.22	N	4.80	S	10.99
(291.8)	found	C	49.34	H	6.15	N	4.77	S	10.92

IR (neat): $\tilde{\nu}$ = 3382 (bs, OH), 3121 (m), 2956 (m, CH_3), 2899 (w, SCH_3), 1602 (w), 1472 (w), 1394 (s), 1359 (w), 1332 (w), 1287 (m), 1247 (m), 1192 (w), 1165 (m), 1121 (s), 1096 (w), 1062 (w), 1006 (m), 946 (m), 916 (w), 886 (w), 844 (w), 820 (w), 794 (m), 740 (s) cm^{-1}.

The ^1H and ^{13}C NMR data are contained in Tables 27-29, p. 310-312.

8.5.7 Synthesis of pyrrolidinediols

Experiment 98 (FJS 29; LR 175)

(2*S*,3*S*,4*R*,5*S*)-3,4-Dihydroxy-2-(4-methoxyphenyl)-5-methylpyrrolidine hydrochloride (96·HCl)

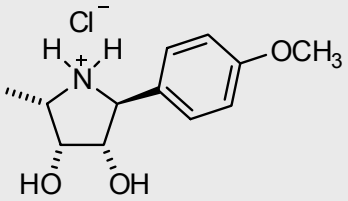

96·HCl

TLP 5: Typical Laboratory Procedure for the hydrolysis of the 3,4-O-isopropylidene protecting group using concentrated hydrochloric oder hydrobromic acid

The cyclic amine **86** (112 mg, 0.425 mmol) in MeOH (5 mL) was cooled to 0 °C and concentrated hydrochloric acid (0.6 mL) was added. After stirring overnight at room temp., the solvents were removed on the rotary evaporator (25 °C/10 mbar). The remaining water was removed azeotropically with toluene, then finally at high vacuum (10^{-3} mbar, P_4O_{10}). This provided the crude product as a red resin. A small amount of methanol was added, followed by enough diethyl ether to induce liophilisation (colourless solid crashes out; cooling overnight in the fridge may help, if this does not occur immediately). The solvents were removed once more on the rotary evaporator and the light-red solid was recrystallised using the diffusion method as follows: the pyrrolidine salt was placed in a oval-shaped flask ('Spitzkolben') and dissolved in ca. 1 mL MeOH with gentle heating. The flask was fitted with an ether bridge, to which a flask containing diethyl ether was attached on to the other end. After 2 d, the product, soluble in methanol, had taken up enough diethyl ether to cause the product to fall out as needle-like crystals. Using a small Büchner funnel, the crystals were filtered off, washed with a small portion of cold diethyl ether (ca. 5 mL) and dried (10^{-2} mbar, P_4O_{10}). This afforded the pyrrolidine hydrochloride **96·HCl** (110 mg, 0.424 mmol, 99 %) as an analytically pure, colourless solid (m. p. 213-215 °C, decomp.). From the crystals, an X-ray

structure determination was made (cf. Sections 5.1.6 and 9.12). This confirmed that methanol was lattice-bound, which explains the deviating values of elemental analysis.

$[\alpha]_D^{20}$ = –6.4 (*c* = 0.5, CH_3OH)

$C_{12}H_{18}ClNO_3$	calc.	C	55.49	H	6.99	N	5.39	Cl	13.66
(259.7)	found	C	53.52	H	7.51	N	4.78	Cl	12.34
$M\cdot(MeOH)_{1.0}$	calc.	C	53.54	H	7.52	N	4.80	Cl	12.15

MS (EI, 70 eV, 440 K): *m/z* (%) = 223.1 (15) $[M]^+$, 206.1 (4), 163.1 (100), 148.1 (14), 136.1 (16), 121.4 (13), 91.1 (5), 77.1 (6), 65.0 (3), 55 (4), 38.0 (8), 35.9 (20), 18.1 (2).

IR (neat): $\tilde{\nu}$ = 3250 (m, NH), 2934 (m), 2838 (w, OCH_3), 1615 (m), 1503 (m), 1246 (m), 1027 (m), 814 (m), 786 (m), 757 (w), 707 (w), 604 (m) cm^{-1}.

The ^1H and ^{13}C NMR data are contained in Tables 27-29, p. 310-312.

Experiment 108 (FJS 24)

(2*S*,3*S*,4*R*,5*S*)-3,4-Dihydroxy-2-(4-methoxyphenyl)-5-methylpyrrolidine (105)

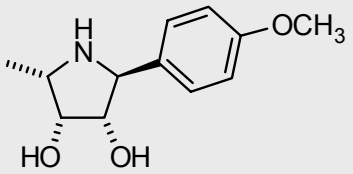

105

Scale: 280 mg (0.905 mmol) pyrrolidine **86**
8.0 mL MeOH, 0.75 conc. HCl

The deprotection was carried out in accordance with TLP 5. The crude product of the pyrrolidine hydrochloride, a red resin-like substance, was purified using 5 g of strongly acidic ion-exchange resin (DOWEX 50WX8, H^+-form, 200-400 mesh; for activation, see notes in Section 8.1). The free amine was eluted with 1 N ammonia (ca. 100 mL). After solvent removal (10 mbar, 40 °C) and drying (10^{-2} mbar, P_4O_{10}), the 2-methoxyphenyl-substituted pyrrolidine diol **105** was obtained (130 mg, 0.5 mmol, 88 %) as a colourless solid (80-81 °C) with slightly deviating elemental analysis.

$[\alpha]_D^{20}$ = –42 (*c* = 0.92, CH_3OH)

$C_{12}H_{17}NO_3$	calc.	C	64.55	H	7.67	N	6.27
(223.3)	found	C	63.11	H	7.66	N	5.98

MS (EI, 70 eV, 360 K): *m/z* (%) = 223.1 (15) $[M]^+$, 206.1 (4), 163.1 (100), 136.1 (18), 121.4 (13), 91.1 (5), 77.1 (6), 65.0 (4), 45.0 (10), 31.0 (20), 18.1 (40).

HRMS (EI, 70 eV): for $C_{12}H_{17}NO_3$: calc. 223.1208; fish 223.1209.

IR (neat): $\tilde{\nu}$ = 3294 (m, NH), 2917 (m), 2837 (w, OCH_3, bend), 2665 (bs), 1612 (m), 1500 (m), 1426 (w), 1374 (w), 1336 (w), 1244 (m), 1179 (w), 1155 (w), 1042 (w), 1028 (m), 982 (w), 803 (m), 787 (w), 707 (w), 604 (m) cm^{-1}.

^{1}H NMR (CD_3OD, 500.1 MHz): δ = 1.21 (d, $J_{5,1'}$ = 6.5 Hz, 3 H, 1'-H), 3.49 ("dq", $J_{4,5}$ = 4.0, $J_{5,1'}$ = 6.5 Hz, 1 H, 5-H), 3.76 (s, 3 H, OCH_3), 3.95 (t, $J_{3,4}$ = $J_{4,5}$ = 4.0 Hz, 1 H, 4-H), 4.06 (d, $J_{2,3}$ = 8.5 Hz, 1 H, 2-H), 4.11 (dd, $J_{2,3}$ = 8.5, $J_{3,4}$ 4.0 Hz, 1 H, 3-H), 6.90 ("dd", $J_{A,B}$ = $J_{A',B'}$ = 8.7 Hz, 2 H, A,A' of AA'BB'), 7.32 ("dd", $J_{A,B}$ = $J_{A',B'}$ = 8.7 Hz, 2 H, B,B' of AA'BB').

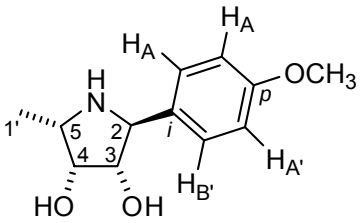

105

^{13}C NMR (CD_3OD, 125.7 MHz): δ = 15.3 (q, C-1'), 55.7 (d, C-5), 56.3 (q, OCH_3), 65.9 (d, C-2), 75.4 (d, C-4), 81.6 (d, C-3), 115.0 (d, *m*-C), 129.4 (s, *i*-C), 135.4 (d, *o*-C), 160.6 (s, *p*-C).

Experiment 111 (LR 109; 113)

(2*S*,3*S*,4*R*,5*S*)-*N*-(*tert*-Butoxycarbonyl)-3,4-dihydroxy-2-(4-methoxyphenyl)-5-methylpyrrolidine (108)

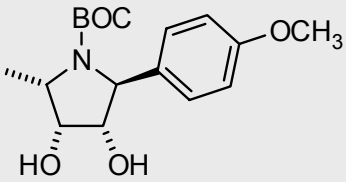

108

To a solution of the pyrrolidine diol **105** (43 mg, 0.193 mmol) in abs. MeOH (2 mL) was added Boc_2O (46 mg, 0.212 mmol, 1.1 Eq.). The solution was stirred at room temp. for 2 d, concentrated on the rotary evaporator, taken up in 3 mL ethyl acetate, and washed with ca. 1 mL NaCl solution. The organic phase was dried ($MgSO_4$) and the solvents removed under vacuum on the rotary evaporator (25 °C/10 mbar). The crude product, a colourless oil that solidified on standing, was subjected to column chromatography (SiO_2, 30 g, 2 cm x 21 cm,

PE:EE = 30:70) to afford the Boc-protected pyrrolidinediol **108** (40 mg, 0.12 mmol, 64 %) as an analytically pure, colourless solid (m. p. 119 °C).

$[\alpha]_D^{20}$ = 0.56 (*c* = 0.96, CH_3OH)

$C_{17}H_{25}NO_5$	calc.	C	63.14	H	7.79	N	4.33
(323.4)	found	C	62.85	H	7.80	N	4.23

IR (neat) $\tilde{\nu}$ = 3400 (bs, OH), 3300 (bs, NH), 2970 (s, CH_2), 1445 (w), 1291 (w), 1195 (w), 1150 (m), 1128 (m), 1043 (s), 1004 (m), 975 (w), 840 (m), 765 (s), 730 (s), 690 (s) cm^{-1}.

^1H NMR (CD_3CN, 500.1 MHz, 298 K): δ = 1.08, 1.41 [2 s of two rotamers; ratio = 2:1; 9 H, $C(CH_3)_3$], 1.31 (d, $J_{5,1'}$ = 6.5 Hz, 3 H, 1'-CH_3), 3.22-3.27 (m, 1 H, 4-OH), 3.55-3.59 (m, 1 H, 3-OH), 3.76 (s, 3 H, OCH_3), 3.77-3.86 (m, 1 H, 3-H), 4.05-4.15 (m, 1 H, 5-H), 4.17-4.25 (m, 1 H, 4-H), 4.57-4.69 ("d", *J* = 50.8 Hz, 1 H, 2-H), 6.85-6.89 (m, 2 H, H_A, $H_{A'}$), 7.04-7.07 (m, 2 H, H_B, $H_{B'}$).

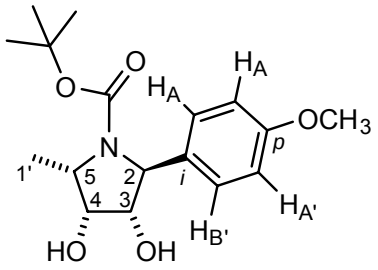

108

^1H NMR (CD_3CN, 300.1 MHz, 343 K): δ = 1.22 [bs, 9 H, $C(CH_3)_3$], 1.33 [d, $J_{5,1'}$ = 6.6 Hz, 1'-CH_3, overlapping with $C(CH_3)_3$], 3.08 (d, $J_{4,OH}$ = 6.0 Hz, 1 H, 4-OH), 3.42 (bs, 1 H, 3-OH), 3.76 (s, 3 H, OCH_3), 3.84 (bs, 1 H, 3-H), 4.08-4.15 (m, 1 H, 5-H), 4.18-4.26 (m, 1 H, 4-H), 4.63 (bs, 1 H, 2-H), 6.86 ("dd", $J_{A,B}$ = $J_{A',B'}$ = 8.7 Hz, 2 H, A,A' of AA'BB'), 7.05 ("dd", $J_{A,B}$ = $J_{A',B'}$ = 8.7 Hz, 2 H, B,B' of AA'BB').

^{13}C NMR (DMSO-d_6, 125.8 MHz, 353 K): δ = 14.0 (q, C-1'), 27.5 [q and s, $C(\underline{C}H_3)_3$, $\underline{C}(CH_3)_3$, overlapping signals], 54.8 (q, OCH_3), 55.2 (d, C-5), 67.0 (d, C-2), 69.0 (d, C-4), 77.6 (d, C-3), 113.3 (d, *m*-C), 126.2 (d and s, *o*-C, *i*-C), 153.0 (s, NCO_2), 157.8 (s, *p*-C).

At room temperature, only badly resolved ^1H and ^{13}C NMR spectra ($CDCl_3$) were obtained. The N-Boc group led to the presence of a ca. 2:1 ratio of rotamers.

Experiment 99 (LR 160; 219)

(2*S*,3*S*,4*R*,5*S*)-2-([1,1'-Biphenyl]-4-yl)-3,4-dihydroxy-5-methylpyrrolidine hydrochloride (97·HCl)

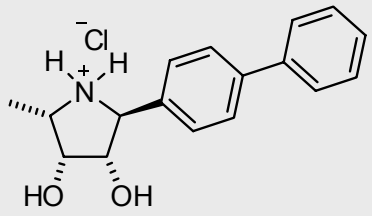

97·HCl

Scale: 280 mg (0.905 mmol) pyrrolidine **87**
8.0 mL MeOH, 0.75 conc. HCl

The reaction, isolation, and recrystallisation was carried out in accordance to TLP 5. After 1 d, needle-like crystals precipitated and were filtered off according to TLP 5. After drying (10^{-3} mbar, P_4O_{10}), the pyrrolidine hydrochloride **97·HCl** was obtained (203 mg, 0.66 mmol, 73 %) as an analytically pure, colourless solid (m. p. 224 °C, decomp.). The filtrate was collected, concentrated and recrystallised once more according to TLP 5. This yielded a further 60 mg (0.196 mmol, 22 %, Σ 95 %) of the analytically pure pyrrolidine **97·HCl**. An X-ray crystal structure was determined (cf. Sections 5.1.6 and 9.13) to provide additional structural proof. Methanol was found to be lattice-bound, which can be inferred from the respective elemental analysis.

$[\alpha]_D^{20}$ = –54 (*c* = 0.99, CH_3OH)

$C_{17}H_{20}ClNO_2$	calc.	C	66.77	H	6.59	N	4.58	Cl	11.59
(305.8)	found	C	63.81	H	7.12	N	4.11	Cl	10.17
$M·(MeOH)_{1.0}$	calc.	C	63.99	H	7.16	N	4.15	Cl	10.49

MS (CI, positive ion, 70 eV, carrier gas: CH_4, 445 K) *m*/*z* (%) = 270.2 (100) $[M+H]^+$, 269.2 (8), 252.2 (4) [-OH], 235.1 (2) [$-H_2O$], 209.1 (90), 182.1 (5), 167.1 (7), 152.1 (4), 132.1 (7), 116.1 (9), 102.1 (2), 74.1 (16), 44.0 (9).

HRMS (CI, 70 eV, carrier gas: CH_4, 445 K) calc. for $C_{17}H_{19}NO_2$: 269.1416; found 269.1415.

IR (neat) $\tilde{\nu}$ = 3400 (bs, OH), 3300 (bs, NH), 2970 (s, CH_2), 1598 (s, N^+H_2), 1445 (w), 1291 (w), 1195 (w), 1150 (m), 1128 (m), 1043 (s), 1004 (m), 840 (m), 765 (s), 730 (s), 690 (s) cm^{-1}.

^1H and ^{13}C NMR data is displayed in Tables 27-29 below, p. 310-312.

Experiment 100 (LR 335)

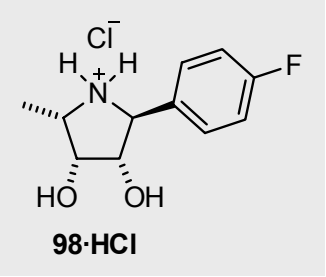

98·HCl

(2*S*,3*S*,4*R*,5*S*)-2-(4-Fluorophenyl)-3,4-dihydroxy-5-methylpyrrolidine hydrochloride (98·HCl)

Scale: 105 mg (0.418 mmol) pyrrolidine **88**
3.0 mL MeOH, 0.8 mL conc. HCl

The reaction, isolation, and recrystallisation was carried out as stated in TLP 5. After 1 d, the crystals obtained were filtered off to yield the pyrrolidine hydrochloride **98·HCl** (98 mg, 0.396 mmol, 95 %) as a analytically pure, colourless solid (m. p. > 200 °C; decomp.).

$[\alpha]_D^{20}$ = –64 (*c* = 1.00, CH_3OH)

$C_{11}H_{15}ClFNO_2$	calc.	C	53.34	H	6.10	N	5.65	Cl	14.31
(247.7)	found	C	53.40	H	6.13	N	5.58	Cl	14.61

IR (neat): $\tilde{\nu}$ = 3484 (w), 3314 (s), 2903 (bs), 2781 (m), 2715 (m), 2534 (m), 1597 (m), 1519 (s), 1447 (w), 1424 (w), 1402 (m), 1376 (m), 1321 (w), 1260 (m), 1234 (s), 1140 (m), 1119 (s), 998 (m), 985 (m), 858 (m), 837 (m), 828 (m), 803 (s), 643 (m), 578 (s), 569 (s) cm^{-1}.

^1H and ^{13}C NMR data is displayed in Tables 27-29 below, p. 310-312.

Experiment 101 (LR 159)

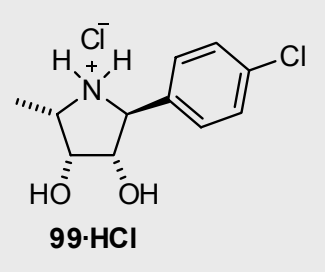

99·HCl

(2*S*,3*S*,4*R*,5*S*)-2-(4-Chlorophenyl)-3,4-dihydroxy-5-methylpyrrolidine hydrochloride (99·HCl)

Scale: 158 mg (0.59 mmol) pyrrolidine **89**
7 mL MeOH, 0.5 mL conc. HCl

The reaction and product isolation was carried out as stated in TLP 5. This gave the pyrrolidine hydrochloride salt **99·HCl** (152 mg, 0.576 mmol, 98 %) as a spectroscopically

pure, dark-red solid. This substance was recrystallised using the method stated in TLP 5. After 1 d, the appearance of colourless, needle-like crystals was observed. Filtration and drying furnished the hydrochloride salt **99·HCl** (134 mg, 5.07 mmol, 86 %) as an analytically pure, colourless solid. A second recrystallisation of the filtrate produced an additional 6.7 mg of pyrrolidine **99·HCl** (0.0254 mmol, 4 %, Σ 90 %) in analytically pure form (m. p. 151 °C, decomp.). The X-ray crystal structure was elucidated to provide additional structural proof (data in Section 9.14). This also confirmed the presence of lattice-bound methanol, also shown to be present from the adjusted elemental analysis values.

$[\alpha]_D^{20}$ = –61 (*c* = 0.985, CH_3OH)

$C_{11}H_{15}Cl_2NO_2$	calc.	C	50.02	H	5.72	N	5.30	Cl	26.84
(264.1)	found	C	48.66	H	6.46	N	4.72	Cl	23.97
$M·(MeOH)_{1.0}$	calc.	C	48.71	H	6.35	N	4.72	Cl	24.32

HRMS (ESI, positive ion) calc. for $C_{11}H_{14}NO_2 + H^+$: 228.0786; found 228.0778.

^1H and ^{13}C NMR data is displayed in Tables 27-29 below, p. 310-312.

Experiment 109 (LR 115)

(2*S*,3*S*,4*R*,5*S*)-2-(4-Chlorophenyl)-3,4-dihydroxy-5-methylpyrrolidine (106)

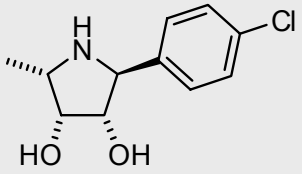

106

Scale: 329 mg (1.229 mmol) 2-(4-chlorophenyl)-pyrrolidine **89**
15 mL MeOH, 1.1 mL conc. HCl

The reaction and the removal of the solvents were carried out in accordance to TLP 5. This afforded the corresponding pyrrolidine hydrochloride which was purified using ion-exchange column (4 g, Dowex 50 WX8, Fluka, strong acid; H^+-form, 200-400 mesh). The crude product was taken up in methanol, added to the column in one go and the impurities were washed out with 100 mL MeOH and 100 mL H_2O. The polyhydroxylated pyrrolidine was eluted with 1 N NH_3 (140 mL) which, after removal of solvents followed by drying (P_4O_{10}, 10^{-3} mbar) yielded the pyrrolidine diol **106** (265 mg, 1.164 mmol, 95 %) as a light-yellow, spectroscopically pure, resin-like solid (m. p. >180 °C, decomp.).